NUREG/CR-6158
EGG-2644

# Implications for Accident Management of Adding Water to a Degrading Reactor Core

Prepared by
P. Kuan, D. J. Hanson, D. J. Pafford, K. S. Quick, R. J. Witt

Idaho National Engineering Laboratory
EG&G Idaho, Inc.

Prepared for
U.S. Nuclear Regulatory Commission

NUREG/CR-6158
EGG-2644

# Implications for Accident Management of Adding Water to a Degrading Reactor Core

Manuscript Completed: December 1993
Date Published: February 1994

Prepared by
P. Kuan, D. J. Hanson, D. J. Pafford, K. S. Quick, R. J. Witt

Idaho National Engineering Laboratory
Managed by the U.S. Department of Energy

EG&G Idaho, Inc.
Idaho Falls, ID 83415

**Prepared for**
**Division of Systems Research**
**Office of Nuclear Regulatory Research**
**U.S. Nuclear Regulatory Commission**
**Washington, DC 20555-0001**
**NRC FIN B5995**
**Under DOE Contract No. DE-AC07-76ID01570**

## ABSTRACT

This report evaluates both the positive and negative consequences of adding water to a degraded reactor core during a severe accident. The evaluation discusses the earliest possible stage at which an accident can be terminated and how plant personnel can best respond to undesired results. Specifically discussed are (a) the potential for plant personnel to add water for a range of severe accidents, (b) the time available for plant personnel to act, (c) possible plant responses to water added during the various stages of core degradation, (d) plant instrumentation available to understand the core condition and (e) the expected response of the instrumentation during the various stages of severe accidents.

# CONTENTS


ABSTRACT ..... iii

EXECUTIVE SUMMARY ..... ix

ACKNOWLEDGMENTS ..... xvii

1 INTRODUCTION ..... 1

2 BENEFITS OF WATER ADDITION, RECOVERY STRATEGIES, AND TIMING OF RECOVERY ..... 2

2.1 The Surrey Plant Results ..... 3

2.2 The Zion Plant Results ..... 5

2.3 The Sequoyah Plant Results ..... 5

2.4 The Peach Bottom Plant Results ..... 6

2.5 The Grand Gulf Plant Results ..... 7

3. THE PROGRESSIVE STAGES OF CORE DAMAGE AND THE EFFECTS OF INJECTING WATER AT THE VARIOUS STAGES ..... 8

3.1 High-Pressure Sequence ..... 8

3.2 Low-Pressure Sequence ..... 19

4. INSTRUMENT RESPONSE DURING CORE DAMAGE AND WATER ADDITION ..... 22

4.1 Instrumentation ..... 22

4.2 Distinguishing Stages of Core Degradation ..... 25

5. CHARACTERIZATION OF THE EFFECTS OF ADDING WATER AT DIFFERENT CORE DAMAGE STAGES ..... 31

5.1 Simple Model Results ..... 31

5.2 SCDAP/RELAP5/MOD3 Calculation Results ..... 34

6. CONCLUSIONS AND RECOMMENDATIONS ..... 50

7. REFERENCES ..... 57

Appendix A—Examination of Water Addition Capabilities for the Five NUREG-1150 Plants ..... A-1

Appendix B—Phenomenology of the Consequences of Adding Water to Degraded Reactor Cores ..... B-1

Appendix C—SCDAP/RELAP5/MOD3 Surry Model Description ..... C-1

# LIST OF FIGURES


1. Core damage progression, showing consequences of adding sufficient water ..... 9
2. Fuel rod ballooning and failure around 1100 K in the central part of the core ..... 13
3. Formation of the lower crust from relocated control material ..... 15
4. Growth of a cohesive debris bed in the central part of the core ..... 16
5. Formation of a particulate debris bed on top of the cohesive bed ..... 17
6. Melting of the interior of a cohesive debris bed, with corresponding thinning of its crust ..... 18
7. Crust failure and relocation of core material to the lower plenum ..... 19
8. Cladding surface temperatures along the center fuel channel for Calculation 1 ..... 38
9. Core collapsed liquid level for Calculation 1 ..... 38
10. System pressure for Calculation 1 ..... 39
11. HPIS mass flow rate for Loop A in Calculation 1 ..... 39
12. Hydrogen mass generated through oxidation in Calculation 1 ..... 40
13. A comparison of system pressures for Calculations 1 and 2 ..... 41
14. A comparison of HPIS flow rates for Calculations 1 and 2 ..... 42
15. A comparison of core collapsed liquid levels for Calculations 1 and 2 ..... 42
16. Cladding surface temperatures along the center fuel channel for Calculation 2 ..... 43
17. Cladding surface temperatures along the center fuel channel for Calculation 3 ..... 44
18. Comparison of core levels for Calculations 1 and 3 ..... 44
19. Comparison of system pressures for Calculations 1 and 3 ..... 45
20. Comparison of HPIS flow rates for Calculations 1 and 3 ..... 46
21. Comparison of the hydrogen mass generated for Calculations 1 and 3 ..... 46
22. Cladding surface temperatures along the center fuel channel for Calculation 4 ..... 47
23. Collapsed core liquid level for Calculation 4 ..... 48
24. System pressure for Calculation 4 ..... 49
25. HPIS mass flow rate for Loop A in Calculation 4 ..... 49

# LIST OF TABLES


ES-1 Effects of water addition on a degraded core ..... xi

1. Description of injection system failure mechanism characteristics ..... 3

2. Summary of potential reductions in core damage frequency resulting from implementation of accident management strategies ..... 4

3. Possible instrument response for core damage stages ..... 26

4. Nominal PWR parameters ..... 32

5. Energy from decay heat of a nominal PWR ..... 32

6. Summary of the different parameters between the four calculations ..... 36

7. Effects of water addition on a degraded core ..... 51

# EXECUTIVE SUMMARY

Preventing severe accidents or mitigating their consequences may require implementation of strategies that add water to the reactor core. However, the consequences of adding water may be difficult to detect during the advanced stages of core degradation using current plant instrumentation. Under certain degraded core conditions, adding water may have negative consequences, such as enhanced hydrogen production or induced changes in core geometry, that complicate the removing of core energy and allow core damage to progress. We have evaluated the consequences of adding water to a degraded core to ensure that (a) undesirable consequences are understood so their effects can be minimized and the accident can be terminated at the earliest possible stage, and (b) plant personnel can be better prepared to deal with undesired plant responses.

We place emphasis on the severe accident behavior of a pressurized water reactor (PWR). However, the major events in the progression of core damage during a severe accident in a boiling water reactor (BWR) are expected to be similar to those for a PWR. Where appropriate, we discuss important differences in behavior between PWRs and BWRs. The capability of existing PWR plant instrumentation to follow core damage progression should also be applicable to BWRs with proper recognition given to the differences in BWR instrument types and locations.

We first evaluated the capability of systems to add water and prevent core damage during the early stages of potential severe accidents. As part of the evaluation, we reviewed accident sequences from *Severe Accident Risks: An Assessment of Five U.S. Nuclear Power Plants* (NUREG-1150). Results from this review indicate that 80 percent or more of core damage frequency originates from sequences where core uncovery could be prevented if additional and innovative recovery actions are implemented. Time frames necessary to implement these actions highly depend on the accident sequence and on plant-specific conditions. If the time available for initiating water addition is relatively short (for example less than 1 hour) the likelihood for success is low. However, the duration of many accident sequences are much longer, some exceeding 17 hours. For these sequences, the likelihood of successful operator intervention is high.

The progression of core damage during severe accidents can be described in terms of the following stages:

1. From core uncovery to fuel rod ballooning
2. Ballooning and rupture of fuel rod cladding
3. Early rapid oxidation of zircaloy cladding by steam
4. Late rapid oxidation of zircaloy cladding by steam
5. Formation of a debris bed in the lower regions of the reactor core or at the lower core support plate from relocated molten zircaloy and liquefied fuel
6. Relocation of core materials to the lower plenum of the reactor vessel.

Concurrent with the formation of a cohesive debris bed near the bottom of the core, a particulate debris bed may also form from fuel pellets or oxidized cladding that relocate to the top of the cohesive bed. The five stages of core damage progression are characterized by temperatures ranging from approximately 1100 K (ballooning of the fuel rod cladding) up to 3100 K (melting of the $UO_2$ fuel).

The effects of adding water during the early core damage stages were evaluated in two ways. First, relatively simple models were developed to estimate the effects of the water on core energy removal. Second, we used the SCDAP/RELAP5/MOD3 computer code, which has phenomenologically based models for severe accident behavior to simulate the effects of adding water during a station blackout (TMLB')

at the Surry nuclear power plant. Results from these two sources, together with results from severe accident experiments, were used to develop a general description of the effects of adding water during the core damage stages. Table ES-1 lists the stages of core damage and discusses the possible positive and negative consequences of adding water, potential accident management strategies to prevent progression to the next damage stage, and potential long-term management strategies to mitigate accident consequences.

The calculations at all core damage stages show that the capability to maintain long-term core energy removal depends on the amount of energy being transferred from the core to the water or steam, the amount of energy being removed from the reactor coolant system (RCS), and the operational characteristics of the safety injection systems. There is the possibility that the reactor core will reach a condition such that a portion of the core remains uncovered for a long period of time if (a) the injection system head is low, or (b) the injection system flow strongly depends on RCS pressure, and (c) the energy transferred from the core to the water exceeds the energy being removed from the RCS. Even if core damage is initially stopped by injecting water, the core may uncover again, and core damage will proceed unless the energy removed from the RCS is equal to or exceeds the core decay heat.

Not all of the accident management strategies discussed in Table ES-1 are evaluated in this report. Selection of many of the strategies was based on results from strategy evaluations sponsored by the Nuclear Regulatory Commission or performed by the nuclear industry. Table ES-1 shows that accident management strategies for the early core damage stages concentrate on ensuring there is adequate water injection and RCS heat removal. During the latter stages of core degradation, strategies are added to prevent vessel failure and to control hydrogen and fission products. Strategies to prevent containment failure were not included in this study.

Results from both the simple and code calculations indicate that core damage progress can be stopped and the core can be recovered (core material returned to near saturation temperature) if the high-pressure injection system (HPIS) operates at full capacity prior to temperatures reaching about 1200 K (the fuel rod ballooning stage). The reactor vessel level monitoring system (RVLMS) would detect the approach to this core damage stage and, initially, the temperature of the fuel rods would be indicated by core exit thermocouple (CET) or hot-leg resistance temperature device (RTD) readings in excess of fluid saturation temperature. A possible negative consequence of adding water at this stage would be pressurization of the reactor coolant system (RCS). High pressure could reduce the HPIS flow rate, which could allow core damage to progress. Whether or not there would be a reduction in HPIS flow would depend on the HPIS pump characteristics, which are plant-specific. No other significant adverse effects were identified.

If core temperatures are greater than 1500 K but less than 2100 K (the rapid oxidation stage), the simple calculations indicate the HPIS flow rate would be below the water addition capacity required to prevent core damage from progressing to a higher stage. However, the SCDAP/RELAP5/MOD3 results indicate that HPIS injection is adequate to prevent progression to the next core damage stage if the HPIS is injecting at its nominal rate. The code predicts that some zircaloy has relocated and that it is not available for further oxidation. As a result, nominal HPIS flow is adequate to cool the remaining cladding and the fuel rods. It should be possible to identify the onset of rapid oxidation from the CETs. However, this core damage stage lasts only a short time and any accident management action would need to be implemented quickly. Methods for depressurizing the RCS to maintain HPIS at or above its nominal flow conditions, for example opening the power-operated relief valves (PORVs), were found to be effective.

Additional hydrogen will be produced when water is injected during the rapid oxidation core damage stage, but the amount is not significant

**Table ES-1.** Effects of adding water on a degraded core.

| Core damage stage (temperature range) | Potential positive consequences of water addition | Potential negative consequences of water addition | Potential accident management strategies to prevent progression to next damage stage | Potential long-term accident management strategies to mitigate accident consequences |
|---|---|---|---|---|
| From core uncovery to ballooning of fuel rod cladding (saturation to 1100 K) | Injection at nominal HPIS rates or greater would prevent advance to the next stage (clad ballooning stage with temperatures >1100 K). Instruments remain well within measurement ranges. | Steam generated during recovery could pressurize the RCS, which could reduce HPIS injection rates. | Use HPIS if RCS pressure is low enough for nominal HPIS flows or use LPIS if pressure is low.<br>If initial RCS pressure is above pressure for nominal HPIS flows, use steam generator feed and bleed to reduce RCS pressure so that HPIS flow is at least nominal, or use RCS feed and bleed.<br>Depressurize the steam generator for temporary reduction of RCS pressure.<br>Restart RCS pumps for temporary core cooling. | Ensure long-term borated ECC water supplies (refill BWST from external sources, etc.) |
| Fuel rod cladding ballooning and rupture (1100 K to 1500 K) | Injection at nominal HPIS rates or greater would prevent advance to the next stage (rapid zircaloy oxidation with temperatures >1500 K). Instruments remain within measurement ranges. | Steam generated during recovery could pressurize the RCS, which could reduce HPIS injection rates. A small amount of hydrogen would be generated but its effects on the system would not be significant. | Use HPIS if RCS pressure is low enough for nominal HPIS flows or use LPIS if pressure is low.<br>If initial RCS pressure is above pressure for nominal HPIS flows, use steam generator feed and bleed to reduce RCS pressure so that HPIS flow is at least nominal, or use RCS feed and bleed.<br>Depressurize the steam generator for temporary reduction of RCS pressure.<br>Restart RCS pumps for temporary core cooling. | Ensure long-term borated ECC water supplies (refill BWST from external sources, etc.)<br>Depressurize the RCS using the PORVs to initiate the accumulators or the LPIS if HPIS is not available. |

**Table ES-1.** (continued).

| Core damage stage (temperature range) | Potential positive consequences of water addition | Potential negative consequences of water addition | Potential accident management strategies to prevent progression to next damage stage | Potential long-term accident management strategies to mitigate accident consequences |
|---|---|---|---|---|
| Early rapid zircaloy oxidation (1500 K to 1800 K) | HPIS injection rates will likely prevent advance to the late rapid oxidation stage (temperatures >1800 K). The uncertainty that injection will be successful in stopping core damage is much larger than during the previous stage. | Steam and hydrogen generated would cause pressurization of the RCS. Significant amounts of hydrogen may be produced. The effectiveness of adding water will be difficult to determine because CETs will approach their limits. Relocation of control material may begin. | Use HPIS if RCS pressure is low enough for nominal HPIS flows or use LPIS if pressure is low.<br>Restart RCS pumps for temporary core cooling. | Ensure long-term borated ECC water supplies (refill BWST from external sources, etc.)<br>If initial RCS pressure is above pressure for nominal HPIS flows, use steam generator feed and bleed to reduce RCS pressure so that HPIS flow is at least nominal, or use RCS feed and bleed.<br>Depressurize the RCS using the PORVs to initiate the accumulators or the LPIS if HPIS is not available. |
| Late rapid zircaloy oxidation (1800 K to 2100 K) | Simple calculations indicate very high (near full accumulator) rates may prevent the advance to stages where debris beds are formed. Code calculations predict HPIS rates will prevent advance to the next core damage stage but there is a large degree of uncertainty in the results because a debris bed is predicted to form. Although it is predicted to cool, modeling may have contributed to excessive heat transfer. | Injection rates must be high because core heatup is proceeding rapidly. Delay times (resulting from filling piping, downcomer, and lower plenum) would become more important for adding water. Hydrogen and steam generation would cause rapid system pressurization. The effectiveness of adding water would be difficult to determine because many CETs would not be operating properly. | Inject at very high ECC rates, if possible. If very high rates are not possible, the effectiveness of adding water to prevent progress to the next core damage stage is not assured. | Inject ECC at the maximum rates possible.<br>If pressure is high, depressurize the RCS using the PORVs to increase HPIS and initiate the accumulators or the LPIS.<br>Ensure long-term borated ECC water supplies (refill BWST from external sources, etc.)<br>Initiate vessel cavity flooding if it is projected to be effective for the plant conditions. |
| Particulate debris bed formation (>2100 K, depending on conditions) | There is potential that adding water could cool and prevent advance to the next core damage stage. There is also the potential that water injected during this stage would cool debris during later stages if it relocates to the lower plenum. | There is the potential that adding water will not cool the debris. Steam generation could be high, depending on the debris bed porosity, power level, and temperature. Hydrogen generation could be high, depending on the amount of unoxidized zircaloy, its location, porosity, and temperature. Water injection may cause CETs to give low temperature readings when core temperatures remain high. | The effectiveness of adding water in preventing progress to the next core damage stage is not assured. | Inject ECC at the maximum rates possible.<br>Ensure long-term borated ECC water supplies (refill BWST from external sources, etc.)<br>Initiate vessel cavity flooding if it is projected to be effective for the plant conditions.<br>Initiate hydrogen control measures.<br>Initiate fission product control measures. |

**Table ES-1.** (continued).

| Core damage stage (temperature range) | Potential positive consequences of water addition | Potential negative consequences of water addition | Potential accident management strategies to prevent progression to next damage stage | Potential long-term accident management strategies to mitigate accident consequences |
|---|---|---|---|---|
| Cohesive debris bed formation (>2100 K depending on conditions) | There is the potential that water addition will cool and stabilize the crust preventing relocation. The molten pool will also begin to cool and eventually solidify. | There is a high likelihood that the crust will not stabilize and relocation will occur. Interaction between the molten fuel and the injected water could cause steam explosions. It will be difficult for plant accident management personnel to recognize this stage. Peripheral thermocouples may show the core is cool when it is not. | The effectiveness of adding water in preventing progress to the next core damage stage is not assured. | Inject ECC at the maximum rates possible.<br>Ensure long-term borated ECC water supplies (refill BWST from external sources, etc.).<br>Initiate vessel cavity flooding if it is projected to be effective for the plant conditions.<br>Initiate hydrogen control measures.<br>Initiate fission product control measures. |
| Lower head attack by molten core debris (>1700 K for metals, >2700 K for ceramics) | Failure of the lower head may be prevented. | Steam and hydrogen generated may raise the RCS pressure so that the vessel will fail earlier than otherwise. The melt ejection will be more dispersed, which will increase the likelihood of DCH. Use of water to cool the outside of the lower head may be delayed if operators believe adding water is being effective in stabilizing the core. | The effectiveness of adding water to prevent progress to the next core damage stage is not assured. | Inject ECC at the maximum rates possible.<br>Ensure long-term borated ECC water supplies (refill BWST from external sources, etc.)<br>Initiate vessel cavity flooding if it is projected to be effective for the plant conditions.<br>Initiate hydrogen control measures.<br>Initiate fission product control measures. |

compared to the hydrogen that would be produced if the core damage progress is unmitigated. Because temperature measurements would become unreliable during this stage, confirmation of core recovery would require examination of the long-term trends of many instruments. Hydrogen detection monitors could identify this stage but there would likely be a substantial delay between the time hydrogen generation begins and when the hydrogen is detected.

Relocation of core materials first occurs when the stainless steel cladding of the control rods fails. In addition to molten stainless steel, relocating materials would include control material (generally Ag-In-Cd or $B_4C$). Zircaloy from the fuel assembly guide tubes may also be liquified by the molten control materials during this stage. If unborated water is added to the core after the control materials have relocated, there is a possibility of re-criticality of the reactor. However, it is beyond the scope of this report to address the recriticality issue.

If a cohesive debris bed is formed in the core region from the relocation of core materials, removal of energy from the degraded core cannot be assured even if unlimited amounts of water are added to the vessel. The SCDAP/RELAP5/MOD3 calculation with HPIS initiated at 1800 K predicts the intact fuel rods will quench but predicts formation of a small cohesive debris bed. The calculation indicates the debris bed cools slowly, but the cooling is likely influenced by the modeling of the bed, which includes some porosity. The capability of water to remove energy from a cohesive debris bed depends on the bed's size and the power density, the porosity, and the thermal conductivity of the materials composing the bed. The power density and the thermal conductivities depend on the design and operating parameters of the reactor. Although the code predicts cooling of the debris bed, the success of adding water is uncertain for this and more advanced core damage stages because the debris bed characteristics and configuration are uncertain. As a result, alternate accident management strategies, such as water injection into the reactor vessel cavity, should be considered when CETs exceed 1800 K or significant quantities of hydrogen are detected. Implementation of alternate strategies would need to be pursued until there were long-term indication of core recovery.

A cohesive debris bed or a more advanced stage of core degradation would be very difficult to detect using instrumentation currently installed in nuclear power plants. Temperature measurements would not be accurate and would not have signatures unique to these damage stages. Interpreting the response of RCS pressure to adding water after the formation of a cohesive debris bed could be counterintuitive. Core materials could be in several configurations simultaneously: a cohesive bed, a particulate bed, and loose debris. A large cohesive debris bed and particulate bed would result in small amounts of material in the form of loose debris. If adding water to the core produces a rapid pressure rise, it is likely that the cohesive and the particulate beds would be small and core energy would be easily removed by the incoming water. If there is only a small RCS pressure rise during water addition, the debris bed is likely to be large, and energy cannot be efficiently removed from its interior. Because it cannot be easily cooled, the interior of a large cohesive debris bed is likely to melt portions of the crust, causing it to thin. The thinned crust will eventually fail, and molten material will relocate to the reactor vessel lower plenum.

The possibility of steam explosions at the time of relocation of molten material is not evaluated in this work. This complex issue is currently being evaluated by separate programs within the NRC.

Results in this report can be used to identify and integrate effective strategies for accident management and to identify limits on the capability of instrumentation in determining when strategies should be implemented. However, plant-specific information would be necessary for the development of an accident management plan for a nuclear power plant. The special characteristics of the specific nuclear power plant should be considered when developing its core damage progression stages. For example, the pressure range over which the HPIS flow is maximized is very important. The individual plant instrument

response to adding water at each stage of core degradation would also need to be quantified as a function of the instrument type and its location within the plant.

## ACKNOWLEDGMENTS

The authors express appreciation to Dr. Frank Odar, the NRC Project Manager, and to those within the NRC who have offered ideas and suggestions for improving this report. We thank R. J. Witt of the University of Wisconsin for his insights in the subject of low-pressure sequences and instrumentation signatures. We thank D. A. Brownson, C. A. Dobbe, and L. D. Schlenker for reviewing the report and offering helpful suggestions.

# Implications for Accident Management of Adding Water to a Degrading Reactor Core

## 1. INTRODUCTION

Significant capabilities for the management of accidents currently exist at nuclear power generation plants in the United States, which are generally directed toward preventing core damage, preventing containment failure, and minimizing public health risks. Although some capabilities exist for mitigating the effects of severe accidents, the effectiveness of these capabilities to reduce risk for a broad range of credible severe accidents has not been fully demonstrated. As a result, the staff of the Nuclear Regulatory Commission (NRC) have concluded that the risk associated with severe core damage can be further reduced by extending current accident management practices.

Preventing severe accidents or mitigating their consequences will require implementation of strategies to add water to the reactor core. However, for advanced stages of core degradation, there is no guarantee that adding water will immediately terminate the progress of core damage. Under certain degraded core conditions, adding water may have negative consequences, such as enhancing hydrogen production or inducing changes in core geometry that complicate core energy removal and recovery.

Our primary objective of evaluating the consequences of adding water to a degraded core is to identify and examine the potential benefits and undesirable consequences, so that (a) the benefits can be enhanced and the effects of the undesirable consequences can be minimized, (b) the accident can be terminated at the earliest possible stage, and (c) plant personnel can be better prepared to deal with plant responses that appear contrary to desired outcomes when water is added. We have accomplished this objective by evaluating the potential for plant personnel to add water for a range of severe accidents, the time available for the plant personnel to act, the plant instrumentation available to identify the core status and the expected response of this instrumentation during the various stages of core degradation, and the possible core and plant responses during water addition for severe accidents.

Much has been learned since the TMI-2 accident in understanding core damage progression during severe accidents. Researchers have analyzed the TMI-2 plant responses to the accident, examined the damaged TMI-2 core, performed in-pile severe fuel damage experiments both in the U.S. and overseas laboratories, performed separate-effects experiments that address various specific aspects of the core degradation process, and developed and applied computer codes to the analysis of severe accidents. This research has resulted in a fairly consistent scenario of unmitigated core degradation, which includes (a) fuel rod ballooning and rupture, (b) rapid oxidation of the zircaloy clad by steam, (c) failure of control rods, (d) formation of a cohesive debris bed from molten core materials relocated to the lower elevations of the reactor core, and (e) relocation of core materials to the reactor vessel lower plenum.

In this report, we emphasize the severe accident behavior of a pressurized water reactor (PWR). However, the major events in the core damage progression sequence for a boiling water reactor (BWR) are expected to be similar to those for a PWR. We discuss important differences in behavior between PWRs and BWRs where appropriate. Discussion of the capability of instrumentation to follow core degradation should also be applicable to BWRs if one recognizes the differences in BWR instrument types and location.

# 2. BENEFITS OF WATER ADDITION, RECOVERY STRATEGIES, AND TIMING OF RECOVERY

The capability to add water during core degradation will depend on the availability of both safety and nonsafety-grade injection systems and the ability of the plant operators to recognize which systems are available and to initiate their use. Action by the operators may also be necessary during some accident sequences to modify the conditions in the RCS to allow available systems to be used more effectively. To aid in understanding the availability of safety-grade systems during core damage sequences, we have evaluated several nuclear power plants to (a) identify postulated sequences where water added into the primary will reduce the core damage frequency (CDF), (b) estimate the time at which the core uncovers for the identified accident sequences, and (c) review factors that may prevent the addition of water.

To examine the availability of safety-grade injection systems at typical nuclear power plants, we examined the sequences for the five plants studied in the NUREG-1150 program.[1] Postulated sequences were identified where adding water into the primary system would reduce the core damage frequency (CDF) as determined in the NUREG-1150 and supporting documentation such as NUREG/CR-4550 (Reference 3). These accident sequences were then examined to determine which injection systems are available for adding water. Injection system failure mechanisms and times were identified and the core uncovery time was estimated. The contributions to the core damage frequency were then determined for the various injection system failure mechanisms. Plant conditions that may prevent sufficient water addition were also reviewed. A more detailed description of the overall methodology used in this study follows.

We obtained the dominant accident sequences and their descriptions from the NUREG/CR-4550 analyses of the Surry plant (a three-loop PWR with a subatmospheric containment), Zion (a four-loop PWR with a large dry containment), Sequoyah (a four-loop PWR with an ice condenser containment), Peach Bottom [a boiling water reactor/4 (BWR/4) with a Mark I containment], and Grand Gulf (a BWR/6 with a Mark III containment).[2,3,4,5,6] For all plants examined except Grand Gulf, the core damage frequency information for the sequences were obtained from the respective NUREG/CR-4550 analyses. The Grand Gulf NUREG/CR-4550 analysis was unique among the five plants in that some of the accident sequences were split among different plant damage states (PDSs). However, the contribution of each accident sequence to each PDS was not presented in the NUREG/CR-4550. Therefore, an alternative method for Grand Gulf was necessary. Appendix A describes this alternative method in more detail.

The contribution to the core damage frequency of each injection system failure mechanism, identified in the previous step, was determined using two substeps. First, each sequence was placed in one of three bins, based on the following characteristic failure mechanisms: (a) the source or cause of the injection failure, (b) which injection system failed, and (c) the time that the system failed. Second, similar characteristic combinations were sorted to obtain the contribution of each failure mechanism to the total CDF. Table 1 summarizes the three characteristic descriptions used for all five plants.

In the following sections, we briefly discuss the results for the five NUREG-1150 plants. Appendix A presents a more detailed description of the approach and results. All reductions in CDF should be considered as the maximum possible, since implementation of accident management strategies would be necessary to realize these reductions. The likelihood of successfully implementing accident management strategies depends strongly on the capabilities of the personnel and the time they have available. Time available for implementation of less than 1 hour would result in a very low likelihood of successfully diagnosing the conditions and initiating the

**Table 1.** Description of injection system failure mechanism characteristics.

| Attribute-mnemonic | Description |
|---|---|
| | **Characteristic 1—Injection system failure mechanism** |
| POWER | Injection system does not operate because of total or partial power failure. |
| RECIRC | Injection system operates initially, fails in the recirculation mode. |
| FAIL | Injection system fails owing to hardware failure. |
| ATWS | Injection system fails owing to ATWS induced events. |
| OPERATOR | Injection system fails owing to operator error. |
| CCW/SW | Injection system fails owing to loss of component cooling water/service water. |
| SAFETY | Injection system does not operate owing to safety injection actuation failure. |
| | **Characteristic 2—Failed injection system** |
| HPI | High-pressure injection system is failed. |
| LPI | Low-pressure injection system is failed. |
| | **Characteristic 3Time of failure** |
| INIT | Injection system fails at moment of request or soon after. |
| RECIRC | Injection system fails in the recirculation mode. |
| LATE | Injection system operates for some time, then fails. |

appropriate strategies. For times greater than 1 hour, likelihood increases significantly as time increases. Table 2 summarizes the potential for reducing CDF for each plant, assuming that all strategies would be successfully implemented.

## 2.1 The Surry Plant Results

Applying the methodology to the Surry plant shows that about 83% of the CDF is due to sequences in which core uncovery might be prevented if additional and innovative recovery actions were implemented. This percentage can be broken down as follows:

- CDF could be reduced up to 67% if additional onsite ac power sources with the capability to power the injection pumps were provided
- CDF could be reduced up to 10% if the reactor coolant system were depressurized so that available low-pressure injection systems could be used
- CDF could be reduced up to 4% if water were available for long-term injection, for example, additional stored water sources or the capability to refill the refueling water

**Table 2.** Summary of potential reductions in core damage frequency resulting from implementation of accident management strategies.

| Plant | Additional ac or dc power available (%) | RCS depressurization (%) | Additional long-term water source (%) | Eliminate recirculation failures (%) |
|---|---|---|---|---|
| Surrey | 67 | 10 | 4 | |
| Zion | 4 | — | 3.5 | — |
| Sequoyah | 26 | 5 | 4 | 46 |
| Peach Bottom | 5[a] | — | — | — |
| Grand Gulf | 95[b] | 1.5 | — | — |

a. Could be increased to 46% if vessel depressurization is combined with additional ac power sources.

b. Includes reductions from powering systems other than injection systems.

storage tank (RWST) over an indefinite period of time

- CDF could be reduced up to 2% if additional reactor scram procedures and devices were implemented.

The remaining 17% of the CDF is the result of sequences involving injection system failures for which no feasible recovery action could be implemented to prevent the onset of core damage. These sequences include interfacing system loss-of-coolant accidents (V sequences), large and medium break loss-of-coolant accidents (LOCAs), and anticipated transients without scram (ATWS) events.

Of those sequences that might be prevented if additional onsite ac power sources were provided, the injection systems are not available following accident initiation. For approximately 27% (based upon CDF) of these sequences, the core uncovers in approximately 1 hour and accident management action would not likely be successful in this time. For the remaining 73%, the time of core uncovery ranges from approximately 2 to 7 hours, which could significantly increase the likelihood of successfully implementing accident management strategies.

For those sequences that might be prevented if the reactor vessel were depressurized so that available low-pressure injection systems could be used, the high-pressure injection system is failed at the initiation of the accident. For 21% of these sequences, the time to core uncovery ranges from approximately 15 to 50 minutes, which is a relatively short time for accomplishing accident management actions necessary to successfully depressurize the RCS. For about 26% of the sequences, the time of core uncovery ranges from approximately 50 minutes to 17 hours, which should enable personnel to successfully cope with the accident. For the remainder (approximately 53%) of these sequences, the time at which the core uncovers is not specified in NUREG-1150.

For those sequences that might be prevented if additional stored water sources were provided or if refilling of the RWST could be continued for an indefinite period of time, the high-pressure system fails in the recirculation mode. The time of core uncovery is greater than 10 hours for all of these sequences, which should allow personnel

sufficient time to implement accident management strategies.

The high-pressure injection systems fail immediately for those sequences that might be prevented if additional reactor scram procedures and devices were implemented. The time to core uncovery for these sequences is not specified in the available documentation.

## 2.2 Zion Results

At Zion, 95.6% of the CDF is due to PDSs in which core uncovery might be prevented if additional and innovative recovery actions were implemented. The breakdown of these PDS are as follows:

- The CDF could be reduced up to 4% if additional onsite ac power sources with the capability to power the injection pumps were provided
- The CDF could be reduced up to 3.5% if water were available for long-term injection, for example, additional stored water sources or the capability to refill and maintain water in the RWST for an indefinite period of time
- The CDF could be reduced up to 86% if pump seal LOCAs, loss-of-component cooling, or loss-of-service-water supplies could be prevented
- The CDF could be reduced up to 2% if additional reactor scram procedures and devices were available.

Only 4.4% of the CDF is due to plant damage states (PDSs) involving injection system failures in which no feasible recovery action could be implemented. These PDSs involve V sequences, and large and medium break LOCAs.

The approximate failure times for injection systems at Zion are included in the following paragraph. However, estimates of the time to core uncovery were not available for most of the PDSs and are consequently omitted.

For those PDSs that might be prevented if pump seal LOCAs, loss-of-component cooling, and loss of service water could be prevented, the injection systems fail immediately. For those PDSs that might be prevented if additional onsite ac power sources were provided, approximately 50% (based on CDF) involve initial failures of the high-pressure injection systems. The remaining 50% involve failures of the high-pressure injection systems in the recirculation mode. Of those PDSs that might be prevented if additional stored water sources or if refilling of the RWST could be continued for an indefinite period of time, all involve failures of the high-pressure injection system in the recirculation mode. Finally, of those PDSs that might be prevented if additional reactor scram procedures and devices were available, all involve initial failures of the high-pressure injection systems.

## 2.3 The Sequoyah Plant Results

At Sequoyah, 80% of the CDF is due to sequences in which core uncovery might be prevented if additional and innovative recovery actions were implemented. The breakdown of the CDF is as follows:

- The CDF could be reduced up to 46% if failures of the high- and low-pressure recirculation systems could be eliminated
- The CDF could be reduced up to 26% if additional onsite ac power sources with the capability to power the injection pumps were provided
- The CDF could be reduced up to 5% if the reactor coolant system were depressurized so that available low-pressure injection systems could be used
- The CDF could be reduced and up to 4%, if water was available for long term injection, for example, additional stored water sources or the capability to refill and maintain water

in the RWST for an indefinite period of time.

The remaining 20% of the CDF is due to sequences involving injection system failures in which no feasible recovery action could be implemented. The sequences include a V sequence, large and medium break LOCAs, and ATWS events.

For those sequences that might be prevented if failures of the high and low pressure recirculation systems were eliminated, the injection system failures occur in the recirculation mode. For 76% (based upon CDF) of these sequences, the time to core uncovery is estimated as being greater than 17 hours which is adequate time for a wide range of accident management actions. For the remaining 24%, the range of time to core uncovery is estimated as being from 45 minutes to 17 hours.

For those sequences that might be prevented if additional onsite ac power sources were provided, all involve initial failures of the high pressure injection system. For 68% of the sequences, the time to core uncovery is approximately 1 hour. This amount of time is short for successfully implementing the needed accident management actions. For the remaining 32%, the time of core uncovery ranges from approximately two to 7 hours. Accident management actions to initiate additional power sources likely could be accomplished in this time if there was sufficient advanced preparation.

Of those sequences that might be prevented if the reactor coolant system was depressurized so that available low pressure injection systems could be utilized, all involve initial failures of the high pressure injection system. The time to core uncovery for these sequences is not specified.

Of those sequences that might be prevented if additional stored water sources or if refilling of the RWST could be continued for an indefinite period of time, all involve failure of the high-pressure injection system in the recirculation mode. The time to core uncovery for these sequences is not specified.

## 2.4 The Peach Bottom Plant Results

At Peach Bottom, 82% of the CDF is due to sequences in which core uncovery might be prevented if additional and innovative recovery actions were implemented. The breakdown of the CDF is as follows:

- The CDF could be reduced up to 42% if a combination of additional reactor vessel depressurization mechanisms and additional onsite ac power supplies to the low-pressure injection systems were implemented

- The CDF could be reduced up to 5% if only additional onsite ac power sources with the capability to power the injection pumps were provided (no coincident depressurization)

- The CDF could be reduced up to 35% if a combination of additional reactor scram and reactor depressurization mechanisms were implemented.

The remaining 18% of the CDF is due to sequences involving injection system failures in which no feasible recovery action could be implemented. The sequences include large- and medium-break LOCAs, and very short-term ATWS events.

For those sequences that might be prevented if a combination of additional reactor vessel depressurization mechanisms and additional onsite ac power supplies to the low-pressure injection systems were implemented, the high pressure core injection (HPCI) and reactor core isolation cooling (RCIC) systems fail in approximately 10 hours owing to loss-of-room cooling or battery depletion. For these sequences, the core uncovers in about 10 to 13 hours. This time frame should be adequate for implementation of accident management strategies.

For those sequences that might be prevented if only additional onsite ac power sources were provided (no coincident depressurization), the HPCI and RCIC systems fail at the start of the sequence.

For these sequences, the time to core uncovery is approximately 1 hour. Implementation of accident management strategies in this short time period could have a low likelihood of success.

For those sequences that might be prevented if a combination of additional reactor scram and reactor depressurization mechanisms were implemented, the HPCI and RCIC systems fail in less than one half hour owing to high suppression pool temperature. The control rod drive (CRD) injection system is operating but cannot mitigate the sequence. For these sequences, the time to core uncovery is not specified.

## 2.5 The Grand Gulf Plant Results

At Grand Gulf, all of the CDF is due to sequences in which core uncovery might be prevented if additional and innovative recovery actions were implemented. The major contributors to the CDF are as follows:

- The CDF could be reduced up to 95% if additional onsite ac and dc power sources with the capability to power needed systems were provided
- The CDF could be reduced up to 1.5% if additional reactor vessel depressurization mechanisms were implemented
- The CDF could be reduced up to 1.5% if additional pump room cooling was provided
- The CDF could be reduced up to 1.6% if a combination of all of the recovery actions were implemented.

For those sequences that might be prevented if additional onsite ac and dc power sources were provided, 99% of the sequences (based upon CDF) involve initial failure of the HPI systems. The time to core uncovery for these sequences is approximately 1 hour. This time is short to successfully implement accident managemen' strategies. The remaining 1% involve failure of the operator to activate the firewater system late in the transient. The time to core uncovery for these sequences is approximately 12 hours.

For those sequences that might be prevented if additional reactor vessel depressurization mechanisms were implemented, more than 99% involve initial failure of the high-pressure core spray system (HPCS). For these sequences, the CRD and RCIC systems are operating but are not sufficient to make up the coolant loss. The time to core uncovery is approximately 1 hour.

The sequence that might be prevented if additional pump room cooling were provided involves late failure of the HPCS owing to pump room heatup. The CRD and RCIC systems are operating but are not sufficient to make up the coolant loss. The time to core uncovery is estimated as more than 12 hours.

Finally, the sequence that might be prevented if a combination of all of the recovery actions were implemented involves a late failure of the firewater system. The time of core uncovery is estimated to be more than 12 hours.

The majority of the Grand Gulf sequences proceed to core damage in about 1 hour. Therefore, accident management actions would need to be well-planned and executed to successfully prevent core damage.

# 3. THE PROGRESSIVE STAGES OF CORE DAMAGE AND THE EFFECTS OF INJECTING WATER AT THE VARIOUS STAGES

The response of a plant during a severe accident will depend to some degree on the plant design, the accident initiator, the mitigation actions initiated by the plant personnel or hardware, and the performance of the personnel and hardware. However, results from a variety of severe fuel damage experiments and the TMI-2 accident show that the progression of unmitigated core damage can be characterized by a sequence of distinct stages.[7] Although some details of the timing or the phenomena for these stages may be altered by system conditions, such as high versus low pressure, the general progression is very similar among plants.

Following is a description of the core damage stages for severe accident sequences that remain at high pressure during the entire core damage period. For these stages, core uncovery is caused by the boil-off of water from the core region, which causes a relatively slow depletion of the core water inventory. This type of core uncovery is typical of sequences where loss of water from the system is slow, for example, small-break loss-of-coolant accidents or station blackout sequences. It would also be typical of sequences where mass is depleted rapidly during the early stages of the accident but is replaced by injection systems, such as the accumulators in a pressurized water reactor. We describe the core damage states for high-pressure sequences, then the differences in the core damage states caused by low-pressure sequences. Appendix B presents more detailed information on the core damage stages.

## 3.1 High-Pressure Sequence

Figure 1 shows the expected sequence of core damage stages typical of high-pressure boil-off accident conditions. This sequence can apply to both PWRs and BWRs. However, to simplify the discussion we describe the sequence mainly in terms of the expected behavior of PWRs; only where differences in behavior are expected to be significant do we discuss the behavior of BWRs. The sequence starts with core uncovery and ends in either the termination of the damage progression for a particular state or melt through of the lower head of the reactor vessel. The stages of core damage progression can be characterized by a temperature scale: from a temperature that is within the operating range of the plant coolant (560 K), to a temperature above the melting point of $UO_2$ (3100 K). The potential consequences of adding water at each major stage of core damage are also shown in the sequence.

At the time of core uncovery for a sequence involving high-pressure boiloff, steam occupies the volume of the primary system above the top of the reactor core, while a two-phase mixture of steam and liquid water occupies the volume below. The temperature of the fuel rods stays near the saturation temperature of the water. As long as the fuel rods are in a two-phase fluid environment, even up to very high void fractions, heatup of the fuel rods will not be significant.[8]

If water fails to enter the core following initiation of core uncovery, the water in the core will be boiled off gradually, and the upper part of the fuel rods will be exposed to a steam environment and they will heat up. Above a temperature of approximately 1100 K, the zircaloy cladding can fail because of loss of mechanical strength, either from ballooning (localized radial expansion) and bursting[a,9,10,11] when the internal pressure of the rods exceeds the system pressure, or from collapsing when the pressure inside the rods is below the system pressure. Figure 2 depicts the damage state of the core with ballooned and burst cladding of fuel rods.

Collapse of cladding onto fuel pellets does not affect subsequent cooling of the core as water is added, but ballooning of cladding may block a substantial portion of the flow area of the core and restrict the flow of water. The blocked region may continue to heat up to the next stage of core

a. M. H. Schankula et al., "Recent Post-Irradiation Examination Results from Battelle FLHT-2 and FLHT-4 Test Assemblies," presentation at the Severe Accident Research Program Partners Review Meeting, Idaho Falls, Idaho, April 1–14, 1989.

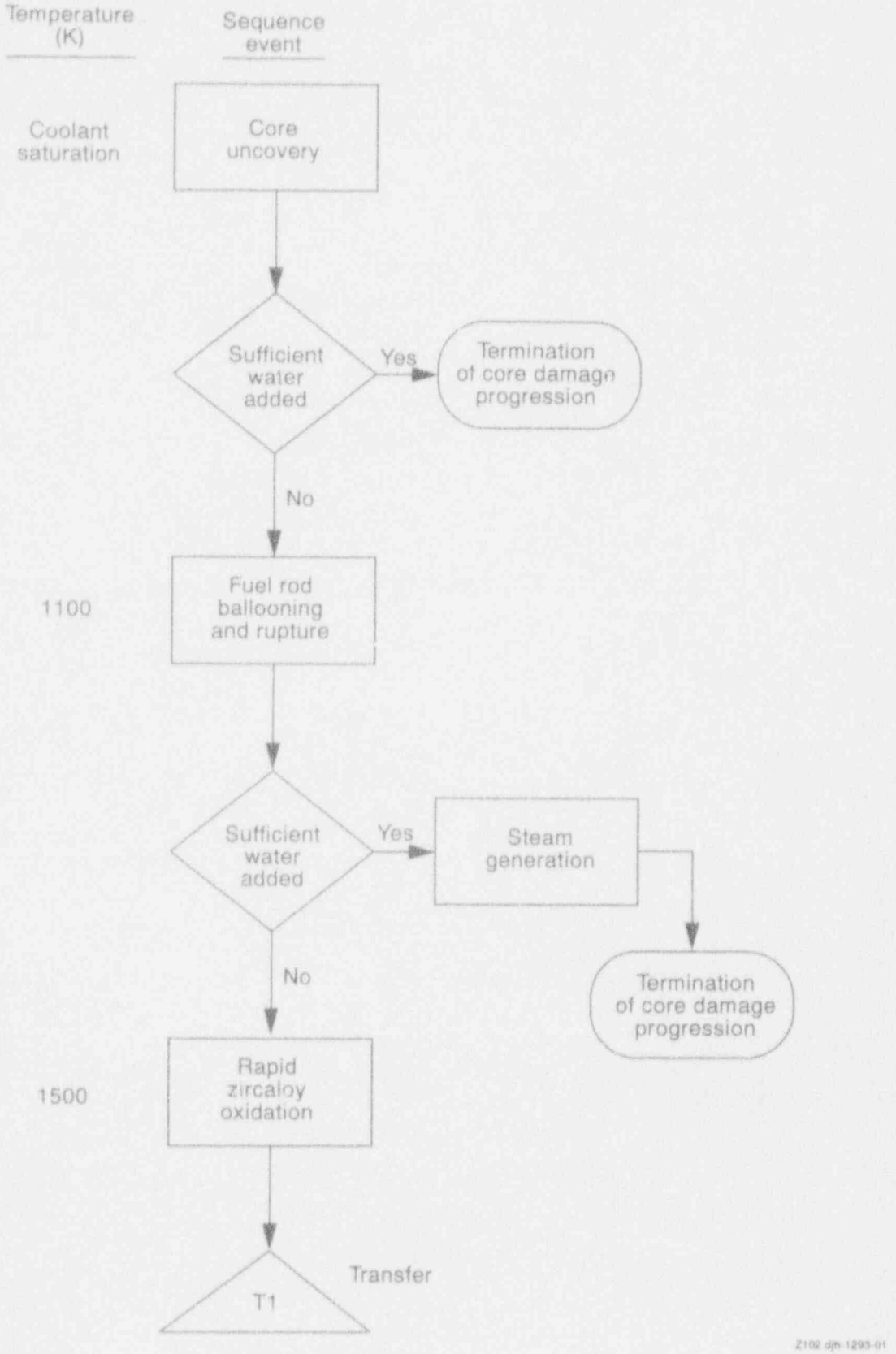


**Figure 1.** Core damage progression, showing consequences of adding sufficient water.

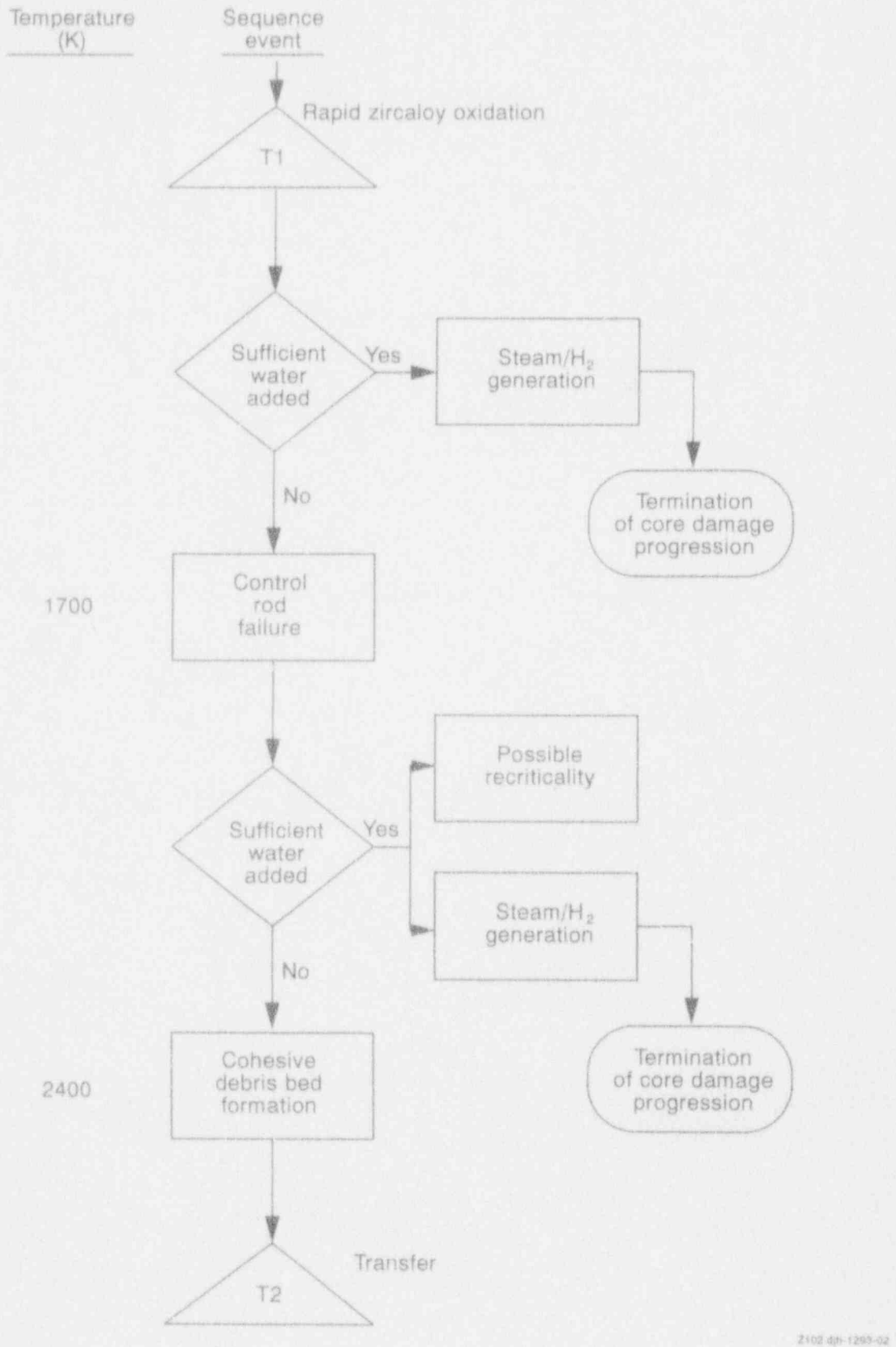


**Figure 1.** (continued).

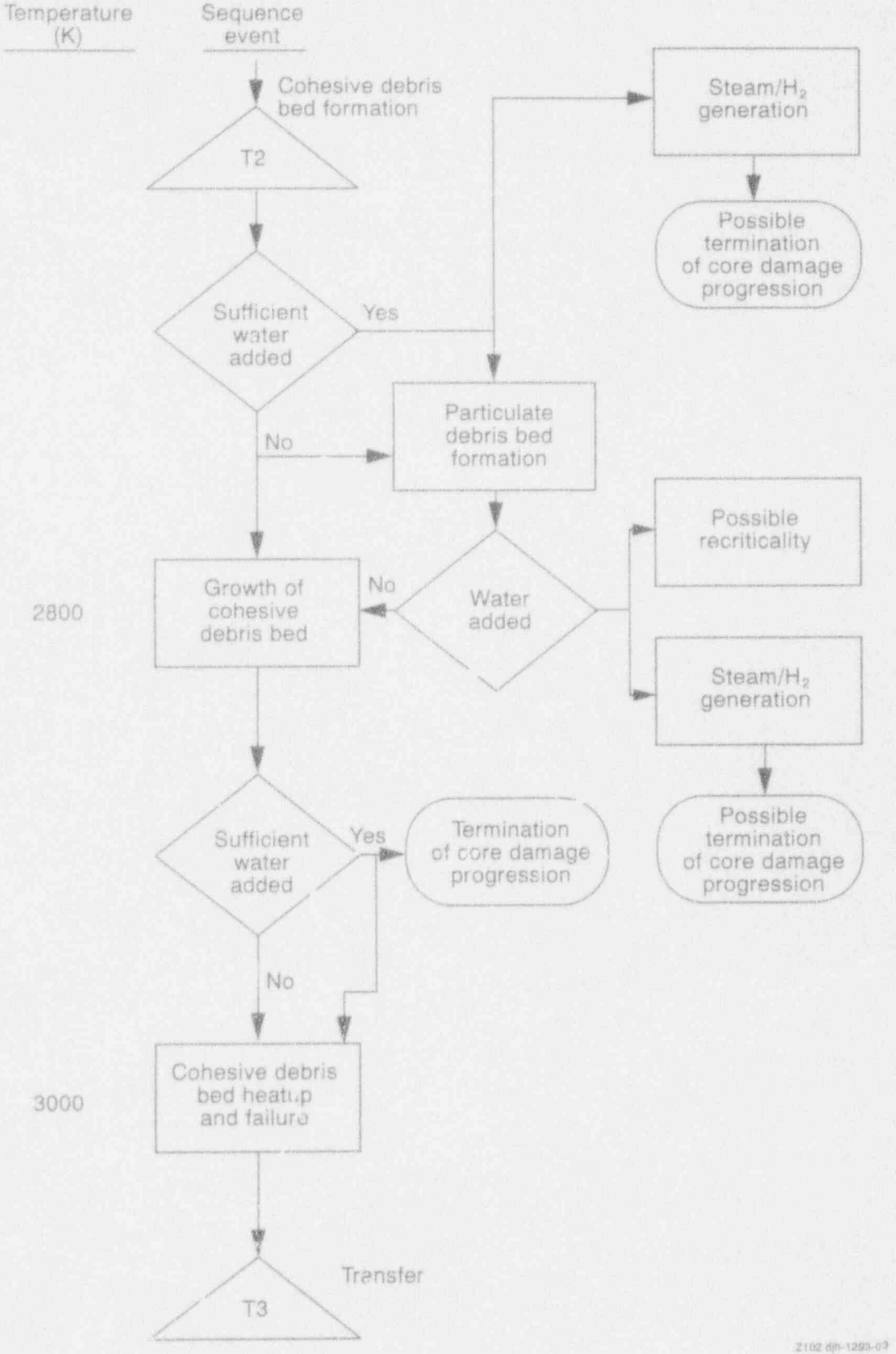


**Figure 1.** (continued).

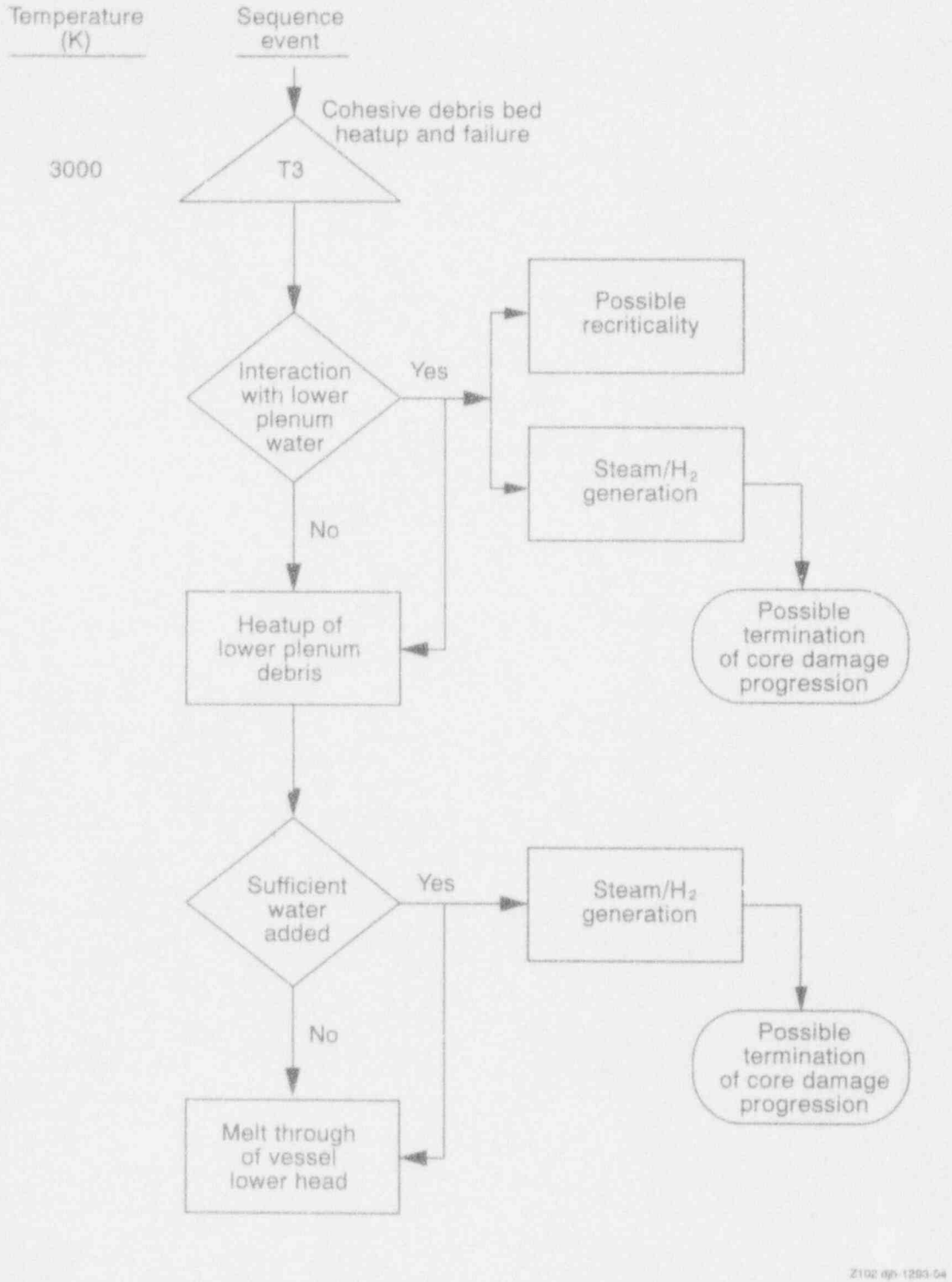


Z192 dpi-1293-04

**Figure 1.** (continued).

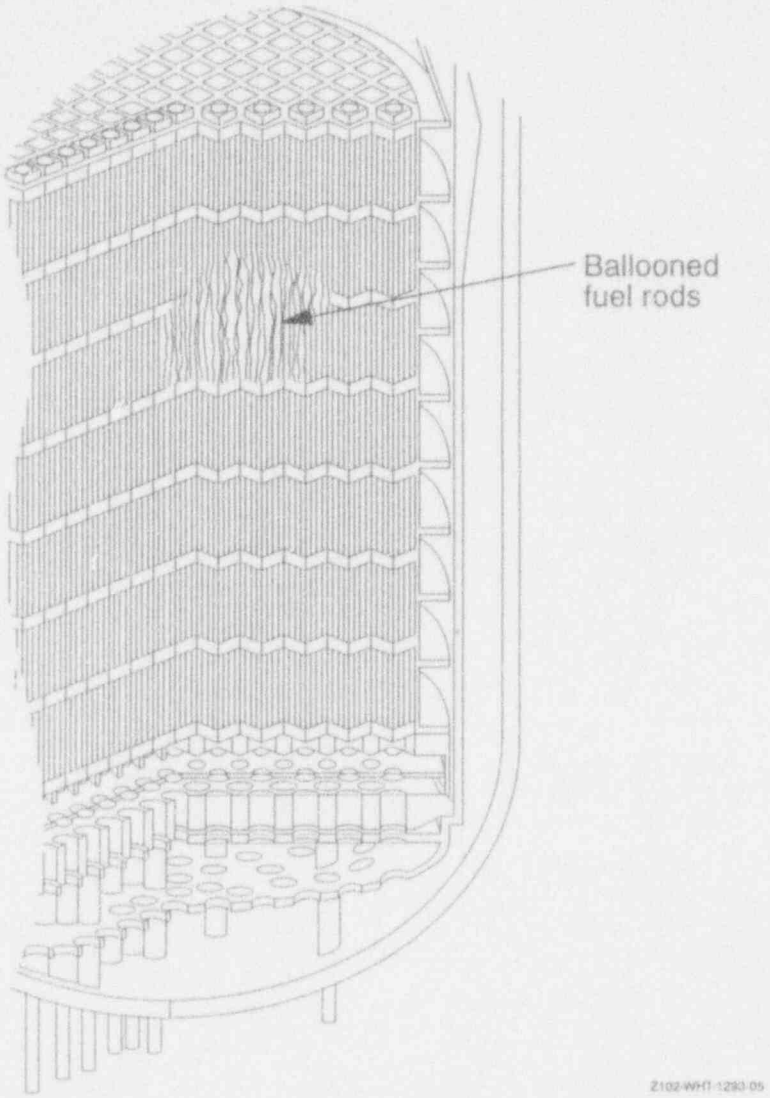


**Figure 2.** Fuel rod ballooning and failure around 1100 K in the central part of the core.

degradation. However, complete blockage of the core is unlikely. At this stage, sufficient water to thecore can terminate further core heatup. We estimate the required rate of water flow through the core in Section 5.

The next stage of core degradation, beginning at approximately 1500 K, is the rapid oxidation of the zircaloy cladding of the fuel rods by steam. In the process, hydrogen is produced and a substantial amount of heat is released. For small increases in temperature, the oxidation rate increases exponentially. Since the oxidation of the zircaloy cladding by steam is exothermic, the oxidation is autocatalytic in character. The rate of oxidation increases with temperature, which is increased by the energy release from the oxidation, so the process feeds on itself. At approximately 1500 K, the rate of energy release from the oxidation of the cladding exceeds that from decay heat. At higher temperatures, it can be several orders of magnitude higher than the power from decay heat, unless the oxidation rate is limited by the supply of zircaloy or steam.

During the rapid oxidation stage in the absence of emergency coolant injection, the flow of steam through the core may be insufficient to supply all the steam that can be consumed in the oxidation of the zircaloy in the core. In small-scale experiments that simulate the boiloff of water inventory in the core, such as the PBF Severe Fuel Damage (SFD) experiments,[12,13] the steam supply through the experimental fuel bundle completely converts to hydrogen when the bundle temperature exceeds approximately 1500 K. Although the

temperature of the fuel rods in the upper part of the bundle is over 1500 K, rapid oxidation does not take place because of the lack of steam in the upper part of the bundle is "steam starved." A similar restriction of oxidation in the upper part of the core from steam starvation is expected in a PWR experiencing a high-pressure boil-off.

If water is added to the core during the rapid oxidation stage, steam will be rapidly generated because of the high rate of heat transfer from the fuel rods to the incoming water, but the rate of hydrogen generation will depend on the temperature response of the core. In the lower region of the core where fuel rods are quenched, hydrogen generation will stop. However, in the upper part of the core where the oxidation of zircaloy may have been steam-starved before water is added, the addition of water to the core would provide the steam necessary for oxidation. If the sudden revival of oxidation in the upper part of the core generates energy at a rate higher than the rate of heat transfer to the water, the temperature of the rods will escalate. This could happen when the temperature of the rods is high, when the oxide layer on the surface of the cladding is thin, or when the water causes the oxide shell to break up, exposing unoxidized zircaloy. All of these conditions contribute to high oxidation rates.[14]

If water is added to the core at a sufficiently rapid rate during the early phase of oxidation when the core temperature is less than 1500 K, the core can be quenched and core damage progress will cease. However, if the addition of water is slow or intermittent, or if the core is not completely covered with water, the core will heat up to the next stage of degradation. We estimate the required rate of water flow through the core to stop further core damage in Section 5.

When the temperature in the core reaches about 1700 K, the stainless steel cladding of the control rods melts. The control material, Ag-In-Cd in the case of most PWRs, will already be molten at this time (the melting point is approximately 1100 K) and will be released upon failure of the control rod cladding. In the case of BWRs, the control blades may fail at a slightly lower temperature (approximately 1600 K) owing to the interaction of the control material ($B_4C$) with the stainless steel cladding.[15] After its release from the rods, the control material flows to the lower part of the core where the temperature is low, and it solidifies in the space between the fuel rods. The solidified control material may become part of a lower crust in the subsequent development of a cohesive debris bed in the core,[16] or it may eventually relocate to the lower plenum if the temperatures in the lower core region become high.

Besides producing steam and hydrogen, adding water to the core after loss of the control material in the upper part of the core may also lead to recriticality if the incoming water contains little or no boron to absorb neutrons. To determine the specific conditions that would lead to recriticality, one would need analyze the combined thermal-hydraulic response, core damage states, and neutronic behavior.

With the onset of rapid oxidation of zircaloy, the temperature in the core can escalate to the melting point of zircaloy (approximately 2150 K) in a few minutes. The melting of the zircaloy cladding usually does not immediately lead to a downward flow of the zircaloy if it is constrained by a protective layer of zirconium dioxide from earlier oxidation of the zircaloy. If the molten zircaloy stays in place, it will start to dissolve some $UO_2$ fuel.[17] Upon cladding breach, the molten zircaloy and some dissolved $UO_2$ flow downward and freeze in the cooler, lower region of the core. Together with the solidified control material from earlier downflows, the relocated zircaloy and $UO_2$ form the lower crust of a developing cohesive debris bed. Because of limited heat losses, the molten material relocated to the top of the crust eventually stops freezing. Figure 3 presents the conceptual state of the core at this stage.

The next stage of development of the lower crust is its radial growth from the center toward the periphery of the core. Because of decreasing temperatures near the periphery (from slower heatup because of decreasing power densities and enhanced steam cooling), relocating materials freeze at higher elevations toward the periphery of the core. Thus, the lower crust is expected to

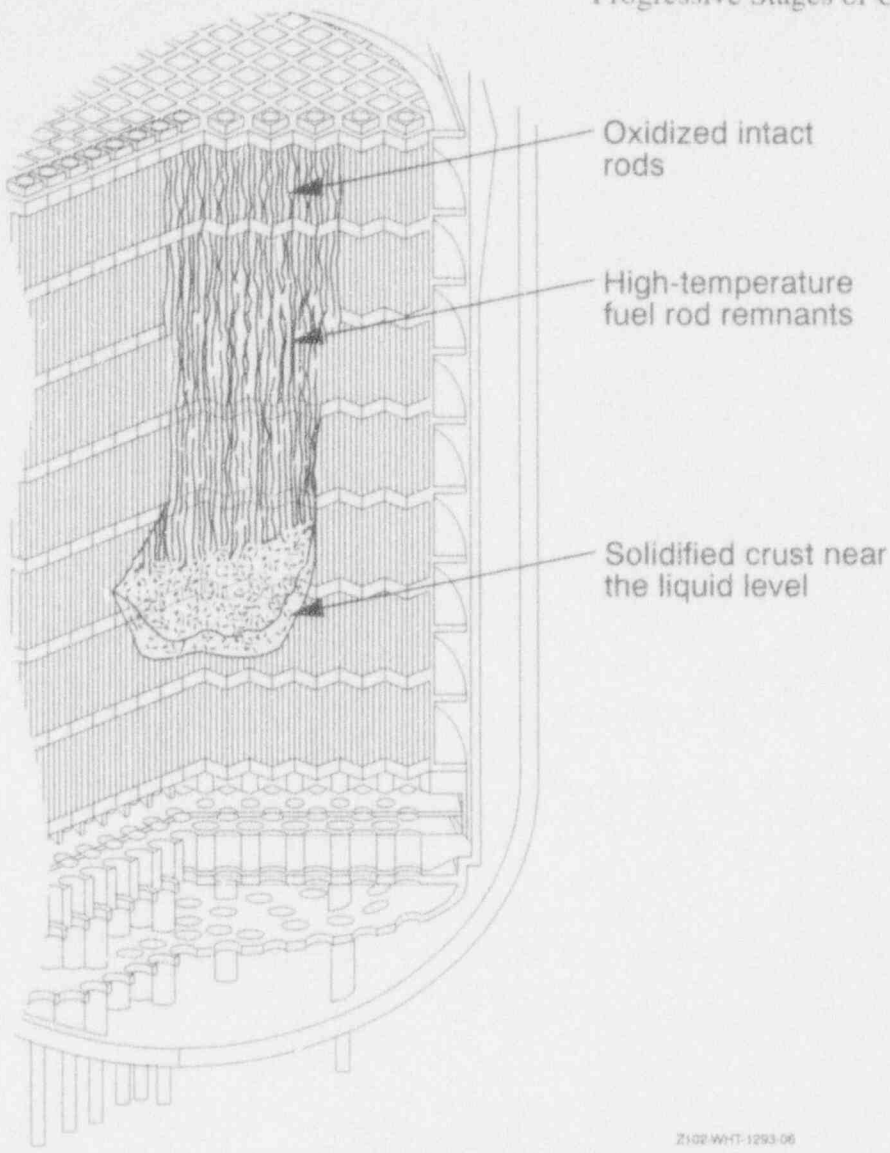


**Figure 3.** Formation of the lower crust from relocated control material.

take the shape of a crucible. The materia' ,· ported by the crust will be a pool of molten m... rial and submerged rod stubs in the process of melting. As the submerged rod stubs melt away, mechanical support of rod stubs above the molten pool is lost, and further slumping of the rod stubs into the pool occurs. Some fuel rod remnants are expected to be submerged in the pool as long as some rod remnants stand above the pool. Figure 4 illustrates the state of the core at this stage of core damage progression.

If water is added to the core before complete slumping of fuel rod remnants into the molten pool occurs, the top surface of the molten pool may freeze to form an upper crust (Figure 5) and the fuel rod remnants above that surface may be shattered to form a particulate bed, as is believed to have happened during the TMI-2 coolant pump transient.[17,18] If the temperature of the peripheral fuel rods is still below the temperature for rapid oxidation of zircaloy by steam, they will be quenched by the incoming water.[19] Since the average temperature of the core at this stage of core heatup is fairly high, copious production of steam is expected. As a result, the pressure of primary system will rise. The generation of hydrogen will also increase as water is added to the core. It is estimated that, in the TMI-2 accident, one-third of the hydrogen generated during the entire accident was produced within a few minutes after water was delivered to the core at 174 min into the accident by a reactor coolant

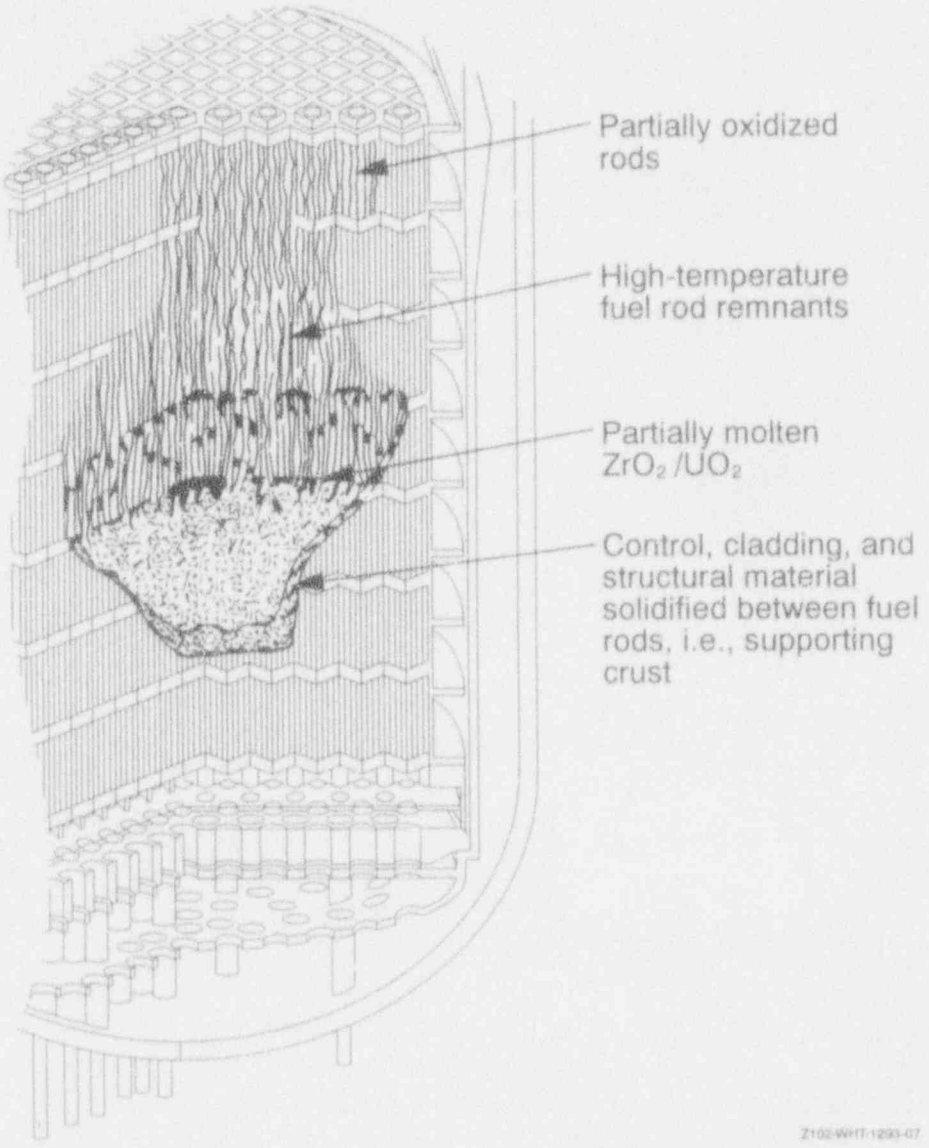


**Figure 4.** Growth of a cohesive debris bed in the central part of the core.

pump.[20,21] Similarly, high rates of hydrogen generation were also observed in the PBF SFD-ST[22] and the LOFT LP-FP-2[23] tests when the test bundles were being reflooded after liquefaction of the cladding and fuel occurred.

If no water is added to the core during the growth of the cohesive debris bed, the entire upper part of the core will eventually sink into the molten pool in the center of the core. Before its complete immersion into the molten pool, the upper part of the core may retain a rod-like geometry, or, alternatively, it may disintegrate into small particles even without the addition of water. The possibility of the latter scenario has been demonstrated in the PBF SFD 1-4 experiment. A particulate debris bed was formed in the upper part of the SFD 1-4 test bundle, though the bundle was never reflooded by water.[13] The formation of a particulate debris bed in this experiment was due to the shattering of irradiated fuel pellets after the cladding had relocated to the lower part of the core.

If the particulate bed is shallow or composed of relatively large particles, the continued adding of water will quench the particulate bed. In the process, steam and hydrogen will be generated. However, because of limited water ingress into the particulate debris bed, the steam and hydrogen generation rate will be quite low and

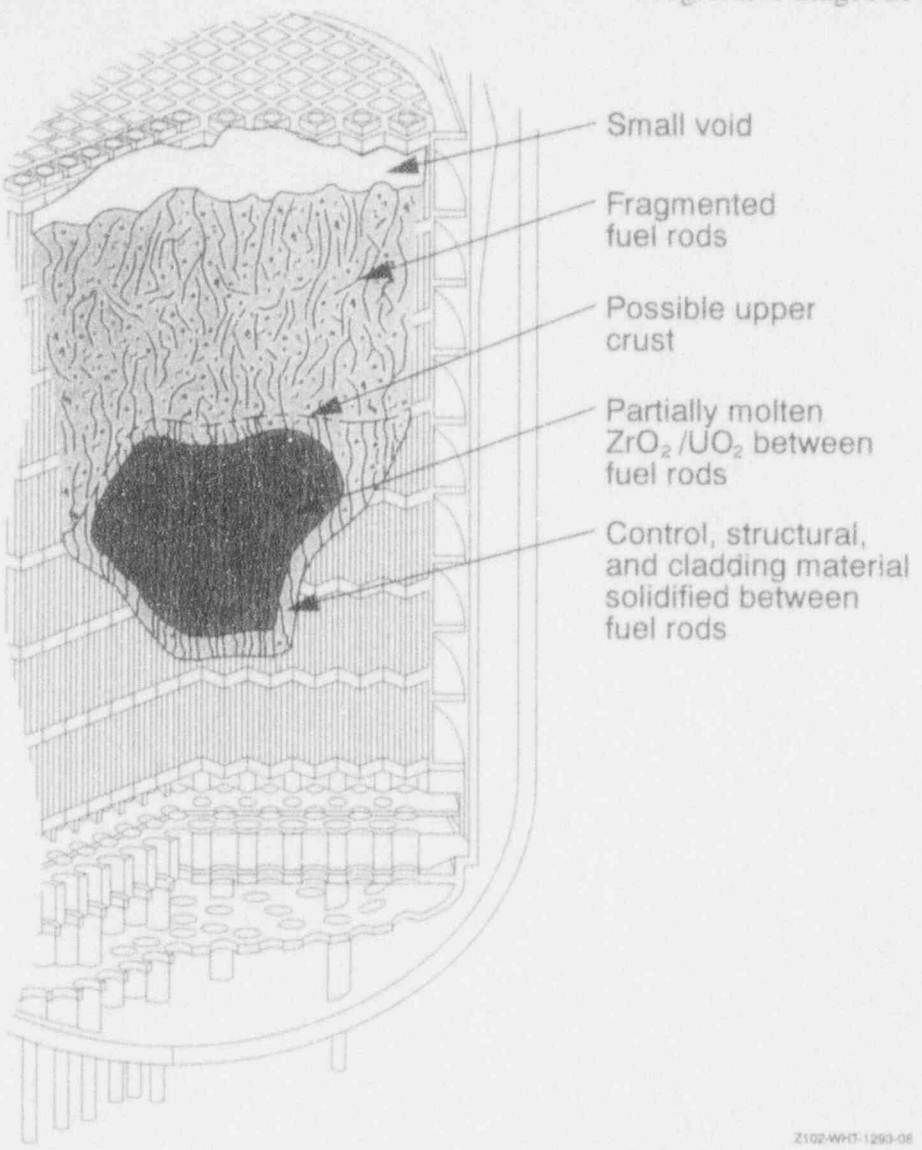


**Figure 5.** Formation of a particulate debris bed on top of the cohesive bed.

independent of the rate of water added to the core, as long as water covers the debris bed. Because control material would have relocated to the lower part of the core at the time of particulate debris bed formation, recriticality may be a concern if unborated water penetrates the debris bed.

If the particulate bed of shattered fuel pellets in the upper part of the core is sufficiently deep or is composed of sufficiently small particles, water can be prevented from penetrating the bed. This is usually referred to as dryout of the particulate bed. The dryout of particulate beds have been studied extensively, both theoretically and experimentally.[24–28] (The conditions for dryout are discussed in Appendix B). After dryout, cooling of the particulate bed by natural convection of steam inside the bed is generally inefficient and gradual heatup of the bed will eventually lead to melting of the particles,[29] which will add to the growth of the cohesive debris bed.

If the cohesive bed is radially thin and small, adding water may gradually cool the bed and the progress of core damage may be stopped. However, a thin and small cohesive bed could mean that a large fraction of core material remains outside of the cohesive bed and may have formed a deep particulate bed that is beyond the dryout limit. Such a particulate bed resting on the cohesive bed shields water from the upper surface of the cohesive bed and prevents it from being cooled.

If the cohesive bed is large, its subsequent evolution depends little on water addition.[31] Its interior will continue to heat up and melt until only a thin crust remains, regardless of water addition (Figure 6). Failure of the crust, either mechanically or by melt-through, can lead to the relocation of the enclosed molten core material to the lower plenum of the vessel (Figure 7). The relocated amount depends on the amount of molten material in the core and on the location of the failure point on the crust.

For most severe accidents, there is generally a pool of water in the lower plenum of the vessel at the time of core relocation. Release of molten core material into water invariably generates large amounts of steam. In addition, if the molten stream of core material breaks up rapidly in water, a steam explosion is also possible,[31] though it is not likely at high pressures. At the time of relocation, any unoxidized zirconium in the molten material can be oxidized by steam to release energy and produce hydrogen. Recriticality could also be a problem if the control material is left behind in the core and the relocated material breaks up in unborated water in the lower plenum. However, it is extremely unlikely that the molten core material would attain the proper geometry to reach criticality.

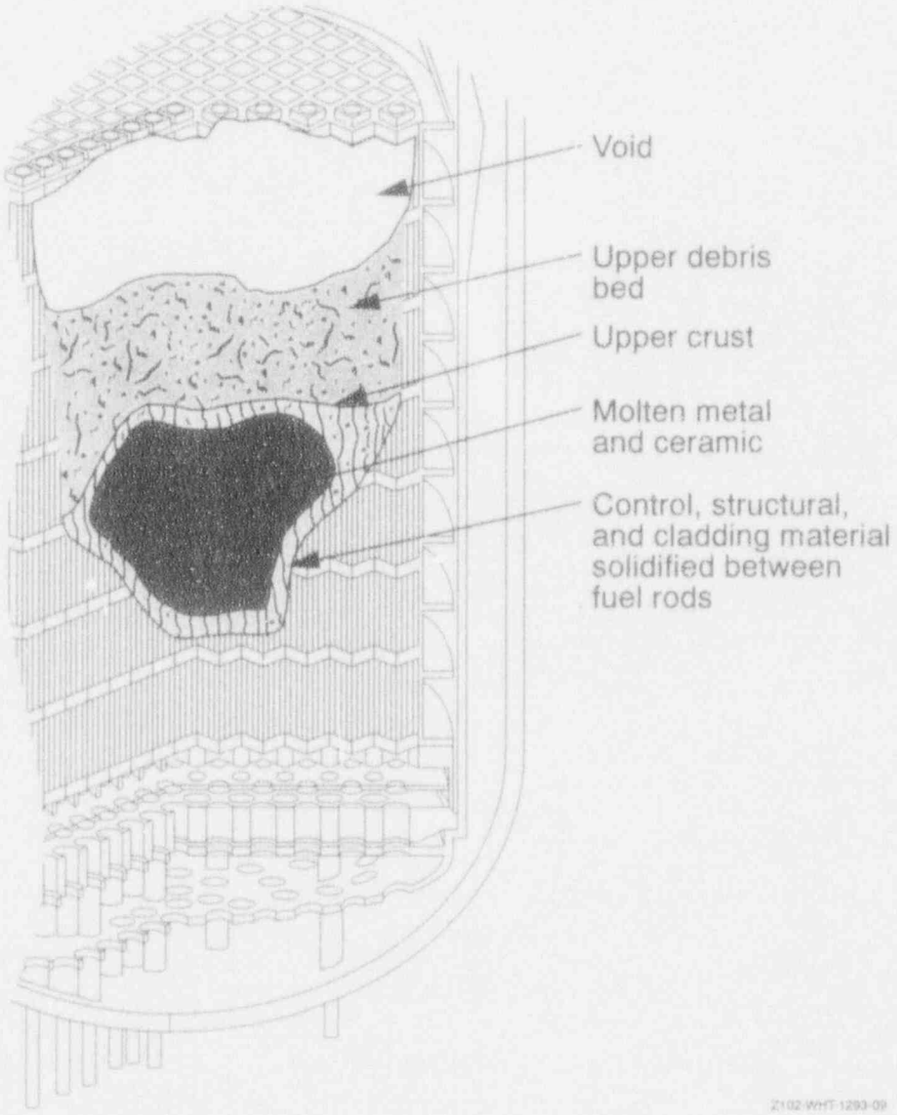


**Figure 6.** Melting of the interior of a cohesive debris bed, with corresponding thinning of its crust.

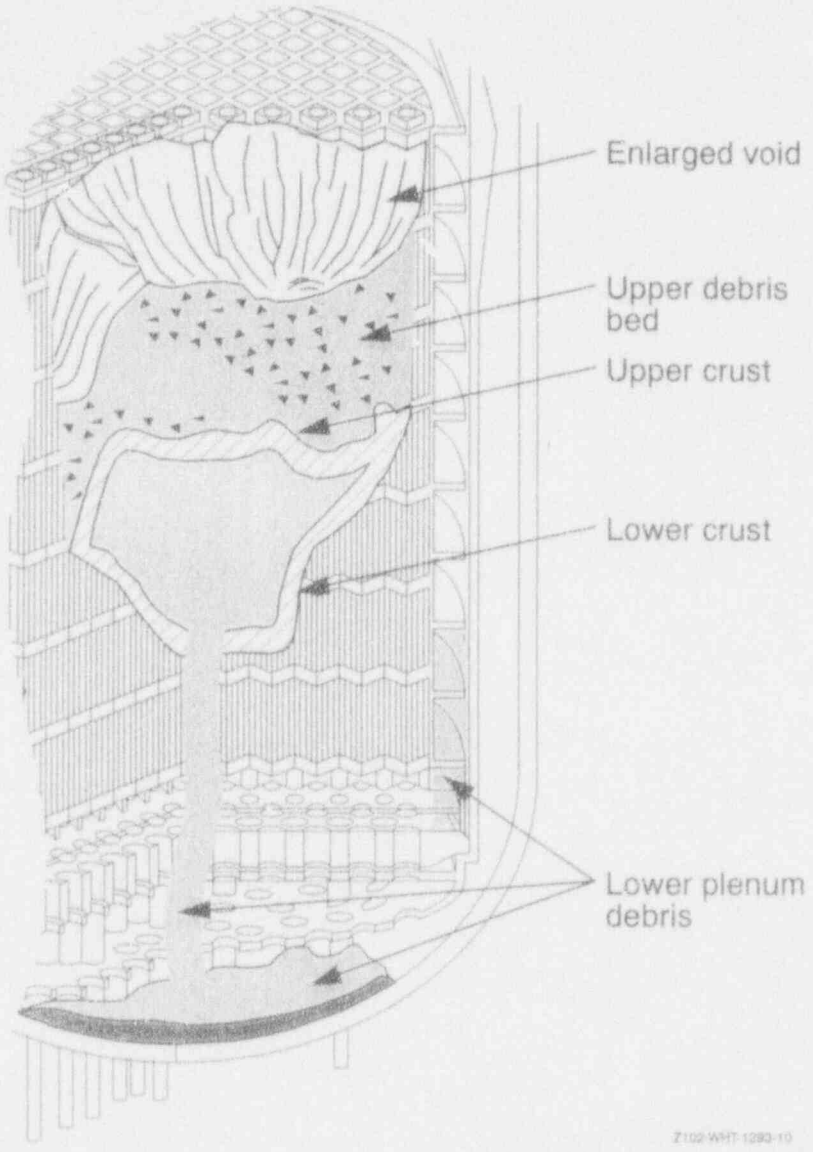


**Figure 7.** Crust failure and relocation of core material to the lower plenum.

In the TMI-2 accident, the progress of core damage was essentially terminated with the relocation of approximately 20 metric tons of core material into the lower plenum of the vessel. The material partially broke up to form a particulate bed and was quenched by the water in the lower plenum. The increase in pressure of the primary system at the time of relocation (224 min into the accident) indicates that both hydrogen and steam were produced for a short period of time after the relocation. There is no evidence that the reactor ever became critical again. For postulated accident scenarios in general, however, relocation of core materials to the lower plenum is not limited to 20 metric tons. Calculations show that, for sufficiently large amounts of core material in consolidated form, the presence of water in the lower plenum cannot prevent the heatup of the material.[32,33] In addition, the inner surface of the vessel may be ablated by the relocating core material, and the vessel is likely to fail from creep rupture of the vessel lower head.[34] The failure mode of the reactor pressure vessel and the subsequent accident progression to the exterior of the vessel is not part of the scope of the present report.

## 3.2 Low-Pressure Sequence

The sequence of core damage stages in a low-pressure environment is typical of large or

intermediate loss-of-coolant accidents or other sequences where the system depressurizes quickly. Core uncovery that results in substantial core damage will likely still be typical of a slow boil-off because the accumulator safety injection system should keep the core relatively cool until the inventory is depleted or until the system pressure is sufficiently high to permanently terminate injection. Many of the phenomena are similar in the high- and low-system-pressure environments, so only differences between the two need be discussed. These differences include cladding ballooning behavior, control rod rupture, and steam explosions. One difference not explicit in these states but important in later calculations is that the total injection capacity for the low pressure case includes both the high- and low-system-pressure emergency core coolant injection systems.

**3.2.1 Cladding Ballooning.** The scenarios for ballooning and bursting of fuel rod cladding is different for accidents at high and low system pressures. In the high-system-pressure environment, the differential pressure between the fuel-clauding gap and the system is small, so the cladding undergoes substantial ballooning before it ruptures at an elevated temperature (about 1250 K or higher). In a low-system-pressure environment, the differential pressure is high, so the cladding experiences little ballooning before it violently bursts. Negligible circumferential expansion of the cladding prior to bursting is expected, so flow restriction is not an issue.

While ballooning in a low-system-pressure environment is not expected to produce significant flow restrictions, as in the high system pressure case, bursting at low system pressure presents a different kind of problem. In the high-system-pressure environment, bursting of the cladding is not expected to move the fuel pellets because of low differential pressure between the inside and the outside of the fuel rods. With a low system pressure, bursting is violent because at the instant of bursting the gas inside the fuel rods, which is at a much higher pressure than the system, causes the pellet adjacent to the bursting site to slam toward the opening. Since fuel pellets are highly fragmented after a brief period of reactor operation, the pellets near the bursting site will be expelled from the fuel rod at the instant of bursting of the cladding. However, the remainder of the pellets in the rod are likely to be unaffected. Approximately two of the three hundred pellets stacked in the fuel rod may be immediately expelled, settling on the lower core support plate as relatively cool shards and fragments of fractured fuel. This does not constitute fuel relocation in the TMI-2 sense, but the displaced mass is still significant. Two-thirds of one percent of the core corresponds to a fuel mass of several hundred kilograms.

**3.2.2 Control Rod Failure.** When control rods fail, the time to failure and the distribution of control materials in the low-system-pressure environment will be quite different than in the high-pressure case. When the control rod cladding fails in a high-system-pressure environment, the control materials slump to the bottom of the core. In a low-system-pressure environment, control rod failure occurs much sooner after reactor scram. Were the cladding to fail, the control materials, driven by the cadmium pressure, would spray from the ruptured rods onto adjacent rods. If the molten control material sticks to the fuel rods, the timing of material relocation and the spatial distribution of relocated and refrozen material may be altered, which can affect the formation of the lower crust for latter core damage states.

**3.2.3 Steam Explosions.** When molten core materials come in contact with water at system pressures lower than about 5 MPa, steam explosions are more likely than at higher pressures. The mechanics of steam explosions can be partitioned into four stages: (a) quiescent mixing of fuel and coolant, (b) triggering of the explosion, (c) escalation and propagation of the explosion, and (d) vapor expansion and work production.[35] It is the mechanics of triggering that makes steam explosions improbable under high-pressure conditions and a major concern under low-pressure conditions. In the fuel-coolant interaction prior to triggering a steam explosion, a vapor film exists between molten fuel and the coolant. This film is susceptible to hydrodynamic instabilities, which may be initiated by a number of different external

sources. The result of the instabilities is local film collapse, which permits coolant jets to impinge on the molten surface. Coolant then penetrates into the molten mass and, as the coolant turns to vapor and expands, it induces breakup of the melt. Under high system pressures, however, the vapor film is substantially more resistant to collapse. Although no experiments have been conducted at a pressure of about 5 MPa, an extrapolation of the results of small-scale experiments suggests that an external pulse of about 14 MPa would be required to trigger an explosion at this pressure. At pressure of a few atmospheres, on the other hand, pressure pulses of a few atmospheres may be sufficient to trigger an explosion. External perturbations to system pressures of this order may occur from a number of different sources so that, at low pressures, steam explosion becomes an issue whenever coolant and molten core materials come into contact. With respect to the sequence of core damage states, the issue of steam explosion appears when molten control materials are released from the control rods, when the zircaloy melts and liquefies the fuel, and when molten materials are released from the cohesive debris bed toward lower elevations in the reactor vessel.

# 4. INSTRUMENT RESPONSE DURING CORE DAMAGE AND WATER ADDITION

Recognizing the capabilities and limitations of the plant instrumentation is crucial in understanding the state of the core during an accident, particularly when water is added. In this section we describe the types of instrumentation that have the capability to identify the status of the core during a severe accident, we discuss how this instrumentation could be used to determine the stages of core degradation (see Figure 1), and we discuss the effects of adding water to the system. We describe the instrumentation in general terms, but recognize that the number of instruments available, installation locations, and methods of installation can vary from plant to plant. For each stage in the core damage sequence, we discuss potential instrument response and correlate this response with other instrument responses.

## 4.1 Instrumentation

From the perspective of accident management personnel, there are three main types of measurements available for monitoring the state of the core: water level, temperature, and pressure. There are also other measurements that could indirectly support a determination of core conditions, for example, source range power measurements as an indication of core liquid level. A brief description of each of these types of measurements follows.

**4.1.1 Water Level Measurements.** Reactor vessel water level is measured using one of two different types of systems. One system uses heated junction thermocouples located at five elevations in the upper plenum to indicate when the water level passes certain points in the upper plenum, including a position near the top of the core. This measurement does not extend into the core region and, therefore, does not provide any information on the water level in the core or lower plenum regions. If the core has uncovered and reached high temperatures, the performance of the heated junction thermocouple may be degraded and their capability to accurately indicate water level may be compromised during core recovery. However, they should indicate the presence of coolant in the upper plenum, which would provide evidence that water was reaching the core region.

The second system uses sensing lines at the top of the vessel and the hot legs in conjunction with a sensing line at the bottom of the vessel to provide inferred water level measurements based on differential pressure. Two separate measurements of level are made: one from the hot leg to the bottom of the vessel, the other from the top of the vessel to the bottom of the vessel. Both of these measurements would provide information on the approach to core uncovery as well as an indication of the level of water in the core and lower plenum regions.

System conditions must be taken into account when using differential pressure for measuring water level in the vessel. For severe accidents that occur over long periods of time and characterized by a slow core boiloff, the vessel flows are low and do not contribute greatly to overall pressure drop. In this situation, the measured differential pressure can provide accurate estimates of the water level. However, in severe accidents where transient and two-phase-flow conditions are present, the indicated water level is much less accurate because of uncertainties in frictional pressure losses.

Pressurizer level could provide an early indication of mass depletion in the RCS if there is not water leaking from the upper regions of the pressurizer (either through a break or a failed relief valve). This measurement could be used to project core uncovery time. However, there would be large uncertainties in this time for accidents where inventory is decreasing at a slow rate, because the pressurized is at a much higher elevation than the core, and there is a significant amount of inventory that must be depleted between the time that the pressurizer empties and the core uncovers.

**4.1.2 Temperature Measurements.** Understanding the core temperature conditions is an

important contributor in determining the state of the core during severe accidents. Two measurements are used in PWRs as an indication of core temperature: core exit thermocouples (CETs) and hot-leg resistance temperature devices (RTDs). Both of these measurements are considered to be indirect measurements of core temperature because there are situations that could occur when these measurements would not accurately indicate core temperature.

Core exit temperature measurements are obtained from chromel-alumel thermocouples located in the upper core support plate. The thermocouple junctions are mounted horizontally in flow holes on the upper core support plate about six to eight inches above the top of about 30 to 40 percent of the fuel bundles. As this distance is about an assembly width, the thermocouples provide a representative value of the outlet temperature of the fluid flowing out of the individual assemblies. In plants designed by Westinghouse and Combustion Engineering, the thermocouples enter through the top of the reactor vessel. In plants designed by Babcock and Wilcox, the thermocouples enter through the bottom of the reactor vessel and are routed through instrument tubes that pass through the core region. The routing of these thermocouples through the core exposes them to high temperatures during severe accidents, which can affect their accuracy.

These sensors are qualified to 1533 K, though the temperature uncertainty has the potential to increase significantly above about 1470 K. At temperatures exceeding 1670 K, temperature errors may be large, and the trends of the indicated temperatures may also be unreliable. (For example, the indicated temperature may be relatively flat while the actual temperature continues to climb.) Recognizing these limits, the sensors can provide useful information during the early stages of core degradation, but will likely be unreliable in later stages.

RTDs contain precision temperature sensing devices made of platinum wire that undergo a change in resistance when the temperature changes. These assemblies are mounted in thermowells installed in the hot-leg pipes. The time response of the RTDs is affected by the mating between the elements and the cavity in the thermowell and by the thickness of the thermowell walls. The range of the hot leg RTDs is generally specified as 644 k (700°F), which is substantially below the upper limit that would be needed for the latter stages of severe accidents. However, the range could be increased significantly (up to about 1200 K) to provide additional information during severe accidents.

The hot-leg RTDs would provide an indication of core temperature but would significantly lag the time-temperature response of the core. Major contributors to the lag would be heat transfer to the upper plenum and hot-leg structures, which would cool or heat the effluent from the core, and the transit time of the fluid. The transit time would vary during a severe accident and could be significantly different for different types of severe accidents. These restrictions on performance must be considered when relying on hot-leg RTDs to indicate core temperatures.

**4.1.3 RCS Pressure Measurements.** Pressure sensors exist at several locations in the primary cooling system. Measurements may be taken at the hot-leg outlets and in the pressurizer. The sensors at the hot-leg outlets provide absolute pressure measurements with a very short response time and have a range of zero to 20.7 MPa. Low pressures are read from a narrow-range scale (zero to 4.1 MPa) and are accurate down to approximately 1.5 MPa. The uncertainty in the measurement increases rapidly below this pressure level, however, so that there can be little confidence in an absolute measurement on the order of an atmosphere. Four sensors providing absolute measurement of pressure also exist in the pressurizer. These sensors operate over a more restricted range (11.7 to 17.2 MPa) and also have a very short response time.

**4.1.4 Other Measurements.** Though not originally designed for this purpose, measurements other than those discussed above can contribute valuable information for understanding the progression of core damage. The following measurements are discussed: source range monitors,

self-powered neutron detectors (SPNDs), plant radiation measurements, hydrogen measurements, containment pressure, and containment temperature.

Ex-vessel source range monitors are used during plant startup to measure power by detecting neutrons. During the TMI-2 accident, the source range detectors exhibited an increased signal output when the core uncovered and when the core relocated to the lower plenum.[36] Although these ex-core detectors may be useful for substantiating information from instrumentation installed in the RCS, caution should be used in relying on them as the primary source of information. Because the detectors are located outside the vessel, it is not possible to determine whether changes in their signals result from changes in water level or core configuration in the core region, changes in water level in the downcomer region, or simultaneous changes in both regions. Use of the source range detectors to understand degraded core conditions for a plant would require a study of such plant-specific details as location of the detectors, their range, their sensitivity to a wide range of core and downcomer water levels and core material distributions, and correlation of their outputs for various detector locations.

SPNDs are fission source chambers used in reactors to obtain estimates of thermal neutron flux. Although the detectors are intended to provide measurements during full-power operation, they can be used during accidents to detect changes in neutron fluxes at signal levels a few times above background noise when the most sensitive range is selected.[37,38] A means to display the SPND output (current) would likely be needed to adequately identify the small changes indicative of changes in vessel water level and relocation of core material.

SPNDs in PWRs are generally configured in one of two ways. In some plants the SPNDs are built into instrument thimbles at fixed axial locations and are installed at various radial locations in the core so they can be used to provide both radial and axial neutron flux profiles. In other plants the SPNDs are part of a system that allows them to be stored outside of the reactor vessel and inserted axially into specially designed core instrument thimbles located throughout the core. There is, therefore, the possibility that these movable SPND could be inserted into the core during a severe accident to monitor degraded core conditions in local regions and map the extent of core damage. However, because the specially designed core instrument thimbles form part of the pressure boundary for the RCS, their failure when the movable SPND system is in use would provide a direct path for fluid, fission products, and possibly core material to escape into the containment. The capability of this system to operate under severe accident conditions and the possible negative consequences from the use of the system would require further evaluation before it is considered an acceptable tool for appraising the condition of a degraded core. Further evaluation would require additional plant-specific information and is beyond the scope of this report.

Radiation monitors or radiation measurements using sampling systems could be used to indicate when appreciable fission products have been released from the fuel. These systems would need to have sufficient sensitivity that accident management personnel could distinguish between fission products present in the coolant under normal operating conditions and the additional fission products released during core degradation. Radiation monitors on RCS letdown systems and sampling systems for the RCS coolant could provide important information if the RCS leak rates are small. For large RCS leak rates, more global radiation measurements would likely provide early indications of core damage.

Hydrogen monitors or measurements of hydrogen concentration from sampling systems could be used to estimate the time when core temperatures were high enough to initiate cladding oxidation. Time delays in transporting the hydrogen to the detectors and in obtaining samples and analyses would need to be included in the time estimates.

Containment pressure and temperature would provide information that could help distinguish some of the latter stages of core degradation.

High containment pressures and temperatures could be used in conjunction with other measurements to indicate reactor vessel lower head failure.

Other measurements that support severe accident management may be available from plant process instrumentation. The types of information available and how they would be used would depend on systems and conditions that are plant-specific. For example, in some plants an estimate of cavity temperature may be available from heating and ventilation system temperature measurements. The capability to exploit these temperature measurements for a wide spectrum of severe accident conditions would depend on such variables as the location of the measurements, their capability to survive harsh environments, and the availability of support systems such as site battery electrical power. Because of the plant-specific nature of these systems, we do not included them in our following discussion.

## 4.2 Distinguishing Stages of Core Degradation

An understanding of core conditions would aid accident management personnel in determining which accident management strategies could be most effective and in assessing the effectiveness of them. We examined the capability of instrumentation to identify the stages of core damage for PWRs, as shown in Figure 1. Table 3 summarizes the expected instrument responses, and the following discussion additionally explains the core damage stages. We discuss temperature, pressure, and level measurements and other selected measurements that may be useful for identifying the state of the core and the effects of adding water.

### 4.2.1 Accident Initiation to Core Uncovery.

***Temperature.*** Core exit thermocouples (CETs) would generally be ineffective in identifying the approach to core uncovery prior to fuel rod heat up. RTDs would also be relatively ineffective but may indicate the small amount of superheat that results from a loss of inventory in the hot leg for sequences where inventory depletion is not rapid and the pressure is declining. A sustained measurement of subcooling from the RTDs or the CETs should indicate the effectiveness of adding water during this stage of accident progress.

***Pressure.*** Pressure response could assist in identifying some accident sequences, but would not be effective in determining whether core uncovery is imminent or has occurred. Pressure history, however, could be correlated with other measurement responses to indicate that core uncovery is likely. Pressure measurements would assist in identifying systems with the capability to inject water when there are failures in ECC systems. An increase in pressure following water addition should indicate effective core cooling for sequences where inventory loss is slow, whereas negligible RCS or containment pressure increases would indicate large system breaks.

***Level.*** If the sequence is proceeding slowly and the primary coolant pumps are not running, the heated junction thermocouple-based system would provide an accurate water level measurement and indicate the approach to core uncovery. The differential pressure-based system would track the water level in the upper plenum, the core, and the lower plenum. Both systems may be inaccurate for rapidly progressing transients or when the primary coolant pumps are running. The pressurizer level would early indicate RCS inventory depletion. It could be used to project time to core uncovery as long as the possibility of large uncertainties is recognized. Raising water level measurements would indicate effective water addition.

***Other Measurements.*** Source range monitor output and SPND output may not correlate well with the approach to core uncovery because a lowering of the upper plenum water level may result in only small changes in their output. Reductions in RCS pump power or pump current measurements could be used to identify a reduction in RCS inventory if the pumps continue to run during this portion of an accident.

**Table 3.** Possible instrument response for core damage stages.

| Core damage stage (temperature range) | Temperature instruments | RCS pressure instruments | Level instruments | Other instruments |
|---|---|---|---|---|
| Accident initiation to core uncovery | CETs: ineffective in indicating the approach to core uncovery.<br><br>RTDs: may indicate slight superheat after hot leg empties, depending on the RCS pressure response. | Ineffective in indicating the approach to core uncovery but necessary to indicate which ECC systems may be effectively used. | Heated TC: will indicate the approach to core uncovery if the RCS pumps are not running.<br><br>Vessel DP: will indicate the approach to core uncovery. | Subcooled monitor: not an accurate indicator of the approach to core uncovery. |
| Core uncovery to ballooning of fuel rod cladding (saturation to 1100 K) | CETs: a reasonable indicator of core uncovery. Would exceed saturation and could approach core fuel rod temperatures.<br><br>RTDs: should exceed saturation temperature but would be much less than fuel rod temperatures. | Ineffective in indicating core uncovery but necessary to indicate which ECC systems may be effectively used. An increase after water addition would indicate core cooling of some fuel rods. | Heated TC: will indicate core uncovery if RCS pumps are stopped. Would not indicate core level.<br><br>Vessel DP: will indicate core uncovery. Should track level in core and lower plenum. | Source Range Monitor: may indicate decrease in core level. Very low signal would require proper interpretation.<br><br>SPNDs: may indicate decrease in core level. Would require special interpretation. |
| Fuel rod cladding ballooning and rupture (1100 K to 1500 K) | CETs: could follow trends in fuel rod temperature. Relation to core temperature would depend on steam flow and droplet entrainment rates.<br><br>RTDs: would show superheat but would lag core temperatures and may reach upper range limit. | Ineffective in indicating core heat up but necessary to indicate which ECC systems may be effectively used. An increase after water addition would indicate core cooling of some fuel rods. | Heated TC: will indicate core is uncovered but not how far core damage has progressed.<br><br>Vessel DP: will indicate approximate level in core or lower plenum. | Source Range Monitor and SPNDs: may track changes in core level with proper interpretation.<br><br>Radiation Monitors: should indicate fuel rod gap release but there may be a large time delay, depending on instrument location and accident conditions. |

**Table 3.** (continued).

| Core damage stage (temperature range) | Temperature instruments | RCS pressure instruments | Level instruments | Other instruments |
|---|---|---|---|---|
| Early and late rapid zircaloy oxidation (1500 K to 2100 K) | CETs: should follow early trends in fuel rod temperature. Upper temperature range may be exceeded later (1644 K).<br><br>RTDs: would show superheat but would lag core temperatures and may reach upper range limit. | A large RCS pressure increase may occur when cladding oxidation is rapid and RCS leaks are small. It may be difficult to distinguish this increase from other accident progression pressure changes. Necessary to indicate which ECC systems may be effectively used. | Heated TC: will indicate core is uncovered but not how far core damage has progressed. Upper range may be exceeded. Junction relocation may occur.<br><br>Vessel DP: will indicate approximate level in core or lower plenum. Metallic relocation may block pressure tap during latter portions of this stage. | Source range monitor and SPNDs: may track changes in core level with proper interpretation.<br><br>Radiation monitors: should indicate radiation release but there may be a large time delay, depending on instrument location and accident conditions.<br><br>Hydrogen monitors: hydrogen may be detected indicating high core temperatures. |
| Debris bed formation (>2100 K depending on conditions) | CETs: failure would occur in high-temperature regions. CETs output may seem reasonable after failure as false junctions may form.<br><br>RTDs: temperatures would likely exceed their upper range. | Pressure changes will depend on the amount of cooling. If debris beds are not coolable, pressure changes could be small. May observe a large pressure increase when the core relocates. It may be difficult to distinguish from other accident-related pressure changes. | Level instruments would likely be failed but their failure may not be obvious. | Radiation monitors: should indicate radiation release but there may be a large time delay, depending on instrument location and accident conditions.<br><br>Hydrogen monitors: hydrogen from zircaloy oxidation would likely be measured but would not help distinguish this damage stage. |
| Lower head attack by molten core debris (>1700 K for metals, >2700 K for ceramics) | CETs: failure would occur in high-temperature regions. However, the output of the CETs may seem reasonable as false junctions could form.<br><br>RTDs: temperatures would likely exceed their upper range. | Pressure would not be effective in indicating lower head attack. A sharp reduction in pressure and a reading equal to containment pressure would indicate RCS boundary failure. It would be difficult to distinguish vessel and ex-vessel failures. | Level instruments would likely be failed but their failure may not be obvious. | Radiation monitors: should indicate radiation release but there may be a large time delay, depending on instrument location and accident conditions.<br><br>Hydrogen monitors: hydrogen from zircaloy oxidation would likely be measured but would not help distinguish this damage stage. |

### 4.2.2 Core Uncovery to Ballooning of Fuel Rod Cladding.

***Temperature.*** CETs would depart significantly from system saturation temperature and may approach 1100 K for some core conditions. Strong radial temperature differences will likely be indicated by the CETs. Hot Leg RTDs should be higher than saturation temperatures but significantly lower than core temperatures. A measurement of decreasing superheat by CETs and RTDs would signify energy removal from the core but should only be considered as indicative of core recovery when a continuing, long-term decrease is measured. Entrainment of fluid from the core or draining of pressurizer liquid may produce a short-term decrease in superheat while core temperatures remain high. CET- and RTD-measured temperatures would continue to rise if water addition was ineffective.

***Pressure.*** Pressure response would not distinguish this core damage stage from the previous one. It could be used to estimate when fuel rod ballooning conditions are reached if it is combined with a reliable indication of core temperature. A continued measurement of pressure would be important in the selection of ECC systems with the capability to deliver needed quantities of water. A sharp increase in RCS pressure following water addition should indicate effective core energy removal, but no RCS pressure increase would be experienced for large breaks. Containment pressure trends would be difficult to use in identifying this core damage stage.

***Level.*** Core level would be below the range of heated junction thermocouple-based systems. Differential pressure-based level measurements would indicate core and lower plenum levels if the transient is slow and the primary coolant pumps are not running. Long-term trends of increasing level would indicate effective water addition during this core damage stage.

***Other Measurements.*** Source range monitor and SPND outputs should correlate with vessel water level changes. Use of special signal conditioning and display equipment for the source range monitor and SPND signals may be necessary to ensure that changes in vessel water level will be observed. Accident management personnel may need training to properly interpret level changes from the signal trends.

### 4.2.3 Fuel Rod Cladding Ballooning and Rupture

***Temperature.*** CETs should follow the trends of core temperature, though entrained liquid may still be present at some radial locations and could cool the associated CETs. As a result, there may be large radial variations in indicated temperatures. RTDs will respond more slowly to rising core temperatures. Although their temperatures should be much lower than the CETs, it is likely that their upper range (672 K) will be exceeded. Effective water addition would be indicated by a long-term decrease in both CET and RTD temperatures.

***Pressure.*** Pressure response could not be used to distinguish this core damage stage from the previous one. A continued measurement of pressure would be important in the selection of ECC systems with the capability to deliver needed quantities of water. A sharp increase in RCS pressure following water addition should indicate effective core energy removal, but no RCS pressure increase would be experienced for large breaks. Containment pressure trends would be difficult to use in identifying this core damage stage.

***Level.*** Core level would be below the range of heated junction thermocouple-based systems. Differential pressure-based level measurements would indicate core and lower plenum levels if the transient is slow and the primary coolant pumps are not running. Long-term trends of increasing level would indicate effective water addition during this core damage stage.

***Other Measurements.*** Source range monitor and SPND outputs should correlate with vessel water level changes. There may be a need for special signal conditioning, displays, and operator training to ensure that the signals are properly interpreted. Plant radiation monitors would measure increased radiation levels following cladding rupture. The measured increase could be

delayed significantly from the actual rupture time, depending on the accident type and conditions and the monitor location. Radiation monitors would not provide reliable indications of the effectiveness of water addition.

### 4.2.4 Early and Late Rapid Zircaloy Oxidation

***Temperature.*** CET-measured temperatures should be high and should indicate a rapidly increasing temperature. If temperature history is plotted, a change in the rate of temperature increase may be obvious as oxidation begins. Errors in CET-measured temperatures will increase when core temperatures exceed 1450 K. Errors may be either positive or negative, depending on the routing of the CETs into the vessel (from the bottom through the lower plenum and core or from the top through the upper plenum) and on the magnitude of the temperature. The upper range (1644 K) of some CETs may be exceeded. There is potential for the CETs to provide inaccurate trend information (indicating near constant temperatures when core temperatures are rapidly increasing). RTDs may indicate a much higher rate of temperature increase. The RTD-measured temperatures would likely exceed their upper limit. The effects on core temperature of adding water could be difficult to determine because in the short term there is potential for increased oxidation, which would increase fuel rod temperatures.

***Pressure.*** If the system is closed or has a small break, the pressure should increase rapidly. Since there are other conditions that can cause a rapid pressure increase, this measurement would need to be correlated with other measurements. Pressure alone would not distinguish this core damage stage, but continued measurement of pressure would be important in selecting ECC systems with the capability to deliver needed quantities of water.

***Level.*** Core level would be below the range of heated junction thermocouple-based systems. There is the possibility that some heated thermocouples would form false junctions during this phase. This condition could result in erroneous readings if the core is cooled. Differential pressure-based level measurements may indicate core and lower plenum levels if the transient is slow and the primary coolant pumps are not running. However, metals may begin to relocate during the latter part of this core damage stage. This metal could cover or otherwise interfere with the pressure tap in the lower vessel, which would cause level errors. Level would not help to distinguish this core state from the previous one.

***Other Measurements.*** Source range monitor and SPND outputs should correlate with vessel water level changes if the level is still in the core region. The need for special conditioning and training for these measurements would apply. Plant radiation monitors would continue to measure increased radiation levels. The measured increase could be delayed significantly from the actual rupture time, depending on the accident type and conditions and the monitor location. Radiation monitors would not provide reliable indications of the effectiveness of adding water. Measurement of hydrogen by monitors or sampling stations would indicate that this core damage stage was occurring. There may be a time delay, depending on RCS leak rates, leak location, and measurement method and location.

### 4.2.5 Debris Bed Formation

***Temperature.*** CET temperature readings could have significant errors in both magnitude and trend. RTD measurements would not distinguish this core state from the previous state and would likely be outside their operating range. It is unlikely that the effects of adding water will be accurately indicated. Long-term temperature reductions measured by the CETs may not indicate adequate core cooling since false thermocouple junctions may have formed outside of the hottest regions (for plants where the CETs are routed through the core).

***Pressure.*** A sharp increase in pressure would likely occur as core material relocates to the lower plenum if water is present. The magnitude of the pressure increase would depend on the material and system conditions not measured and

so would not be understood by accident management personnel. Identifying the time of core material relocation would require close correlation of the plant measurements, together with a knowledge of ongoing operator and plant control actions that would affect pressure.

***Level.*** Level magnitudes and trends would not distinguish this core state. Relocated material would likely cover the lower differential pressure tap, which would cause large errors in the measurement. Whether the relocation of material would result in level changes that are sufficiently large that they could be distinguished from other level changes is not known. The water level may be low or it may be high and increasing while core material melts and a debris bed forms and grows.

***Other Measurements.*** Most SPNDs would be failed, though the failure of some may not be obvious. Source range monitors would likely indicate different flux levels when materials relocate. Correlation of source range monitor output with pressure measurements may allow identification of material relocation, but this has not been confirmed. Hydrogen and radiation level measurements would not help distinguish this core state from the previous core state.

### 4.2.6 Lower Head Attack by Molten Core Debris

There are no commonly installed instruments that would indicate the heatup of the debris in the lower plenum or of the wall of the reactor vessel lower plenum.

***Temperature.*** Neither the CETs nor the RTDs would reliably indicate lower head failure. There are no commonly installed temperature instruments for the vessel lower head material. Containment temperature could rise sharply but may be insensitive to core relocation for long time periods, depending on the measurement location.

***Pressure.*** A rapid drop in pressure could indicate failure of the RCS boundary. However, the lower head is just one of many possible RCS failure locations.

***Level.*** The effect of the relocated core material on the pressure tap in the lower head would cause this measurement to be unreliable.

***Other Measurements.*** The effect of the molten core material on the source range detectors is not known. Hydrogen and radiation level measurements would be very high but would not help distinguish this core state from several of the previous core states. Containment pressure would show a rapid increase, but this would also be the case with the failure of other locations in the RCS. Identification of core relocation may be possible if gases generated during core concrete interaction can be detected, for example high concentrations of CO or $CO_2$.

# 5. CHARACTERIZATION OF THE EFFECTS OF ADDING WATER AT DIFFERENT CORE DAMAGE STAGES

We performed two types of calculations to characterize the effects of adding water at various stages of core damage. Initially, we developed a simple model that approximated the energy transfer processes and mass balances for adding water during the initial stages of core degradation. We used this model to estimate the amount of water that would be necessary to prevent progression from one core damage state to the next. We then used a SCDAP/RELAP5/MOD3 model of a PWR to examine the effects of adding water at several core damage stages. Results from both of these calculations follow.

## 5.1 Simple Model Results

In this section, we present results from simplified bounding calculations to estimate the minimum rate of water addition that could prevent the core degradation from progressing to a higher state. We also estimate the time required and the total amount of water injected through the core to remove its energy. The calculations include those for a core at the following initial temperatures: (a) 1000 K (predamage state), (b) 1200 K (the ballooning state), (c) 1500 K (the early rapid oxidation state), and (d) 2000 K (late rapid oxidation state). When debris beds are formed in the core, because of the degradation of heat transfer resulting from drastic decreases in heat transfer areas, the rate of water being added becomes secondary to the ability of water to remove energy from the debris bed. We have estimated the critical limits of heat removal for the debris beds as a function of their characteristics, which we present in Appendix B.

**5.1.1 Calculation Parameters.** The simple calculations for determining the amount of water necessary to prevent progress to the next core damage state use nominal parameter values calculated from information contained in Standard Safety Analysis Reports for a Westinghouse four-loop reactor[39] and a B&W 205 reactor.[40] Values of nominal parameters are within approximately 10% of the specific values of large PWRs. General Electric's BWR/6 reactor design[41] is used as a model BWR whenever it is necessary to differentiate between BWRs and PWRs.

Sources of energy in the core after reactor scram can be examined based on the nominal parameter values. These sources include the decay heat, the release of energy from oxidation of zircaloy in the core, and the energy stored in core materials, which is a function of average core temperature. We evaluated the relative magnitudes of these energy sources during severe accidents based on nominal PWR values. Appendix B, Section B-3, summarizes the details from this evaluation. To simplify the analysis, we consider only $UO_2$ and zircaloy in the early stages of core degradation; $ZrO_2$ is added to the analysis as the zircaloy is oxidized by steam.

Table 4 presents the nominal values of PWR parameters used in the evaluation of parameters and for the bounding analyses performed in the remainder of this section. Note that zircaloy comprises approximately 19% of the total core mass. The fuel mass in a BWR[41] is much higher than that in a PWR (157,000 kg for a BWR versus 100,000 kg for a PWR) and, more significantly, the zircaloy in a BWR as a fraction of total core mass is also higher (30% for a BWR versus 19% for a PWR) because of the presence of zircaloy channel boxes around the fuel assemblies.

Decay heat from radioactive materials is the predominant energy source in a reactor after scram. Over a short time interval, the oxidation of zircaloy by steam can also be a significant energy source. In the first hour after scram in a small-break LOCA, most of the stored heat in the fuel during reactor operation (relative to coolant saturation temperatures), residual fission heat, and decay heat would be transferred to the coolant. The core temperature would be near the saturation temperature of the coolant. Therefore, energy release during the first hour of a small-break LOCA may be ignored in calculating the stored

**Table 4.** Nominal PWR parameters.

| | |
|---|---|
| Rated power ($MW_t$) | 3500 |
| $UO_2$ mass (kg) | 100000 |
| Zircaloy mass (kg) | 23000 |
| Cladding thickness (mm) | 0.65 |
| Fuel rod outside diameter (mm) | 9.75 |
| Number of fuel rods | 53000 |
| Core height (m) | 3.66 |
| Volume of fuel rods ($m^3$) | 14.5 |
| Core region free volume ($m^3$) | 17.6 |
| Core bypass and inlet annulus volume ($m^3$) | 21.6 |
| Primary system volume ($m^3$) | 350 |

energy of core materials. For this reason, we compute the decay energy release only for times after the first hour after scram. Table 5 presents the results. The assumptions used in the computations are that (a) the reactor has operated continuously for one year at full power after a fresh loading of fuel, and (b) the conversion fraction of U-238 to an actinide for each fission of U-235 is 0.9. The 1979 ANSI Standard[42] is used as the decay heat model. The decay heat data shown in Table 5 can be used to estimate the time required to dry out the core after core uncovery.

**5.1.2 Calculation Approach.** The objective of adding water to degraded cores is to arrest core damage progress and stabilize the core so that recovery from heatup of the core can be achieved. To prevent further heatup of the core, the rate of adding water must be such that the rate of heat transfer from the core to the water must be greater than the rate of heat generation within the core. Heat transfer from core materials to the incoming water includes vaporization of the water and superheating the steam to nearly the peak temperature of the core materials. In the subsequent formulation, it is assumed that injected water flows to the core through the downcomer and the lower

**Table 5.** Energy from decay heat of a nominal PWR.

| | Time after scram (h) | | | | | | | |
|---|---|---|---|---|---|---|---|---|
| | 1 | 2 | 3 | 4 | 5 | 6 | 7 | 8 |
| Cumulative energy (GJ) | 0 | 137 | 252 | 354 | 448 | 536 | 619 | 698 |
| Energy addition in preceding time interval (MJ) | — | 137 | 115 | 102 | 94 | 88 | 83 | 79 |
| Average power in preceding time interval (MW) | — | 38 | 32 | 28 | 26 | 24 | 23 | 22 |
| Average power in preceding time interval (% of full power) | — | 1.09 | 0.98 | 0.81 | 0.75 | 0.7 | 0.66 | 0.63 |

plenum of the reactor vessel. It is further assumed that the incoming water is heated to saturation before it reaches the high-temperature portion of the core, so there is no heat transfer to subcooled water from the high-temperature portion of the core. Vaporization takes place in the lower elevations of the core, and the steam is superheated in the upper elevations of the core. Reflooding a core at high temperatures is a complicated process that involves film boiling, transition boiling, and nucleate boiling. The purpose of this study is not to model the reflooding process in detail, but rather to provide rough estimates of water addition rates that can adequately remove energy from degraded cores. These estimates can then be used as guides for detailed code calculations if more precisely defined rates are desired. Based on this philosophy, nominal values of heat transfer coefficients or heat transfer fluxes will be used in the calculations. Appendix B documents detail the model developed for the simplified calculations.

**5.1.3 Water Addition During Predamage and Ballooning Stages.** The temperature range during predamage core heatup can be considered to be from the saturation temperature of the water to 1100 K, when fuel rod ballooning is expected to occur. Based on the formulation described in Appendix B, we perform a representative calculation for a temperature at 1000 K over a 2.75-m height of core (75% of the height of the core). The system pressure is taken as 6.9 MPa. The criterion determining the minimum rate of adding water to the core is that the core be prevented from heating up to 1100 K. Between 1000 K and 1100 K, the oxidation of zircaloy is negligible, so only the decay heat is considered in the core heatup during quench. The minimum rate of adding water is determined to be 30 kg/s, or 470 gpm (water volume measured at 300 K). This is within the injection capacity of most PWR high-pressure injection systems if most of the injected water goes through the core. The time required to completely quench the core is calculated to be 225 s, and the total amount of water added to the core during quench is 6700 kg.

We performed a calculation for the ballooning stage to determine the minimum rate of water addition to prevent the core from heating up to the rapid oxidation stage. The initial temperature of the core is taken to be 1200 K, the limiting temperature of the core to be 1500 K, and the minimum temperature for the core to have entered the rapid oxidation stage. Again, the high temperature portion of the core is taken to be 2.75 m in height. Unlike the calculations for the predamage stage, the calculations for the ballooning stage include energy input from oxidation. At 1500 K, the power from oxidation of zircaloy is approximately 1.8 times that from decay heat.

In the calculations for the ballooning stage, it is assumed that the fuel rods in the central 80% of the core have ballooned, and the flow area in the ballooned region is reduced by 40%. Consequently, the hydraulic diameter in the ballooned region is reduced by approximately 50%. The calculations yield a minimum required rate of water addition at 34.4 kg/s for the ballooned region. The calculated flow through the unblocked peripheral region is calculated based on the assumption that the pressure drop in the core is uniform across the core. This gives a required minimum rate of flow through the peripheral region at 17.3 kg/s. The total minimum required flow through the core is 51.7 kg/s, or 820 gpm, again within the capacity of the high-pressure injection system (a minimum of two operating pumps) if most of the injected water goes through the core. The time required to completely quench the core is calculated to be 192 s, and the total amount of water added to the core during quench is 9930 kg. Note that the stored energy in three-fourths of the core at 1200 K is equivalent to the heat of vaporization of 12,000 kg of water (see Table 4). The minimum required amount of water calculated is somewhat less than that. This is due to the effect of steam cooling, which more than compensates for the heating of the upper portion of the core during quenching the lower part of the core.

The above results show that a core heated to less than 1200 K can be recovered with full-capacity injection from the high-pressure injection system if most of the injected water goes through the core. However, to translate water injection rates into the primary cooling system to rates of water flow through the core, detailed code

calculations for specific loss-of-coolant scenarios are necessary.

**5.1.4 Water Addition During Rapid Oxidation Stage**. We performed two calculations to determine the minimum required rates of water addition to a degraded core during the rapid oxidation stage, one at an initial temperature of 1500 K (early rapid oxidation stage), the other at an initial temperature of 2000 K (late rapid oxidation stage). For the early rapid oxidation stage, the determining criterion is that the core be prevented from heating up to 1800 K, a temperature slightly below the transition temperature from the slower Cathcart-Pawel oxidation kinetics[43] to the more rapid Urbanic-Heidrick kinetics.[44] For the late oxidation stage, the determining criterion is that the core be prevented from heating up to the melting point of zircaloy, or 2100 K. Above 2100 K, large debris beds may form in the core from material relocation.

The height of the high-temperature portion of the core is again assumed to be 2.75 m, and all the fuel rods are assumed to have ballooned, contributing to a flow blockage of 40%, as indicated by code calculations.[10] The minimum required rates of water addition are calculated to be 148 kg/s, or 2350 gpm, for an initial temperature of 1500 K, and 1230 kg/s, or 19,500 gpm, for an initial temperature of 2000 K. These required rates are clearly much above the water addition capacity of the high pressure injection system, but they are within the injection capacity of the accumulators if the system pressure is lowered to 0.7 MPa below the accumulator set-point (approximately 4.2 MPa). If the cold legs of the primary cooling system are filled with water, operation of the reactor coolant pumps can also provide the necessary flow through the core.

For an initial core temperature of 1500 K, the time required to completely quench the core is calculated to be 64.6 s, and the total amount of water added to the core during quench is 9540 kg. For an initial core temperature of 2000 K, the time required to completely quench the core is calculated to be 7.6 s and the total amount of water added during the quench is 9350 kg. Note that for a core at high temperature, the time required to cool the core is much shorter than for a core at low temperature, otherwise the core would progress to a higher stage (higher temperature) of degradation. This is because of the rapid escalation of temperature caused by the rapidly increasing oxidation rate as the temperature increases. Because of heat transfer to superheated steam, the total amount of water required to cool the core is not very sensitive to the initial core temperature.

If the rates of water added to the core are higher than those calculated above, the additional hydrogen production during the brief periods of temperature escalation before the complete cooldown of the core is calculated to be limited to 55 kg during the early oxidation stage, and to 20 kg during the late oxidation stage.

## 5.2 SCDAP/RELAP5/MOD3 Calculation Results

The following describes our water addition calculations performed using the SCDAP/RELAP5/MOD3[b] computer code.

**5.2.1 Approach.** We used the SCDAP/RELAP5/MOD3[b] (series 87) computer code to calculate the transient response of the Surry plant during a TMLB' station blackout scenario. The plant model has the capability of calculating the potential effects of RCP seal leakage, countercurrent natural circulation in the hot legs, and creep rupture failure of the ex-vessel piping resulting from high-temperature and high-pressure conditions. We selected the Surry plant for this analysis because the model had already been developed and TMLB' calculations suitable to initialize calculations for the present analysis had been performed.[c] Appendix C describes the Surry plant model in detail.

The station blackout calculations assumed the accident was initiated by the loss of all onsite and offsite ac power. Coincident with the TMLB' initiation was the initiation of reactor coolant pump (RCP) seal leaks of 21 gpm, which represent the

b. C. M. Allison et al. (Eds.), *SCDAP/RELAP5/MOD3 Code Manual*, to be published as a NUREG.

maximum leakage with which the plant would be allowed to operate. The seal leakage increased to 250 gpm when the liquid at the pump reached saturation temperature, simulating partial failure of the pump seals. The loss of electrical power resulted in a reactor scram and coastdown of the reactor coolant and main feedwater pumps. The main feedwater and turbine stop valves closed, causing the steam generator pressure to increase to the relief valve set point. Initially, the steam generators were the principal means of removing energy from the RCS when the pump seal leaks, resulting in a much smaller amount of energy removal. The secondary water inventory decreased as heat transferred by natural circulation from the primary to the secondary system vaporized the secondary side water. Once the steam generator secondary side inventory had boiled away, the heat removal capability of the steam generators was significantly diminished. As a result, the core decay heat exceeded the energy dissipated through the liquid flow out of the seal leaks, and the heat transferred to the vapor in the steam generator secondaries. The temperatures and pressures in the RCS increased until the pressure reached the PORV set point. The RCS pressure remained high until the voiding in the cold legs uncovered the RCP seal leaks. At this time, the vapor discharge out the seal leaks in combination with heat transfer to the vessel and ex-vessel structures exceeded decay power, resulting in gradual RCS depressurization. During this depressurization, the core uncovered and heated up to relatively high temperatures. Water addition was initiated during the core heatup phase.

We performed four calculations with SCDAP/RELAP5/MOD3 to evaluate the effects of adding water. These calculations differ from previous station blackout calculations[d] because they assume that the operator is successful in restoring power to the high-pressure injection system (HPIS). Restoration was assumed when the core reached temperatures that correspond to the threshold of several early core damage stages.

We used simple models of the HPIS and its control logic in this analysis. The control logic for the HPIS contains a pump curve that controls the flow rate based on the pressure of the plant. We developed a head-versus-flow curve from information in the Surry Final Safety Analysis Report. Two out of three HPIS pumps were assumed to be operating with flow into the three cold legs. The shutoff head for the pumps was modeled as 17.9 MPa and the total flow into each of the three loops with no back pressure on the pumps was modeled as 25.11 Kg/s. The coolant from the HPIS was modeled as entering the cold leg just upstream of the vessel cold leg nozzle.

In Calculation 1, the HPIS was initiated when the maximum core cladding surface temperature reached 1500 K. We chose this temperature because it corresponded to the initial temperature of the rapid oxidation stage. This temperature occurred at 208 minutes after the station blackout began. Interaction between the relatively cold HPIS fluid and the hot cladding resulted in shattering of some of the oxide shell that had formed on the fuel rods. The SCDAP oxide shattering models used for this calculation are based on best-estimate assumptions derived from applicable experimental data.[45] The primary reason for allowing oxide shattering is to account for the effect of cooling on the brittle zirconium oxide formed on the exterior of the fuel rods. This cooling shatters the oxide which exposes fresh zircaloy to RCS steam and allows oxidation to continue at a rapid rate when it previously would have substantially slowed. Criteria in the model

c. C. A. Dobbe and D. L. Knudson, "SCDAP/RELAP5/MOD3 Analysis of a Surry 'TMLB' Sequence for FIN A6884," Volumes 1 and 2, AF 108.000, EG&G Idaho, Inc., Idaho, 1992.

d. K. S. Quick and D. L. Knudson, "SCDAP/RELAP5/MOD3 Analysis of RCS Water Addition via HPI During a 'TMLB' Scenario in the Surry Power Station," Analysis Notebook, EG&G Idaho, Inc., 1993.

that must be met for oxide shattering to take place are

1. A beta phase thickness of less than or equal to 0.1 mm

2. A cooling rate greater than 2 K/s for four consecutive time steps within the temperature range of 1150 K to 1560 K.

Calculation 2 was identical to the first calculation, with the exception that the PORVs were latched open after the fuel rods had quenched. As will be explained in the following section, we ran this calculation because the fuel rods began heating up again after the initial quench. We anticipated that opening the PORVs would remove additional energy, which would reduce the RCS pressure and keep the HPI flow rates at a higher level. Because the amount of coolant entering the system in this scenario would be much greater, the core would be much more likely to stay covered with water.

Calculation 3 was identical to the first calculation, with the exception that the HPIS was initiated when the maximum core surface temperature reached 1800 K, rather than 1500 K. As will be explained in the following subsection, the first two calculations indicate that adequate energy could be removed from the core to stop core damage progression if HPI water were added if the core temperatures had not exceeded 1500 K. This calculation was run to determine whether core damage progression could be stopped if the core was at a higher temperature when the HPI water began entering the system.

There are uncertainties as to the capability of the zircaloy shattering models to predict the energy generated from oxidation because this model was developed recently and has not undergone significant testing against experimental data. As a result of these uncertainties, we performed an additional calculation at a lower temperature where oxidation and shattering of the cladding were not as strong an influence on the calculated temperatures. Calculation 4 was identical to the first calculation, with the exception that the HPIS was initiated when the maximum core surface temperature reached 1200 K, rather than 1500 K. We chose this temperature because it represents an earlier stage of core damage than occurred in Calculation 1.

The following section describes and explains the four calculations. Table 6 summarizes the different parameters between the four calculations. The calculations generally would not run to later times than are presented because of problems with condensation and the effect of noncondensible gases.

**5.2.2 Results.** Our discussion of results from the four calculations concentrates on the time frame of the station blackout transient that follows HPIS initiation. As a result, the parameters used to illustrate the system behavior for the calculations will only show the transient response beyond the approximate time when the HPIS is initiated. We briefly discussed the portion of the transient that took place prior to HPI initiation in the previous section; Reference 46 discusses the TMLB' sequence in detail.

***Calculation 1, HPIS Actuation at 1500 K.*** The HPIS was initiated when the maximum core surface temperature reached 1500 K, which was 208 minutes after the station blackout transient began. Examination of the calculation's results show that zircaloy oxidation began about 24 minutes prior to this time (about 184 minutes after the sequence began). During this 24-minute period, about 30 kg of hydrogen was produced, and the rate of oxidation was continually increasing.

**Table 6.** Summary of the different parameters between the four calculations.

| | Calculation | | | |
|---|---|---|---|---|
| Parameter | 1 | 2 | 3 | 4 |
| HPIS initiated at 1500 K | X | X | — | — |
| HPIS initiated at 1800 K | — | — | X | — |
| HPIS initiated at 1200 K | — | — | — | X |
| PORV latched open | — | X | — | — |

About five minutes after HPIS injection was initiated, there was sufficient cooling of the high-temperature portions of some fuel rods that the modeling conditions were met for oxide shattering. Sufficient water reached the core that the rods were cooled and oxide shattering only occurred for a brief period. By 215 minutes, all in-core oxidation had ceased, and by 220 minutes the cladding was quenched. This rapid reduction of core temperatures prevented core damage from progressing to the next core damage stage, where oxidation would become more rapid. The large quantities of steam produced during core quenching caused the RCS pressure to rise. This pressure rise resulted in a reduction of HPIS flow, and the core liquid level began to decrease by 225 minutes. The collapsed liquid level in the core dropped to about 1.5 meters above the bottom of the core (about 40% of the core height) at 260 minutes before increasing HPI flow rates began to add water to the core region and raise the core level again. The calculation was halted shortly after 275 minutes, as the system was reaching a state where the energy being removed from the core was approximately equivalent to the energy being removed from the system, primarily through the pump seal leaks.

Figure 8 shows the cladding surface temperatures along the center (high power) fuel channel for Calculation 1. Quenching of the lower elevations of the hot channel begin shortly after injection is initiated at 208 minutes, and the upper elevations are quenched by about 217 minutes. The entire core was quenched by about 220 minutes. At about 240 minutes, the temperature of the upper elevations of the core begin to increase again and reach 1000 K at 270 minutes. A slight reduction in temperature at the upper elevations follows.

The cladding temperature response closely follows the collapsed liquid level in the core, as shown in Figure 9. Water enters the core following HPIS injection and causes the collapsed level to slowly rise until it approaches the top of the core region at about 220 minutes. The sharp drop and recovery in level between about 222 and 226 minutes appears to be the result of rapid condensation in the cold legs during this time period. Following recovery at about 226 minutes, the collapsed level slowly drops until it is below the core midplane at 265 minutes. The increase in level after this time results in the temperature decreases observed in Figure 8.

Changes in the collapsed core liquid level can be related directly to interactions between the system pressure and the HPIS flow rates. Figure 10 shows the system pressure for the period following 200 minutes. At HPIS initiation (208 minutes), the pressure has decreased to about 11 MPa as a result of flow through the pump seal leaks and energy transfer to the steam generators and the system structure. Following HPI initiation, the pressure rises in response to the steam being produced by the HPIS fluid flashing as it cools the fuel rods. The pressure remains relatively constant from about 215 minutes until about 220 minutes as the core quenches. Following core quench, the pressure declines slowly and then drops rapidly between about 222 and 226 minutes. This rapid drop in pressure corresponds to high rates of condensation taking place in all cold legs. At about 226 minutes, all pump seals are calculated to be covered, and water is flowing from the system rather than steam. Since the flow of water through the leaks removes less energy than steam, the pressure begins increasing again until 240 minutes, where it has reached 13.7 MPa. As the top of the core uncovers, energy transfer from the fuel rods to the system decreases. This reduction in energy transfer to the system results in a reduction in pressure during the period between 240 and 270 minutes. From 270 minutes until the calculation was stopped, the pressure increases slowly and appears to be approaching a quasi-steady value.

Figure 11 shows the HPIS mass flow rates for one coolant loop. Initially, the HPIS mass flow rates increase from 0 to 17.5 kg/s over about a two-minute period. Because of the initial pressure rise described above, the HPIS flow rates begin decreasing by 211 minutes and drop to about 12 kg/s by 215 minutes. As a result of the pressure decline between 215 and 226 minutes, the HPI flow rates increase back to about 17.5 kg/s.

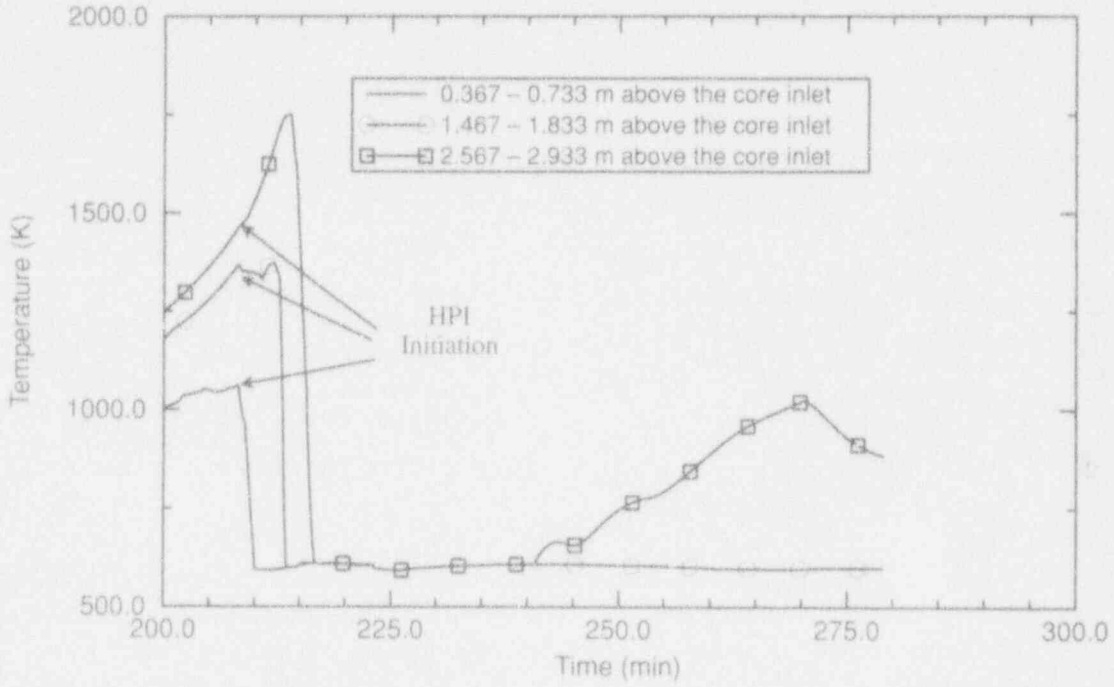


**Figure 8.** Cladding surface temperatures along the center fuel channel for Calculation 1.

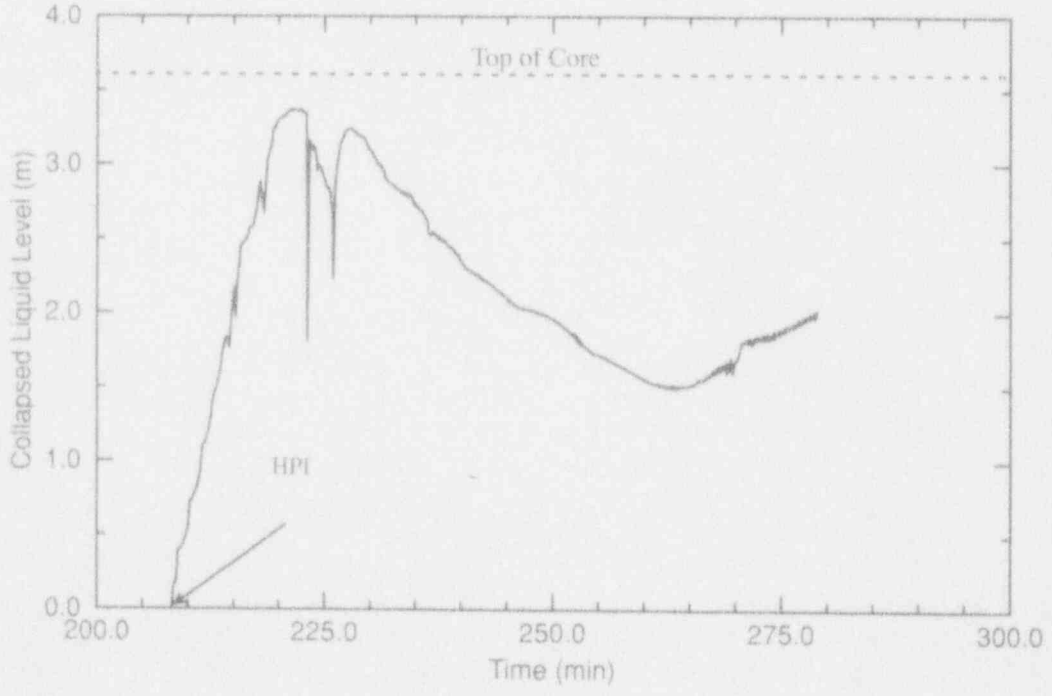


**Figure 9.** Core collapsed liquid level for Calculation 1.

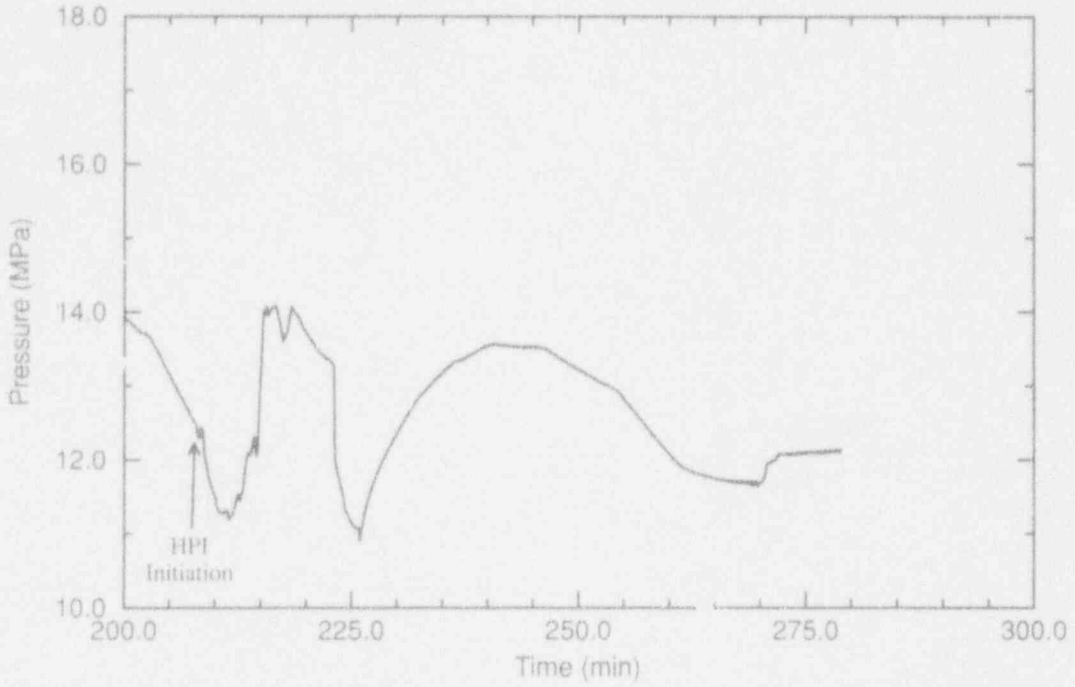


**Figure 10.** System pressure for Calculation 1.

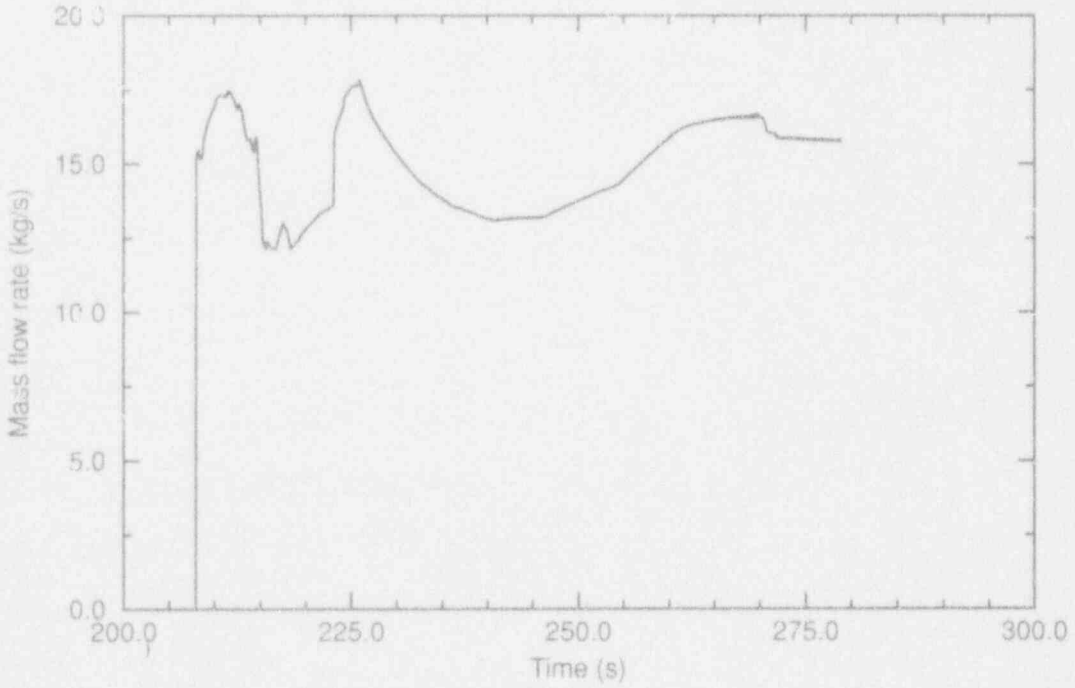


**Figure 11.** HPIS mass flow rate for Loop A in Calculation 1.

The pressure increase between 226 and 240 minutes results in the reduction of HPIS flow rates to 13 kg/s by 240 minutes. Between 240 and 270 minutes, the mass flow rates increase because of a pressure decline over this period. Beyond 270 minutes, the HPI mass flow rates flatten out as the system approaches equilibrium.

Figure 12 shows the mass of hydrogen created as a result of oxidation of the zircaloy cladding. From 200 to 215 minutes, the hydrogen mass increases at a steady rate, while limited oxidation takes place in the upper levels of the core. By 215 minutes, the core has been cooled below the temperature criterion for oxidation. The total mass of hydrogen generated for this calculation is approximately 67 kg.

Results from Calculation 1 show that HPIS injection rates have the capability to initially remove the stored energy from the fuel rods if the HPIS is initiated before the maximum core temperature exceeds 1500 K. It also shows that a second uncovery of the core and heat-up of the upper portions of the fuel rods is possible. Whether the core level recovers and the upper portions of the fuel rods remain cool in the long term depends on the size of the breaks and the characteristics of the HPIS pumps. If the breaks are not large enough to remove the core decay heat, the pressure will rise and reduce the amount of water injected. A quasi-steady condition will be reached where the upper portion of the core will uncover until the energy removal from the break is equivalent to the energy being removed from the portion of the core that is cooled. We investigated in Calculation 2 a possible accident management strategy to prevent core damage when the break is too small to remove core decay heat.

***Calculation 2, HPIS Actuation at 1500 K, PORV Opened Following Initial Core Quench.*** A management strategy to remove additional energy from the system could be effective for sequences where the break size is not large enough to remove core decay heat. Feeding and bleeding the secondary side of the steam generators, or opening the pressurizer PORVs would be the likely means of removing the energy. Opening the pressurizer PORVs was selected for

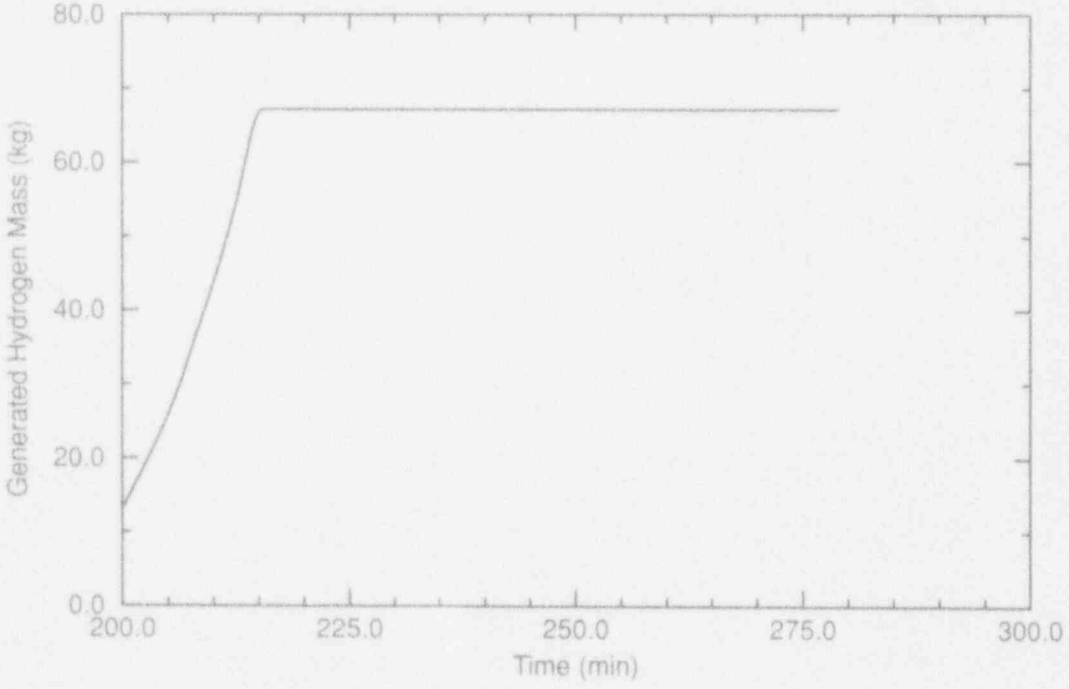


**Figure 12.** Hydrogen mass generated through oxidation in Calculation 1.

evaluation because recovery of feedwater was believed to be more unlikely for the TMLB' sequence. With the HPIS operational, this represents a primary feed and bleed strategy.

Calculation 2 duplicated the initial portion of Calculation 1 up to the time of the second core heat up. The PORVs are latched open at 225.75 minutes, which corresponds to the time of minimum pressure (following HPIS injection) for Calculation 1. This action prevents the pressure from increasing, which allows the HPIS to continue injecting at high mass flow rates. With a large amount of coolant entering the system, the second heat-up observed in Calculation 1 is prevented. The calculation was halted at 250 minutes because it was apparent that the core damage progression had been stopped.

A comparison of the system pressures for Calculations 1 and 2 is shown in Figure 13. Opening the PORVs rapidly reduces the pressure to the saturation pressure of the hotter portions of the RCS. The pressure stabilizes about 2 MPa lower than the minimum pressure predicted for Calculation 1. The lower pressures for Calculation 2 produce much higher HPIS mass flow rates, as shown in Figure 14. The additional mass injected causes the core collapsed liquid level (Figure 15) to initially decrease owing to steam condensation, and then to increase after about 226 minutes as the injection rapidly adds water to the system. At the time the calculation was stopped the core was about seventy percent full, with the level increasing as the HPIS flow rates remained high.

Figure 16 shows the cladding surface temperatures along the center fuel channel. Since the open PORV will maintain the RCS pressure at a relatively low value, HPIS injection rates remain high, and the core will remain covered, resulting in low core temperatures.

Results from Calculation 2 indicate that use of primary system feed and bleed after the initial core recovery will prevent core damage from progressing to a more severe core damage state. Without this capability or some other means of removing decay heat from the system, there is a range of break sizes and HPIS flow characteristics where a second heatup could occur, which would result in additional core damage at upper levels of the core.

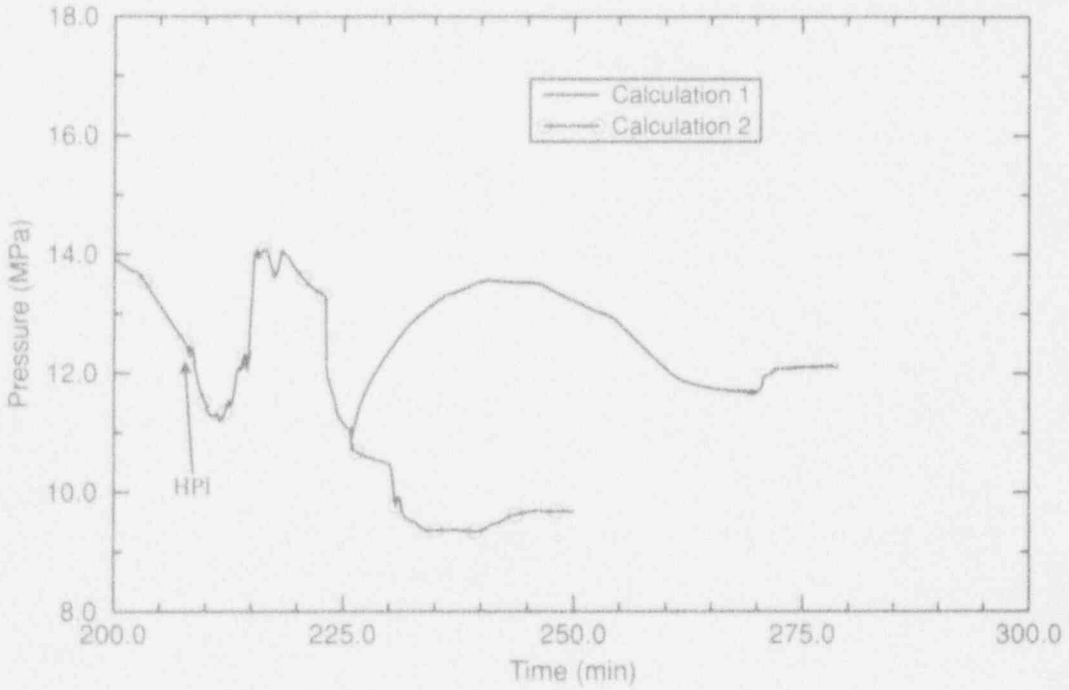


**Figure 13.** A comparison of system pressures for Calculations 1 and 2.

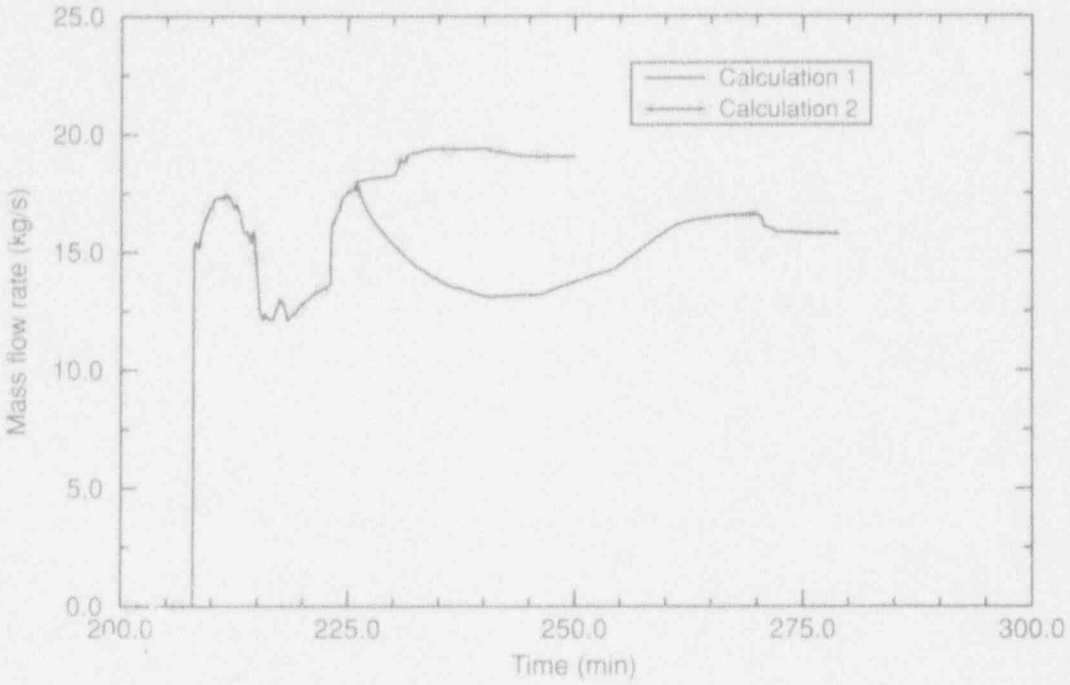


**Figure 14.** A comparison of HPIS flow rates for Calculations 1 and 2.

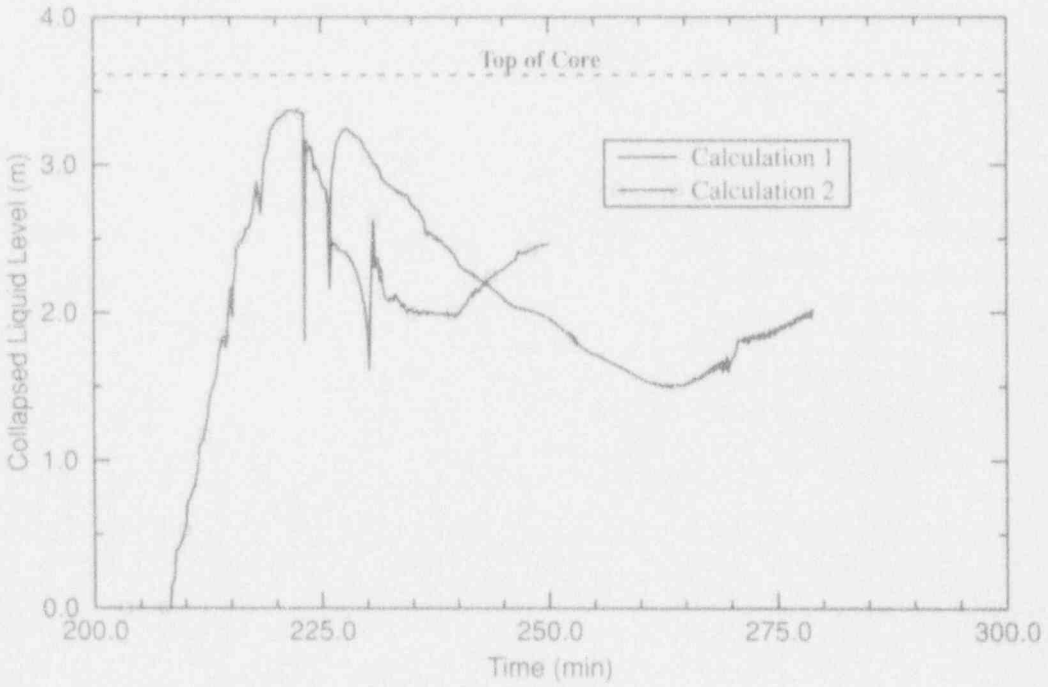


**Figure 15.** A comparison of core collapsed liquid levels for Calculations 1 and 2.

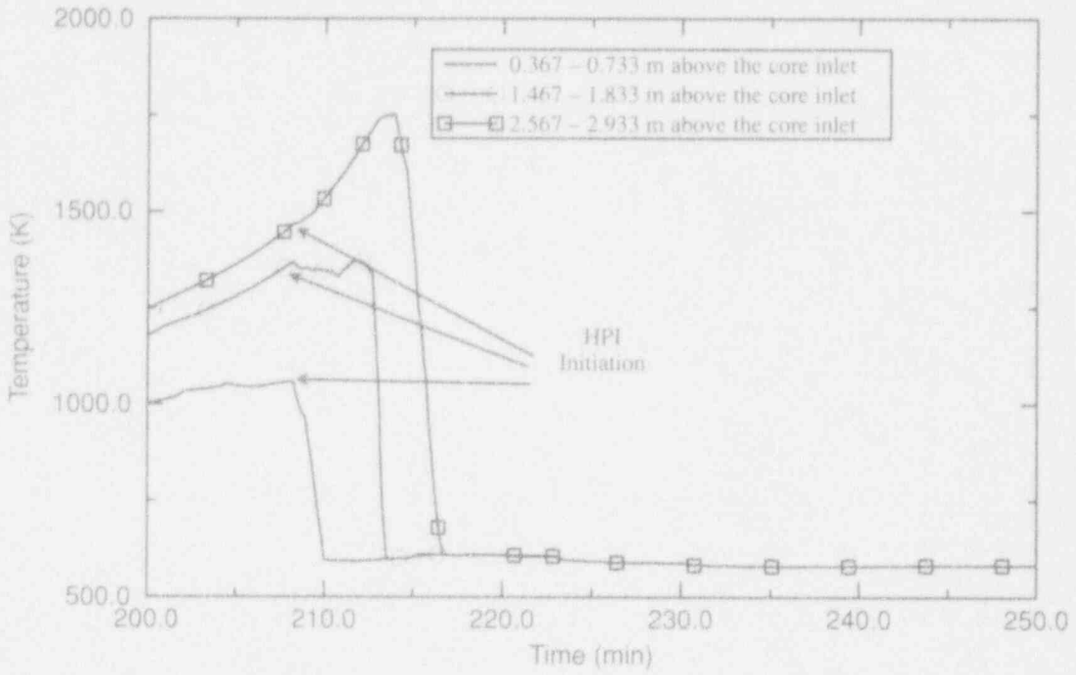


**Figure 16.** Cladding surface temperatures along the center fuel channel for Calculation 2.

***Calculation 3, HPIS Actuation at 1800 K.*** Calculation 3 assumes that the HPIS initiates when the maximum core surface temperature reaches 1800 K. This temperature occurs 212 minutes after the station blackout sequence begins, which is about 28 minutes after cladding oxidation begins. During this 28 minute period, approximately 58 kg of hydrogen is produced and the rate of oxidation increases rapidly at the time of HPIS initiation.

Following HPIS initiation, the injected coolant enters the vessel and begins filling the core. The stored energy in the core is greater in this calculation than in the first two and results in larger amounts of vapor being formed as the HPIS water flashes in the core. The rate at which the core fills in this calculation is, therefore, slower than Calculations 1 and 2, and the core does not totally fill with water until about 230 minutes. At approximately 214 minutes (about 2 minutes after HPIS initiation), a cohesive debris bed forms in the center channel near the bottom of the core. The results indicate that this debris bed is cooled over a period of time and remains cooled even though the upper regions of the core uncover and begin to heat up in the latter part of the calculation.

Figure 17 shows cladding surface temperatures along the center fuel channel. Quenching of the lower elevation of the core begins shortly after the HPIS is initiated at 212 minutes, and the upper locations are quenched by about 225 minutes. A second heatup is shown for the upper elevations of the core similar to Calculation 1.

Examination of the results for all axial and radial core locations shows that a cohesive debris bed is calculated to form in the center channel at axial nodes 3 and 4 (between 0.73 and 1.5 meters from the bottom of the core), but no debris beds are calculated for other core locations. The debris bed temperature in Figure 17 shows a rapid heat up to about 1900 K at 215 minutes. The debris is calculated to begin cooling shortly after it is covered with water, and this cooling trend continues for the remainder of the calculation. The debris bed cools to about 875 K at about 264 minutes, when the temperature of the upper portions of the core exceed the temperature of the debris bed.

Figure 18 compares the core collapsed liquid level for Calculations 1 and 3. As in Calculation 1, the level for Calculation 3 shows a steady increase until the core is full (about 228 minutes).

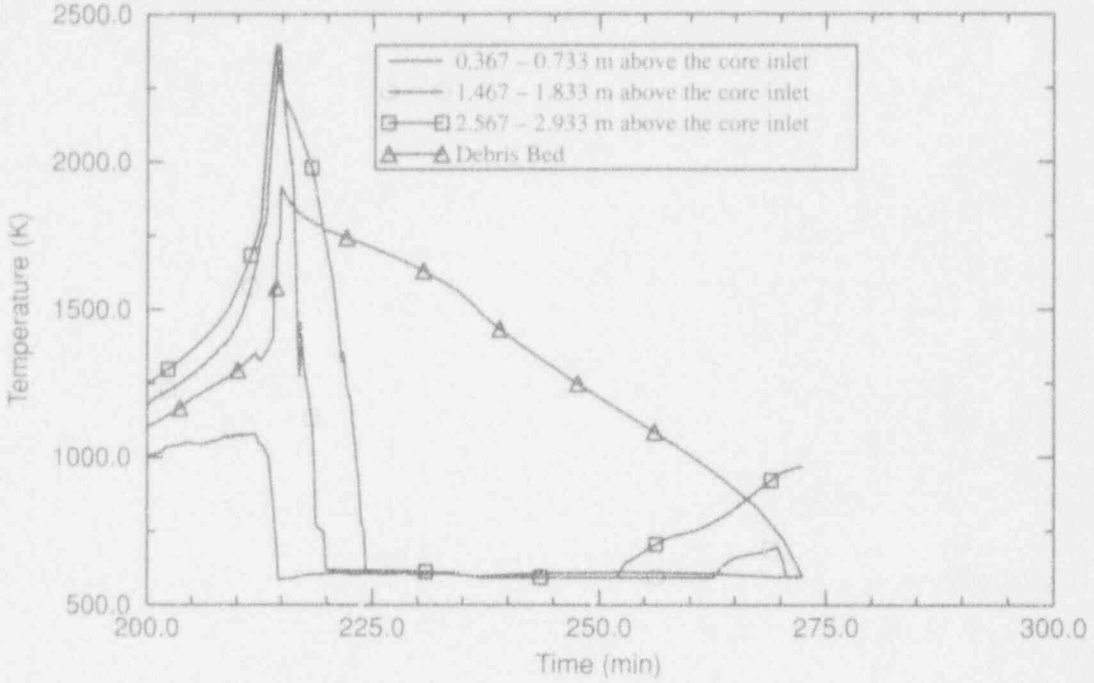


**Figure 17.** Cladding surface temperatures along the center fuel channel for Calculation 3.

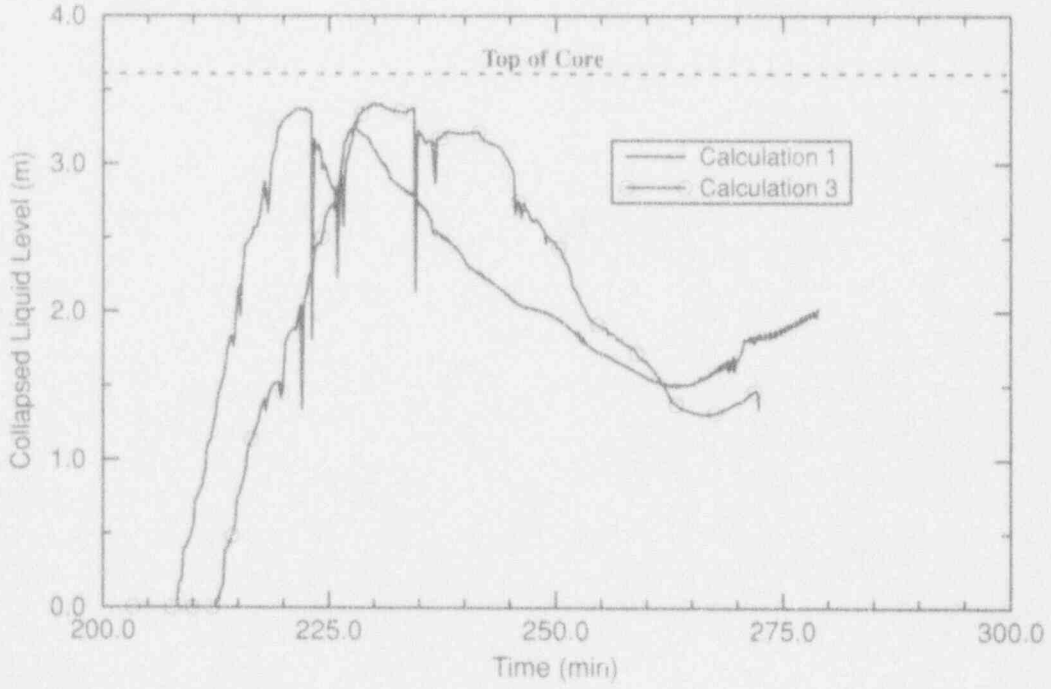


**Figure 18.** Comparison of core levels for Calculations 1 and 3.

Rapid condensation in the cold legs causes a slight reduction in level at about 235 minutes. By 240 minutes, the level begins a steady decline, and the level decreases to about 40% of the total core level at 270 minutes, then it begins to increase just before the calculation was stopped.

Figure 19 shows the system pressure for this calculation. Following HPIS initiation, the pressure initially decreased to 10 MPa as a result of condensation in the cold leg. As the HPIS-injected water begins to cool the core, the energy removed from the fuel rods vaporizes the water, and energy added from oxidation combines to rapidly increase the pressure from 10 MPa to 16 MPa. The magnitude of the pressure rise is about 2 MPa larger than Calculation 1 because there is additional stored energy and because the oxidation rates are higher. At 219 minutes, the pressure levels off for a brief period before showing a steady decline between 227 and 237 minutes, where it reaches a low of 11.5 MPa. Several factors contribute to this pressure decline. First, the HPIS injection reduces the fuel rod temperatures to below 1100 K, so cladding oxidation would no longer be important (see Figure 17). Rapid condensation in the cold legs should also occur at about 235 minutes, which causes a rapid decrease in the pressure. At about 237 minutes flow from the pump seal leaks transition from steam to liquid, which decreases the amount of energy being removed from the system. After this time, the pressure begins to rise, and the general trends are similar to those discussed for Calculation 1.

HPIS mass flow rates were strongly influenced by the pressure swings discussed above. Figure 20 shows that the general trends in flow for Calculation 3 are similar to Calculation 1, but the flow rate magnitudes show wider swings because the pressure changes are larger. Both the pressure and HPIS flows for both calculations approach a quasi-steady value at the end of the calculations.

Figure 21 compares the hydrogen generated for Calculations 1 and 3. Well over twice as much hydrogen is generated when HPIS injection is delayed until the peak cladding temperature reaches 1800 K. Although core damage progression was stopped in both calculations, the larger amounts of hydrogen from Calculation 2 would require additional accident management measures to ensure that detonation or deflagration do

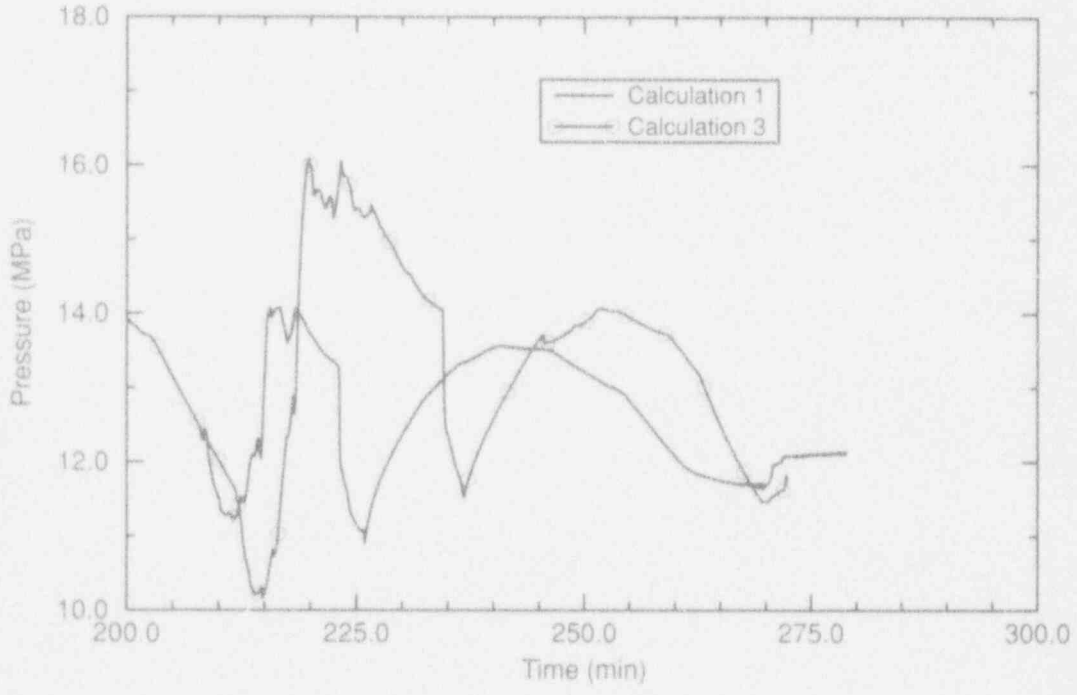


**Figure 19.** Comparison of system pressures for Calculations 1 and 3.

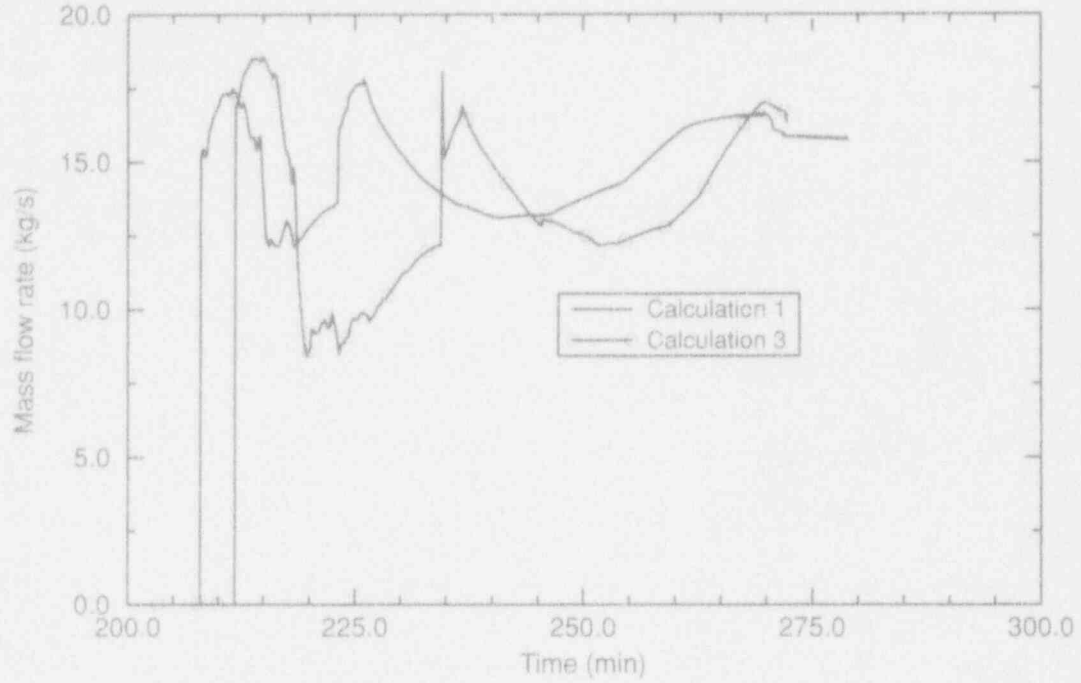


**Figure 20.** Comparison of HPIS flow rates for Calculations 1 and 3.

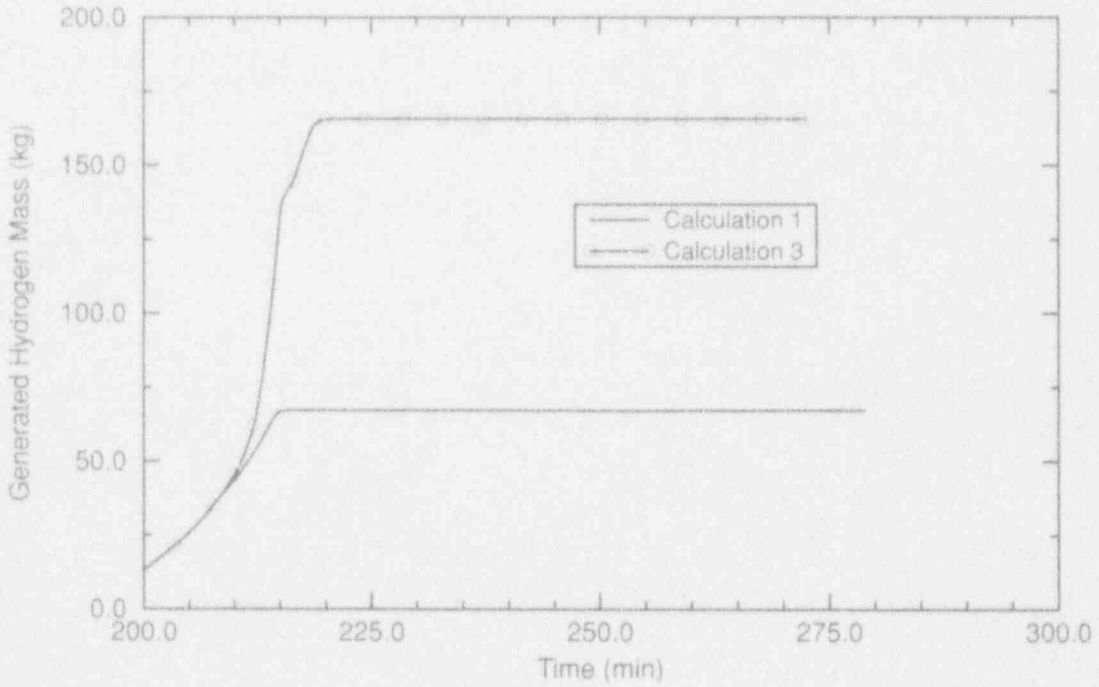


**Figure 21.** Comparison of the hydrogen mass generated for Calculations 1 and 3.

not threaten containment integrity or damage critical equipment.

This calculation, unlike Calculations 1 and 2, predicts the formation of a cohesive debris bed in the core. Although this debris bed is calculated to cool, there is uncertainty in the capability of the water to cool a debris bed this thick, based on the modeling assumptions used in the Surry model. Although the calculation predicts that the debris bed cools, there is sufficient uncertainty in the debris bed heat transfer that injection of water when the core reaches 1800 K should be considered as having a low probability of successfully preventing core damage progression. The second core uncovery and heat up for this calculation could be mitigated using the same feed and bleed accident management strategy demonstrated in Calculation 2.

***Calculation 4, HPIS Actuation at 1200 K.*** The calculations performed for HPIS injection at 1500 K to 1800 K have uncertainties associated with the capability of the oxidation models and the debris bed models to accurately predict the energy removal from the core. To increase assurance that the HPIS injection would stop core damage progression, we performed a fourth calculation that assumed the HPIS was initiated at a maximum core surface temperature of 1200 K. This temperature corresponds to a time 198 minutes after the station blackout transient begins. This is approximately 14 minutes after cladding oxidation begins. During this 14-minute period, only 10 kg of hydrogen has been produced, and the oxidation rates are small at the time of HPIS initiation.

Figure 22 shows the cladding surface temperatures along the center fuel channel. Shortly after HPIS injection is initiated, the fuel rod cladding temperatures all decrease rapidly to saturation, and the entire core is quenched by 208 minutes. Figure 23 shows the collapsed liquid level in the core and, as expected, the level rises rapidly until the core is reflooded at 208 minutes. The core level approaches a quasi-steady value before the calculation stops. The level could eventually decrease and a second heatup would take place, depending on the size of the break and the characteristics of the HPIS system.

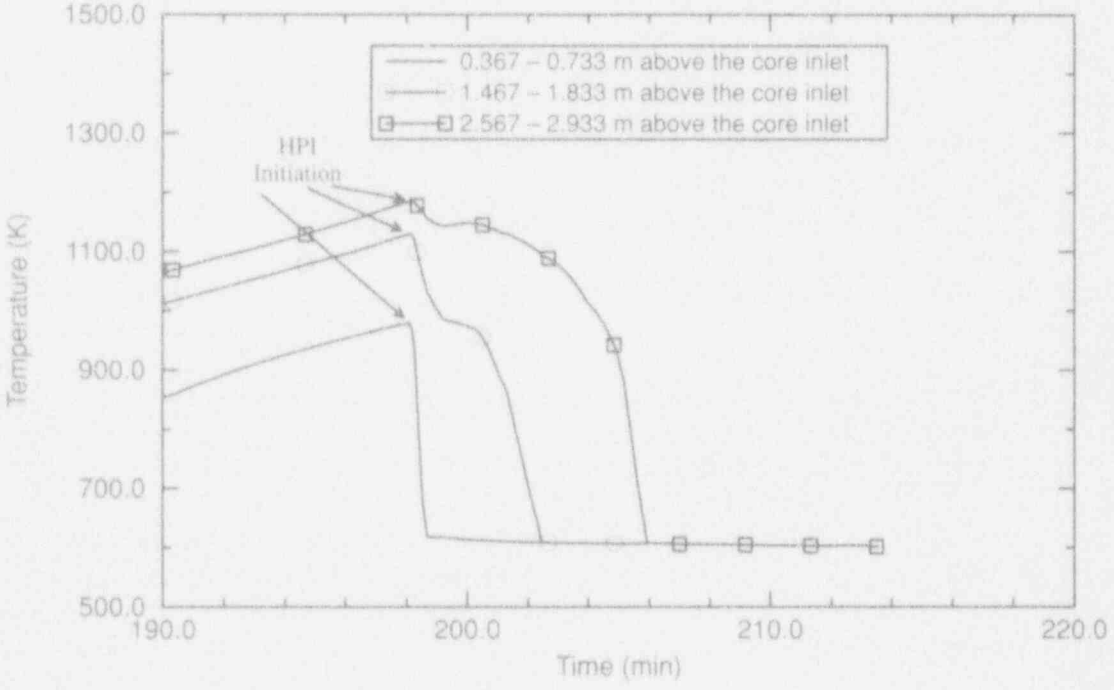


**Figure 22.** Cladding surface temperatures along the center fuel channel for Calculation 4.

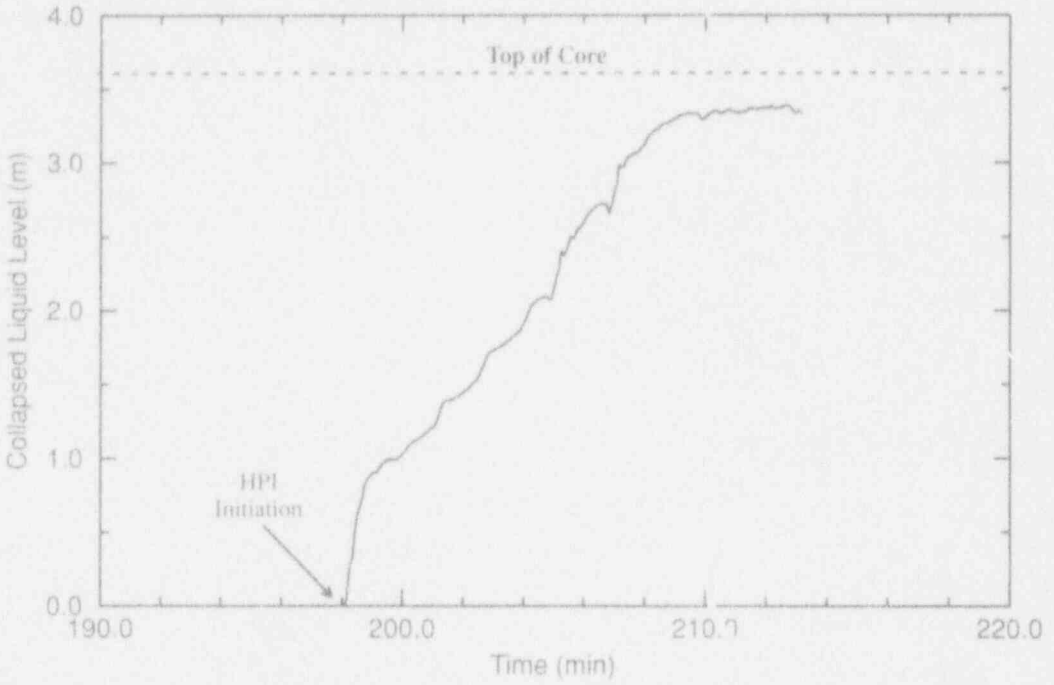


**Figure 23.** Collapsed core liquid level for Calculation 4.

Figure 24 shows the system pressures for Calculation 4. The period of time shown in the plot is from 190 minutes to 215 minutes, where the calculation was stopped. At HPI initiation (198 minutes), the pressure shows a slight decrease caused by condensation, followed by a rapid increase as HPIS fluid is flashed in the core. The HPIS water cools the core rapidly, and the pressure increase lasts for only one minute, until the energy being transferred from the fuel rods is relieved through the pump seal leaks. After the initial increase, the pressure decreases for the remainder of the calculation.

Figure 25 shows the HPIS mass flow rates, which because of the inverse relationship with pressure, shows steadily increasing rates from 199 minutes to the end of the calculation. The flow rates slow from 12.5 kg/s to 10 kg/s shortly after initiation as a result of the brief pressure rise described above. After this period, the increasing mass flow rates go to 15 kg/s by the end of the calculation.

The results from this calculation show that the system has a high probability of recovering if access to the HPIS is gained when core stored energy is lower, and the energy added by cladding oxidation is small. The amount of hydrogen generated is small, so major accident management measures to deal with the hydrogen would not be necessary. It is still possible, however, that the PORVs would need to be opened so that energy can be removed from the system and the HPIS can operate near full capacity.

**5.2.3 Conclusions.** Results from the SCDAP/RELAP5/MOD3 computer code indicate that HPIS injection will initially prevent progress to higher stages of core damage if the HPIS is initiated when peak core temperatures range from 1200 K to 1800 K. However, as the temperatures get higher, there is greater uncertainty in the outcome of water injection. Above 1500 K, debris beds are calculated to be formed and there are large uncertainties in the capability to provide long-term energy removal. Depending on the size of the break and the characteristics of the HPI pumps, there is also the possibility of a second heat up for the TMLB' sequence. An accident management strategy involving use of the PORVs to initiate RCS bleed and continued injection with the HPIS to feed the RCS was demonstrated to be successful.

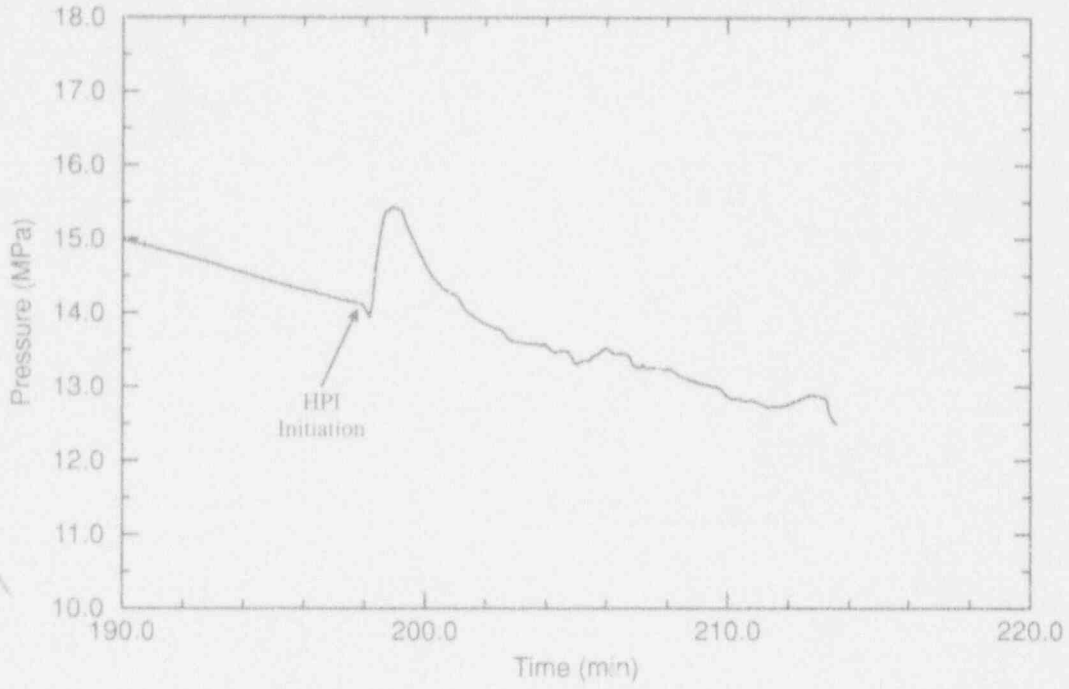


**Figure 24.** System pressure for Calculation 4.

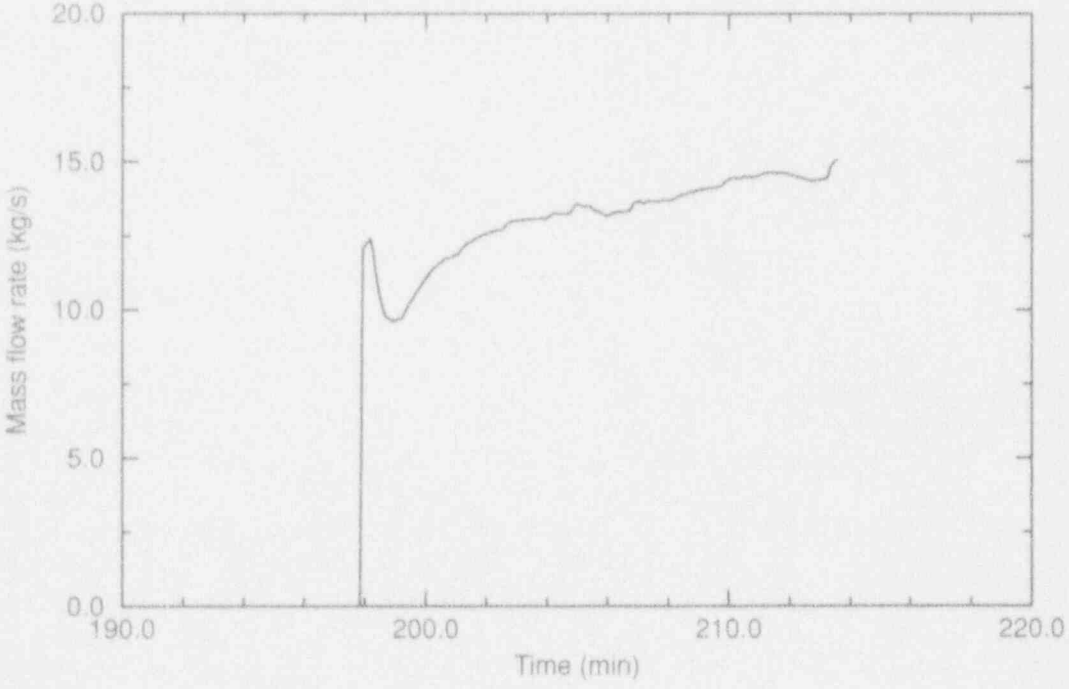


**Figure 25.** HPIS mass flow rate for Loop A in Calculation 4.

# 6. CONCLUSIONS AND RECOMMENDATIONS

An evaluation of the capability of adding water to prevent core damage was completed for the five plants examined in Severe Accident Risks: An Assessment of Five U.S. Nuclear Power Plants (draft) (NUREG-1150). Results indicate that 80 percent or more of the core damage frequency is due to sequences where core uncovery may be prevented if additional and innovative recovery actions are implemented. Time frames necessary to implement these actions depend very much on the plant and the accident sequence. If times available for initiation are relatively short, (for example, less than 1 hour) the likelihood for success would be low. Some of the times are much longer, exceeding 17 hours. For these sequences, the likelihood of successful operator intervention would be high.

The unmitigated core damage sequence presented in this study consists of the following stages: (a) core uncovery to fuel rod ballooning, (b) ballooning and rupture of fuel rod cladding, (c) early rapid oxidation of zircaloy cladding by steam, (d) late rapid oxidation of zircaloy cladding by steam, (e) formation of a debris region from relocated molten zircaloy and liquefied fuel in lower regions of the reactor core or at the lower core support plate, and (f) the relocation of core debris to the lower plenum of the reactor vessel. Concurrent with the formation of a cohesive debris bed near the bottom of the core, a particulate debris bed may also form on top of the cohesive debris bed from fuel pellets or oxidized cladding. These five stages of core damage are characterized by temperatures ranging from 1100 K (ballooning of the fuel rod cladding) to 3100 K (melting of the $UO_2$ fuel). Table 7 lists the core damage states and their temperature ranges and describes the possible positive consequences of adding water, the potential negative consequences, potential accident management strategies to prevent progressing to the next core damage stage, and potential long-term accident management strategies to mitigate accident consequences.

Not all of the accident management strategies discussed in Table 7 were evaluated in this report. Many were selected from reviews of strategy evaluations sponsored by the Nuclear Regulatory Commission or performed by the nuclear industry. The results show that accident management strategies for the early core damage stages concentrate on ensuring there is adequate water injection and RCS heat removal. During the latter stages of core degradation, strategies are added to prevent vessel failure and to control hydrogen and fission products. Strategies to prevent containment failure are not included in this study.

Results from Table 7 indicate that core damage progression can be stopped and the core can be recovered (core material returned to near saturation temperature) if the high-pressure injection system operates at full capacity prior to the fuel rod ballooning stage. The inventory depletion that precedes core uncovery can be determined using the RVLMS, and initial heatup of the fuel rods would be measured by core exit thermocouples or hot-leg RTD readings in excess of fluid saturation temperature. Injection by the HPIS would stop the core damage progression. A possible negative consequence of adding water would be pressurization of the RCS, which would reduce HPIS water flow into the system. Other adverse effects would likely be insignificant.

The calculated results at all core damage stages show that the capability to maintain long-term core energy removal depends on the amount of energy being transferred from the core to the water or steam, the amount of energy being removed from the RCS, and the characteristics of the safety injection system. If the injection system head is low or the flow strongly depends on pressure and the energy transferred from the core to the water exceeds the energy being removed from the RCS, the reactor core may reach a stable condition where a portion of the core remains uncovered for a long period of time. Even if core damage is initially stopped by injection, the core may uncover again, and core damage could proceed unless the energy removal from the RCS is equal to or exceeds the core decay heat.

**Table 7.** Effects of water addition on a degraded core.

| Core damage stage (temperature range) | Potential positive consequences of water addition | Potential negative consequences of water addition | Potential accident management strategies to prevent progression to next damage stage | Potential long-term accident management strategies to mitigate accident consequences |
|---|---|---|---|---|
| From core uncovery to ballooning of fuel rod cladding (saturation to 1100 K) | Injection at nominal HPIS rates or greater would prevent advance to the next stage (clad ballooning stage with temperatures >1100 K). Instruments remain well within measurement ranges. | Steam generated during recovery could pressurize the RCS, which could reduce HPIS injection rates. | Use HPIS if RCS pressure is low enough for nominal HPIS flows or use LPIS if pressure is low.<br>If initial RCS pressure is above pressure for nominal HPIS flows, use steam generator feed and bleed to reduce RCS pressure so that HPIS flow is at least nominal, or use RCS feed and bleed.<br>Depressurize the steam generator for temporary reduction of RCS pressure.<br>Restart RCS pumps for temporary core cooling | Ensure long-term borated ECC water supplies (refill BWST from external sources, etc.) |
| Fuel rod cladding ballooning and rupture (1100 K to 1500 K) | Injection at nominal HPIS rates or greater would prevent advance to the next stage (rapid zircaloy oxidation with temperatures >1500 K). Instruments remain within measurement ranges. | Steam generated during recovery could pressurize the RCS, which could reduce HPIS injection rates. A small amount of hydrogen would be generated but its effects on the system would not be significant. | Use HPIS if RCS pressure is low enough for nominal HPIS flows or use LPIS if pressure is low.<br>If initial RCS pressure is above pressure for nominal HPIS flows, use steam generator feed and bleed to reduce RCS pressure so that HPIS flow is at least nominal, or use RCS feed and bleed.<br>Depressurize the steam generator for temporary reduction of RCS pressure.<br>Restart RCS pumps for temporary core cooling | Ensure long-term borated ECC water supplies (refill BWST from external sources, etc.)<br>Depressurize the RCS using the PORVs to initiate the accumulators or the LPIS if HPIS is not available. |
| Early rapid zircaloy oxidation (1500 K to 1800 K) | HPIS injection rates will likely prevent advance to the late rapid oxidation stage (temperatures >1800 K). The uncertainty that injection will be successful in stopping core damage is much larger than during the previous stage. | Steam and hydrogen generated would cause pressurization of the RCS. Significant amounts of hydrogen may be produced. The effectiveness of adding water will be difficult to determine because CETs will approach their limits. Relocation of control material may begin. | Use HPIS if RCS pressure is low enough for nominal HPIS flows or use LPIS if pressure is low.<br>Restart RCS pumps for temporary core cooling. | Ensure long-term borated ECC water supplies (refill BWST from external sources, etc.)<br>If initial RCS pressure is above pressure for nominal HPIS flows, use steam generator feed and bleed to reduce RCS pressure so that HPIS flow is at least nominal, or use RCS feed and bleed.<br>Depressurize the RCS using the PORVs to initiate the accumulators or the LPIS if HPIS is not available. |

**Table 7.** (continued).

| Core damage stage (temperature range) | Potential positive consequences of water addition | Potential negative consequences of water addition | Potential accident management strategies to prevent progression to next damage stage | Potential long-term accident management strategies to mitigate accident consequences |
|---|---|---|---|---|
| Late rapid zircaloy oxidation (1800 K to 2100 K) | Simple calculations indicate very high (near full accumulator) rates may prevent the advance to stages where debris beds are formed. Code calculations predict HPIS rates will prevent advance to the next core damage stage but there is a large degree of uncertainty in the results because a debris bed is predicted to form. Although it is predicted to cool, modeling may have contributed to excessive heat transfer. | Injection rates must be high because core heatup is proceeding rapidly. Delay times (resulting from filling piping, downcomer and lower plenum) would become more important for adding water. Hydrogen and steam generation would cause rapid system pressurization. The effectiveness of adding water would be difficult to determine because many CETs would not be operating properly. | Inject at very high ECC rates, if possible. If very high rates are not possible, the effectiveness of adding water to prevent progress to the next core damage stage is not assured. | Inject ECC at the maximum rates possible.<br>If pressure is high, depressurize the RCS using the PORVs to increase HPIS and initiate the accumulators or the LPIS.<br>Ensure long-term borated ECC water supplies (refill BWST from external sources, etc.)<br>Initiate vessel cavity flooding if it is projected to be effective for the plant conditions. |
| Particulate debris bed formation (>2100 K, depending on conditions) | There is potential that adding water could cool and prevent advance to the next core damage stage. There is also the potential that water injected during this stage would cool debris during later stages if it relocates to the lower plenum. | There is the potential that adding water will not cool the debris. Steam generation could be high, depending on the debris bed porosity, power level, and temperature. Hydrogen generation could be high, depending on the amount of unoxidized zircaloy, its location, porosity, and temperature. Water injection may cause CETs to give low temperature readings when core temperatures remain high. | The effectiveness of adding water in preventing progress to the next core damage stage is not assured. | Inject ECC at the maximum rates possible.<br>Ensure long-term borated ECC water supplies (refill BWST from external sources, etc.)<br>Initiate vessel cavity flooding if it is projected to be effective for the plant conditions.<br>Initiate hydrogen control measures.<br>Initiate fission product control measures. |
| Cohesive debris bed formation (>2100 K depending on conditions) | There is the potential that water addition will cool and stabilize the crust preventing relocation. The molten pool will also begin to cool and eventually solidify. | There is a high likelihood that the crust will not stabilize and relocation will occur. Interaction between the molten fuel and the injected water could cause steam explosions. It will be difficult for plant accident management personnel to recognize this stage. Peripheral thermocouples may show the core is cool when it is not. | The effectiveness of adding water in preventing progress to the next core damage stage is not assured. | Inject ECC at the maximum rates possible.<br>Ensure long-term borated ECC water supplies (refill BWST from external sources, etc.)<br>Initiate vessel cavity flooding if it is projected to be effective for the plant conditions.<br>Initiate hydrogen control measures.<br>Initiate fission product control measures. |

**Table 7.** (continued).

| Core damage stage (temperature range) | Potential positive consequences of water addition | Potential negative consequences of water addition | Potential accident management strategies to prevent progression to next damage stage | Potential long-term accident management strategies to mitigate accident consequences |
|---|---|---|---|---|
| Lower head attack by molten core debris (>1700 K for metals, >2700 K for ceramics) | Failure of the lower head may be prevented. | Steam and hydrogen generated may raise the RCS pressure so that the vessel will fail earlier than otherwise. The melt ejection will be more dispersed, which will increase the likelihood of DCH. Use of water to cool the outside of the lower head may be delayed if operators believe adding water is being effective in stabilizing the core. | The effectiveness of adding water to prevent progress to the next core damage stage is not assured. | Inject ECC at the maximum rates possible.<br>Ensure long-term borated ECC water supplies (refill BWST from external sources, etc.)<br>Initiate vessel cavity flooding if it is projected to be effective for the plant conditions.<br>Initiate hydrogen control measures.<br>Initiate fission product control measures. |

If the core temperatures are greater than 1500 K (the rapid oxidation stage), the simple calculations indicate the HPIS flow rate would be below the water addition capacity that would prevent core damage from progressing to a higher stage. However, the SCDAP/RELAP5/ MOD3 results indicate that HPIS injection is adequate to prevent progression to the next core damage stage when it is injecting at its nominal rate. It should be possible to identify the onset of rapid oxidation from the CETs. However, this stage lasts only a short time, so actions to add water would need to be implemented very quickly. Methods for depressurizing the RCS, for example, opening the power-operated relief valves (PORVs), were found to be effective in removing decay heat when the break is relatively small.

Additional hydrogen will be produced when water is injected during the rapid oxidation stage, but the amount is not significant compared with the hydrogen that would be produced if the core damage progression is unmitigated. Because temperature measurements would become unreliable during this stage, confirmation of core recovery would require examination of the long-term trends of many instruments. Hydrogen detection monitors could identify this stage, but there would likely be a substantial delay between the time when hydrogen generation begins and when the hydrogen is detected.

Relocation of core materials first occurs when the stainless steel cladding of the control rods fails. Besides molten stainless steel, the relocating materials would also include control material (generally Ag-In-Cd or $B_4C$). Some zircaloy may also be liquified by the molten control materials at this stage. If unborated water is added to the core after the control materials have relocated, there is the possibility of re-criticality of the reactor. However, the recriticality issue is beyond the scope of this report.

If a cohesive debris bed is formed in the core region from the relocation of core materials (stainless steel, control materials, zircaloy, fuel, and their eutectics), energy removal from the degraded core cannot be assured, even if unlimited amounts of water are added to the vessel. Code calculations with HPIS initiated at 1800 K predict that the intact fuel rods would quench but formation of a small debris bed is predicted. The calculation indicates that this debris bed cools slowly, but this cooling is likely influenced by the modeling of the bed, which includes some porosity of the bed. The capability of water to remove energy from a cohesive debris bed depends on the bed's size, the power density of the bed, the porosity, and the thermal conductivity of the materials composing the bed. The power density and the thermal conductivities depend on the design and operating parameters of the reactor. Although the code predicts cooling of this debris bed, the success of adding water is uncertain for this and more advanced core damage stages because the debris bed characteristics are uncertain. As a result, alternate accident management strategies, such as adding water to the reactor vessel cavity, should be considered when CETs exceed 1500 to 1800 K or significant quantities of hydrogen are detected. Implementation of these alternate strategies would need to be pursued until there were long-term indications of core recovery.

Detection of the formation of cohesive debris beds and more advanced stages of core degradation would be very difficult using instrumentation currently installed in nuclear power plants. Temperature measurements would not be accurate and would not have signatures unique to these core damage stages. Interpreting the response of system pressure to water addition after the formation of a cohesive debris bed could be counterintuitive. Core materials would be in several configurations simultaneously: a cohesive bed, a particulate bed, and loose debris. Larger cohesive debris beds and particulate beds would result in smaller amounts of materials in the form of loose debris. If adding water to the core produces a rapid pressure rise, it is more likely that the cohesive and the particulate beds are small, and energy can be easily removed from them by the incoming water. If there is only a small system pressure rise

during water addition, the debris beds are more likely to be large, and energy cannot be efficiently removed from their interiors. Because they cannot be easily cooled, the interiors of large debris beds are likely to melt and eventually relocate to the reactor vessel lower plenum.

The possibility of steam explosions at the time of relocation of molten materials to the lower plenum is a negative effect that has not been evaluated in this work. This complex issue is currently being evaluated by separate programs within the NRC.

# 7. REFERENCES


1. U.S. NRC, *Severe Accident Risks: An Assessment of Five U.S. Nuclear Power Plants*, NUREG-1150, Revision 1, June 1989.

2. R. C. Bertucio and J. A. Julius, *Analysis of Core Damage Frequency: Surry Unit 1 Internal Events*, NUREG/CR-4550, Volume 3, Revision 1, Parts 1 and 2, SAND86-2084, April 1990.

3. M. B. Sattison and K. W. Hall, *Analysis of Core Damage Frequency: Zion Unit 1 Internal Events*, NUREG/CR-4550, Volume 7, Revision 1, EGG-2554, May 1990.

4. R. C. Bertucio and S. R. Brown, *Analysis of Core Damage Frequency: Sequoyah Unit 1 Internal Events*, NUREG/CR-4550, Volume 5, Revision 1, Parts 1 and 2, SAND86-2084, April 1990.

5. A. M. Kolaczkowski et al., *Analysis of Core Damage Frequency: Peach Bottom Unit 2 Internal Events*, NUREG/CR-4550, Volume 4, Revision 1, Parts 1 and 2, SAND86-2084, August 1989.

6. M. T. Drouin et al., *Analysis of Core Damage Frequency: Grand Gulf Unit 1 Internal Events*, NUREG/CR-4550, Volume 6, Revision 1, Parts 1 and 2, SAND86-2084, September 1989.

7. R. Hobbins et al., *Review of Experimental Results on Light Water Reactor Core Melt Progression*, *Nuclear Technology*, *95*, September 1991.

8. P. D. Bayless, *Experiment Results Report for LOFT Nuclear Experiment L3-5, L3-6, and L8-1*, EGG-LOFT-5471, Idaho National Engineering Laboratory, July 1981.

9. W. J. Camp et al., *MELPROG-PWR/MOD0: A Mechanistic Code for Analysis of Reactor Core Melt Progression and Vessel Attack under Severe Accident Conditions*, NUREG/CR-4909, SAND85-0237, April 1987.

10. C. M. Allison and S. T. Polkinghorne, "SCDAP/MOD1 Analysis of the Progression of Core Damage during the TMI-2 Accident," EGG-SAR-7104, Idaho National Engineering Laboratory, November 1985.

11. P. D. Bayless, "Analysis of Natural Circulation during a Surry Station Blackout using SCDAP/RELAP5," NUREG/CR-5214, EGG-2547, October 1988.

12. Z. R. Martinson, D. A. Petti, and B. A. Cook, *PBF Severe Fuel Damage Test 1-1 Test Results Report*, NUREG/CR-4684, EGG-2643, Vol. 1-2, October 1986.

13. D. A. Petti et al., "Power Burst Facility (PBF) Severe Fuel Damage Test 1-4 Test Results Report," NUREG/CR-5136, EGG-2542, April 1989.

14. P. Kuan, "Stability of Zircaloy Oxidation During Severe LWR Accidents," *Heat Transfer—Pittsburgh 1987, AIChE Symposium Series, 83*, 257, August 1987, pp. 297–300.

15. R. O. Gauntt, R. D. Gasser, and L. J. Ott, *The DF-4 BWR Control Blade/Channel Box Fuel Damage Experiment*, NUREG/CR-4671, SAND86-1443, March 1988.

16. J. M. Broughton et al., "A Scenario of the Three Mile Island Unit 2 Accident," *Nuclear Technology*, *87*, August 1989, pp. 34–53.

17. P. Hofmann et al, "Reactor Core Materials Interactions at Very High Temperatures," *Nuclear Technology, 87*, August 1989, pp. 146–186.

18. P. Kuan and D. W. Golden, "Thermal Behavior of Cohesive Debris Beds in a Degraded Nuclear Reactor," *AIChE Symposium Series, 85*, 69, August 1989, pp. 42–47.

19. T. L. Van Witbeck and J. Putnam, "Three Mile Island Unit 2, Annotated Sequence of Events, March 18, 1979," TDR-044, GPUN Corporation.

20. P. Kuan, J. L. Anderson, and E. L. Tolman, "Thermal Interactions during the TMI-2 2-B Coolant Pump Transient," *Transactions American Nuclear Society, 57*, October–November 1988, pp. 410–411.

21. P. Kuan, J. L. Anderson, and E. L. Tolman, "Thermal Interactions during the TMI-2 2-B Coolant Pump Transient," *Nuclear Technology, 87*, 1, August 1989.

22. A. D. Knipe, S. A. Ploger, and D. J. Osetek, *PBF Severe Fuel Damage Scoping Test—Test Results Report*, NUREG/CR-4683, EGG-2413, August 1986.

23. J. P. Adams et al., *Quick-Look Report on OECD LOFT Experiment LP-FP-2*, OECD LOFT-T-3804, Idaho National Engineering Laboratory, September 1985.

24. E. S. Sowa et al., "Heat Transfer Experiments through Beds of $UO_2$ in Boiling Sodium," *Transactions American Nuclear Society, 14*, November 1981, p. 725.

25. R. J. Lipinski, *A Model for Boiling and Dryout in Particle Beds*, NUREG/CR-2646, SAND82-0765, June 1982.

26. D. Squarer, L. E. Hochreiter, and A. T. Pieczynski, "Modes of Heat Removal from a Heat-Generating Debris Bed," *Nuclear Technology, 65*, April 1984, pp. 16–22.

27. G. Hofmann, "Dryout in Very Deep Particulate Beds," *Nuclear Engineering Design, 99*, 1987, p. 177.

28. A. W. Reed et al., *DCC-1/DCC-2 Degraded Core Coolability Analysis*, NUREG/CR-4390, SAND85-1967, October 1985.

29. S. S. Dosanjh, *Melt Progression in Severely Damaged Reactor Cores*, NUREG/CR-5029, December 1987.

30. E. L. Tolman and R. Moore, "TMI-2 Degraded Core Heatup and Cooldown Analysis," *Transactions American Nuclear Society, 57*, October 1988, p. 411.

31. D. E. Mitchell, M. L. Corradini, and W. W. Tarbell, *Intermediate Scale Steam Explosion Phenomena: Experiment and Analysis*, NUREG/CR-2145, SAND81-0124, September 1981.

32. R. Moore, *TMI-2 Reactor Vessel Lower Head Heatup Calculations*, EGG-TMI-7784, Idaho National Engineering Laboratory, September 1987.

33. J. L. Rempe et al., *Light Water Reactor Lower Head Failure Analysis*, NUREG/CR-5642, EGG-2618, October 1993.

34. G. L. Thinnes and R. L. Moore, "Comparison of Thermal and Mechanical Responses of the Three Mile Island Unit 2 Reactor Vessel," *Nuclear Technology, 87*, 1, August 1989.

35. T. G. Theofanous et al., *An assessment of Steam-Explosion-Induced Containment Failure*, NUREG/CR-5050, February 1989.

36. Anthony J. Baratta et al., "The Overall Source Range Monitor Response During the Three Mile Island Unit 2 Accident," *Nuclear Technology, 87*, 4, December 1989.

37. J. P. Adams and V. T. Berta, "Monitoring Reactor Vessel Liquid Level With a Vertical String of Self-Powered Neutron Detectors," *Nuclear Science and Engineering, 88*, 1984, pp. 367–375.

38. J. P. Adams and V. T. Berta, "Response of LOFT Self-Powered Neutron Detectors to Reactor Coolant Density Variations During LOCA Simulations," *Nuclear Technology, 58*, August 1982.

39. Reference Safety Analysis Report, Westinghouse Nuclear Energy Systems, 1975.

40. Babcock & Wilcox, *Standard Safety Analysis Report*, 1978.

41. BWR/6, *Standard Safety Analysis Report*, General Electric Corporation.

42. ANSI/ANS-5.1, *1979 Decay Heat Standard for Light Water Reactors*.

43. R. E. Pawel, J. V. Cathcart, and R. A. McKee, "The Kinetics of Oxidation of Zircaloy-4 in Steam at High Temperatures," *Electrical Chemical Science and Technology, 126*, 7, July 1979.

44. V. F. Urbanic and T. R. Heidrick, "High-Temperature Oxidation of Zircaloy-2 and Zircaloy-4 in Steam," *Journal of Nuclear Materials, 75*, 1978, pp. 251–261.

45. E. W. Coryell et al., *DESIGN REPORT: SCDAP/RELAP5 REFLOOD OXIDATION MODEL*" Informal Report, EGG-RAAM–10307, Idaho National Engineering Laboratory, Idaho, October 1992.

46. D. L. Knudson and C. A. Dobbe, *Assessment of the Potential for High Pressure Melt Ejection Resulting from a Surry Station Blackout Transient*, NUREG/CR-5949, EGG-2689, December 1993.

# Appendix A

# Examination of Water Addition Capabilities for the Five NUREG-1150 Plants

Marc D. Rumminger
Daniel J. Pafford

# EXAMINATION OF WATER ADDITION CAPABILITIES FOR THE FIVE NUREG-1150 PLANTS

MARC D. RUMMINGER AND DANIEL J. PAFFORD

OCTOBER 1991

EG&G Idaho, Inc.
Idaho Falls, Idaho 83415

Prepared for the
U.S. Nuclear Regulatory Commission
Under DOE Idaho Operations Office
Contract No. DE-AC07-76ID01570

# CONTENTS


1. SUMMARY . . . . . A-7

2. INTRODUCTION . . . . . A-13

3. PLANT FEATURES . . . . . A-15

4. METHODOLOGY . . . . . A-23

   4.1 Overall Methodology . . . . . A-23

   4.2 Plant Specific Methodology . . . . . A-24

5. RESULTS . . . . . A-31

   5.1 Surry Results . . . . . A-31

   5.2 Zion Results . . . . . A-40

   5.3 Sequoyah Results . . . . . A-54

   5.4 Peach Bottom Results . . . . . A-62

   5.5 Grand Gulf Results . . . . . A-69

6. CONCLUSIONS . . . . . A-77

7. REFERENCES . . . . . A-83


# TABLES


1. Summary of design features at Surry Unit 1 . . . . . A-16

2. Summary of design features at Zion Unit 1 . . . . . A-17

3. Summary of design features at Sequoyah Unit 1 . . . . . A-18

4. Summary of design features at Peach Bottom Unit 2 . . . . . A-19

5. Summary of design features at Grand Gulf Unit 1 . . . . . A-21

6. Description of injection system failure mechanism characteristics . . . . . A-25

7. Injection failure mechanism descriptions for the dominant accident sequences at Surry . . . . . A-34

8. Injection system failure mechanism characteristics for the dominant accident sequences at Surry . . . . . A-38

9. Contribution by injection system failure mechanisms to the total core damage frequency at Surry . . . . . A-39

10. Injection failure mechanism descriptions for the dominant plant damage states at Zion . . . . . A-44

11. Injection system failure mechanisms characteristics for the dominant plant damage states at Zion . . . . . A-51

12. Contribution by injection system failure mechanisms to the total core damage frequency at Zion . . . . . A-53

13. Injection failure mechanism descriptions for the dominant accident sequences at Sequoyah . . . . . A-57

14. Injection system failure mechanism characteristics for the dominant accident sequences at Sequoyah . . . . . A-60

15. Contribution by injection system failure mechanisms to the total core damage frequency at Sequoyah . . . . . A-61

16. Injection failure mechanism descriptions for the dominant accident sequences at Peach Bottom . . . . . A-64

17. Injection system failure mechanism characteristics for the dominant accident sequences at Peach Bottom . . . . . A-67

18. Contribution by injection system failure mechanisms to the total core damage frequency at Peach Bottom . . . . . A-68

19. Injection failure mechanism descriptions for the dominant accident sequences at Grand Gulf . . . . . A-72

20. Injection system failure mechanism characteristics for the dominant accident sequences at Grand Gulf . . . . . A-75

21. Contribution by injection system failure mechanisms to the total core damage frequency at Grand Gulf . . . . . A-76

# 1. SUMMARY

This report identifies postulated sequences where water addition into the primary system will reduce the core damage frequency (CDF) as determined in the NUREG-1150 and supporting documentation such as NUREG/CR-4550 for the five plants described therein. The timing of the water injection system failures is estimated based upon the defined sequence of events. Plant conditions which may prevent sufficient water addition are reviewed.

For the five plants studied in the NUREG-1150 program, examination of the postulated sequences has revealed that insufficient water being added to prevent core damage occurs in all of the sequences. The results for the five plants are summarized below.

Surry

At Surry, 17% of the CDF is due to sequences involving injection system failures in which no feasible recovery action could be implemented. The sequences involve interfacing system (V sequence) loss of coolant accidents (LOCAs), large and medium break LOCAs, and anticipated transients without scram (ATWS) events. However, the remaining 83% of the CDF is due to sequences in which core uncovery might be prevented if additional and innovative recovery actions were implemented. The CDF could be reduced up to 67%, if additional onsite ac power sources were provided; up to 10%, if the reactor vessel was depressurized so that available low pressure injection systems could be utilized; up to 4%, if additional stored water sources or if refilling of the refueling water supply storage tank (RWST) could be continued for an indefinite period of time; and up to 2%, if additional reactor scram procedures and devices were implemented.

Of those sequences that might be prevented if additional onsite ac power sources were provided, the injection systems are not available beginning at the accident initiation. For approximately 27% (based upon CDF) of these sequences, the core uncovers in approximately one hour and successful accident management actions would have to be initiated within this time frame to

prevent core damage. For the remaining 73%, the time of core uncovery ranges from approximately two to seven hours, which allows more time for actions to be taken.

For those sequences that might be prevented if the reactor vessel was depressurized so that available low pressure injection systems could be utilized, the high pressure injection system is failed immediately. For approximately 53% of these sequences, the time at which the core uncovers is not specified in the NUREG-1150 documentation. For 21% of these sequences, the time to core uncovery ranges from approximately 15 to 50 minutes which is a relatively short period of time for initiation of the necessary accident management actions. For the remaining 26%, the time of core uncovery ranges from approximately 50 minutes to 17 hours.

For those sequences that might be prevented if additional stored water sources were provided or if refilling of the RWST could be continued for an indefinite period of time, the high pressure system fails in the recirculation mode. The time of core uncovery is greater than ten hours for all of these sequences which should allow personnel sufficient time to complete the necessary actions.

For those sequences that might be prevented if additional reactor scram procedures and devices were implemented the high pressure injection systems are failed immediately. The time to core uncovery for these sequences is not specified in the available documentation.

Zion

At Zion, only 4.4% of the CDF is due to plant damage states (PDSs) involving injection system failures in which no feasible recovery action could be implemented. These PDSs involve V sequences, and large and medium break LOCAs. However, the remaining 95.6% of the CDF is due to PDSs in which core uncovery might be prevented if additional and innovative recovery actions were implemented. The CDF could be reduced up to 86%, if pump seal LOCAs, loss of component cooling, or loss of service water supplies could be prevented; up to 4%, if additional onsite ac power sources were provided; up to 3.5%, if

additional stored water sources or if refilling of the RWST could be continued for an indefinite period of time; and up to 2%, if additional reactor scram procedures and devices were available.

The times of injection system failures at Zion are summarized below. However, estimates of the time to core uncovery were not available for most of the PDSs and are omitted.

For those PDSs that might be prevented if pump seal LOCAs, loss of component cooling, and loss of service water could be prevented, the injection systems are failed initially. For those PDSs that might be prevented if additional onsite ac power sources were provided, approximately 50% (based on CDF) involve initial failures of the high pressure injection systems. The remaining 50% involve failures of the high pressure injection systems in the recirculation mode. Of those PDSs that might be prevented if additional stored water sources or if refilling of the RWST could be continued for an indefinite period of time, all involve failures of the high pressure injection system in the recirculation mode. Finally, of those PDSs that might be prevented if additional reactor scram procedures and devices were available, all involve initial failures of the high pressure injection systems.

Sequoyah

At Sequoyah, 20% of the CDF is due to sequences involving injection system failures in which no feasible recovery action could be implemented. The sequences include a V sequence, large and medium break LOCAs, and ATWS events. However, the remaining 80% of the CDF is due to sequences in which core uncovery might be prevented if additional and innovative recovery actions were implemented. The CDF could be reduced up to 46%, if failures of the high and low pressure recirculation systems could be eliminated; up to 26%, if additional onsite ac power sources were provided; up to 5% if the reactor vessel was depressurized so that available low pressure injection systems could be utilized; and up to 4%, if additional stored water sources or if refilling of the RWST could be continued for an indefinite period of time.

For those sequences that might be prevented if failures of the high and low pressure recirculation systems were be eliminated, the injection system failures occur in the recirculation mode. For 76% (based upon CDF) of these sequences, the time to core uncovery is estimated as being greater than 17 hours which is adequate time for a wide range of accident management actions. For the remaining 24%, the range of time to core uncovery is estimated as being from 45 minutes to 17 hours.

For those sequences that might be prevented if additional onsite ac power sources were provided, all involve initial failures of the high pressure injection system. For 68% of the sequences, the time to core uncovery is approximately one hour. For the remaining 32%, the time of core uncovery ranges from approximately two to seven hours.

Of those sequences that might be prevented if the reactor vessel was depressurized so that available low pressure injection systems could be utilized, all involve initial failures of the high pressure injection system. The time to core uncovery for these sequences is not specified.

Of those sequences that might be prevented if additional stored water sources or if refilling of the RWST could be continued for an indefinite period of time, all involve failure of the high pressure injection system in the recirculation mode. The time to core uncovery for these sequences is not specified.

**Peach Bottom**

At Peach Bottom, 18% of the CDF is due to sequences involving injection system failures in which no feasible recovery action could be implemented. The sequences include large and medium break LOCAs, and very short term ATWS events. However, the remaining 82% of the CDF is due to sequences in which core uncovery might be prevented if additional and innovative recovery actions were implemented. The CDF could be reduced up to 42%, if a combination of additional reactor vessel depressurization mechanisms and additional onsite ac power supplies to the low pressure injection systems were implemented; up to 5%, if only additional onsite ac power sources were provided; and up to 36%,

if a combination of additional reactor scram and reactor depressurization mechanisms were implemented.

For those sequences that might be prevented if a combination of additional reactor vessel depressurization mechanisms and additional onsite ac power supplies to the low pressure injection systems were implemented, the high pressure core injection (HPCI) and reactor core isolation cooling (RCIC) systems fail in approximately ten hours due to loss of room cooling or battery depletion. For these sequences, the core uncovers in approximately 10 to 13 hours. This time frame should be adequate for implementation of accident management strategies.

For those sequences that might be prevented if only additional onsite ac power sources were provided, the HPCI and RCIC systems fail at the start of the sequence. For these sequences the time to core uncovery is approximately one hour. Implementation of accident management strategies in this short time period could have a low likelihood of success unless they were well planned and executed.

For those sequences that might be prevented if a combination of additional reactor scram and reactor depressurization mechanisms were implemented, the HPCI and RCIC systems fail in less than one half hour due to high suppression pool temperature. The control rod drive (CRD) injection system is operating, but cannot mitigate the sequence. For these sequences, the time to core uncovery is not specified.

**Grand Gulf**

At Grand Gulf, all of the CDF is due to sequences in which core uncovery might be prevented if additional and innovative recovery actions were implemented. The CDF could be reduced up to 95%, if additional onsite ac and dc power sources were provided; up to 1.5%, if additional reactor vessel depressurization mechanisms were implemented; up to 1.5%, if additional pump room cooling was provided; and up to 1.6%, if a combination of all of the recovery actions were implemented.

For those sequences that might be prevented if additional onsite ac and dc power sources were provided, 99% of the sequences (based upon CDF) involve initial failures of the HPI systems. The time to core uncovery for these sequences is approximately one hour. The remaining 1% involve late failures of the operator to activate the firewater system. The time to core uncovery for these sequences is approximately twelve hours.

For those sequences that might be prevented if additional reactor vessel depressurization mechanisms were implemented, more than 99% involve initial failure of the high pressure core spray system (HPCS). For these sequences, the CRD and RCIC systems are operating, but are not sufficient to make up the coolant loss. The time to core uncovery is approximately one hour.

The sequence that might be prevented if additional pump room cooling was provided involves late failure of the HPCS due to pump room heatup. The CRD and RCIC systems are operating, but are not sufficient to make up the coolant loss. The time to core uncovery is estimated as more than 12 hours.

Finally, the sequence that might be prevented if a combination of all of the recovery actions were implemented involves a late failure of the firewater system. The time of core uncovery is estimated as more than 12 hours.

The majority of the Grand Gulf sequences proceed to core damage in about one hour. Therefore, accident management actions would need to be well planned and executed to successfully prevent core damage.

# 2. INTRODUCTION

Understanding the potential consequences of water addition to a degraded core during a severe core accident is important for the development of effective accident management strategies. While the need to add water to cool the damaged core is not at issue, the effects of water addition on the system must be understood to ensure proper strategies can be developed. This issue arises primarily because 1) water contacting high temperature corium can generate pressures which may, for example, threaten the primary system boundary or require immediate operator action to mitigate, 2) unborated water entering the core may lead to recriticality, and 3) steam generation accompanying water addition may lead to rapid oxidation of zircaloy cladding and significant hydrogen generation rates which may require specific operator action. Obviously, to correctly assess these effects and thereby optimize management strategies requires a knowledge of the characteristics of the damaged core states in terms of configuration and coolability during the accident sequences.

Results presented in the NUREG-1150 program identify potentially important system failures. Identification of the dominant accident sequences and plant damage states (PDSs) conveys the most probable sequences to accident managers and system modelers. With detailed information about the dominant accident sequences, accidents can be more effectively modeled. Knowledge of sequence progression and timing can enable accident managers to focus on vulnerable systems and develop innovative accident mitigation procedures.

This report is part of a program to assess the potential effects of water addition to the vessel during a severe accident. The objectives of this project are 1) to identify postulated sequences where water addition into the primary will reduce the core damage frequency as determined for the five plants studied in the NUREG-1150 program, 2) to estimate the time at which the core uncovers for identified accident sequences, and 3) to review factors that may prevent addition of water.

This report presents an examination of the five plants studied in and the results obtained from the NUREG-1150 program.[1] The accident sequences defined there are examined in terms of what injection systems are or are not available for the addition of water. Injection system failure mechanisms are identified and the time of failure and the time at which the core uncovers are estimated. The contributions to the core damage frequency are determined for the various injection system failure mechanisms. Results from this examination can be used to identify the sequences and systems that should be modeled for other tasks in this program to evaluate the potential consequences of water addition to a degraded core.

Descriptions and important system design features of the five plants analyzed are described in Section 3. The methodology used to obtain the information is discussed in Section 4. Section 5 presents, for each plant, the dominant accident sequences, the injection system failure mechanisms, the estimated time of failure, the estimated time at which the core uncovers for each sequence, and the contribution of each injection system failure mechanism to the total plant core damage frequency.

# 3. PLANT FEATURES

The five commercial plants examined in this report are those that were analyzed in the NUREG-1150 program (see Reference 1.) The five plants are:

- Surry Unit 1; a three-loop Westinghouse PWR rated at 788 MWe and housed in a sub-atmospheric containment.

- Zion Unit 1; a four-loop Westinghouse PWR rated at 1100 MWe and housed in a large, dry containment.

- Sequoyah Unit 1; a four-loop Westinghouse PWR rated at 1148 MWe and housed in an ice condenser containment.

- Peach Bottom Unit 2; a General Electric BWR-4 rated at 1150 MWe and housed in a Mark I containment.

- Grand Gulf Unit 1; a General Electric BWR-6 rated at 1250 MWe and housed in a Mark III containment.

Important system design features for the five plants are described in Tables 1 through 5.

**Table 1.** Summary of design features at Surry Unit 1.[1]

| | |
|---|---|
| 1. High Pressure Injection (HPI) | a. Safety injection and recirculation system with 2 trains and 3 pumps.<br>b. Charging system provides normal makeup flow with safety injection crosstie to Unit 2. |
| 2. Low Pressure Injection (LPI) | a. Low-pressure injection and recirculation system with 2 trains and 3 pumps. |
| 3. Heat Removal Systems | a. Power conversion system.<br>b. Auxiliary feedwater system (AFWS) with 3 trains and 3 pumps (2 motor driven pumps, 1 turbine driven) and crosstie to Unit 2 AFWS. |
| 4. Reactivity Control Systems | a. Control rods.<br>b. Chemical and volume control systems. |
| 5. Key Support Systems | a. dc power provided by 2-hour design basis station batteries.<br>b. Emergency ac power provided by 1 dedicated and 1 swing diesel generator (both self-cooled).<br>c. Component cooling water provides normal cooling to reactor coolant pump thermal barriers.<br>d. Service water is gravity-fed system that provides heat removal from containment following an accident. |

Table 2. Summary of design features at Zion Unit 1.[1]

| | |
|---|---|
| 1. High Pressure Injection (HPI) | a. Two centrifugal charging pumps.<br>b. Two 1500 psig safety injection (SI) pumps.<br>c. Charging pumps inject through boron injection tank.<br>d. Provides seal injection flow.<br>e. Requires component cooling water. |
| 2. Low Pressure Injection (LPI) | a. Two residual heat removal (RHR) pumps deliver flow when RCS is below about 170 psig.<br>b. Heat exchangers downstream of pumps provide recirculation heat removal.<br>c. Recirculation mode takes suction on containment sump and discharges to the RCS, HPI suction, and/or containment spray pump suction.<br>d. Pumps and heat exchangers require component cooling water. |
| 3. Auxiliary Feedwater | a. Two 50 percent motor driven pumps and one 100 percent turbine driven pump.<br>b. Pumps take suction from own unit condensate storage tank (CST) but can be manually crosstied to the other unit's CST. |
| 4. Emergency Power System | a. Each unit consists of three 4160 VAC class IE buses, each feeding one 480 VAC class 1E bus and motor control center.<br>b. For the 2 units there are 5 diesel generators, with one being a swing diesel generator shared by both units.<br>c. Three trains of dc power are supplied from the inverters and 3 unit batteries. |
| 5. Component Cooling Water | a. Shared system between both units.<br>b. Consists of 5 pumps, 3 heat exchangers, and 2 surge tanks.<br>c. Cools RHR heat exchangers, reactor coolant pump motors and thermal barriers, RHR pumps, SI pumps, and charging pumps.<br>d. One of 5 pumps can provide sufficient flow. |
| 6. Service Water | a. Shared system between both units.<br>b. Consists of 6 pumps and 2 supply headers.<br>c. Cools component cooling heat exchangers, containment fan coolers, diesel generator coolers, auxiliary feedwater pumps.<br>d. Two of 6 pumps can supply sufficient flow. |

**Table 3.** Summary of design features at Sequoyah Unit 1.[1]

| | |
|---|---|
| 1. High Pressure Injection (HPI) | a. Charging system provides feed and bleed cooling and seal injection flow to the reactor coolant pump (RCP) seals, with 2 centrifugal charging pumps.<br>b. Safety injection system provides high head injection, with 2 trains and 2 pumps. |
| 2. Low Pressure Injection (LPI) | a. Low pressure injection/recirculation system provides emergency coolant injection and recirculation following LOCA, with 2 trains and 2 pumps. |
| 3. Heat Removal Systems | a. Power conversion system.<br>b. Auxiliary feedwater system, with 3 trains and 2 pumps (2 motor driven pumps, 1 turbine driven pump.) |
| 4. Reactivity Control Systems | a. Control rods.<br>b. Chemical and volume control systems. |
| 5. Key Support Systems | a. dc power, with 2-hour station batteries.<br>b. Emergency ac power, with 2 diesel generators for each unit, each diesel generator dedicated to a 6.9 kV emergency bus (these buses can be crosstied to each other via a shutdown utility bus.)<br>c. Component cooling water provides cooling water to RCP thermal barriers and selected ECCS equipment, with 5 pumps and 3 heat exchangers for both Units 1 and 2.<br>d. Service water system, with 8 self cooled pumps for both Units 1 and 2. |

**Table 4.** Summary of design features at Peach Bottom Unit 2.[1]

| | |
|---|---|
| 1. High Pressure Injection Systems (HPI) | a. High pressure coolant injection (HPCI) system provides coolant to the reactor vessel during accidents in which system pressure remains high, with 1 train and 1 turbine driven pump (TDP).<br>b. Reactor core isolation cooling (RCIC) system provides coolant to the reactor vessel during accidents in which system pressure remains high, with 1 train and 1 (TDP).<br>c. Control rod drive system provides backup source of high pressure injection, with 2 pumps/210 gpm (total)/1,100 psia. |
| 2. Low Pressure Injection Systems (LPI) | a. Low pressure core spray (LPCS) system provides coolant to the reactor vessel during accidents in which vessel pressure is low, with 2 trains and 4 motor driven pumps (MDP).<br>b. Low pressure coolant injection (LPCI) system provides coolant to the reactor vessel during accidents in which vessel pressure is low, with 2 trains and 4 pumps.<br>c. High pressure service water crosstie system provides coolant makeup source to the reactor vessel during accidents in which normal sources of emergency injection have failed (low RPV pressure), with 1 train and 4 pumps for crosstie.<br>d. Automatic depressurization system for depressurizing the reactor vessel to a pressure at which the LPI systems can inject coolant to the reactor vessel; 5 ADS relief valves/capacity 820,000 lb/hr. |
| 3. Key Support Systems | a. dc power with up to 12 hour station batteries.<br>b. Emergency ac power from 4 diesel generators shared between 2 units.<br>c. Emergency service water provides cooling water to safety systems and components shared by 2 units. |

Table 4. Continued.

| | |
|---|---|
| 4. Heat Removal Systems | a. Residual heat removal/suppression pool cooling system to remove heat from the suppression pool during accidents, with 2 trains and 4 pumps.<br>b. Residual heat removal/shutdown cooling system to remove decay heat during accidents in which reactor vessel integrity is maintained and reactor at low pressure, with 2 trains and 4 pumps.<br>c. Residual heat removal/containment spray system to suppress pressure and remove decay heat in the containment during accidents, with 2 trains and 4 pumps. |
| 5. Reactivity Control Systems | a. Control rods.<br>b. Standby liquid control system, with 2 parallel positive displacement pumps rated at 43 gpm, but each with 86 gpm equivalent because of the enriched boron. |

Table 5. Sum of design features at Grand Gulf Unit 1.[1]

| | |
|---|---|
| 1. High Pressure Injection Systems (HPI) | a. High pressure core spray (HPCS) system provides coolant to the reactor vessel during accidents in which system pressure remains high or low, with 1 train and 1 diesel driven pump (DDP).<br>b. Reactor core isolation cooling (RCIC) system provides coolant to the reactor vessel during accidents in which system pressure remains high, with 1 train and 1 turbine driven pump (TDP).<br>c. Control rod drive system provides backup source of high pressure injection, with 2 pumps/238 gpm (total)/1103 psia. |
| 2. Low Pressure Injection Systems (LPI) | a. Low pressure core spray (LPCS) system provides coolant to the reactor vessel during accidents in which vessel pressure is low, with 1 train and 1 motor driven pump (MDP).<br>b. Low pressure coolant injection (LPI) system provides coolant to the reactor vessel during accidents in which vessel pressure is low, with 3 trains and 3 pumps.<br>c. Standby service water crosstie system provides coolant makeup source to the reactor vessel during accidents in which normal sources of emergency injection have failed, with 1 train and 1 pump (for crosstie.)<br>d. Firewater system is used as a last resort source of low pressure coolant injection to the reactor vessel, with 3 trains, 1 MDP, 2 DDP.<br>e. Condensate system used as a backup injection source.<br>f. Automatic depressurization system depressurizes the reactor vessel to a pressure at which the LPI systems can inject coolant to the reactor vessel, with 8 relief valves/capacity 900,000 lb/hr. |

Table 5. Continued.

| | |
|---|---|
| 3. Heat Removal Systems | a. Residual heat removal (RHR)/suppression pool cooling system removes decay heat from the suppression pool during accidents, with 2 trains and 2 pumps.<br>b. RHR/shutdown cooling system removes decay heat during accidents in which reactor vessel integrity is maintained and reactor is at low pressure, with 2 trains and 2 pumps.<br>c. RHR/containment spray system suppresses pressure in the containment during accidents, with 2 trains and 2 pumps. |
| 4. Reactivity Control Systems | a. Control rods.<br>b. Standby liquid control system, with 2 parallel positive displacement pumps rated at 43 gpm. |
| 5. Key Support Systems | a. dc power with 12-hour station batteries.<br>b. Emergency ac power, with 2 diesel generators and third diesel generator dedicated to HPCS but with crossties.<br>c. Suppression pool makeup system provides water from the upper containment pool to the suppression pool following a LOCA.<br>d. Standby service water provides cooling water to safety systems and components. |

# 4. METHODOLOGY

This section first describes the overall methodology used in examining accident sequences in terms of the injection system failure mechanisms, the estimated times of failure, the estimated time at which the core uncovers, and the contribution of each injection system failure mechanism to the total core damage frequency (CDF). This general description is followed by the details of the methodology used for each plant. While the overall methodology was similar for the five plants, some plant specific difference were encountered. These differences were most commonly due to differences in the types of injection systems, to the types of failures identified, or to the basic approach used in the NUREG/CR-4550 analyses.

## 4.1 Overall Methodology

The overall methodology used is as follows. The dominant accident sequences and their descriptions were obtained from the NUREG/CR-4550 analyses of Surry, Zion, Sequoyah, Peach Bottom, and Grand Gulf.[2,3,4,5,6] For all of the plants examined except Grand Gulf, the CDF information for the sequences were obtained from the respective NUREG/CR-4550 analyses. The Grand Gulf NUREG/CR-4550 analysis was unique among the five plants in that some of the accident sequences were split among different plant damage states (PDSs). However, the contribution of each accident sequence to each PDS was not presented in the NUREG/CR-4550. Therefore, an alternative method for Grand Gulf was necessary. This alternative method is described later in the Grand Gulf plant specific methodology.

The contribution to the CDF of each injection system failure mechanism identified in the step above was derived from the gathered information. This derivation consisted of two steps. First, each sequence was binned with a simplified three characteristic failure mechanism description which consisted of the source or cause of the injection failure mechanism, which injection system is failed, and at what time the system fails. The second step involved sorting the similar characteristic combinations to obtain the contribution of

each failure mechanism to the total CDF. Table 6 summarizes the three characteristic descriptions used for all five plants.

## 4.2 Plant Specific Methodology

### Surry

The first plant analyzed was Surry. Twenty eight dominant accident sequences were identified in the NUREG/CR-4550 analysis (see Reference 2.) These accident sequences were grouped into seven PDSs, also identified in the NUREG/CR-4550 analysis. For each sequence, the mean CDF, the contribution of that sequence to the PDS CDF, and to the total plant CDF were obtained from Tables 5-3 and 5-4 of Reference 2. The status of the high pressure (HPI) and low pressure injection (LPI) systems and the motor and turbine driven auxiliary feedwater systems (AFWS) were identified from information presented in Sections 4.4 and 5.2 of Reference 2. Finally, for each sequence a brief description of the reactor coolant system status and predicted range of times at which the core uncovers were obtained from the same reference. All of this information was tabulated collectively.

In determining the CDF contribution of each injection system failure mechanism, not all of the characteristic descriptions in Table 6 are applicable for Surry. For the first characteristic, only the POWER, RECIRC, FAIL, and ATWS attributes apply; for the second characteristic, both the HPI and LPI attributes apply; and for the third characteristic, only the INIT and RECIRC attributes apply.

### Zion

The next plant analyzed was Zion. For this plant, 205 accident sequences with a CDF greater than $1.0 \times 10^{-9}$ per reactor year were identified in the NUREG/CR-4550 analysis (see Table 5-4, Reference 3.) Because of the large number of accident sequences for this plant, the material gathered from the NUREG/CR-4550 was categorized by PDSs rather than by accident sequence. The number of PDSs identified for this plant was 58. These PDSs were then

Table 6. Description of injection system failure mechanism characteristics.

| Attribute-Mnemonic | Description |
|---|---|
| **Characteristic 1 - Injection system failure mechanism** | |
| POWER | Injection system does not operate because of total or partial power failure. |
| RECIRC | Injection system operates initially, fails in recirculation mode. |
| FAIL | Injection system fails due to hardware failure. |
| ATWS | Injection system fails due to ATWS induced events. |
| OPERATOR | Injection system fails due to operator error. |
| CCW/SW | Injection system fails due to loss of component cooling water/service water. |
| SAFETY | Injection system does not operate due to safety injection actuation failure. |
| **Characteristic 2 - Failed injection system** | |
| HPI | High pressure injection system is failed. |
| LPI | Low pressure injection system is failed. |
| **Characteristic 3 - Time of failure** | |
| INIT | Injection system fails at moment of request or soon after. |
| RECIRC | Injection system fails in recirculation mode. |
| LATE | Injection system operates for some time, then fails. |

arranged into five plant damage state groups (PDSGs). The five PDSGs were defined in the Zion accident progression event tree analysis.[7] Similar to that done for Surry, for each of the 58 PDSs, the CDF, the contribution of that PDS to the PDSG CDF, and to the total plant CDF were obtained from Tables 5-2 and 5-4 of Reference 3. Point estimates of the CDF are reported here instead of the mean values because only a limited data uncertainty analysis was performed in the Zion NUREG/CR-4550 analysis. The status of the HPI and LPI systems and the motor and turbine driven AFW systems were obtained from Sections 4.4 and 5.1 of Reference 3. Finally, for each sequence, a brief description of the reactor coolant system status and predicted range of times at which the core uncovers were obtained from the same reference. All of this information was tabulated collectively.

The failure mechanism contributions to the total CDF were obtained using the same method used for Surry. However, some additional characteristic attributes were used in grouping the injection system failure mechanisms. The characteristic attributes listed in Table 6 applicable for Zion were for the first characteristic: POWER, RECIRC, FAIL, ATWS, OPERATOR, CCW/SW, and SAFETY; for the second characteristic: HPI and LPI; and for the third characteristic: INIT and RECIRC.

In labeling the failure characteristics, two of the PDSs were split into more than one failure characteristic descriptions. PDS S1IBYYYYY was split between FAIL-LPI-INIT and OPERATOR-LPI-RECIRC. The PDS CDF was split between the two failure descriptions as 5.3E-07 and 4.9E-06, respectively. The split information for this PDS was obtained from Tables 4.4-21 and 5-4 of Reference 3. Similarly, PDS TLCYNNYY was split between ATWS-HPI-INIT and FAIL-HPI-INIT. This PDS CDF was split between the two failure descriptions as 5.8E-06 and 2.7E-07, respectively. The split information for this PDS was obtained from Tables 4.4-51, 4.4-61, 4.4-91, 4.4-101, 4.4-131, 4.4-141, and 5-4 of the same reference.

**Sequoyah**

The next plant analyzed was Sequoyah. Twenty three dominant accident sequences were identified in the NUREG/CR-4550 analysis (see Reference 4.) These accident sequences were grouped into seven PDSs. As was done for the previous two PWR plants, for each sequence, the mean CDF, the contribution to the PDS CDF, the contribution to the total plant CDF, the status of the HPI and LPI systems, the status of the AFW systems, the status of the reactor coolant system, and the predicted range of times at which the core uncovers were obtained. The accident sequences and mean CDFs were obtained from Table 5-3 of Reference 4. The qualitative descriptions of the injection systems, feedwater systems, and the RCS status were obtained from Sections 4.4 and 5.2 of the same reference.

The failure mechanism contributions to the total CDF were obtained using the same method used for the two previous PWR plants analyzed. The characteristic attributes used in grouping the injection system failure modes for Sequoyah were for the first characteristic: POWER, RECIRC, FAIL, and ATWS; for the second characteristic: HPI and LPI; and for the third characteristic: INIT and RECIRC.

**Peach Bottom**

The next plant analyzed was Peach Bottom. Eighteen dominant accident sequences leading to core damage were identified in the NUREG/CR-4550 analysis (see Reference 5.) These accident sequences were grouped into four super PDSs. For each sequence, the mean CDF, the contribution to the PDS CDF, the contribution to the total plant CDF, the status of the HPI and LPI systems, the status of the reactor coolant system, and the predicted range of times at which the core uncovers were obtained. The accident sequences and mean CDFs were obtained from Table 5-7 of Reference 5. The qualitative descriptions of the injection systems and the RCS status were obtained from Sections 4.4 and 5.2 of the same reference.

The HPI systems examined include the three systems listed in Table 4: the high pressure coolant injection (HPCI) system, the reactor core isolation

cooling (RCIC) system, and the control rod drive (CRD) system. The status of all three systems are tabulated in the results section.

The LPI systems examined include the three systems listed in Table 4: the low pressure coolant injection (LPCI) system, the low pressure core spray (LPCS) system, and the high pressure service water (HPSW) system. The status of all three systems are tabulated.

The contribution of the injection system failure mechanisms to the total core damage frequency was obtained using the same method used for the PWR plants. The characteristic attributes used in grouping the injection system failure modes for Peach Bottom were for the first characteristic: POWER, FAIL, ATWS, and OPERATOR; for the second characteristic: HPI and LPI; and for the third characteristic: INIT and LATE.

**Grand Gulf**

The final plant analyzed was Grand Gulf. Seven accident sequences leading to core damage were identified in the NUREG/CR-4550 analysis (see Table 4.10-3 of Reference 6.) These accident sequences were grouped into twelve PDSs. Of the five plants studied in the NUREG-1150 analysis, this is the only plant in which individual accident sequence groups were split among more than one PDS. This was accomplished by splitting the cut sets that make up each accident sequence group into the appropriate PDSs. Of the seven accident sequence groups, six were split into two or more PDSs. Only accident sequence T1B-13 was not split. The accident sequences that were split between more than one PDS were as follows. The three accident sequences, T1B-16, T1B-17, and T1B-21, were split among PDS-1, PDS-2, PDS-3, and PDS-7; accident sequence T1B-4 was split between PDS-4, PDS-5, and PDS-6; accident sequence TC-74 was split between PDS-9 and PDS-10; and, finally, accident sequence T2-56 was split between PDS-11 and PDS-12. This atypical approach in the NUREG/CR-4550 analysis required that an alternative method be used here to determine the CDF contribution of each accident sequence to each of the PDSs. This alternative method is outlined later in this section.

Similar to the other plants studied, the information obtained for this BWR plant included, for each sequence (split and unsplit), the mean CDF; the contribution to the PDS CDF; the contribution to the total plant CDF; the status of the HPI and LPI systems; the status of the reactor coolant system; and the predicted range of times at which the core uncovers.

The HPI systems examined include the three systems listed in Table 5: the high pressure core spray (HPCS) system, the RCIC system, and the CRD system. The status of all three systems are tabulated in the results section.

The LPI systems examined include the five systems listed in Table 5: the LPCI system, the LPCS system, the standby service water (SSW) system, the condensate system, and the firewater system. The status of all five systems are tabulated.

The contribution of the split accident sequences to each PDS CDF was not presented explicitly in the NUREG/CR-4550 and had to be determined. Two methods were used. The first method utilized information presented in Appendix D of Reference 6. For some of the accident sequences, a complete listing of how the accident sequence cut sets were distributed to the various PDSs was provided. Sequences T1B-4, TC-74, and T2-56 were analyzed with this method. For the remaining accident sequences, this method was not possible because the number of cut sets was so large that the complete list was not presented in the NUREG/CR-4550 documentation. For these accident sequences, a second method was required to determine the contribution to the PDS CDF.

The second approach utilized the Integrated Reliability and Risk Analysis System (IRRAS), Version 2.5,[a] loaded with the latest Grand Gulf data base.[b] IRRAS is a microcomputer based probabilistic risk assessment model

---

a. IRRAS Version 2.5, April 1, 1991, Idaho National Engineering Laboratory, EG&G Idaho, Inc., Idaho Falls, Idaho.

b. Letter Report entitled Grand Gulf Unit 1 Probabilistic Risk Assessment Related Data Base, Richard D. Fowler, et. al., EG&G Idaho, Inc., Idaho Falls, Idaho, November 9, 1990.

development and analysis tool. Using IRRAS, the contribution of three accident sequences to four PDSs CDFs was determined. The three sequences analyzed using IRRAS were T1B-16, T1B-17, and T1B-21.

In analyzing the split sequences with IRRAS, the sequences were renamed. Sequence T1B-16 was split into sequences SEQ16-A, SEQ16-B, SEQ16-C, and SEQ16-D, which were distributed to PDS-1, PDS-2, PDS-3, and PDS-7, respectively. The splits for sequences T1B-17 and T1B-21 were similarly defined. The mean CDF for each of the split sequences was determined using the Latin Hypercube Sampling (LHS) algorithm in IRRAS. A LHS random number seed of 3571 was arbitrarily selected for a sample size of 2000. It should be noted that the calculated CDFs are dependent upon the selected random seed and sample values. However, the fractional contribution of the split sequences to the total PDS CDF is relatively constant over a wide range of seed and sample values. Therefore, the CDFs for the split sequences were determined by multiplying the IRRAS calculated fractional contributions for each split sequence with the PDSs mean CDFs presented in Table 5.3-1 of Reference 6.

The contribution to the total CDF, of the injection system failure mechanisms identified, was obtained using the same method outlined for the other plants analyzed. The characteristic attributes used in grouping the injection system failure modes for Grand Gulf were for the first characteristic: POWER, FAIL, and OPERATOR; for the second characteristic: HPI and LPI; and for the third characteristic: INIT and LATE.

# 5. RESULTS

In this section, the results are presented on a plant by plant basis. The results include a table of injection failure mechanisms descriptions; a table of simplified, three character injection failure descriptions; and, finally, a table giving the core damage frequency (CDF) contribution for each injection failure mechanism.

## 5.1 Surry Results

The injection failure mechanism descriptions for the dominant accident sequences at Surry are presented in Table 7. Using these descriptions, and the failure characteristic definitions listed in Table 6, simplified, three character descriptions for each accident sequence were obtained. These simplified failure descriptions are presented in Table 8. These three character failure descriptions were then sorted to obtain the CDF contribution for each of the failure characteristics. Table 9 presents the CDF contribution by failure mechanism, by which injection system is failed, and by the time of failure.

### Power Failures

The results in Table 9 indicate that the dominant injection system failure mechanism at Surry is due to the loss of ac power (67% of the total CDF.) The reactor coolant system (RCS) remains at high pressure, so that the injection system required for coolant make up is the high pressure system. This system is unavailable from the start of the sequence and remains so during the duration of the sequence. Even if the RCS could be depressurized, the low pressure injection systems would also be unavailable due to the loss of ac power.

There are eight sequences involving loss of power. In four of these, the core uncovers in approximately 1 hour (SBO-Q, SBO-Q2, SBO-L and SBO-L2.) These four sequences contribute 19% to the total CDF at Surry. For the

remaining four involving loss of power, the time at which the core uncovers varies from 2.5 to 7 hours from the loss of ac power (SBO-BATT, SBO-BATT2, SBO-SLOCA, and SBO-SLOCA2.) The only recovery action possible for these sequences would be to obtain an additional source of backup ac power supply for the injection systems. Whether a backup power supply could be initiated in time to prevent core damage, is sequence dependent and would require specific information on the type of backup supply and the procedures for initiating it.

### Recirculation Failures

Failure of the injection systems in the recirculation mode occurs in 7 sequences which makeup 15% of the CDF. One of these sequences is the V sequence or interfacing systems LOCA (4% of the total CDF.) This sequence results from the high pressure coolant system rupturing the low pressure system, leading to a LOCA which bypasses containment, thereby preventing recirculation cooling. No viable recovery actions exist for this sequence. Another four of the sequences (4% of the total CDF) involve a steam generator tube rupture (SGTR), in which the RCS is not depressurized. This leads to loss of core inventory, depletion of the refueling water storage tank (RWST), and finally the core uncovers after more than ten hours. Possible recovery actions for these sequences include continued refilling of the RWST or adding an additional water source. The remaining two sequences (7% of the total CDF) involve medium and large break loss of coolant accidents (LOCAs), in which the low pressure recirculation cooling is not established. Time at which the core uncovers is less than 50 minutes for the medium LOCA and less than 1 minute for the large LOCA. Because of the very short times involved for these two sequences, no viable recovery actions are apparent.

### Hardware Failures

Failure of the injection systems because of hardware failure occurs in 11 of the sequences (14% of the total CDF.) Of these sequences, eight involve failure of the HPI and three involve failure of the LPI (10% and 4% of the total CDF, respectively.) For all of the sequences, the injection system are failed at the beginning of the sequence. For the HPI system failures, the time at which the core uncovers ranges from less than 15 minutes to more than

seventeen hours, depending upon the RCS break size. For the LPI system failures, the time at which the core uncovers ranges from one to 50 minutes. Because of these very short times, recovery of the LPI system is not viable. For those sequences involving failure of the HPI system, one possible recovery action would be to depressurize the RCS so that the LPI system could be utilized. However, since failure to depressurize the RCS has been accounted for in defining these sequences, new innovative depressurization mechanisms would have to be deduced.

**ATWS Event Failures**

Finally, two sequences (TKRZ and $TKRD_4$; 4% of the total CDF) involve an anticipated transient without scram (ATWS) event which induces an overpressurization which fails the HPI system immediately. Furthermore, in sequence TKRZ, the RCS boundary is also failed by the initial overpressurization and the core uncovers in the early time frame. No viable recovery actions are apparent for this sequence. For the other sequence, the only feasible recovery actions would be to scram the reactor and then depressurize the RCS so that either the HPI or the LPI system could operate. However, since failure to scram the reactor and subsequent failure to depressurize the RCS has been accounted for in defining this sequence, new innovative scram and depressurization mechanisms would have to be deduced.

Table 7. Injection failure mechanism descriptions for the dominant accident sequences at Surry.

| Plant Damage State | Accident Sequence | Mean CDF | Percent Contribution | | Injection System Status | | Auxiliary Feedwater States | | RCS Status |
|---|---|---|---|---|---|---|---|---|---|
| | | | To PDS | To Total CDF | HPI | LPI | Motor Driven | Turbine Driven | |
| PDS-1 Long Term Blackout | SBO-BATT | 1.0SE-05 | 47.6 | 25.3 | See note (a). | See note (a). | See note (a). | Starts successfully and continues to run, but battery depletion occurs at 4 hours. This results in loss of instrumentation and control power. Core uncovers 3 hrs. later. | RCS boundary remains intact. |
| | SBO-SLOCA | 5.3E-06 | 24.0 | 13.3 | See note (a). | See note (a). | See note (a). | Starts successfully and continues to run, but battery depletion occurs at 4 hours. This results in loss of instrumentation and control power. | Seal LOCA starts at 1.5 hours. Time of CU is dependent upon the LOCA size and if the operator depressurizes the RCS. Time of CU varies from 2.5 to 5.9 hours from the loss of AC power. |
| | SBO-SLOCA2 | 3.3E-06 | 15.0 | 8.3 | Same as sequence SBO-SLOCA except at both units. | | | | |
| | SBO-Q | 2.2E-06 | 8.9 | 5.5 | See note (a). | See note (a). | See note (a). | Starts successfully and continues to run. Core uncovers before battery depletion. | Primary coolant discharge from stuck open pressurizer PORV leads to CU in 1 hour. Lack of AC prevents PORV block valves from operating. |
| | SBO-BATT2 | 4.3OE-07 | 2.0 | 1.1 | Same as sequence SBO-BATT except at both units. | | | | |
| | SBO-Q2 | 3.2E-07 | 1.5 | 0.8 | Same as sequence SBO-Q except at both units. | | | | |
| PDS-2 Loss of Coolant Accident | $S_2H_2$ | 1.7SE-06 | 28.5 | 4.4 | Operates. | Operates initially, but fails in recirculation mode. | Operates. | Not required. | Medium size break [2"<D<6"] in the RCS piping. CU time is dependent on break size. For 2" break, CU time is < 50 min., for a 3.5" break, CU time is <15 min. independent of secondary depressurization. |

a. System unavailable at the time the transient is initiated due to lack of AC power.

Table 7. Continued.

| Plant Damage State | Accident Sequence | Mean CDF | Percent Contribution To PDS | Percent Contribution To Total CDF | Injection System Status HPI | Injection System Status LPI | Auxiliary Feedwater Status Motor Driven | Auxiliary Feedwater Status Turbine Driven | RCS Status |
|---|---|---|---|---|---|---|---|---|---|
| PDS-2 Loss of Coolant Accident, cont. | $S_1D_1$ | 8.8E-07 | 14.3 | 2.2 | Fails. | Core damage occurs with RCS at high pressure. | Operates. | Not required. | Same as $S_1H_1$. |
| | $AH_1$ | 8.2E-07 | 13.6 | 2.1 | Not required; RCS at low pressure. | Operates initially, but fails in recirculation mode. | Operates. | Not required. | Large break (6"<D< 29") in the RCS piping. Time of CU is dependent on break size, but is on the order of 1 min. or less. |
| | $S_1D_6$ | 6.7E-07 | 11.6 | 1.7 | Operates. | Fails. | Operates. | Not required. | Same as $S_1H_1$. |
| | $AD_6$ | 6.4E-07 | 10.9 | 1.6 | Not required; RCS at low pressure. | Operates, but accumulators fail to inject borated makeup water leading to core damage. CD time not specified. | Operates. | Not required. | Same as $AH_1$. |
| | $S_3D_1$ | 6.3E-07 | 10.2 | 1.6 | Fails. | Does not operate because RCS is at high pressure. | Operates. | Not required. | Very small break (D < 0.5"). Time of CU is dependent upon the LOCA size and if secondary is depressurized. With secondary depressurized, time to CU is greater than 17 hours. |
| | $S_2D_1$ | 4.4E-07 | 7.5 | 1.1 | Fails. | Does not operate because RCS is at high pressure. | Operates. | Not required. | Small break (0.5"<D<2") in RCS piping. With secondary depressurized, time to CU is 45 min. to 17 hours. |
| | $AD_6$ | 3.1E-07 | 3.4 | 0.8 | Does not operate as RCS is at low pressure. | Fails. | Operates. | Not required. | Same as $AH_1$. |
| PDS-3 Short Term Blackout | SBO-L | 4.7E-06 | 98.1 | 11.8 | See note (a). | See note (a). | See note (a). | Fails. CU occurs at approximately 1 hour. | Remains intact. |
| | SBO-L2 | 9.0E-08 | 1.9 | 0.2 | Same as sequence SBO-L except at both units. | | | | |

a. System unavailable at the time the transient is initiated due to lack of AC power.

Table 7. Continued.

| Plant Damage State | Accident Sequence | Mean CDF | Percent Contribution To PDS | Percent Contribution To Total CDF | Injection System Status: HPI | Injection System Status: LPI | Auxiliary Feedwater Status: Motor Driven | Auxiliary Feedwater Status: Turbine Driven | RCS Status |
|---|---|---|---|---|---|---|---|---|---|
| PDS-4 V | Event V | 1.6E-08 | 100.0 | 4.0 | Operates initially, but unable to recirculate. | Fails initially. | Operates. | Not required. | High pressure system ruptures low pressure system. |
| PDS-5 Transients | $T_2LD_2$ | 9.8E-07 | 50.0 | 2.5 | Fails following AFW failure. | Does not operate because RCS is at high pressure. | Fails. | Does not operate as power conversion system is disabled. | RCS boundary remains intact. |
| | $T_2LP$ | 7.4E-07 | 37.4 | 1.9 | Operates but PORVs fail to open, so feed and bleed cooling fails. | Does not operate because RCS is at high pressure. | Fails. | Does not operate as power conversion system is disabled. | RCS boundary remains intact. |
| | $T_{SA}LP$ | 1.3E-07 | 6.3 | 0.3 | Operates but PORVs fail to open, so feed and bleed cooling fails. | Does not operate because RCS is at high pressure. | Fails. | Does not operate as power conversion system is disabled. | RCS boundary remains intact. |
| | $T_{SB}LP$ | 1.3E-07 | 6.3 | 0.3 | Same as sequence $T_{SA}LP$ except at both units. | | | | |
| PDS-6 ATWS | TKRZ | 8.2E-07 | 52.6 | 2.0 | Disabled by initial pressure rise. | Does not operate because RCS is at high pressure. | Operates. | Not required. | Initial pressure rise fails RCS boundary integrity. |
| | $TKRD_4$ | 6.4E-07 | 42.1 | 1.6 | Emergency boration pumps fail; continued power generation maintains pressure above RV set points. Charging pumps inoperable due to high pressure. | Does not operate because RCS is at high pressure. | Operates. | Not required. | Continued discharge through relief valves leads to core damage. |
| | $T_2KR$ | 1.0E-07 | 5.3 | 0.3 | Operates initially, but unable to recirculate. | Does not operate because RCS is at high pressure. | Operates. | Not required. | Loss of SG integrity and continued high pressure due to ATWS leads to loss of core inventory and CD. |

Table 7. Continued.

| Plant Damage State | Accident Sequence | Mean CDF | Percent Contribution To PDS | Percent Contribution To Total CDF | Injection System Status: HPI | Injection System Status: LPI | Auxiliary Feedwater Status: Motor Driven | Auxiliary Feedwater Status: Turbine Driven | RCS Status |
|---|---|---|---|---|---|---|---|---|---|
| PDS-7 SGTR | $T_3D_0Q_6$ | 1.4E-06 | 76.1 | 3.5 | Operates initially, but unable to recirculate. | Does not operate because RCS is at high pressure. | Operates. | Not required. | Loss of SG integrity and failure to depressurize leads to depletion of RWST inventory and CU. Refilling RWST delays CU. Time to CU > 10 hours. |
| | $T_3D_1Q_6$ | 2.1E-07 | 10.9 | 0.5 | Fails. | Does not operate because RCS is at high pressure. Recirculation is not possible. | Operates. | Not required. | Loss of SG integrity and failure to depressurize leads to CU. |
| | $T_3L_3$ | 1.1E-07 | 6.5 | 0.3 | Operates but feed and bleed is not successful due to RCS depressurization to mitigate SGTR; unable to recirculate. | Does not operate because RCS is at high pressure. | Fails. | Inoperable due to SGTR. | Loss of core inventory through SGTR leads to CU. |
| | $T_3D_0QQ_6$ | 1.1E-07 | 6.5 | 0.3 | Operates initially, but unable to recirculate. | Does not operate because RCS is at high pressure. | Operates. | Not required. | Loss of SG integrity, stuck open PORV, and failure to depressurize leads to depletion of RWST. Refilling RWST delays CU. Time to CU > 10 hours. |

**Table 8.** Injection system failure mechanism characteristics for the dominant accident sequences at Surry.

| Plant Damage State | Sequence | Mean CDF | Failure Characteristics |
|---|---|---|---|
| PDS-1 Long Term Station Blackout | SBO-BATT | 1.1E-05 | POWER-HPI-INIT |
| | SBO-SLOCA | 5.3E-06 | POWER-HPI-INIT |
| | SBO-SLOCA2 | 3.3E-06 | POWER-HPI-INIT |
| | SBO-Q | 2.2E-06 | POWER-HPI-INIT |
| | SBO-BATT2 | 4.3E-07 | POWER-HPI-INIT |
| | SBO-Q2 | 3.2E-07 | POWER-HPI-INIT |
| PDS-2 Loss of Coolant Accident | $S_1H_1$ | 1.8E-06 | RECIRC-LPI-RECIRC |
| | $S_1D_1$ | 8.6E-07 | FAIL-HPI-INIT |
| | $AH_1$ | 8.2E-07 | RECIRC-LPI-RECIRC |
| | $S_1D_6$ | 6.7E-07 | FAIL-LPI-INIT |
| | $AD_6$ | 6.4E-07 | FAIL-LPI-INIT |
| | $S_3D_1$ | 6.3E-07 | FAIL-HPI-INIT |
| | $S_2D_1$ | 4.4E-07 | FAIL-HPI-INIT |
| | $AD_6$ | 3.1E-07 | FAIL-LPI-INIT |
| PDS-3 Short Term Station Blackout | SBO-L | 4.7E-06 | POWER-HPI-INIT |
| | SBO-L2 | 9.0E-08 | POWER-HPI-INIT |
| PDS-4 V | V | 1.6E-06 | RECIRC-HPI-RECIRC |
| PDS-5 Transients | $T_2LD_2$ | 9.8E-07 | FAIL-HPI-INIT |
| | $T_2LP$ | 7.4E-07 | FAIL-HPI-INIT |
| | $T_{5A}LP$ | 1.3E-07 | FAIL-HPI-INIT |
| | $T_{5B}LP$ | 1.3E-07 | FAIL-HPI-INIT |
| PDS-6 ATWS | TKRZ | 8.2E-07 | ATWS-HPI-INIT |
| | $TKRD_4$ | 6.4E-07 | ATWS-HPI-INIT |
| | $T_7KR$ | 1.0E-07 | RECIRC-HPI-RECIRC |
| PDS-7 SGTR | $T_7O_DQ_S$ | 1.4E-06 | RECIRC-HPI-RECIRC |
| | $T_7D_1O_D$ | 2.1E-07 | FAIL-HPI-INIT |
| | $T_7L_3$ | 1.1E-07 | RECIRC-HPI-RECIRC |
| | $T_7O_DQQ_S$ | 1.1E-07 | RECIRC-HPI-RECIRC |
| TOTAL | | 4.0E-05 | |

Table 9. Contribution by injection system failure mechanisms to the total core damage frequency at Surry.

| Failure Mechanism | Number of Sequences | Mean CDF | Percent of Total CDF | Percent of failures by injection system | | | |
|---|---|---|---|---|---|---|---|
| | | | | HPI | | LPI | |
| | | | | Initial | Recirc. | Initial | Recirc. |
| POWER | 8 | 2.7E-05 | 67 | 100 | 0 | 0 | 0 |
| RECIRC | 7 | 5.9E-06 | 15 | 0 | 56 | 0 | 44 |
| FAIL | 11 | 5.7E-06 | 14 | 72 | 0 | 28 | 0 |
| ATWS | 2 | 1.5E-06 | 4 | 100 | 0 | 0 | 0 |
| TOTAL | 28 | 4.0E-05 | 100 | | | | |

## 5.2 Zion Results

The injection failure mechanism descriptions for the dominant plant damage states (PDSs) at Zion are presented in Table 10. The simplified three character failure descriptions are presented in Table 11. These three character failure descriptions were then sorted to obtain the CDF contribution for each of the failure mechanisms. Table 12 presents the CDF contribution by failure mechanism, by which injection system is failed, and by time of failure.

### Component Cooling Water/Service Water Failures

The results presented in Table 12 indicate that the dominant failure mechanism is due to the loss of component cooling water (CCW) or service water (SW) which induces a pump seal LOCA (86% of the CDF.) Twenty eight PDSs contribute to this failure mechanism. Of these PDSs, 26 involve failure of the HPI and two involve failure of the LPI (86% and 0.02%, respectively.)

Of the 26 in which the HPI system is failed, 23 PDSs have the HPI system unavailable from the start of the sequence and remains so for the duration of the sequence (85.8% of the total CDF.) In the remaining three PDSs, the HPI system operates initially, but then fails in the recirculation mode due to loss of CCW or SW (0.2% of the total CDF.) All of these PDSs involve small break sizes (0.5" < D < 2") either due to pump seal failure, or SGTR with RCS depressurized and pump seal failure. For this size break, the time at which the core uncovers is approximately 1.5 hour. One possible recovery action for these PDSs would include be to recover the CCW/SW in the time available to prevent injection system failure. In fact, such recovery actions have already been accounted for in the original NUREG/CR-4550 analysis (see Reference 3, section 4.6.2.12). Furthermore, since the time of the original analysis, the Zion licensee has committed to perform additional actions to prevent the loss of CCW and SW and the resulting reactor coolant pump seal failure (see Reference 1, page 7-3.) These actions include providing an auxiliary water supply to each charging pump's oil cooler via either the SW or fire protection

systems and to replace existing pump seal O-rings with new heat-resistant O-rings which will improve seal survivability.

The two PDSs (ANBYYYNN and ANBYYYNY, 0.02% of the total CDF) in which the CCW failure initially fails the LPI system, involve large LOCAs. The time at which the core uncovers varies from seconds to minutes. Because of this very short time, viable recovery actions of the LPI system are not apparent for these PDSs.

**Power Failures**

Failure of the injection systems because of loss of power occurs in 11 of the PDSs (4% of the total CDF.) Of these PDSs, nine involve failure of the HPI and two involve failure of the LPI (4% and 0.002% of the total CDF, respectively.) Of the nine sequences involving HPI failure, three occur initially from lack of power and six fail in recirculation mode (2% and 2% of the total CDF, respectively.) These latter six involve a partial power loss which fails the equipment necessary for switchover to recirculation mode.

The two PDSs, in which the LPI system fails due to loss of power, involve a medium and large LOCA with the LPI system failed initially (PDSs S1RIYYYYR and ARIYYYYR, respectively.) The time at which the core uncovers is less than 50 minutes for the medium LOCA and less than 1 minute for the large LOCA.

Possible recovery actions for the PDSs involving loss of power would be to obtain an additional source of backup ac power supply for the injection systems and recirculation switchover equipment. Whether a backup power supply could be initiated in time to prevent core damage, is dependent upon the PDS and would require specific information on the type of backup supply and the procedures for initiating it.

**Recirculation Failures**

Failure of the injection systems due to recirculation system failures occurs in two PDSs which makeup 0.5% of the total CDF. The first PDS is the V sequence (0.04% of the total CDF) and is essentially the same as that

described for Surry. As was discussed for that plant, no viable recovery actions exist for this PDS. The second PDS, HICYNXYY (0.5% of the total CDF), involves a SGTR and the RCS is not depressurized. This leads to loss of core inventory, depletion of the RWST, and finally the core uncovers. Possible recovery actions for this PDS include continued refilling of the RWST or adding an additional water source.

**Hardware Failures**

Failure of the injection systems due to hardware failures occurs in six PDSs which makeup 1% of the total CDF. This tally of the PDSs includes PDSs S1IBYYYYY and TLCYNNYY which are split between two failure mechanisms as described in Table 11 and Table 12. Of the six PDSs, three involve failure of the HPI and three involve failure of the LPI (0.13% and 0.87% of the total CDF, respectively.) For all of the PDSs, the injection system are failed initially. The HPI system failures involve transients in which feed and bleed cooling fails due to unavailability of a charging pump and a safety injection pump. The sequence remains at high pressure as the RCS boundary remains intact and is not depressurized. The time at which the core uncovers is not specified for these PDSs. The LPI system failures involve a medium and two large break LOCAs. The time at which the core uncovers ranges from one to 50 minutes. Because of these very short times, recovery of the LPI system is not viable. For those sequences involving failure of the HPI system, one possible recovery action would be to depressurize the RCS so that the LPI system could be utilized. However, since failure to depressurize the RCS using secondary side cooling and the auxiliary feedwater system (AFW) has been accounted for in defining these sequences, new innovative depressurization mechanisms would have to be deduced.

**ATWS Event Failures**

Failure of the injection systems due to an ATWS event which induces an overpressurization which fails the HPI system occurs in four PDSs (2% of the total CDF.) This tally of the PDSs includes TLCYNNYY which is split between two failure mechanisms as described in Table 11 and Table 12. For all of these PDSs, the only viable recovery actions would be to scram the reactor and then depressurize the RCS so that either the HPI or the LPI system could

operate. However, since failure to scram the reactor and subsequent failure to depressurize the RCS using secondary side cooling and the AFW system has been accounted for in defining these sequences, new innovative scram and depressurization mechanisms would have to be deduced.

**Operator Error Failures**

Failure of the injection systems due to operator error occurs in seven PDSs which makeup 6.5% of the total CDF. This tally of the PDSs includes PDS S1IBYYYYY that is split between two failure mechanisms as described in Table 11 and Table 12. For all of these PDSs, the failure occurs in the recirculation mode and the dominant contributor is human error at switchover. Three of these PDSs involve failure of the high pressure recirculation and four involve the low pressure recirculation ( 3% and 3.5% of the total CDF, respectively.) The high pressure recirculation failures involve small break LOCAs. Possible recovery actions for these PDSs include continued refilling of the RWST or adding an additional water source. The low pressure recirculation failures involve medium and large break LOCAs. The time at which the core uncovers is less than 50 minutes for the medium LOCA and less than 1 minute for the large LOCA. Because of the very short times involved for these PDSs, no viable recovery actions are apparent.

**Safety Injection Actuation Failures**

Finally, two PDSs (less than 0.01% of the total CDF) involve failure of the safety injection actuation system to operate which immediately prevents the HPI system from operating. One PDS involves a small LOCA and the other involves a SGTR in which the RCS is depressurized below the steam generator safety valve set points. However, in both PDSs, RCS pressure remains to high to use the LPI system. Feed and bleed cooling is failed and the core uncovers. The only viable recovery actions would be to either bypass the failed safety actuation signal or to depressurize the RCS so that the LPI system could operate. However, since failure to actuate the injection systems and subsequent failure to depressurize the RCS has been accounted for in defining this sequence, new innovative safety actuation and depressurization mechanisms would have to be deduced.

Table 10. Injection failure mechanism descriptions for the dominant plant damage states at Zion.

| Plant Damage State Group | Plant Damage State | CDF Point Estimate | Percent Contribution To PDS6 | Percent Contribution To Total CDF | Injection System Status: HPI | Injection System Status: LPI | Auxiliary Feedwater Status: Motor Driven | Auxiliary Feedwater Status: Turbine Driven | RCS Status |
|---|---|---|---|---|---|---|---|---|---|
| PDS-1 Station Blackout | TRRRRSRR | 4.7E-06 | 90 | 1.7 | See note (a). | See note (a). | See note (a). | Starts successfully and continues to run, but battery depletion occurs at 6 hours. This results in loss of instrumentation and control power. Core uncovers 1.5 hours later. | RCS boundary remains intact. |
| | S2RRRYRR | 4.2E-07 | 8.0 | 0.15 | See note (a). | See note (a). | See note (a). | Operates; SG's depressurized. | Pump seal failure leads to S2 break (0.5"<D<2"). |
| | S2RRRRSRR | 8.2E-08 | 1.6 | 0.03 | See note (a). | See note (a). | See note (a). | Starts successfully and continues to run, but battery depletion occurs at 6 hours. This results in loss of instrumentation and control power. Core uncovers in less than 1.5 hours later. | Pump seal failure leads to S2 break (0.5"<D<2"). |
| PDS-2 Loss of Coolant Accident | S2NBYYYNY | 1.2E-04 | 46 | 43 | Failed due to loss of CCW. | Does not operate because RCS is at high pressure. | Operates. | Not required. | Loss of component cooling water leads to pump seal failure and S2 size break. One exception is for S2 break followed by CCW failure. |
| | S2NBYYYNN | 1.2E-04 | 46 | 43 | Failed due to loss of SW. | Does not operate because RCS is at high pressure. | Operates. | Not required. | Loss of service water leads to pump seal failure and S2 size break. One exception is for S2 break followed by SW failure. |
| | S2IBYYYYY | 8.0E-06 | 3.1 | 2.9 | Operates initially, but fails in recirculation mode; see note (b). | Does not operate because RCS is at high pressure. | Operates. | Not required. | Small break (0.5"<D<2") in RCS piping. Time to CD is not specified. |

a. System unavailable at the time the transient is initiated due to lack of AC power.
b. Dominant contributor to failure is human error at switchover.

Table 10. Continued.

| Plant Damage State Group | Plant Damage State | CDF Point Estimate | Percent Contribution To PDS6 | Percent Contribution To Total CDF | Injection System Status: HPI | Injection System Status: LPI | Auxiliary Feedwater Status: Motor Driven | Auxiliary Feedwater Status: Turbine Driven | RCS Status |
|---|---|---|---|---|---|---|---|---|---|
| PDS-2 Loss of Coolant Accident, cont. | S1IBYYYY | 5.4E-06 | 2.1 | 2.0 | Operates. | Operates initially, but fails in recirculation mode[a] or is failed initially. | Operates. | Not required. | Medium break (2"<D<5") in RCS piping. Time to CU is not specified. |
| | A1BYYYY | 4.9E-06 | 1.9 | 1.8 | Not required; RCS at low pressure. | Operates initially, but fails in recirculation mode; see note [a]. | Not required. | Not required. | Large break (D>6") in RCS piping. Recirculation must be switched on within 20 to 30 min. |
| | ANBYYYY | 1.4E-06 | 0.54 | 0.51 | Not required; RCS at low pressure. | Failed due to common cause failure of both RHR pumps. | Not required. | Not required. | Large break (D>6") in RCS piping. Time of CU from seconds to minutes. |
| | S2NBYYYNR | 3.8E-07 | 0.15 | 0.14 | Failed due to loss of CCW. | Does not operate because RCS is at high pressure. | Operates. | Not required. | Loss of CCW leads to pump seal failure and S2 break. |
| | S2I1YYYNR | 3.3E-07 | 0.13 | 0.12 | Operates initially, fails in recirculation mode due to loss of CCW or SW. | Does not operate because RCS is at high pressure. | Operates. | Not required. | Loss of CCW or SW leads to pump seal failure and S2 size break. |
| | S2NIYYYNN | 2.3E-07 | 0.09 | 0.08 | Failed due to loss of SW. | Does not operate because RCS is at high pressure. | Operates. | Not required. | Loss of SW leads to pump seal failure and S2 size break. |
| | S2NIYYYNY | 1.9E-07 | 0.07 | 0.07 | Failed due to loss of CCW. | Does not operate because RCS is at high pressure. | Operates. | Not required. | Loss of CCW leads to pump seal failure and S2 size break. |
| | S2IBYYYNY | 1.8E-07 | 0.07 | 0.06 | Operated initially, fails in recirculation mode due to loss of CCW or SW. | Does not operate because RCS is at high pressure. | Operates. | Not required. | Loss of CCW or SW leads to pump seal failure and S2 size break. |
| | S2IBYYYNR | 6.8E-08 | 0.03 | 0.02 | Operated initially, fails in recirculation mode due to loss of CCW or SW. | Does not operate because RCS is at high pressure. | Operates. | Not required. | Loss of CCW or SW leads to pump seal failure and S2 size break. |

a. Dominant contributor to failure is human error at switchover.

Table 10. Continued.

| Plant Damage State Group | Plant Damage State | CDF Point Estimate | Percent Contribution To POSG | Percent Contribution To Total CDF | Injection System Status: HPI | Injection System Status: LPI | Auxiliary Feedwater Status: Motor Driven | Auxiliary Feedwater Status: Turbine Driven | RCS Status |
|---|---|---|---|---|---|---|---|---|---|
| POS-2 Loss of Coolant Accident, cont. | SZIIYYYR | 3.8E-08 | 0.01 | 0.01 | Operated initially, but fails in recirculation mode due to partial loss of AC power. | Does not operate because RCS is at high pressure. | Operates. | Not required. | Small break (0.5"<D<2") in RCS piping. Time to CU is not specified. |
| | SZLBYYYNR | 2.1E-08 | 0.01 | 0.01 | Failed due to loss of CCW or SW. | Available to inject when core is uncovered, but cannot because RCS pressure is too high. | Operates. | Not required. | Loss of CCW or SW leads to pump seal failure and S2 size break. |
| | ANBYYYNN | 2.1E-08 | 0.01 | 0.01 | Not required; RCS is at low pressure. | Failed due to loss of SW and thus CCW. | Not required. | Not required. | Large break (D>6") in RCS piping. Time of CU from seconds to minutes. |
| | SINBYYYNN | 2.1E-08 | 0.01 | 0.01 | Failed due to loss of SW and thus CCW. | Failed due to loss of SW and thus CCW. | Operates. | Not required. | Medium break (2"<D<6") in RCS piping. Time of CU is not specified. |
| | SINBYYYNY | 2.1E-08 | 0.01 | 0.01 | Failed due to loss of CCW. | Failed due to loss of CCW. | Operates. | Not required. | Medium break (2"<D<6") in RCS piping. Time of CU is not specified. |
| | ANBYYYNY | 2.1E-08 | 0.01 | 0.01 | Not required; RCS is at low pressure. | Failed due to loss of CCW. | Not required. | Not required. | Large break in RCS piping. Time of CU from sec.-min. |
| | SZLBYYNYY | 1.9E-08 | 0.01 | 0.01 | Disabled due to initial pressure rise of ATWS event. | Available to inject when core is uncovered, but cannot because RCS pressure is too high. | Power excursion is beyond the capability of the AFW system to maintain SG water level. | Not required. | Small break (0.5"<D<2") in RCS piping initiates ATWS. |
| | SINHYNYNR | 1.4E-08 | <0.01 | <0.01 | Failed due to loss of CCW. | Does not operate as RCS is at high pressure. | Operates. | Not required. | Loss of CCW leads to pump seal failure and S2 break. |
| | SZLBYYYNY | 1.3E-08 | <0.01 | <0.01 | Failed due to loss of SW and thus CCW. | Available to inject at CU, but RCS pressure is too high. | Operates. | Not required. | Loss of SW leads to pump seal failure and S2 size break. |
| | SZIIYYYYY | 1.3E-08 | <0.01 | <0.01 | Operated initially, but fails in recirculation mode; see note (a). | Does not operate because RCS is at high pressure. | Operates. | Not required. | Small break (0.5"<D<2") in RCS piping. Time to CU is not specified. |

a. Dominant contributor to failure is human error at switchover.

Table 10. Continued.

| Plant Damage State Group | Plant Damage State | CDF Point Estimate | Percent Contribution To PDSG | Percent Contribution To Total CDF | Injection System Status: MPI | Injection System Status: LPI | Auxiliary Feedwater Status: Motor Driven | Auxiliary Feedwater Status: Turbine Driven | RCS Status |
|---|---|---|---|---|---|---|---|---|---|
| PDS-2 Loss of Coolant Accident, cont. | S2NIYYYNR | 1.2E-08 | <0.01 | <0.01 | Failed due to loss of CCW. | Does not operate as RCS is at high pressure. | Operates. | Not required. | Loss of CCW leads to pump seal failure and S2 break. |
| | S2IIYYNNR | 1.1E-08 | <0.01 | <0.01 | Operates initially, fails in recirculation mode from partial AC power loss. | Does not operate because RCS is at high pressure. | See note (a). | Failed or in maintenance. | Loss of SW leads to pump seal failure and S2 size break. |
| | S2NNYYNN | 1.9E-08 | <0.01 | <0.01 | Failed due to loss of SW. | Does not operate as RCS is at high pressure. | Operates. | Not required. | Loss of SW leads to pump seal failure and S2 break. |
| | S1IIYYYY | 7.8E-09 | <0.01 | <0.01 | Operates. | Operates initially, but fails in recirculation mode; see note (b). | Operates. | Not required. | Medium break (2"<D<6") in RCS piping. Time to CU is not specified. |
| | AIIYYYY | 7.8E-09 | <0.01 | <0.01 | Not required; RCS is at low pressure. | Operates initially, but fails in recirculation mode; see note (b). | Not required. | Not required. | Large break (D>6") in RCS piping. Recirculation must be switched on within 20 to 30 minutes. |
| | S2LBYYYN | 7.7E-09 | <0.01 | <0.01 | Fails due to safety injection actuation signal failure. | Available to inject when core is uncovered, but cannot because RCS pressure is too high. | Operates. | Not required. | Small break (0.5"<D<2") in RCS piping. Time to CU is not specified. |
| | S2NBYYNNY | 6.6E-09 | <0.01 | <0.01 | Failed due to loss of CCW. | Does not operate because RCS is at high pressure. | Failed due to turbine trip failure. | Failed due to turbine trip failure. | Loss of CCW leads to pump seal failure and S2 size break. |
| | S2NBYYNNN | 6.6E-09 | <0.01 | <0.01 | Failed due to loss of SW. | Does not operate because RCS is at high pressure. | Failed due to turbine trip failure. | Failed due to turbine trip failure. | Loss of SW leads to pump seal failure and S2 size break. |
| | S2NNYNYNY | 5.6E-09 | <0.01 | <0.01 | Failed due to loss of CCW. | Does not operate because RCS is at high pressure. | Operates. | Not required. | Loss of CCW leads to pump seal failure and S2 size break. |
| | S2INYYYNR | 3.9E-09 | <0.01 | <0.01 | Same as sequence S2IBYYYNY. | | | | |

a. System unavailable at the time the transient is initiated due to lack of AC power.
b. Dominant contributor to failure is human error at switchover.

Table 10. Continued.

| Plant Damage State Group | Plant Damage State | CDF Point Estimate | Percent Contribution To PDSG | Percent Contribution To Total CDF | Injection System Status: HPI | Injection System Status: LPI | Auxiliary Feedwater Status: Motor Driven | Auxiliary Feedwater Status: Turbine Driven | RCS Status |
|---|---|---|---|---|---|---|---|---|---|
| PDS-2 Loss of Coolant | S2NIYYNNN | 3.6E-09 | <0.01 | <0.01 | Failed due to loss of SW. | Does not operate because RCS is at high pressure. | See note (a). | Failed or in maintenance. | Loss of SW leads to pump seal failure and S2 size break. |
| | ANIYYYY | 2.3E-09 | <0.01 | <0.01 | Same as sequence ANBTYYYY. | | | | |
| | S1RIYYYYR | 2.1E-09 | <0.01 | <0.01 | Operates. | See note (a). | Not required. | Not required. | Medium break (2"<D<6") in RCS piping. Time to CU is not specified. |
| | ARIYYYYR | 2.1E-09 | <0.01 | <0.01 | Not required; RCS at low pressure. | See note (a). | Not required. | Not required. | Large break (D>6") in RCS piping. Time of CU is not specified. |
| | S2IIYYNYR | 1.6E-09 | <0.01 | <0.01 | Operates initially, fails in recirculation mode due to loss of AC power. | Does not operate because RCS is at high pressure. | See note (a). | Failed or in maintenance. | Small break (0.5"<D<2") in RCS piping. Time to CU is not specified. |
| | S2NIYYNNR | 1.1E-09 | <0.01 | <0.01 | Failed due to loss of CCW. | Does not operate because RCS is at high pressure. | See note (a). | Failed or in maintenance. | Loss of CCW leads to pump seal failure and S2 size break. |
| PDS-3 Transients | TLCYNRYY | 6.1E-06 | 52 | 2.2 | Disabled due to initial pressure rise of ATWS event or failed at start of transient. | Available to inject when core is uncovered but cannot because RCS pressure is too high. | Power excursion is past the capability of AFW to maintain SG water level, failure of turbine trip fails AFW or failed at start of transient. | Not required. | RCS boundary remains intact. |
| | TIAYYNYR | 5.2E-06 | 44 | 1.9 | Operates initially, fails in recirc. mode due to partial loss of AC power. | Does not operate as RCS is at high pressure. | See note (a). | Failed or in maintenance. | RCS boundary remains intact. |
| | TICYYNYY | 4.4E-07 | 3.7 | 0.16 | Operates initially, but fails in the recirculation mode; see note (b). | Does not operate because RCS is at high pressure. | Failed due to turbine trip failure or failed at beginning. | Failed due to turbine trip failure or failed at beginning. | RCS boundary remains intact. |

a. System unavailable at the time the transient is initiated due to lack of AC power.
b. Dominant contributor to failure is human error at switchover.

Table 10. Continued.

| Plant Damage State Group | Plant Damage State | CDF Point Estimate | Percent Contribution To PDSG | Percent Contribution To Total CDF | Injection System Status: HPI | Injection System Status: LPI | Auxiliary Feedwater Status: Motor Driven | Auxiliary Feedwater Status: Turbine Driven | RCS Status |
|---|---|---|---|---|---|---|---|---|---|
| PDS-3 Transients, cont. | TINYYNYR | 3.3E-08 | 0.28 | 0.01 | Operates initially, fails in recirc. mode due to partial loss of AC power. | Does not operate because RCS is at pressure. | See note (a). | Failed or in maintenance. | RCS boundary remains intact. |
| | TICYYNYR | 1.9E-08 | 0.16 | 0.01 | Operates initially, but fails in the recirculation mode due to containment fan cooler failing from lack of AC power. | Does not operate because RCS is at high pressure. | See note (b). | Failed or in maintenance. | RCS boundary remains intact. |
| | TLCYNNYR | 1.0E-08 | 0.09 | <0.01 | Feed and bleed cooling fails due to unavailability of a charging or safety injection pump. | Available to inject when core is uncovered but cannot because RCS pressure is too high. | See note (b). | Failed or in maintenance. | RCS boundary remains intact. |
| | TLAYNNYR | 2.5E-09 | <0.01 | <0.01 | Feed and bleed cooling fails due to unavailability of both a charging and safety injection pump. | Available to inject when core is uncovered but cannot because RCS pressure is too high. | See note (a). | Failed or in maintenance. | RCS boundary remains intact. |
| | TLAYNYY | 8.5E-09 | <0.01 | <0.01 | Disabled due to initial pressure rise of ATWS event. | Available to inject when core is uncovered but cannot because RCS pressure is too high. | Power excursion is beyond the capability of the AFW system to maintain SG water level. | Not required | RCS boundary remains intact. |
| | TNCYNNYY | 1.1E-08 | <0.01 | <0.01 | Failed due to loss of CCW. | Failed due to loss of CCW. | Failed or in maintenance. | Failed or in maintenance. | RCS boundary remains intact. |
| | TNCYNNYN | 1.1E-08 | <0.01 | <0.01 | Failed due to loss of SW. | Failed due to loss of SW. | Failed or in maintenance. | Failed or in maintenance. | RCS boundary remains intact. |
| | TNAYNNYN | 1.0E-09 | <0.01 | <0.01 | Failed due to loss of SW. | Failed due to loss of SW. | See note (a). | Failed or in maintenance. | RCS boundary remains intact. |

a. System unavailable at the time the transient is initiated due to lack of AC power.
b. One train unavailable due to lack of AC power or maintenance, and the other is failed or in maintenance at the start of the transient.

Table 10. Continued.

| Plant Damage State Group | Plant Damage State | CDF Point Estimate | Percent Contribution To PDSG | Percent Contribution To Total CDF | Injection System Status: HPI | Injection System Status: LPI | Auxiliary Feedwater Status: Motor Driven | Auxiliary Feedwater Status: Turbine Driven | RCS Status |
|---|---|---|---|---|---|---|---|---|---|
| PDS-4 SGTRs | HICYNXYY | 1.3E-06 | 96 | 0.46 | Operates initially, but fails in the recirculation mode due to core and RWST inventory being lost through SGTR. | Does not operate because RCS is at high pressure. | Operates but SGs are not depressurized. | Not required. | SGTR but RCS is not depressurized below the main safety valve set-points of the SG. Loss of inventory from RCS is never mitigated. |
| | GMCYNYNN | 2.9E-08 | 2.1 | 0.01 | Failed due to loss of SW. | Does not operate because RCS is at high pressure. | Operates. | Not required. | SGTR with RCS depressurized below the main safety valve setpoints of the SG. One sequence involves pump seal failure and S2 size break. |
| | GMCYNYNY | 2.9E-08 | 2.1 | 0.01 | Failed due to loss of CCW. | Does not operate because RCS is at high pressure. | Operates. | Not required. | SGTR with RCS depressurized below the main safety valve setpoints of the SG. One sequence involves pump seal failure and S2 size break. |
| | GMCYNNYY | 5.6E-09 | 0.41 | <0.01 | Fails; large, early overpressurization results in failure of safety injection system check valves and piping. | Does not operate because RCS is at high pressure. | Functional, but loss of inventory prevents adequate heat transfer from core to SG's. | Functional, but loss of inventory prevents adequate heat transfer from core to SG's. | Reactor is not tripped; loss of inventory from SGTR prevents adequate secondary cooling; large, early overpressurization without cooling results in CD. |
| | GMCYNYYN | 2.2E-09 | 0.16 | <0.01 | Failed due to failure of safe-guards actuation system. | Does not operate because RCS is at high pressure. | Operates. | Not required. | SGTR with RCS depressurized below the main safety valve setpoints of of the SG. |
| PDS-5 Event V | V | 1.1E-07 | 100 | 0.04 | Operates initially, but fails in recirculation mode. | Fail by initiating event. | Operates. | Not required. | High pressure system ruptures low pressure system outside of containment. |

**Table 11.** Injection system failure mechanism characteristics for the dominant plant damage states at Zion.

| Plant Damage State Group | Plant Damage State | Point estimate CDF | Failure Characteristics |
|---|---|---|---|
| PDS-1 Station Blackout | TRRRRSRR | 4.7E-06 | POWER-HPI-INIT |
| | S2RRRRYRR | 4.2E-07 | POWER-HPI-INIT |
| | S2RRRRSRR | 8.2E-08 | POWER-HPI-INIT |
| PDS-2 Loss of Coolant Accident | S2NBYYYNY | 1.2E-04 | CCW/SW-HPI-INIT |
| | S2NBYYYNN | 1.2E-04 | CCW/SW-HPI-INIT |
| | S2IBYYYYY | 8.0E-06 | OPERATOR-HPI-RECIRC |
| | S1IBYYYYY[a] | 4.9E-06 | OPERATOR-LPI-RECIRC |
| | S1IBYYYYY[a] | 5.3E-07 | FAIL-LPI-INIT |
| | AIBYYYYY | 4.9E-06 | OPERATOR-LPI-RECIRC |
| | ANBYYYYY | 1.4E-06 | FAIL-LPI-INIT |
| | S2NBYYYNR | 3.8E-07 | CCW/SW-HPI-INIT |
| | S2IIYYYNR | 3.3E-07 | CCW/SW-HPI-INIT |
| | S2NIYYYNN | 2.3E-07 | CCW/SW-HPI-INIT |
| | S2NIYYYNY | 1.9E-07 | CCW/SW-HPI-INIT |
| | S2IBYYYNY | 1.8E-07 | CCW/SW-HPI-RECIRC |
| | S2IBYYYNR | 6.8E-08 | CCW/SW-HPI-RECIRC |
| | S2IIYYYYR | 3.8E-08 | POWER-HPI-RECIRC |
| | S2LBYYYNR | 2.1E-08 | CCW/SW-HPI-INIT |
| | ANBYYYNN | 2.1E-08 | CCW/SW-LPI-INIT |
| | S1NBYYYNN | 2.1E-08 | CCW/SW-HPI-INIT |
| | S1NBYYYNY | 2.1E-08 | CCW/SW-HPI-INIT |
| | ANBYYYNY | 2.1E-08 | CCW/SW-LPI-INIT |
| | S2LBYYNYY | 1.9E-08 | ATWS-HPI-INIT |
| | S2NNYNYNR | 1.4E-08 | CCW/SW-HPI-INIT |
| | S2LBYYYNY | 1.3E-08 | CCW/SW-HPI-INIT |
| | S2IIYYYYY | 1.3E-08 | OPERATOR-HPI-RECIRC |
| | S2NIYYYNR | 1.2E-08 | CCW/SW-HPI-INIT |
| | S2IIYYNNR | 1.1E-08 | POWER-HPI-RECIRC |
| | S2NNYNYNN | 1.0E-08 | CCW/SW-HPI-INIT |
| | S1IIYYYYY | 7.8E-09 | OPERATOR-LPI-RECIRC |
| | AIIYYYYY | 7.8E-09 | OPERATOR-LPI-RECIRC |
| | S2LBYYYYN | 7.7E-09 | SAFETY-HPI-INIT |
| | S2NBYYNNY | 6.6E-09 | CCW/SW-HPI-INIT |
| | S2NBYYNNN | 6.6E-09 | CCW/SW-HPI-INIT |
| | S2NNYNYNY | 5.6E-09 | CCW/SW-HPI-INIT |
| | S2INYYYNR | 3.9E-09 | CCW/SW-HPI-RECIRC |
| | S2NIYYNNN | 3.6E-09 | CCW/SW-HPI-INIT |
| | ANIYYYYY | 2.3E-09 | FAIL-LPI-INIT |
| | S1RIYYYYR | 2.1E-09 | POWER-LPI-INIT |
| | ARIYYYYR | 2.1E-09 | POWER-LPI-INIT |
| | S2IIYYNYR | 1.6E-09 | POWER-HPI-RECIRC |
| | S2NIYYNNR | 1.1E-09 | CCW/SW-HPI-INIT |

a. This PDS is split between the two failure characteristics as shown.

**Table 11.** continued.

| Plant Damage State Group | Plant Damage State | Point estimate CDF | Failure Characteristics |
|---|---|---|---|
| PDS-3 Transients | TLCYNNYY[a] | 5.8E-06 | ATWS-HPI-INIT |
| | TLCYNNYY[a] | 2.7E-07 | FAIL-HPI-INIT |
| | TIAYYNYR | 5.2E-06 | POWER-HPI-RECIRC |
| | TICYYNYY | 4.4E-07 | OPERATOR-HPI-RECIRC |
| | TINYYNYR | 3.3E-08 | POWER-HPI-RECIRC |
| | TICYYNYR | 1.9E-08 | POWER-HPI-RECIRC |
| | TLCYNNYR | 1.0E-08 | FAIL-HPI-INIT |
| | TLAYNNYR | 2.5E-09 | FAIL-HPI-INIT |
| | TLAYNNYY | 8.5E-09 | ATWS-HPI-INIT |
| | TNCYNNYY | 1.1E-09 | CCW/SW-HPI-INIT |
| | TNCYNNYN | 1.1E-09 | CCW/SW-HPI-INIT |
| | TNAYNNYN | 1.0E-09 | CCW/SW-HPI-INIT |
| PDS-4 SGTR | HICYNXYY | 1.3E-06 | RECIRC-HPI-RECIRC |
| | GNCYNYNN | 2.9E-08 | CCW/SW-HPI-INIT |
| | GNCYNYNY | 2.9E-08 | CCW/SW-HPI-INIT |
| | GNCYNNYY | 5.6E-09 | ATWS-HPI-INIT |
| | GNCYNYYN | 2.2E-09 | SAFETY-HPI-INIT |
| PDS-5 V | V | 1.1E-07 | RECIRC-HPI-RECIRC |
| TOTAL | | 2.8E-04 | |

a. This PDS is split between the two failure characteristics as shown.

Table 12. Contribution by injection system failure mechanisms to the total core damage frequency at Zion.

| Failure Mechanism | Number of PDSs | Mean CDF | Percent of Total CDF | Percent of failures by injection system | | | |
|---|---|---|---|---|---|---|---|
| | | | | HPI | | LPI | |
| | | | | Initial | Recirc. | Initial | Recirc. |
| POWER | 11 | 1.1E-05 | 4 | 50 | 50 | <<0.1 | 0 |
| RECIRC | 2 | 1.4E-067 | 0.5 | 0 | 100 | 0 | 0 |
| FAIL | 5[a,b] | 2.2E-06 | 1 | 13 | 0 | 87 | 0 |
| ATWS | 4[b] | 5.9E-06 | 2 | 100 | 0 | 0 | 0 |
| OPERATOR | 7[a] | 1.8E-05 | 6.5 | 0 | 46 | 0 | 54 |
| CCW/SW | 28 | 2.4E-04 | 86 | 99.7 | 0.2 | <<0.1 | 0 |
| SAFETY | 2 | 9.9E-09 | <<0.1 | 100 | 0 | 0 | 0 |
| TOTAL | 60[c] | 2.8E-04 | 100 | | | | |

a. PDS S1IBYYYYY is split between failure mechanisms OPERATOR-LPI-RECIRC and FAIL-LPI-INIT.
b. PDS TLCYNNYY is split between failure mechanisms ATWS-HPI-INIT and FAIL-HPI-INIT.
c. Total tally includes the two split PDSs.

## 5.3 Sequoyah Results

The injection failure mechanism descriptions for the dominant accident sequences at Sequoyah are presented in Table 13. The simplified three character failure descriptions are presented in Table 14. These three character failure descriptions were then sorted to obtain the CDF contribution for each of the failure mechanisms. Table 15 presents the CDF contribution by failure mechanism, by which injection system is failed, and by time of failure.

The results in Table 15 indicate that the dominant failure mechanism at Sequoyah involves recirculation mode failures and occurs in 12 sequences which makeup 64% of the total CDF. One of these sequences is the V sequence (1% of the total CDF.) This sequence is identical to that described for Surry above. As was discussed previously, no viable recovery actions exist for this sequence. Another three of the sequences (4% of the total CDF) involve a SGTR in which the RCS is not depressurized sufficiently to stop the loss of coolant. This leads to loss of core inventory, depletion of the refueling water storage tank (RWST), and finally the core uncovers. Possible recovery actions for these sequences include continued refilling of the RWST or adding an additional water source.

The remaining eight sequences (59% of the total CDF) involve very small, small, medium, and large break LOCAs. Although for some of these sequences, operator failure to properly initiate the recirculation switchover is an important contributor for this failure mechanism, these sequences were not classified as an operator error mechanism as was done for Zion above. The reason for this is that it was not clear from the NUREG/CR-4550 (see Reference 4) which sequences were due to operator error and which were due failures in the recirculation system. Three sequences ($S_3O_CH_2$, $S_3O_CH_3$, and $S_3W_1H_3$) involve small break sizes (break diameter less than a half inch.) These three sequences contribute 35% to the total CDF. The time at which the core uncovers for these sequences is greater than 17 hours. Two sequences ($S_2H_2$ and $S_2H_3$) involve small break sizes (break diameter between 0.5 and 2

inches.) These two sequences contribute 11% to the total CDF. For these sequences, depending upon the break size, the time at which the core uncovers varies from 45 minutes to 17 hours. The remaining three sequences ($S_1H_2$, $S_1H_4$, and $AH_1$) involve medium and large break LOCAs. These three sequences contribute more than 13% to the total CDF. The time at which the core uncovers for these sequences is between 15 and 50 minutes for the medium LOCAs and less than 1 minute for the large LOCA. Possible recovery actions for these sequences can be found in the discussion for Surry.

### Power Failures

Failures due to loss of ac power involve four sequences and accounts for 26% of the total CDF. In all of these sequences, the RCS remains at high pressure, so that the HPI system is required for coolant make up. The system is unavailable from the start of the sequence and remains so for the duration of the sequence. Even if the RCS could be depressurized, the low pressure injection systems would also be unavailable due to the loss of ac power.

Of the four sequences involving loss of power, in two of them, the core uncovers in approximately 1 hour (SBO-Q and SBO-L.) These two sequences contribute 18% to the total CDF at Sequoyah. For the remaining two (SBO-SLOCA and SBO-BATT), the time at which the core uncovers varies from 2.5 to 7 hours. Possible recovery actions for these sequences are the same as those discussed for Surry power failures.

### Hardware Failures

Failure of the injection systems because of hardware failure occurs in 5 of the sequences (7% of the total CDF.) Of these sequences, three involve failure of the HPI and two involve failure of the LPI (4% and 3% of the total CDF, respectively.) For all of the sequences, the injection system are failed at the beginning of the sequence. For the HPI system failures, the sequences all involve transients ($T_2L_1P_1$, $T_{DCI}L_1P_1$, and $T_{DCII}L_1P_1$) which result in loss of main feedwater. Subsequent failure of the power operated relief valves (PORVs) to open for feed and bleed cooling causes the core to uncover. For the LPI system failures, the two sequences involve large break LOCAs ($AD_5$ and

$AD_6$) in which the time at which the core uncovers is less than one minute. Because of this very short time, recovery of the LPI system is not viable. For those sequences involving failure of the HPI system, one possible recovery action would be to depressurize the RCS so that the LPI system could be utilized. However, since failure to depressurize the RCS was accounted for in defining these sequences, new innovative depressurization mechanisms would have to be deduced.

**ATWS Event Failures**

Finally, as was seen for Surry, two sequences (TKRZ and $TKRD_4$; 3% of the total CDF) involve an ATWS event which induces an overpressurization which fails the HPI system immediately. Further discussion on these sequences can be found in the results for Surry.

Table 13. Injection failure mechanism descriptions for the dominant accident sequences at Sequoyah.

| Plant Damage State | Accident Sequence | Mean CDF | Percent Contribution To PDS | Percent Contribution To Total CDF | Injection System Status: HPI | Injection System Status: LPI | Auxiliary Feedwater Status: Motor Driven | Auxiliary Feedwater Status: Turbine Driven | RCS Status |
|---|---|---|---|---|---|---|---|---|---|
| PDS-1 Slow Blackout | SBO-SLOCA | 4.32E-06 | 86.4 | 7.6 | See note (a). | See note (a). | See note (a). | Starts successfully and continues to run, but battery depletion occurs at 4 hours. This results in loss of instrumentation and control power. | Seal LOCA starts at 1.5 hours. Time of CU is dependent upon the LOCA size and if the operator depressurizes the RCS. Time of CU varies from 2.5 to 5.9 hours from the loss of AC power. |
| | SBO-Q | 3.87E-07 | 7.7 | 0.7 | See note (a). | See note (a). | See note (a). | Starts successfully and continues to run. Core uncovers before battery depletion. Fails in sequence T1-22 (14%). | Primary coolant discharge from stuck open pressurizer PORV leads to CU in 1 hour. PORV block valves are unavailable due to no AC. |
| | SBO-BATT | 3.08E-07 | 6.2 | 0.5 | See note (a). | See note (a). | See note (a). | Starts successfully and continues to run, but battery depletion occurs at 4 hours. This results in loss of instrumentation and control power. Core uncovers 3 hrs later. | RCS boundary remains intact. |
| PDS-2 Fast Blackout | SBO-L | 9.64E-06 | 100.0 | 16.9 | See not (a). | See note (a). | See note (a). | Fails CU occurs at approximately 1 hour. | Remains intact. |
| PDS-3 Loss of Coolant Accident | $S_3D_0H_3$ | 1.43E-05 | 40.2 | 25.0 | Operates initially, but fails in recirculation mode. | Not activated as RCS is at high pressure. | Operates. | Not required. | Very small break ($D < 0.5"$). Time of CU dependent upon the LOCA size and if secondary is depressurized. With secondary depressurized, time to CU is greater than 17 hours. |

a. System unavailable at the time the transient is initiated due to lack of AC power.

Table 13. Continued.

| Plant Damage State | Accident Sequence | Mean CDF | Percent Contribution To PDS | Percent Contribution To Total CDF | Injection System Status: HPI | Injection System Status: LPI | Auxiliary Feedwater Status: Motor Driven | Auxiliary Feedwater Status: Turbine Driven | RCS Status |
|---|---|---|---|---|---|---|---|---|---|
| POS-3 Loss of Coolant Accident, cont. | $S_2Q_CH_2$ | 5.02E-06 | 14.1 | 8.8 | Operates. | Operates initially, but fails in recirculation mode. | Operates. | Not required. | Same as $S_2Q_CH_2$. |
| | $S_1H_2$ | 4.88E-06 | 13.7 | 8.5 | Operates initially, but fails in recirculation mode. | Operates initially and in recirculation mode. | Operates. | Not required. | Medium size break (2"<D<6") in the RCS piping. Time of CU is dependent on break size. For 2" break, the time to CU is < 50 min., for 3.5" break, the time to CU is < 15 min. independent of secondary depressurization. |
| | $S_2H_2$ | 4.50E-06 | 12.6 | 7.8 | Operates initially, but fails in recirculation mode. | Not activated, RCS is at high pressure. | Operates. | Not required. | Small break (0.5"<D<2") in RCS piping. With secondary depressurized, time to CU is 45 min. to 17 hours. |
| | $S_1H_4$ | 1.90E-06 | 5.3 | 3.3 | Operates. | Operates initially, but fails in recirculation mode. | Operates. | Not required. | Same as $S_1H_2$. |
| | $S_2H_3$ | 1.72E-06 | 4.8 | 3.0 | Operates initially, but fails in recirculation mode. | Fails to supply coolant to HPI recirculation mode. | Operates. | Not required. | Same as $S_2H_2$. |
| | $AD_5$ | 1.29E-06 | 3.6 | 2.3 | Not required; RCS at low pressure. | Operates, but accumulators fail to inject, leading to core damage. Time of CD is immediate. | Not required. | Not required. | Large break (6"<D< 29") in the RCS piping. Time of CU is dependent on break size, but is on the order of 1 min. or less. |
| | $AH_1$ | 9.98E-07 | 2.8 | 1.7 | Not required; RCS at low pressure. | Operates initially, but fails in recirculation mode. | Not required. | Not required. | Same as $AD_5$. |
| | $S_3W_1H_3$ | 6.34E-07 | 1.8 | 1.1 | Operates. | Operates initially, but fails in recirculation mode. | Operates. | Not required. | Same as $S_3Q_CH_2$. |
| | $AD_6$ | 3.41E-07 | 1.0 | 0.6 | Not activated as RCS is at low pressure. | Fails. | Not required. | Not required. | Same as $AD_5$. |

Table 13. Continued.

| Plant Damage State | Accident Sequence | Mean CDF | Percent Contribution To PDS | Percent Contribution To Total CDF | Injection System Status: HPI | Injection System Status: LPI | Auxiliary Feedwater Status: Motor Driven | Auxiliary Feedwater Status: Turbine Driven | RCS Status |
|---|---|---|---|---|---|---|---|---|---|
| PDS-4 V | Event V | 6.50E-07 | 100.0 | 1.1 | Operates initially, but unable to recirculate. | Fails initially. | Operates. | Not required. | High pressure system ruptures low pressure system. |
| PDS-5 Transients | $T_2L_1P_1$ | 1.93E-06 | 73.9 | 3.4 | Operates but PORVs fail to open, so feed and bleed cooling fails. | Not activated as RCS is at high pressure. | Fails. | Does not operate as power conversion system is disabled. | RCS boundary remains intact. |
| | $T_{DC}L_1P_1$ | 3.38E-07 | 13.0 | 0.6 | Same as sequence $T_2L_1P_1$. | | | | |
| | $T_{DC}L_1P_1$ | 3.38E-07 | 13.0 | 0.6 | Same as sequence $T_2L_1P_1$. | | | | |
| PDS-6 ATWS | TKRZ | 1.40E-06 | 72.2 | 2.4 | Disabled due to initial pressure rise. | Not activated as RCS is at high pressure. | Operates. | Not required. | Initial pressure rise fails RCS boundary integrity. Very small break size. |
| | $TKRD_4$ | 2.39E-07 | 12.3 | 0.4 | Emergency boration pumps fail; continued power generation maintains pressure above RV set points. High pressure fails charging pumps. | Not activated as RCS is at high pressure. | Operates. | Not required. | Continued discharge through relief valves leads to core damage. |
| | $T_{SQ}KR$ | 3.01E-07 | 15.5 | 0.5 | Operates initially, but recirculation is not possible. | Not activated as RCS is at high pressure. | Operates. | Not required. | Loss of SG integrity and continued high pressure due to ATWS leads to loss of core inventory and CU. |
| PDS-7 SGTR | $T_{SQ}Q_3Q_4$ | 1.30E-06 | 76.8 | 2.3 | Operates initially, but recirculation is not possible. | Not activated as RCS is at high pressure; recirculation is not possible. | Operates. | Not required. | Loss of SG integrity and failure to depressurize leads to depletion of RWST inventory and CU. Refilling RWST delays CU. |
| | $T_{SQ}L$ | 4.14E-07 | 24.2 | 0.7 | Operates but feed and bleed is not successful due to RCS depressurization to mitigate SGTR; recirculation is not possible. | Not activated as RCS is at high pressure. | Fails. | Inoperable due to SGTR. | Loss of core inventory through SGTR leads to CU. |

Table 14. Injection system failure mechanism characteristics for the dominant accident sequences at Sequoyah.

| Plant Damage State | Sequence | Mean CDF | Failure Characteristics |
|---|---|---|---|
| PDS-1 Slow Blackout | SBO-SLOCA | 4.32E-06 | POWER-HPI-INIT |
| | SBO-Q | 3.87E-07 | POWER-HPI-INIT |
| | SBO-BATT | 3.08E-07 | POWER-HPI-INIT |
| PDS-2 Fast Blackout | SBO-L | 9.64E-06 | POWER-HPI-INIT |
| PDS-3 Loss of Coolant Accident | $S_3O_CH_2$ | 1.43E-05 | RECIRC-HPI-RECIRC |
| | $S_3O_CH_3$ | 5.02E-06 | RECIRC-LPI-RECIRC |
| | $S_1H_2$ | 4.88E-06 | RECIRC-HPI-RECIRC |
| | $S_2H_2$ | 4.50E-06 | RECIRC-HPI-RECIRC |
| | $S_1H_4$ | 1.90E-06 | RECIRC-LPI-RECIRC |
| | $S_2H_3$ | 1.72E-06 | RECIRC-LPI-RECIRC |
| | $AD_5$ | 1.29E-06 | FAIL-LPI-INIT |
| | $AH_1$ | 9.98E-07 | RECIRC-LPI-RECIRC |
| | $S_3W_1H_3$ | 6.34E-07 | RECIRC-LPI-RECIRC |
| | $AD_6$ | 3.41E-07 | FAIL-LPI-INIT |
| PDS-4 V | V | 6.50E-07 | RECIRC-HPI-RECIRC |
| PDS-5 Transients | $T_2L_1P_1$ | 1.93E-06 | FAIL-HPI-INIT |
| | $T_{DCI}L_1P_1$ | 3.38E-07 | FAIL-HPI-INIT |
| | $T_{DCII}L_1P_1$ | 3.38E-07 | FAIL-HPI-INIT |
| PDS-6 ATWS | TKRZ | 1.40E-06 | ATWS-HPI-INIT |
| | $TKRD_4$ | 2.39E-07 | ATWS-HPI-INIT |
| | $T_{SG}KR$ | 3.01E-07 | RECIRC-HPI-RECIRC |
| PDS-7 SGTR | $T_{SG}O_DQ_S$ | 1.30E-06 | RECIRC-HPI-RECIRC |
| | $T_{SG}L$ | 4.14E-07 | RECIRC-HPI-RECIRC |
| TOTAL | | 5.71E-05 | |

Table 15. Contribution by injection system failure mechanisms to the total core damage frequency at Sequoyah.

| Failure Mechanism | Number of Sequences | Mean CDF | Percent of Total CDF | Percent of failures by injection system | | | |
|---|---|---|---|---|---|---|---|
| | | | | HPI | | LPI | |
| | | | | Initial | Recirc. | Initial | Recirc. |
| POWER | 4 | 1.5E-05 | 26 | 100 | 0 | 0 | 0 |
| RECIRC | 12 | 3.7E-05 | 64 | 0 | 72 | 0 | 28 |
| FAIL | 5 | 4.2E-06 | 7 | 62 | 0 | 38 | 0 |
| ATWS | 2 | 1.6E-06 | 3 | 100 | 0 | 0 | 0 |
| TOTAL | 23 | 5.7E-05 | 100 | | | | |

## 5.4 Peach Bottom Results

The injection failure mechanism descriptions for the dominant accident sequences at Peach Bottom are presented in Table 16. The simplified three character failure descriptions are presented in Table 17. These three character failure descriptions were then sorted to obtain the CDF contribution for each of the failure characteristics. Table 18 presents the CDF contribution by failure mechanism, by which injection system is failed, and by time of failure.

### Power Failures

The results in Table 18 indicate that the dominant failure mechanism at Peach Bottom is due to loss of ac power (46% of the total CDF.) The reactor coolant system (RCS) remains at high pressure, so that either the high pressure coolant injection (HPCI) or the reactor core isolation cooling (RCIC) systems are required for coolant make up. If the RCS can be depressurized, the low pressure injection systems are unavailable due to the loss of ac power.

A total of five sequences involve this scenario. Of these, three (T1-BNU11, T1-P1BNU11, and T1-BU11NU21), involve late failures of the HPCI and RCIC due to either loss of room cooling or due to battery depletion (after about ten hours.) The core is uncovered after about 10 to 13 hours due to coolant boiloff. These three sequences contribute 41% to the total CDF at Peach Bottom. In the remaining two (T1-BU11U21 and T1-P1BU11U21), the core uncovers in approximately 1 hour. These two sequences contribute 4.6% to the total CDF. For the long term sequences, possible recovery actions are to provide an alternative on-site ac power supply to the control rod drive system or to the high pressure service water (HPSW) system for long term core cooling. If the HPSW is to be used the reactor must also be depressurized. For the short term sequences, the only viable recovery would be alternative sources of on-site ac and dc power. However, whether such power sources could be initiated in sufficient time would have to be determined.

**Hardware Failures**

Failure of the injection systems because of a hardware failure occurs in two sequences (T3C-CU11X and T3A-CU11X; 7% of the total CDF.) These involve transients with failure to scram, the SLC operates, the HPCI and RCIC fail, and depressurization fails which precludes low pressure cooling. The core uncovers in less than 15 minutes. There are no feasible recovery actions for these sequences because of the very short times for the core to uncover.

**ATWS Events**

Failure of the injection systems because of an ATWS event occurs in five of the sequences (35% of the total CDF.) Three (T3A-C-SLC, T3B-C-SLC, and T2-C-SLC; 32.6% of the total CDF) involve a transient with failure to scram and standby liquid control (SLC) system failure. The HPCI fails early on high suppression pool temperature. Then the reactor is either not depressurized or is manually depressurized to use the low pressure systems. However in the latter case, the low pressure systems will always fail due to low net positive suction head (NPSH), harsh environments, or the inability to keep the reactor vessel depressurized. The remaining two sequences T3C-C-SLC and T1-C-SLC (3.4% of the total CDF) are similar, except that a safety relief valve is stuck open in the first case and in the latter, the sequence initiator is loss of offsite power. The only feasible recovery actions for these sequences would be to scram the reactor and then depressurize the reactor. However, since failure to scram the reactor and to depressurize the RCS was accounted for in defining these sequences, new innovative depressurization mechanisms would have to be deduced.

**Operator Failures**

Failure of the injection systems because of an operator error occurs in six of the sequences (11% of the total CDF.) All of these sequences involve cases where the low pressure systems are required but operator miscalibration of the reactor pressure sensors prevents the injection valves to open. Five of the sequences involve the equivalent of a medium size LOCA and one involves a large LOCA. For the medium LOCA cases the core uncovers in one to two hours and for the large LOCA in about 15 minutes. Because of the relatively short times involved, there are no feasible recovery actions.

Table 16. Injection failure mechanism descriptions for the dominant accident sequences at Peach Bottom.

| Super Plant Damage State | Accident Sequence | Mean CDF | Percent Contribution To PDS | Percent Contribution To Total CDF | Injection System Status: HPCI and CRD | RCIC | LPCI | LPCS and HPSW | RCS Status |
|---|---|---|---|---|---|---|---|---|---|
| LOSP | T1-BNU11 | 1.6E-06 | 74.3 | 35.8 | HPCI operates initially, but fails in about 10 hours due to loss of room cooling or battery depletion; CRD - see note (a). | Fails in same manner as HPCI. | See note (a). | See note (a). | Core damage occurs in about 13 hours due to coolant boiloff. |
| | T1-BU11U21 | 1.9E-07 | 8.8 | 4.3 | HPCI failed from common cause failure of multiple batteries, followed by failure of diesel generators; CRD - see note (a). | Fails in same manner as HPCI. | See note (a). | See note (a). | Core damage occurs in about one hour. |
| | T1-P1BNU11 | 1.3E-07 | 6.0 | 2.9 | HPCI operates initially, but fails in about 10 hours due to loss of room cooling or battery depletion; CRD - see note (a). | Fails in same manner as HPCI. | See note (a). | See note (a). | Core damage occurs in about 10 to 13 hours. Failed open SRV causes slightly faster boiloff than for T1-BNU11. |
| | T1-BU11NU21 | 1.3E-07 | 6.0 | 2.9 | HPCI fails initially; CRD - see note (a). | RCIC fails following battery depletion or due to harsh environment. | See note (a). | See note (a). | Core damage occurs in about 13 hours due to coolant boiloff. |
| | T1-PZVZ34NU11B | 8.7E-08 | 4.0 | 1.9 | HPCI operates initially, 2 SRVs fail open; fails in about 0.5 to 1.0 hour due to loss of vessel steam pressure; CRD is operating but cannot mitigate the sequence. | Fails in same manner as HPCI. | Fails initially, mainly due to miscalibration of reactor pressure sensors, so injection valves do not open. | LPCS fails in same manner as LPCI; HPSW cannot be connected in time to prevent CD. | The two stuck open SRVs are equivalent to an S1 LOCA. Core damage occurs in 1 to 2 hours. |
| | T1-P1BH11U21 | 1.7E-08 | 0.8 | 0.4 | HPCI failed due to common cause failure of multiple batteries, followed by failure of diesel generators; CRD - see note (a). | Fails in same manner as HPCI. | See note (a). | See note (a). | Core damage occurs in about 1 hour. Failed open SRV causes slightly faster boiloff than for T1-BU11U21. |

a. System unavailable at the time the transient is initiated due to lack of ac power.

Table 16. Continued.

| Super Plant Damage State | Accident Sequence | Mean CDF | Percent Contribution To PDS | Percent Contribution To Total CDF | Injection System Status: HPCI and CRD | RCIC | LPCI | LPCS and HPSW | RCS Status |
|---|---|---|---|---|---|---|---|---|---|
| Loss of Coolant Accident | S1-V2V3V4NU11 | 2.1E-07 | 82.0 | 4.7 | HPCI operates initially, but fails in about 0.5 to 1.0 hour due to loss of vessel steam pressure; CRD is operating but cannot mitigate the LOCA. | Fails in same manner as HPCI. | Fails initially, mainly due to miscalibration of reactor pressure sensors, so injection valves do not open. | LPCS and HPSW fail in same manner as LPCI. | Medium size LOCA leads to core damage in 1 to 2 hours. |
| | A-V2V3 | 4.6E-08 | 18.0 | 1.0 | HPCI not activated as RCS is at low pressure; CRD is operating but cannot mitigate the LOCA. | Fails in same manner as HPCI. | Fails initially, mainly due to miscalibration of reactor pressure sensors, so injection time to prevent CD. valves do not open. | LPCS fails in same manner as LPCI; HPSW cannot be connected in | Large LOCA with no injection leads to core damage in about 15 min. |
| Transient | T2-P2V234NU11 | 5.7E-08 | 41.3 | 1.3 | HPCI operates initially, 2 SRVs fail open. HPCI fails in about 0.5 to 1.0 hour due to loss of vessel steam pressure; CRD is operating but cannot mitigate the sequence. | Fails in same manner as HPCI. | Fails initially, due to miscalibration of reactor pressure sensors, so injection valves do not open. | LPCS and HPSW fail in same manner as LPCI. | The two stuck open SRVs are equivalent to a medium LOCA. Core damage occurs in 1 to 2 hours. |
| | T3B-P2V234NU11 | 5.6E-08 | 40.6 | 1.3 | Same as sequence T2-P2V234NU11. | | | | |
| | T3A-P2V234NU11 | 2.5E-08 | 18.1 | 0.6 | Same as sequence T2-P2V234NU11. | | | | |
| ATWS | T3A-C-SLC | 1.4E-06 | 73.1 | 31.4 | HPCI fails in less than 0.5 hour due to high suppression pool temperature; CRD is operating but cannot mitigate the sequence. | Fails in same manner as HPCI. | Fails because of low net positive suction head, steam in reactor building, or inability to keep the reactor depressurized. | LPCS and HPSW fail in same manner as LPCI. | Reactor protection system and standby liquid control system fail leading to core damage. |
| | T3A-CU11X | 2.8E-07 | 14.6 | 6.3 | HPCI fails either due to component failure, failing to start and run, or being out for maintenance; CRD is operating but cannot mitigate the sequence. | Fails in same manner as HPCI. | Low pressure cooling can not be initiated because reactor depressurization fails. | LPCS and HPSW fail in same manner as LPCI. | Reactor protection system and depressurization fail; 2 SRVs stuck open; core damage occurs in less than fifteen minutes. |

Table 16. Continued.

| Super Plant Damage State | Accident Sequence | Mean CDF | Percent Contribution To PDS | Percent Contribution To Total CDF | Injection System Status: HPCI and CRD | RCIC | LPCI | LPCS and HPSW | RCS Status |
|---|---|---|---|---|---|---|---|---|---|
| ATWS, cont. | T3C-C-SLC | 1.1E-07 | 5.7 | 2.5 | HPCI fails in less than 0.5 hour due to high suppression pool temperature; CRD is operating but cannot mitigate the sequence. | Fails in same manner as HPCI. | Fails because of low net positive suction head, steam in reactor building, or inability to keep the reactor depressurized. | LPCS and HPSW fail in same manner as LPCI | Inadvertent open SRV, reactor protection system and standby liquid control system fails leading to core damage. |
| | T1-C-SLC | 4.4E-08 | 2.3 | 1.0 | Same as sequence T3A-C-SLC. | | | | |
| | T3B-C-SLC | 3.3E-08 | 1.7 | 0.7 | Same as sequence T3A-C-SLC. | | | | |
| | T2-C-SLC | 2.7E-08 | 1.4 | 0.6 | Same as sequence T3A-C-SLC. | | | | |
| | T3C-CV1IX | 2.2E-08 | 1.1 | 0.5 | HPCI fails either due to component failure, failing to start and run, or being out for maintenance; CRD is operating but cannot mitigate the sequence. | Fails in same manner as HPCI. | Low pressure cooling can not be initiated because reactor depressurization fails. | LPCS and HPSW fail in same manner as LPCI. | Inadvertent open SRV, reactor protection system and depressurization fail; core damage occurs in less than fifteen minutes. |

Table 17. Injection system failure mechanism characteristics for the dominant accident sequences at Peach Bottom.

| Super Plant Damage State | Sequence | Mean CDF | Failure Characteristics |
|---|---|---|---|
| LOSP | T1-BNU11 | 1.6E-06 | POWER-HPI-LATE |
| | T1-BU11U21 | 1.9E-07 | POWER-HPI-INIT |
| | T1-P1BNU11 | 1.3E-07 | POWER-HPI-LATE |
| | T1-BU11NU21 | 1.3E-07 | POWER-HPI-LATE |
| | T1-P2V234NU11B | 8.7E-08 | OPERATOR-LPI-INIT |
| | T1-P1BU11U21 | 1.7E-08 | POWER-HPI-INIT |
| LOCA | S1-V2V3V4NU11 | 2.1E-07 | OPERATOR-LPI-INIT |
| | A-V2V3 | 4.6E-08 | OPERATOR-LPI-INIT |
| Transient | T2-P2V234NU11 | 5.7E-08 | OPERATOR-LPI-INIT |
| | T3B-P2V234NU11 | 5.6E-08 | OPERATOR-LPI-INIT |
| | T3A-P2V234NU11 | 2.5E-08 | OPERATOR-LPI-INIT |
| ATWS | T3A-C-SLC | 1.4E-06 | ATWS-HPI-INIT |
| | T3A-CU11X | 2.8E-07 | FAIL-HPI-INIT |
| | T3C-C-SLC | 1.1E-07 | ATWS-HPI-INIT |
| | T1-C-SLC | 4.4E-08 | ATWS-HPI-INIT |
| | T3B-C-SLC | 3.3E-08 | ATWS-HPI-INIT |
| | T2-C-SLC | 2.7E-08 | ATWS-HPI-INIT |
| | T3C-CU11X | 2.2E-08 | FAIL-HPI-INIT |
| TOTAL | | 4.5E-06 | |

Table 18. Contribution by injection system failure mechanisms to the total core damage frequency at Peach Bottom.

| Failure Mechanism | Number of Sequences | Mean CDF | Percent of Total CDF | Percent of failures by injection system | | | |
|---|---|---|---|---|---|---|---|
| | | | | HPI | | LPI | |
| | | | | Initial | Late | Initial | Late |
| POWER | 5 | 2.1E-06 | 46 | 10 | 90 | 0 | 0 |
| FAIL | 2 | 3.0E-07 | 7 | 100 | 0 | 0 | 0 |
| ATWS | 5 | 1.6E-06 | 36 | 100 | 0 | 0 | 0 |
| OPERATOR | 6 | 4.8E-07 | 11 | 0 | 0 | 100 | 0 |
| TOTAL | 18 | 4.5E-06 | 100 | | | | |

## 5.5 Grand Gulf Results

The injection failure mechanism descriptions for the dominant accident sequences at Grand Gulf are presented in Table 19. The simplified three character failure descriptions are presented in Table 20. These three character failure descriptions were then sorted to o' ain the CDF contribution for each of the failure characteristics. Table 21 presents the CDF contribution by failure mechanism, by which injection system is failed, and by time of failure.

### Hardware Failures

The results in Table 21 indicate that the dominant failure mechanism at Grand Gulf is hardware failure which contributes 86% to the total CDF. Nine sequences contribute to this failure mechanism. This tally of sequences includes the split sequences T1B-16, T1B-21, TC-74, and T2-56. The first two sequences (82% of the CDF) involve a loss of offsite power which is recoverable. The vessel is at high pressure and the high pressure core spray (HPCS) and the CRD systems are unavailable because of ac power failure. The RCIC is demanded but fails to run initially and the core uncovers in about one hour. Possible recovery actions for these sequences would involve an alternative source of ac power to the HPCS or CRD systems. Whether such a system could be actuated in time to prevent core damage would have to be determined.

Sequence TC-74 is split between PDSs 9 and 10 (1.2% and 1.5% of the total CDF, respectively.) Both PDSs are initiated by an ATWS, but the sequence of events that follow are different for the two PDSs. In PDS-9, the ATWS event is followed by failure to depressurize the reactor so that all LPI systems cannot operate. The HPCS is required but fails on demand; the RCIC and CRD systems operate but are not sufficient to make up the coolant loss. Core damage occurs in about one hour. In PDS-10, the sequence follows that in PDS-9, except the HPCS operates initially and fails late due to harsh environment. Core damage occurs in over twelve hours. Recovery actions would

have to involve either an innovative mechanism to depressurize the reactor or some method of keeping the HPCS pump room cooled.

Sequence T2-56 (much less than 0.1% of the total CDF) involves a loss of the power conversion system followed by failure to depressurize the reactor. The HPI systems are demanded. The HPCS and CRD system either fail initially and the RCIC fails late or vice versa. The systems fail initially due to miscalibration of the water level sensors and the operator fails to initiate manually. The systems fail late due to pump room heat up. Core damage occurs after 12 hours. Possible recovery actions for this sequence are the same as those discussed for the TC-74 sequence.

Power Failures

Failure of the injection systems because of loss of power occurs in seven sequences (13% of the total CDF.) This tally of sequences includes the split sequences T1B-16, T1B-17, and T1B-21 and the unsplit T1B-13. Sequence T1B-17 is split between PDSs 1, 2, 3, and 7. For this failure mechanism, sequences T1B-16 and T1B-21 only involve PDS-7.

The T1B-17 sequence events are identical for PDSs 1, 2, and 3 (1.2% of the total CDF.) The HPCS, CRD, LPCI, LPCS, and standby service water (SSW) systems are not available because of loss of ac power. Two SRVs are stuck open; the RCIC and firewater systems operate but are not sufficient to make up for the coolant loss. The core uncovers in about one hour. The only feasible recovery actions for this sequence would be to supply additional ac power sources to the HPCS and CRD systems. For PDS-7, the events are identical for sequences T1B-16, T1B-17, and T1B-21 (10.4% of the total CDF.) The HPCS, CRD, LPCI, LPCS, and standby service water (SSW) systems are not available because of loss of ac power. The RCIC system fails due to battery failure and the firewater system is only capable of providing sufficient injection in the long term. The core uncovers in about one hour. The only possible recovery action for these sequences would be to provide an alternative dc battery supply to the RCIC system. Whether such a system could be initiated in time to prevent core damage would have to be determined.

Sequence T1B-13 (1.6% of the total CDF) involves a loss of offsite power in which the HPCS, CRD, LPCI, LPCS, and standby service water (SSW) systems are not available because of loss of ac power. The RCIC system operates initially, but fails late because of high containment pressure. The firewater system operates until the reactor pressure rises above turbine shutoff head. Reactor pressure can not be controlled because of loss of dc power. The core uncovers after 12 hours. Possible recovery actions for this sequence would include a combination of all the recovery actions discussed for this failure mechanism.

**Operator Failures**

Finally, failure of the injection systems because of an operator error occurs in four of the sequences (1% of the total CDF.) This tally of sequences includes the split sequences T1B-14 and T2-56. The T1B-14 sequence is split between PDSs 4, 5, and 6, but the sequence events are identical for all three (1% of the total CDF.) The HPCS, CRD, LPCI, LPCS, and standby service water (SSW) systems are not available because of loss of ac power. The RCIC operates initially, but fails on high containment pressure. The firewater system is available but the operator fails to activate it. The core uncovers after 12 hours. The plant condition that causes the core to be uncovered is loss of ac power to the LPCI and LPCS. Sequence T2-56 involves a loss of the power conversion system in which the reactor is not depressurized and high pressure injection is required (much less than 0.1% of the total CDF.) However, all high pressure systems fail due to miscalibration of the water level sensors and the operator then fails to initiate the systems manually. Core damage occurs in about one hour. Possible recovery actions for these sequences are to provide an innovative depressurization method so as to utilize the low pressure systems.

Table 19. Injection failure mechanism descriptions for the dominant accident sequences at Grand Gulf.

| Plant Damage State | Accident Sequence | Mean CDF | Percent Contribution To PDS | Percent Contribution To Total CDF | Injection System Status: HPCS and CRD | Injection System Status: RCIC | Injection System Status: LPCI | Injection System Status: LPCS, SSW, Firewater and Condensate | RCS Status |
|---|---|---|---|---|---|---|---|---|---|
| PDS-1 SBO with Diesel Generator Failure B2-P3-I5-H2-M2-ST | T1B-16 | 3.0E-06 | 93.25 | 73.1 | See note (a). | Pump fails to start or run. | See note (a). | See notes (a), (b), and (c). | Core damage occurs in about one hour. |
| | T1B-17 | 4.5E-08 | 1.43 | 1.1 | See note (a). | Operates, but is not sufficient to make up for the coolant lost from open SRVs. | See note (a). | See notes (a) and (b); firewater and RCIC together are not sufficient. | Two stuck open SRVs equivalent to an SI LOCA. Core damage occurs in about one hour. |
| | T1B-21 | 1.7E-07 | 5.32 | 4.1 | See note (a). | Pump fails to start or run. | See note (a). | See notes (a), (b), and (c). | One stuck open SRV is equivalent to an SI LOCA. Core damage occurs in about one hour. |
| PDS-2 SBO with Diesel Generator Failure B2-P3-I5-H1-M2-ST | T1B-16 | 3.9E-08 | 80.57 | 0.95 | Same as sequence T1B-16 of PDS-1. | | | | |
| | T1B-17 | 8.0E-10 | 1.66 | 0.020 | Same as sequence T1B-17 of PDS-1. | | | | |
| | T1B-21 | 8.6E-09 | 17.77 | 0.21 | Same as sequence T1B-21 of PDS-1. | | | | |
| PDS-3 SBO with Diesel Generator Failure B2-P3-I3-H1-M2-ST | T1B-16 | 1.7E-07 | 94.80 | 4.1 | Same as sequence T1B-16 of PDS-1. | | | | |
| | T1B-17 | 3.1E-09 | 1.70 | 0.076 | Same as sequence T1B-17 of PDS-1. | | | | |
| | T1B-21 | 6.4E-09 | 3.50 | 0.16 | Same as sequence T1B-21 of PDS-1. | | | | |
| PDS-4 SBO with Diesel Generator Failure B2-P4-I5-H2-M2-LT | T1B-14 | 3.9E-08 | 100 | 0.95 | See note (a). | Initially operates, but high containment pressure causes RCIC turbine trip. | See note (a). | Operator fails to activate firewater system for coolant injection; also see notes (a) and (c). | Core damage occurs after 12 hours. |
| PDS-5 SBO with Diesel Generator Failure B2-P3-I5-H1-M2-LT | T1B-14 | 1.3E-09 | 100 | 0.032 | Same as sequence T1B-14 of PDS-4. | | | | |

a. HPCS, CRD, LPCI, LPCS, and SSW systems unavailable because of AC power failure; available only upon restoration of either offsite or onsite power.
b. Firewater system is only capable of providing sufficient injection in the long term (i.e., when coolant makeup has been provided for a period of time.)
c. Condensate system is unavailable because of AC power failure; available only upon restoration of offsite power.

Table 19. Continued.

| Plant Damage State | Accident Sequence | Mean CDF | Percent Contribution To PDS | Percent Contribution To Total CDF | Injection System Status: HPCS and CRD | Injection System Status: RCIC | Injection System Status: LPCI | Injection System Status: LPCS, SSW, Firewater and Condensate | RCS Status |
|---|---|---|---|---|---|---|---|---|---|
| PDS-6 SBO with Diesel Generator Failure B2-P4-I2-H1-M2-LT | T1B-14 | 2.0E-09 | 100 | 0.049 | Same as sequence T1B-14 of PDS-4. | | | | |
| PDS-7 SBO with no DC power; Non-recoverable B1-P1-I1-H1-M1-ST | T1B-16 | 4.1E-07 | 95.94 | 10.0 | See note (a). | Does not operate because of battery failure. | See note (a). | See notes (a) and (b). | Core damage occurs in about one hour. |
| | T1B-17 | 5.6E-10 | 0.13 | 0.014 | See note (a). | Does not operate because of battery failure. | See note (a). | See notes (a) and (b). | Two stuck open SRVs are equivalent to an S1 LOCA. Core damage occurs in about one hour. |
| | T1B-21 | 1.7E-08 | 3.93 | 0.41 | See note (a). | Does not operate because of battery failure. | See note (a). | See notes (a) and (b). | One stuck open SRV is equivalent to an S2 LOCA. Core damage occurs in about one hour. |
| PDS-8 SBO with no DC power; Non-recoverable B1-P1-I1-H1-M1-LT | T1B-13 | 6.6E-08 | 100 | 1.6 | See note (a). | Initially operates, but high containment pressure causes RCIC turbine trip. | See note (a). | Firewater operates initially, fails when reactor pressure rises above turbine shutoff head; also see note (a). | Core damage occurs some time after 12 hours. |
| PDS-9 ATWS TC-P2-I6-H3-M3-ST | TC-74 | 5.0E-08 | 100 | 1.2 | HPCS fails on demand due to hardware or MOV failure; CRD flow is not sufficient to make up coolant loss. | Operates, but is not sufficient to make up coolant loss. | Low pressure cooling cannot be initiated because reactor depressurization fails. | Fail in same manner as LPCI. | Reactor is not scrammed; core damage occurs in about one hour. |
| PDS-10 ATWS TC-P2-I4-H3-M3-LT | TC-74 | 6.3E-08 | 100 | 1.5 | HPCS operates initially but fails late due to room heatup; CRD flow is not sufficient to make coolant loss. | Operates, but is not sufficient to make up coolant loss. | Low pressure cooling cannot be initiated because reactor depressurization fails. | Fail in same manner as LPCI. | Reactor is not scrammed; core damage occurs in over twelve hours. |

a. HPCS, CRD, LPCI, LPCS, and SSW systems unavailable because of AC and DC power failure; systems are not recoverable when power is restored.
b. Firewater system is only capable of providing sufficient injection in the long term (i.e., when coolant makeup has been provided for a period of time.)

Table I9. Continued.

| Plant Damage State | Accident Sequence | Mean CDF | Percent Contribution To PDS | Percent Contribution To Total CDF | Injection System Status: HPCS and CRD | Injection System Status: RCIC | Injection System Status: LPCI | Injection System Status: LPCS, SSW, Firewater and Condensate | RCS Status |
|---|---|---|---|---|---|---|---|---|---|
| PDS-11 PCS T2-P2-I5-H3-M3-ST | T2-S6 | 1.2E-08 | 100 | 0.29 | Fail initially due to miscalibration of water level sensors and operator fails to initiate manually. | Fails in same manner as HPCS. | Low pressure cooling cannot be initiated because reactor depressurization fails. | Fail in same manner as LPCI. | Core damage occurs in about one hour. |
| PDS-12 PCS T2-P2-I5-H3-M3-LT | T2-S6 | 2.7E-10 | 100 | 0.0066 | Either, fail late due to room heatup or fail initially due to miscalibration of water level sensors and operator fails to initiate manually. | Fails in opposite reason to HPCS. | Low pressure cooling cannot be initiated because reactor depressurization fails. | Fail in same manner as LPCI. | Core damage occurs some time after 12 hours. |

Table 20. Injection system failure mechanism characteristics for the dominant accident sequences at Grand Gulf.

| Plant Damage State | | Sequence | Mean CDF | Failure Characteristics |
|---|---|---|---|---|
| PDS-1 | SBO<br>B2-P3-I5-H2-M2-ST | T1B-16<br>T1B-17<br>T1B-21 | 3.0E-06<br>4.5E-08<br>1.7E-07 | FAIL-HPI-INIT<br>POWER-HPI-INIT<br>FAIL-HPI-INIT |
| PDS-2 | SBO<br>B2-P3-I5-H1-M2-ST | T1B-16<br>T1B-17<br>T1B-21 | 3.9E-08<br>8.0E-10<br>8.6E-09 | FAIL-HPI-INIT<br>POWER-HPI-INIT<br>FAIL-HPI-INIT |
| PDS-3 | SBO<br>B2-P3-I3-H1-M2-ST | T1B-16<br>T1B-17<br>T1B-21 | 1.7E-07<br>3.1E-09<br>6.4E-09 | FAIL-HPI-INIT<br>POWER-HPI-INIT<br>FAIL-HPI-INIT |
| PDS-4 | SBO<br>B2-P4-I5-H2-M2-LT | T1B-14 | 3.9E-08 | OPERATOR-LPI-LATE |
| PDS-5 | SBO<br>B2-P3-I5-H1-M2-LT | T1B-14 | 1.3E-09 | OPERATOR-LPI-LATE |
| PDS-6 | SBO<br>B2-P4-I2-H1-M2-LT | T1B-14 | 2.0E-09 | OPERATOR-LPI-LATE |
| PDS-7 | SBO<br>B1-P1-I1-H1-M1-ST | T1B-16<br>T1B-17<br>T1B-21 | 4.1E-07<br>4.7E-10<br>1.7E-08 | POWER-HPI-INIT<br>POWER-HPI-INIT<br>POWER-HPI-INIT |
| PDS-8 | SBO<br>B1-P1-I1-H1-M1-LT | T1B-13 | 6.6E-08 | POWER-LPI-LATE |
| PDS-9 | ATWS<br>TC-P2-I6-H3-M3-ST | TC-74 | 5.0E-08 | FAIL-HPI-INIT |
| PDS-10 | ATWS<br>TC-P2-I4-H3-M3-LT | TC-74 | 6.3E-08 | FAIL-HPI-LATE |
| PDS-11 | PCS<br>T2-P2-I5-H3-M3-ST | T2-56 | 1.2E-08 | OPERATOR-HPI-INIT |
| PDS-12 | PCS<br>T2-P2-I5-H3-M3-LT | T2-56 | 2.7E-10 | FAIL-HPI-LATE |
| | TOTAL | | 4.1E-06 | |

Table 21. Contribution by injection system failure mechanisms to the total core damage frequency at Grand Gulf.

| Failure Mechanism | Number of Sequences[a] | Mean CDF | Percent of Total CDF | Percent of failures by injection system | | | |
|---|---|---|---|---|---|---|---|
| | | | | HPI | | LPI | |
| | | | | Initial | Late | Initial | Late |
| POWER | 7 | 5.4E-07 | 13 | 88 | 0 | 0 | 12 |
| FAIL | 9 | 3.5E-06 | 86 | 98 | 2 | 0 | 0 |
| OPERATOR | 4 | 5.4E-08 | 1 | 22 | 0 | 0 | 78 |
| TOTAL | 20 | 4.1E-06 | 100 | | | | |

a. Of the seven dominant accident sequences for this plant, six are divided into 19 split sequences and one is not divided, to make a total of 20 split and unsplit accident sequences.

# 6. CONCLUSIONS

For the five plants studied in the NUREG-1150 program, examination of the postulated sequences has revealed that insufficient water was added to prevent core damage in all of the sequences. The plant conditions which prevented water addition have been examined. The results for the five plants are summarized below.

Surry

At Surry, 17% of the CDF is due to sequences involving injection system failures in which no feasible recovery action could be implemented. The sequences involve interfacing system (V sequence) loss of coolant accidents (LOCAs), large and medium break LOCAs, and anticipated transients without scram (ATWS) events. However, the remaining 83% of the CDF is due to sequences in which core uncovery might be prevented if additional and innovative recovery actions were implemented. The CDF could be reduced up to 67%, if additional onsite ac power sources were provided; up to 10%, if the reactor vessel was depressurized so that available low pressure injection systems could be utilized; up to 4%, if additional stored water sources or if refilling of the refueling water supply storage tank (RWST) could be continued for an indefinite period of time; and up to 2%, if additional reactor scram procedures and devices were implemented.

Of those sequences that might be prevented if additional onsite ac power sources were provided, the injection systems are not available beginning at the accident initiation. For approximately 27% (based upon CDF) of these sequences, the core uncovers in approximately one hour and successful accident management actions would have to be initiated within this time frame to prevent core damage. For the remaining 73%, the time of core uncovery ranges from approximately two to seven hours, which allows more time for actions to be taken.

For those sequences that might be prevented if the reactor vessel was depressurized so that available low pressure injection systems could be

utilized, the high pressure injection system is failed immediately. For approximately 53% of these sequences, the time at which the core uncovers is not specified in the NUREG-1150 documentation. For 21% of these sequences, the time to core uncovery ranges from approximately 15 to 50 minutes which is a relatively short period of time for initiation of the necessary accident management actions. For the remaining 26%, the time of core uncovery ranges from approximately 50 minutes to 17 hours.

For those sequences that might be prevented if additional stored water sources were provided or if refilling of the RWST could be continued for an indefinite period of time, the high pressure system fails in the recirculation mode. The time of core uncovery is greater than ten hours for all of these sequences which should allow personnel sufficient time to complete the necessary actions.

For those sequences that might be prevented if additional reactor scram procedures and devices were implemented the high pressure injection systems are failed immediately. The time to core uncovery for these sequences is not specified in the available documentation.

Zion

At Zion, only 4.4% of the CDF is due to plant damage states (PDSs) involving injection system failures in which no feasible recovery action could be implemented. These PDSs involve V sequences, and large and medium break LOCAs. However, the remaining 95.6% of the CDF is due to PDSs in which core uncovery might be prevented if additional and innovative recovery actions were implemented. The CDF could be reduced up to 86%, if pump seal LOCAs, loss of component cooling, or loss of service water supplies could be prevented; up to 4%, if additional onsite ac power sources were provided; up to 3.5%, if additional stored water sources or if refilling of the RWST could be continued for an indefinite period of time; and up to 2%, if additional reactor scram procedures and devices were available.

The times of injection system failures at Zion are summarized below. However, estimates of the time to core uncovery were not available for most of the PDSs and are omitted.

For those PDSs that might be prevented if pump seal LOCAs, loss of component cooling, and loss of service water could be prevented, the injection systems are failed initially. For those PDSs that might be prevented if additional onsite ac power sources were provided, approximately 50% (based on CDF) involve initial failures of the high pressure injection systems. The remaining 50% involve failures of the high pressure injection systems in the recirculation mode. Of those PDSs that might be prevented if additional stored water sources or if refilling of the RWST could be continued for an indefinite period of time, all involve failures of the high pressure injection system in the recirculation mode. Finally, of those PDSs that might be prevented if additional reactor scram procedures and devices were available, all involve initial failures of the high pressure injection systems.

Sequoyah

At Sequoyah, 20% of the CDF is due to sequences involving injection system failures in which no feasible recovery action could be implemented. The sequences include a V sequence, large and medium break LOCAs, and ATWS events. However, the remaining 80% of the CDF is due to sequences in which core uncovery might be prevented if additional and innovative recovery actions were implemented. The CDF could be reduced up to 46%, if failures of the high and low pressure recirculation systems could be eliminated; up to 26%, if additional onsite ac power sources were provided; up to 5% if the reactor vessel was depressurized so that available low pressure injection systems could be utilized; and up to 4%, if additional stored water sources or if refilling of the RWST could be continued for an indefinite period of time.

For those sequences that might be prevented if failures of the high and low pressure recirculation systems were be eliminated, the injection system failures occur in the recirculation mode. For 76% (based upon CDF) of these sequences, the time to core uncovery is estimated as being greater than 17 hours which is adequate time for a wide range of accident management actions.

For the remaining 24%, the range of time to core uncovery is estimated as being from 45 minutes to 17 hours.

For those sequences that might be prevented if additional onsite ac power sources were provided, all involve initial failures of the high pressure injection system. For 68% of the sequences, the time to core uncovery is approximately one hour. For the remaining 32%, the time of core uncovery ranges from approximately two to seven hours.

Of those sequences that might be prevented if the reactor vessel was depressurized so that available low pressure injection systems could be utilized, all involve initial failures of the high pressure injection system. The time to core uncovery for these sequences is not specified.

Of those sequences that might be prevented if additional stored water sources or if refilling of the RWST could be continued for an indefinite period of time, all involve failure of the high pressure injection system in the recirculation mode. The time to core uncovery for these sequences is not specified.

**Peach Bottom**

At Peach Bottom, 18% of the CDF is due to sequences involving injection system failures in which no feasible recovery action could be implemented. The sequences include large and medium break LOCAs, and very short term ATWS events. However, the remaining 82% of the CDF is due to sequences in which core uncovery might be prevented if additional and innovative recovery actions were implemented. The CDF could be reduced up to 42%, if a combination of additional reactor vessel depressurization mechanisms and additional onsite ac power supplies to the low pressure injection systems were implemented; up to 5%, if only additional onsite ac power sources were provided; and up to 36%, if a combination of additional reactor scram and reactor depressurization mechanisms were implemented.

For those sequences that might be prevented if a combination of additional reactor vessel depressurization mechanisms and additional onsite ac

power supplies to the low pressure injection systems were implemented, the high pressure core injection (HPCI) and reactor core isolation cooling (RCIC) systems fail in approximately ten hours due to loss of room cooling or battery depletion. For these sequences, the core uncovers in approximately 10 to 13 hours. This time frame should be adequate for implementation of accident management strategies.

For those sequences that might be prevented if only additional onsite ac power sources were provided, the HPCI and RCIC systems fail at the start of the sequence. For these sequences the time to core uncovery is approximately one hour. Implementation of accident management strategies in this short time period could have a low likelihood of success unless they were well planned and executed.

For those sequences that might be prevented if a combination of additional reactor scram and reactor depressurization mechanisms were implemented, the HPCI and RCIC systems fail in less than one half hour due to high suppression pool temperature. The control rod drive (CRD) injection system is operating, but cannot mitigate the sequence. For these sequences, the time to core uncovery is not specified.

Grand Gulf

At Grand Gulf, all of the CDF is due to sequences in which core uncovery might be prevented if additional and innovative recovery actions were implemented. The CDF could be reduced up to 95%, if additional onsite ac and dc power sources were provided; up to 1.5%, if additional reactor vessel depressurization mechanisms were implemented; up to 1.5%, if additional pump room cooling was provided; and up to 1.6%, if a combination of all of the recovery actions were implemented.

For those sequences that might be prevented if additional onsite ac and dc power sources were provided, 99% of the sequences (based upon CDF) involve initial failures of the HPI systems. The time to core uncovery for these sequences is approximately one hour. The remaining 1% involve late failures

of the operator to activate the firewater system. The time to core uncovery for these sequences is approximately twelve hours.

For those sequences that might be prevented if additional reactor vessel depressurization mechanisms were implemented, more than 99% involve initial failure of the high pressure core spray system (HPCS). For these sequences, the CRD and RCIC systems are operating, but are not sufficient to make up the coolant loss. The time to core uncovery is approximately one hour.

The sequence that might be prevented if additional pump room cooling was provided involves late failure of the HPCS due to pump room heatup. The CRD and RCIC systems are operating, but are not sufficient to make up the coolant loss. The time to core uncovery is estimated as more than 12 hours.

Finally, the sequence that might be prevented if a combination of all of the recovery actions were implemented involves a late failure of the firewater system. The time of core uncovery is estimated as more than 12 hours.

The majority of the Grand Gulf sequences proceed to core damage in about one hour. Therefore, accident management actions would need to be well planned and executed to successfully prevent core damage.

# 7. REFERENCES


1. U.S. NRC, *Severe Accident Risks: An Assessment of Five U.S. Nuclear Power Plants*, (Draft), NUREG-1150, Revision 1, June 1989.

2. R. C. Bertucio and J. A. Julius, *Analysis of Core Damage Frequency: Surry Unit 1 Internal Events*, NUREG/CR-4550, Volume 3, Revision 1, Parts 1 and 2, SAND86-2084, April 1990.

3. M. B. Sattison and K. W. Hall, *Analysis of Core Damage Frequency: Zion Unit 1 Internal Events*, NUREG/CR-4550, Volume 7, Revision 1, EGG-2554, May 1990.

4. R. C. Bertucio and S. R. Brown, *Analysis of Core Damage Frequency: Sequoyah Unit 1 Internal Events*, NUREG/CR-4550, Volume 5, Revision 1, Parts 1 and 2, SAND86-2084, April 1990.

5. A. M. Kolaczkowski, et. al., *Analysis of Core Damage Frequency: Peach Bottom Unit 2 Internal Events*, NUREG/CR-4550, Volume 4, Revision 1, Parts 1 and 2, SAND86-2084, August 1989.

6. M. T. Drouin, et. al., *Analysis of Core Damage Frequency: Grand Gulf Unit 1 Internal Events*, NUREG/CR-4550, Volume 6, Revision 1, Parts 1 and 2, SAND86-2084, September 1989.

7. C. K. Park, et al., *Evaluation of Severe Accident Risks: Zion Unit 1*, NUREG/CR-4551, Volume 7, Draft Revision 1, BNL/NUREG-52029, July 1989.

# Appendix B

# Phenomenology of the Consequences of Adding Water to Degraded Reactor Cores

## ABSTRACT

A sequence of core damage states is developed as a basis to evaluate the consequences of water addition to a degraded core. The amount and rate of water addition required to remove energy from degraded cores and to arrest core damage progression are estimated for various stages of core degradation. Such information can be useful in the development of accident management plans.

## SUMMARY

Preventing severe accidents or mitigating their consequences requires implementation of strategies to add water to the reactor core. However, for advanced stages of core degradation, there is no assurance that water addition can immediately terminate the progression of core damage. Under certain degraded core conditions, adding water may enhance hydrogen production, induce changes in core geometry that complicate recovery, cause steam explosions, or make the reactor core critical again if unborated water is used. A primary purpose of an evaluation of the consequences of water addition to a degraded core is, therefore, to ensure that these undesirable consequences are understood so that: (1) their effects can be minimized and the accident can be terminated at the earliest possible stage, and (2) plant personnel can be better prepared to deal with plant responses that appear contrary to desired outcomes when water is added during a core degradation transient.

An unmitigated core damage sequence is developed in this study to serve as a framework for the discussion of the consequences of water addition to degraded cores. The sequence consists of: (1) Ballooning and rupture of fuel rod cladding, (2) rapid oxidation of zircaloy by steam, (3) failure of control rods, (4) formation of debris beds in the reactor core, and (5) the relocation of core materials to the lower plenum of the reactor vessel. The above sequence of core damage is essentially a temperature sequence, ranging from ballooning of the fuel rod cladding at approximately 1100 K to melting of the $UO_2$ fuel at 3100 K.

The consequences of water addition to a degraded core are identified for the above sequence of core damage states ranging from fuel rod ballooning and bursting to the relocation of molten core materials to the lower plenum of the vessel. For sufficiently high rates of water addition to a core prior to significant movement of core materials, the core can be cooled after a brief period of steam and hydrogen production. After the relocation of control materials in the core, re-criticality of the reactor could be a concern if unborated water is added to the core. With the formation of cohesive and particulate beds in the core, adding water to the core can no longer ensure that enough energy can be quickly removed from the core materials to prevent their melting, and further movement of core materials to the lower plenum of the vessel in molten form should be anticipated. When a significant amount of molten core materials interacts with water, rapid steam and hydrogen production, or even steam explosions, may complicate subsequent efforts of recovery from an accident.

Simple, bounding calculations are performed to evaluate the capability of water addition to degraded cores to arrest the progression of their damage. The results indicate that for a core that has progressed up to the stage of fuel rod ballooning and bursting, water addition to the core using the high pressure injection system can prevent the core from heating up to the rapid oxidation stage if most of the injected water goes through the core. If a core has heated up to the rapid oxidation stage, accumulator injection, or rapid delivery of water by the reactor coolant pumps, is necessary to prevent core melting. If the required amount of water is delivered to the core at a sufficiently high rate to prevent it from heating to the melting point of zircaloy, additional hydrogen will be produced, but will not be in amounts that are significant compared to the total production of hydrogen prior to water addition. Hydrogen production during water addition that can shatter the fuel rods is not evaluated because of insufficient knowledge of the phenomenology involved.

Energy removal from cohesive and particulate debris beds is also evaluated, assuming that there is sufficient water to cover the beds. The results are presented in maps showing regions of stability for cohesive beds and regions of dryout for particulate beds. The criterion for stability of a cohesive bed is that heat generation in the debris bed will not melt so much of its interior that only a thin crust remains (say, comprising only three-fourths of the mass of the debris bed). The determining factors for stability of a cohesive bed are the size of the bed (represented by the diameter of a spherical bed), the thermal conductivity of the material comprising the bed, and the power density in the bed. The dryout limits of particulate beds are calculated based theories of dryout of heat-generating particulate beds. The determining factors for dryout of a particulate bed are the bed's porosity, the size of the particles (surface-area-weighted equivalent diameter) comprising the bed, and the power density in the bed. The dryout of particulate beds eventually leads to melting of the particles. Both the stability map for cohesive debris beds and the dryout map for particulate beds indicate that, once core degradation has progressed to the stage of their formation, the possibility of melting in their interiors cannot be ruled out. The molten material may eventually relocate to the lower plenum of the vessel.

## CONTENTS

ABSTRACT ..... B-3

SUMMARY ..... B-5

1. INTRODUCTION ..... B-9

2. SEQUENCE OF CORE DAMAGE STATES ..... B-11

3. CHARACTERIZATION OF CORE DAMAGE STATES ..... B-24

   3.1 Nominal Values of PWR Parameters ..... B-24

   3.2 Energy Sources in a Reactor Core ..... B-24

   3.3 Energy Stored in a Degraded Core ..... B-26

4. ENERGY REMOVAL FROM DEGRADED CORES ..... B-29

   4.1 Criteria for Minimum Required Rates of Water Addition to Degraded Cores .. B-29

   4.2 Adiabatic Heatup of the Core ..... B-32

   4.3 Water Addition During Pre-Damage and Ballooning Stages ..... B-34

   4.4 Water Addition During Rapid Oxidation Stage ..... B-35

   4.5 The Effects of the Geometry of a Degraded Core on Its Energy Removal ..... B-36

      4.5.1 Stability Limits of Cohesive Debris Beds ..... B-37
      4.5.2 Stability (Dryout) Limits of Particulate Debris Beds ..... B-39

5. SUMMARY AND CONCLUSION ..... B-42

6. REFERENCES ..... B-45

## FIGURES

1. Core damage progression showing consequences of water addition ..... B-12

2. Fuel rod ballooning and failure around 1100 K in the central part of the core ..... B-16

3. Formation of the lower crust from relocated control materials, zircaloy, and liquefied fuel shortly after rapid oxidation of the zircaloy cladding ..... B-18

4. Growth of a cohesive debris bed in the central part of the core supported by a crucible-shaped lower crust containing partially molten core material ..... B-19

5. Formation of a particulate debris bed atop a cohesive debris bed as water is added to the core during cohesive bed growth ..... B-20

6. Melting of the interior of a cohesive debris bed with corresponding thinning of its crust ..... B-21

7. Failure of crust around cohesive bed and release of molten core materials to lower plenum of vessel ..... B-22

8. Adiabatic heatup of a reactor core ..... B-34

9. Power density (P) contours separating stable region from unstable region for spherical cohesive debris beds ..... B-38

10. Dryout heat flux ($q_d$) contours delineating dryout boundaries in the particle size - porosity plane for a one-dimensional particulate debris bed ..... B-40

## TABLES

1. Nominal PWR parameters ..... B-25

2. Energy from decay heat of a nominal PWR ..... B-25

3. Specific heats and heats of fusion of uranium dioxide and zircaloy ..... B-27

4. Stored energy in a degraded core ..... B-27

# CONSEQUENCES OF WATER ADDITION TO DEGRADED REACTOR CORES

## 1. INTRODUCTION

Preventing severe accidents or mitigating their consequences requires implementation of strategies to add wate. to the reactor core. However, for advanced stages of core degradation, there is no assurance that water addition can immediateiy terminate the progression of core damage. Under certain degraded core conditions, adding water may enhance hydrogen production, induce changes in core geometry that complicate recovery, cause steam explosions, or make the reactor core critical again if unborated water is used. A primary purpose of an evaluation of the consequences of water addition to a degraded core is, therefore, to ensure that these undesirable consequences are understood so that: (1) their effects can be minimized and the accident can be terminated at the earliest possible stage, and (2) plant personnel can be better prepared to deal with plant responses that appear contrary to desired outcomes when water is added during a core degradation transient.

Significant progress has been made since the TMI-2 accident in understanding the progression of core damage during a severe accident. Such progress has come from the analysis of the TMI-2 plant responses to the accident, the examination of the damaged TMI-2 core, in-pile severe fuel damage experiments performed both in the U.S. and overseas laboratories, the separate-effects experiments that address various specific aspects of the core degradation process, and the development and application of computer codes to the analysis of severe accidents. These efforts have resulted in a fairly consistent scenario of unmitigated core degradation. This scenario consists of: (1) The initial failure of fuel rods from cladding ballooning and rupture, (2) the rapid oxidation of zircaloy by steam, (3) the failure of control rods, (4) the formation of a cohesive region in the lower regions of the reactor core from relocated molten core materials, and (5) the relocation of core materials to the lower plenum of the reactor vessel.

As part of the overall Nuclear Regulatory Commission (NRC) Severe Accident Management program, this study provides information on our present understanding of the progression of an unmitigated core damage for a loss-of-coolant accident (LOCA), and on instrumentation that may be available to the operator during a severe accident to substantiate the core damage status. Such information may help the operators to better understand the nature of the progression of severe core damage and to be better equipped to deal with the complexities of the consequences of water addition to a degraded core.

In this report, we emphasize the behavior of a pressurized water reactor (PWR), which is perhaps better characterized than that of a boiling water reactor (BWR) for a core in an advanced stage of core degradation because of the extensive studies of the TMI-2 accident. Because differences in plant design and core construction invariably introduce complexities and individual characteristics in the core damage sequence, whenever appropriate, we also attempt to identify significant differences in behavior between PWRs and BWRs in the discussion. However, it is believed that the major events in the sequence of core degradation of a BWR are quite similar to those of a PWR. Therefore, much of the discussion for PWRs should also be valid for BWRs.

In Section 2, an unmitigated core damage sequence is described for a small-break LOCA. At each stage of core degradation, the effects of adding water to the core are considered. The discussion of the damage sequence is intended to identify issues or possible consequences of adding water to a reactor core at different stages of degradation. Although the discussion refers specifically to a small-break LOCA, the core damage sequence is fairly generic and is believed to adequately describe in general the core damage sequence resulting from inadequate cooling of the core.

In Section 3, characterizations of core damage states are presented. These include the energy sources and energy contents of the core. The basic parameters presented in this section are subsequently used to determine the
rate and amount of water addition to the core to prevent further damage, and to assess the limits of energy removal from cores in debris bed form.

In Section 4, bounding calculations are made to estimate the rate and the amount of water addition to the core during the ballooning stage to prevent the core from heating up to the rapid oxidation stage, and during the rapid oxidation stage to prevent the cladding from melting. Hydrogen production from water addition during the rapid oxidation stage is estimated. In this section, the energy removal limits for cohesive and particulate debris beds are also determined.

Finally, in Section 5, the results of this study are summarized and general conclusions are drawn on the consequences of water addition to degraded reactor cores. The limitations of this study and additional work needed to understand certain aspects of water addition to degraded cores are also discussed.

## 2. SEQUENCE OF CORE DAMAGE STATES

In a small-break LOCA (break size less than approximately 0.01 $m^2$) with no emergency core coolant injection, as in the TMI-2 accident, core uncovery typically happens between one to two hours after the initiation of coolant loss. Core damage progression then begins as the coolant in the core is boiled off. Although the details of core damage progression depend on plant design and the postulated size and location of the break, severe fuel damage experiments and the TMI-2 accident show that unmitigated core damage can be characterized by a sequence of distinct core damage states.

Figure 1 shows a conceptual sequence of core damage states for a small-break LOCA. The sequence can apply to both PWRs and BWRs. However, the sequence will be discussed mainly in terms of the expected behavior of PWRs; only significant differences in behavior for BWRs will be pointed out in the discussion. The sequence starts with core uncovery and ends in either the termination of the damage progression or meltthrough of the lower head of the reactor vessel. The stages of core damage progression can be characterized by a temperature scale from approximately the saturation temperature of water (560 K at a system pressure of 7 MPa) to a temperature above the melting point of $UO_2$ (3100 K). The potential consequences of water addition at each major stage of core damage are also shown in the sequence.

At the time of core uncovery, steam occupies the volume of the primary system above the top of the reactor core, while a two-phase mixture of steam and liquid water occupies the volume below. The temperature of the fuel rods stays near the saturation temperature of the water. As long as the fuel rods are in a two-phase fluid environment, even up to very high void fractions, heatup of the fuel rods will not be significant [1].

If water fails to enter the core following core uncovery, the water in the core will be boiled off gradually, and the upper part of the fuel rods will be exposed to a steam environment. Inadequate cooling then leads to heatup of the fuel rods. Above a temperature of approximately 1100 K, because of loss of mechanical strength, the zircaloy cladding can fail either from ballooning (localized radial expansion) and bursting [2, 3, 4, 5] when the internal pressure of the rods exceeds the system pressure, or from collapsing when the pressure inside the rods is below the system pressure. The damage state of the core with ballooned and burst cladding of fuel rods is depicted in Figure 2.

Collapse of cladding onto fuel pellets does not affect subsequent cooling of the core as water is added, but ballooning of cladding may block a substantial portion of the flow area of the core and restrict the flow of water. The blocked region may continue to heat up to the next stage of core degradation. However, complete blockage of the core is unlikely. At this stage, sufficient water addition to the core can terminate further core heatup. An estimate of the required rate of water flow through the core is given in Section 4.3.

The next stage of core degradation, beginning at approximately 1500 K, is the rapid oxidation of the zircaloy cladding of the fuel rods by steam. In the process hydrogen is produced and a substantial amount of heat is released. For small increases in temperature, the oxidation rate increases exponentially with the increase in temperature. Since the oxidation of the zircaloy cladding by steam is exothermic, the oxidation is autocatalytic in character: The rate of oxidation increases with temperature, which is increased by the energy release from the oxidation, so the process feeds on itself. At approximately 1500 K, the rate of energy release from the oxidation of the cladding

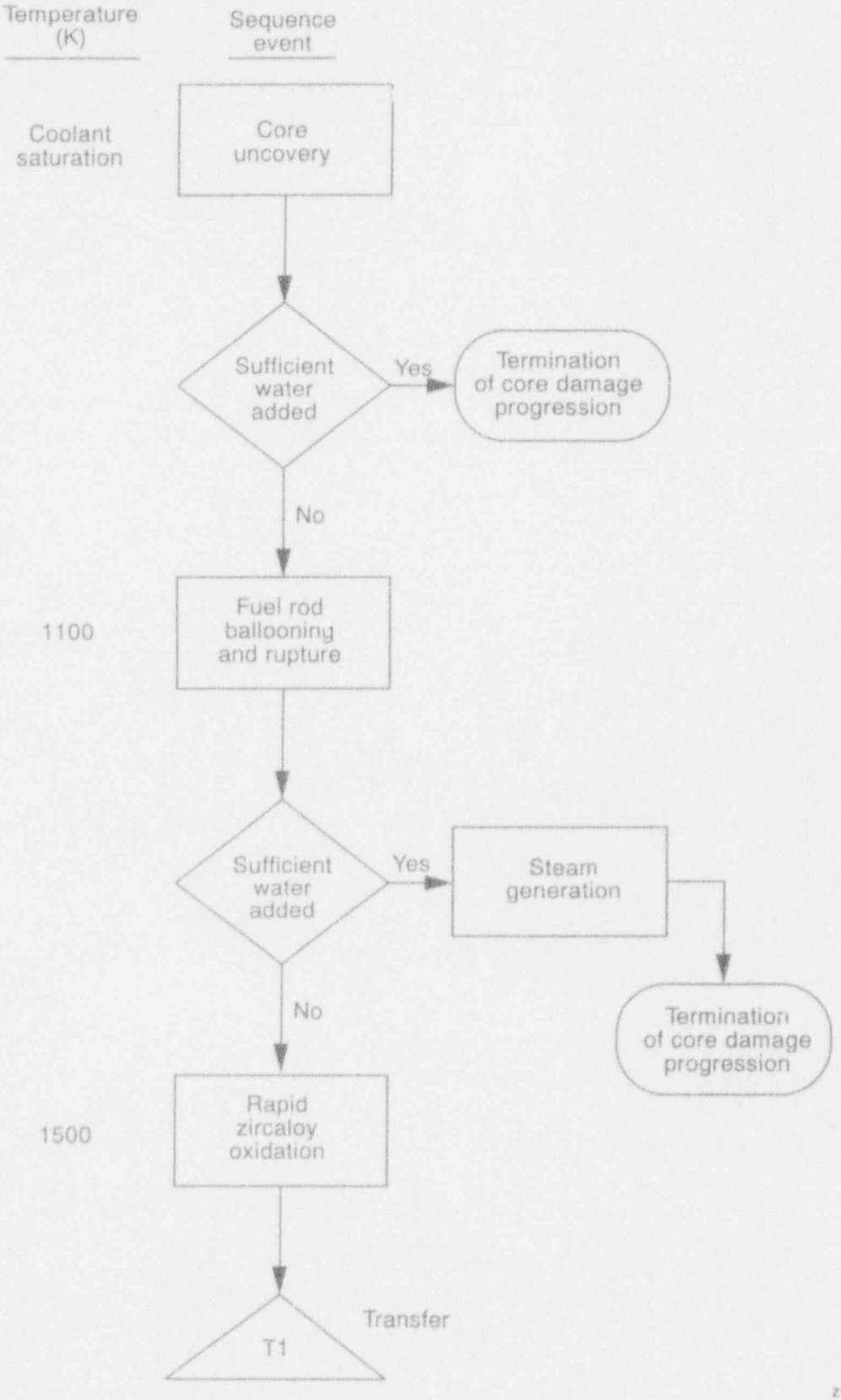


**Figure 1.** Core damage progression showing consequences of water addition.

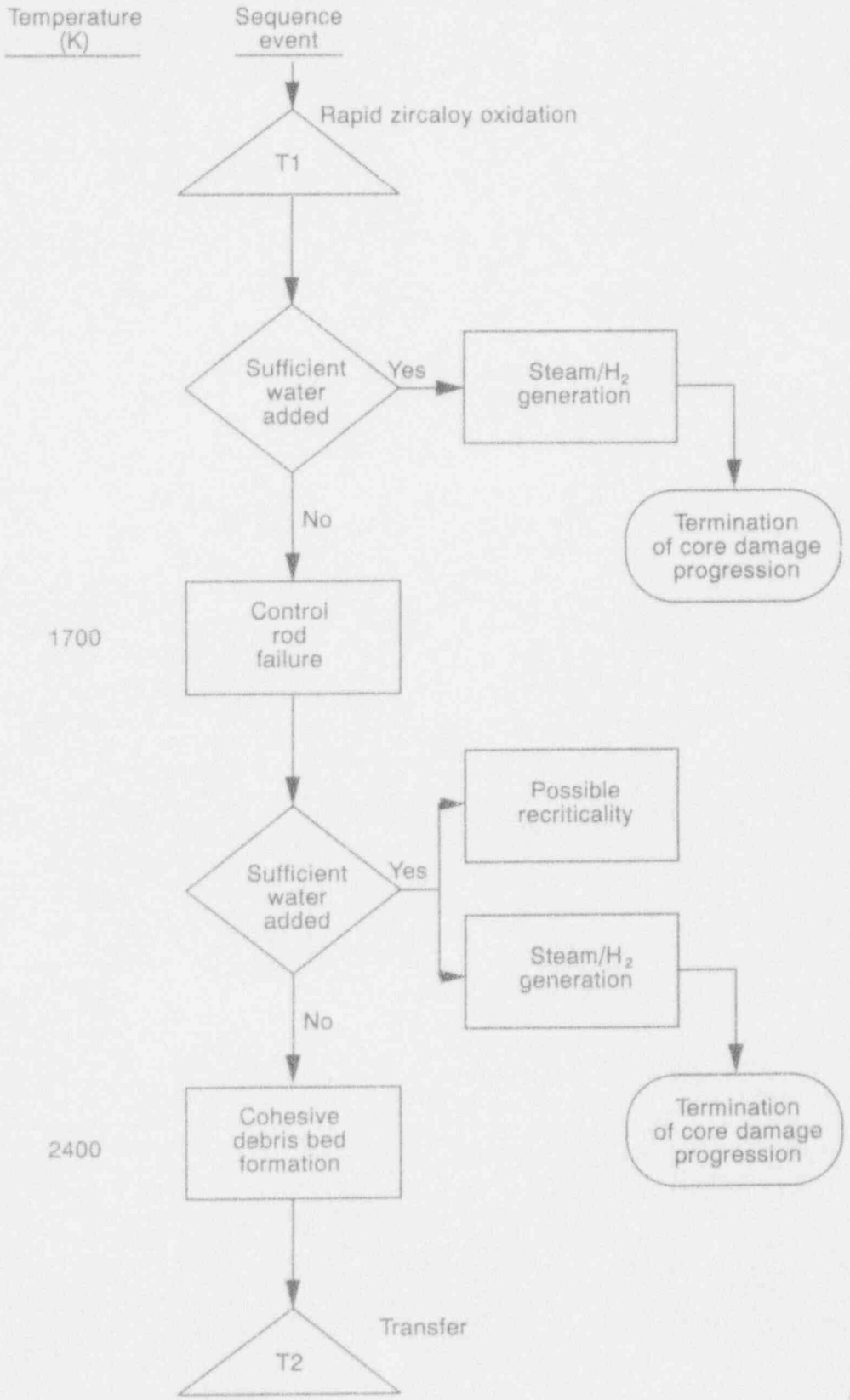


**Figure 1.** (continued).

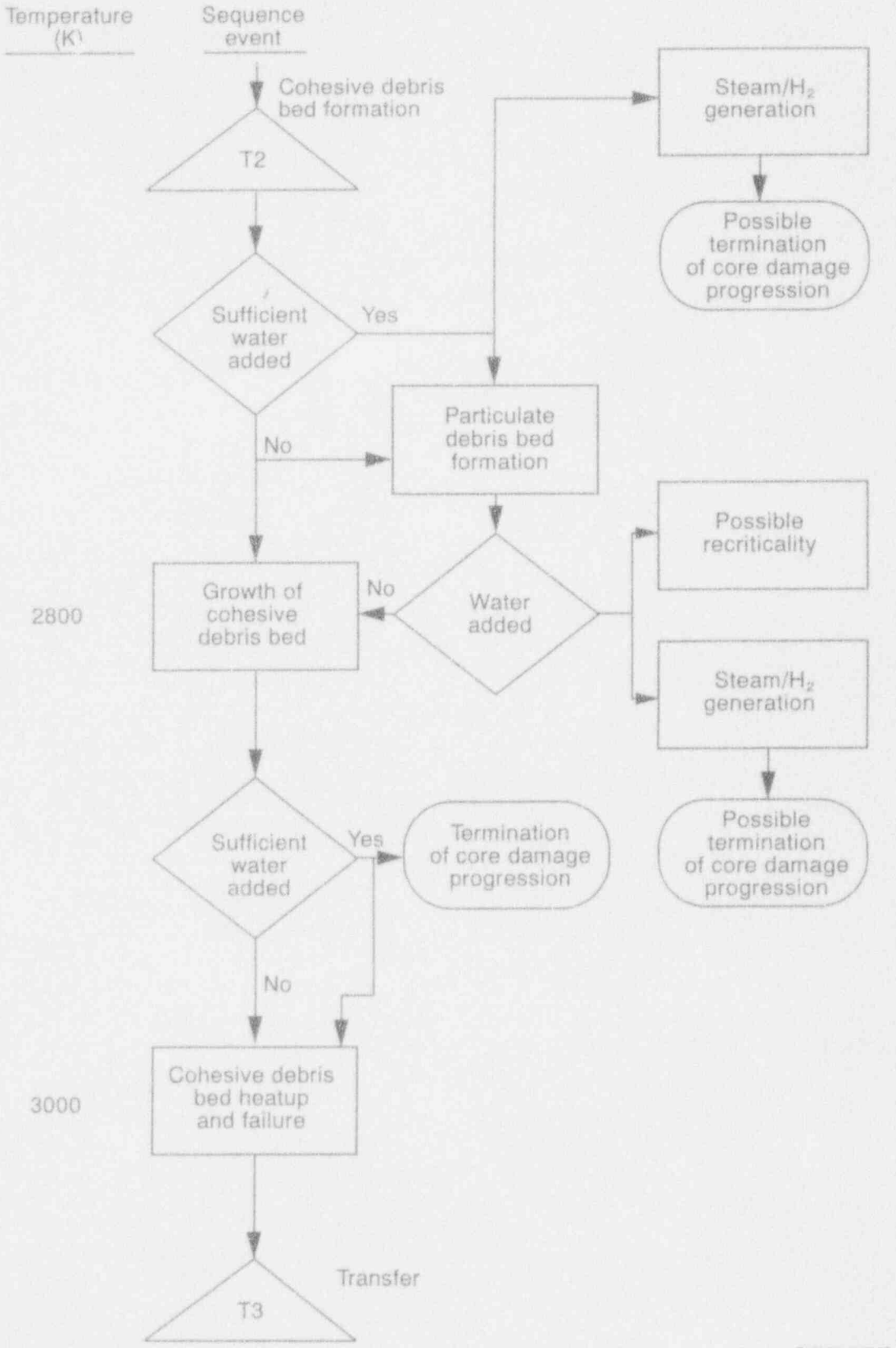


**Figure 1.** (continued).

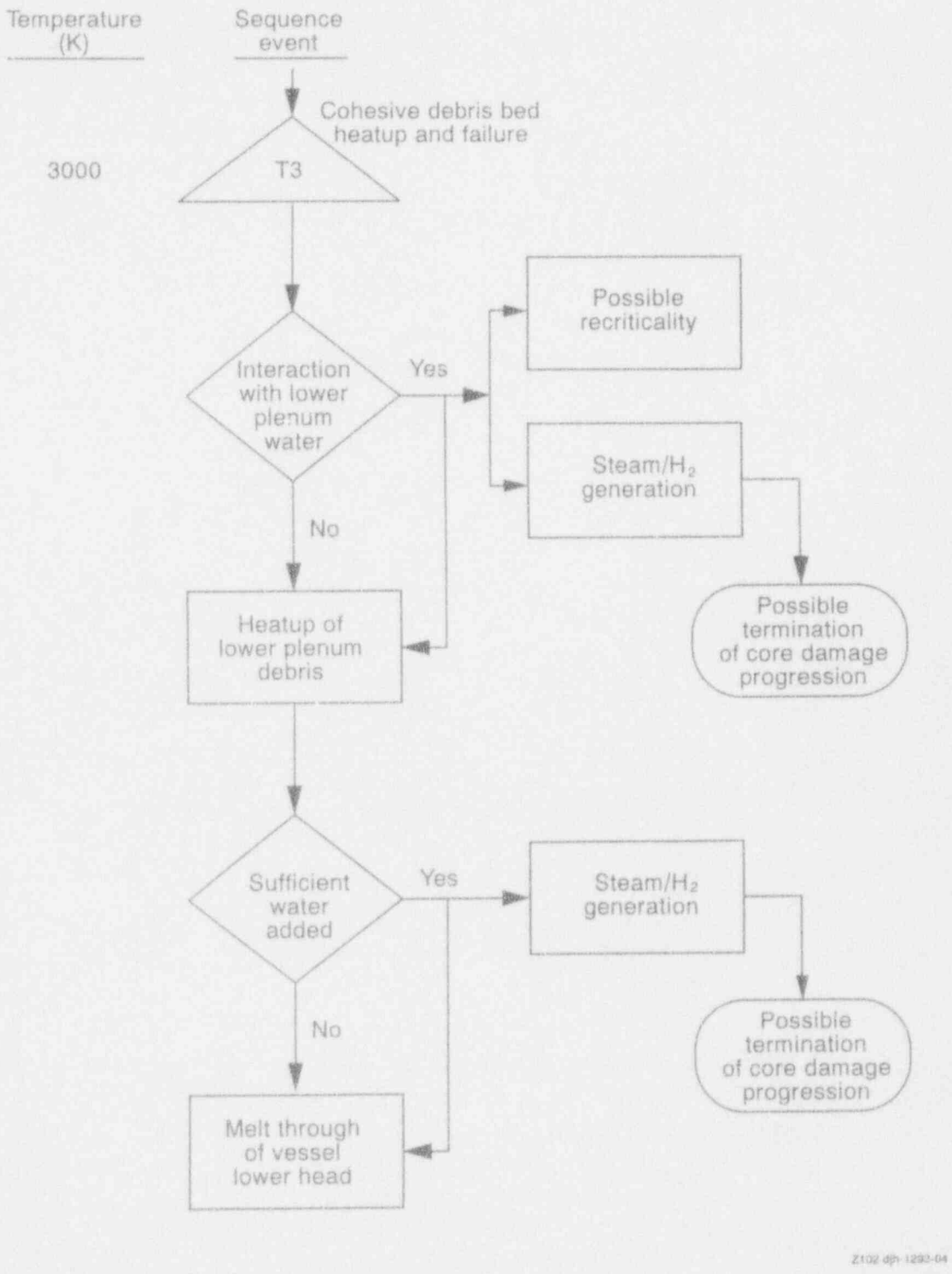


**Figure 1.** (continued).

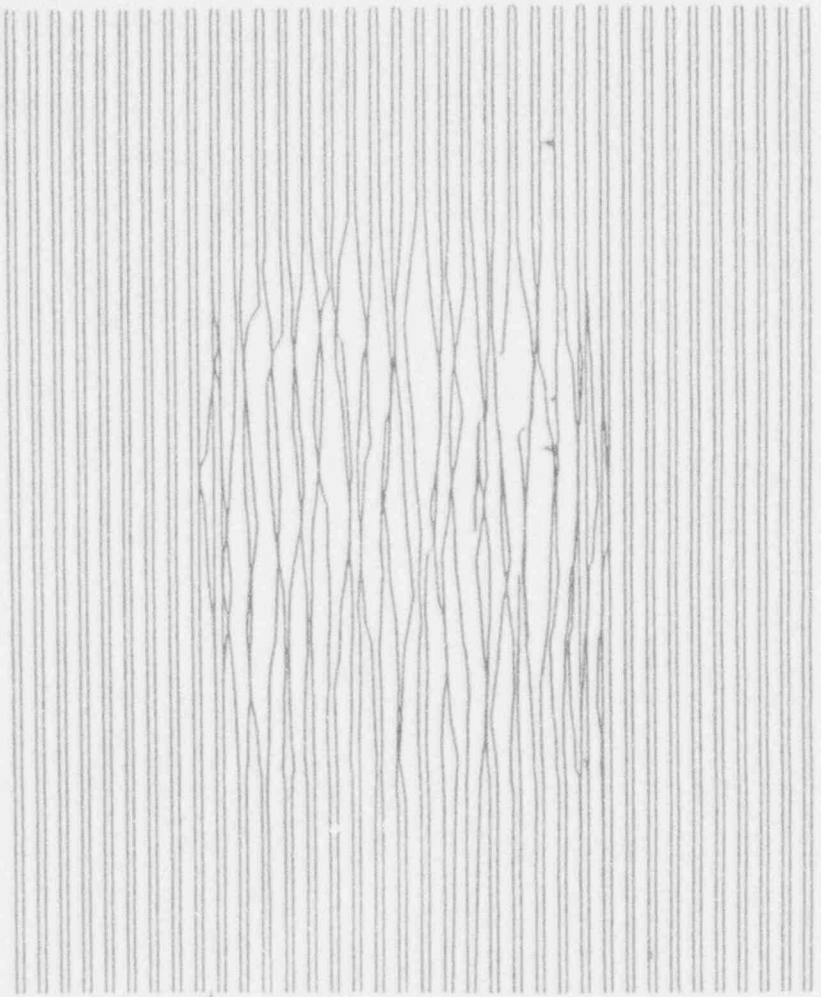


S89 PUB-1089-02

**Figure 2.** Fuel rod ballooning and failure around 1100 K in the central part of the core.

exceeds that from decay heat. At higher temperatures, it can reach tens of times the power from decay heat unless the oxidation rate is limited by the supply of zircaloy or steam.

During the rapid oxidation stage, in the absence of emergency coolant injection, the flow of steam through the core may be insufficient to supply all the steam that can be consumed in the oxidation of the zircaloy in the core. In small, scaled experiments that simulate the boiloff of water inventory in the core, such as the PBF Severe Fuel Damage (SFD) experiments [6, 7], the steam supply through the experimental fuel bundle was completely converted to hydrogen when the bundle temperature exceeds approximately 1500 K. Although the temperature of the fuel rods in the upper part of the bundle was over 1500 K, rapid oxidation did not take place because of lack of steam. In other words, the upper part of the bundle was "steam starved." Similar lack of oxidation in the upper part of the core due to steam starvation is expected in a small-break LOCA in a PWR.

If water is added to the core during the rapid oxidation stage, steam will be rapidly generated because of the high rate of heat transfer from the fuel rods to the incoming water, but the rate of

hydrogen generation will depend on the temperature response of the core. In the lower region of the core where fuel rods are quenched, hydrogen generation will stop. However, in the upper part of the core where the oxidation of zircaloy may have been steam-starved before water is added, the addition of water to the core would provide the necessary steam for oxidation. If the sudden revival of oxidation in the upper part of the core releases energy at a rate that is higher than the rate of heat transfer to the water, the temperature there will escalate. This could happen when the temperature of the rods is high, when the oxide layer on the surface of the cladding is thin, or when the water causes the oxide shell to break up, exposing unoxidized zircaloy; all these conditions contribute to high rates of oxidation [8].

If water is added to the core at a sufficiently rapid rate during the early phase of oxidation when the core temperature is less than 1500 K, the core can be quenched and core damage progression will cease. However, if the addition of water is slow or intermittent, or if the core is not completely covered with water, the core will heat up to the next stage of degradation. An estimate of the required rate of water flow through the core to stop further core damage is given in Section 4.4.

When the temperature in the core reaches about 1700 K, the stainless steel cladding of the control rods melts. The control material, Ag-In-Cd in the case of PWRs, will have already melted by this time (melting point approximately 1100 K), and will be released from the control rods upon failure of the cladding. In the case of BWRs, the control blades may fail at a slightly lower temperature (approximately 1600 K) due to the interaction of the control material $B_4C$ with the stainless steel cladding [9]. After its release from the rods, the control material flows to the lower part of the core where the temperature is low and solidifies in the space between the fuel rods. The solidified control material may become part of a lower crust in the subsequent development of a cohesive debris bed in the core [10].

Besides producing steam and hydrogen, water addition to the core after loss of control materials in the upper part of the core may also lead to recriticality if the incoming water contains little or no boron to absorb neutrons. Combined analyses of the thermal-hydraulic response, core damage states, and neutronic behavior are needed to determine the specific conditions that would lead to recriticality.

With the onset of rapid oxidation of zircaloy, the temperature in the core can escalate to the melting point of zircaloy (approximately 2150 K) in a few minutes. The melting of the zircaloy cladding usually does not immediately lead to a downward flow of the zircaloy if it is constrained by a protective layer of zirconium dioxide from earlier oxidation of the zircaloy. If the molten zircaloy stays in place, it will start to dissolve some $UO_2$ fuel [11]. Upon cladding breach, the molten zircaloy and some dissolved $UO_2$ flow downward and freeze in the cooler, lower region of the core. Together with the solidified control materials from earlier downflows, the relocated zircaloy and $UO_2$ form the lower crust of a developing cohesive debris bed. Because of limited heat losses, molten material relocated to the top of the crust eventually stops freezing. The conceptual state of the core at this stage is shown in Figure 3.

The next stage of development of the lower crust is its radial growth toward the periphery of the core. Because of decreasing temperatures toward the periphery of the core (from slower heatup because of decreasing power densities and enhanced steam cooling), relocating materials freeze at

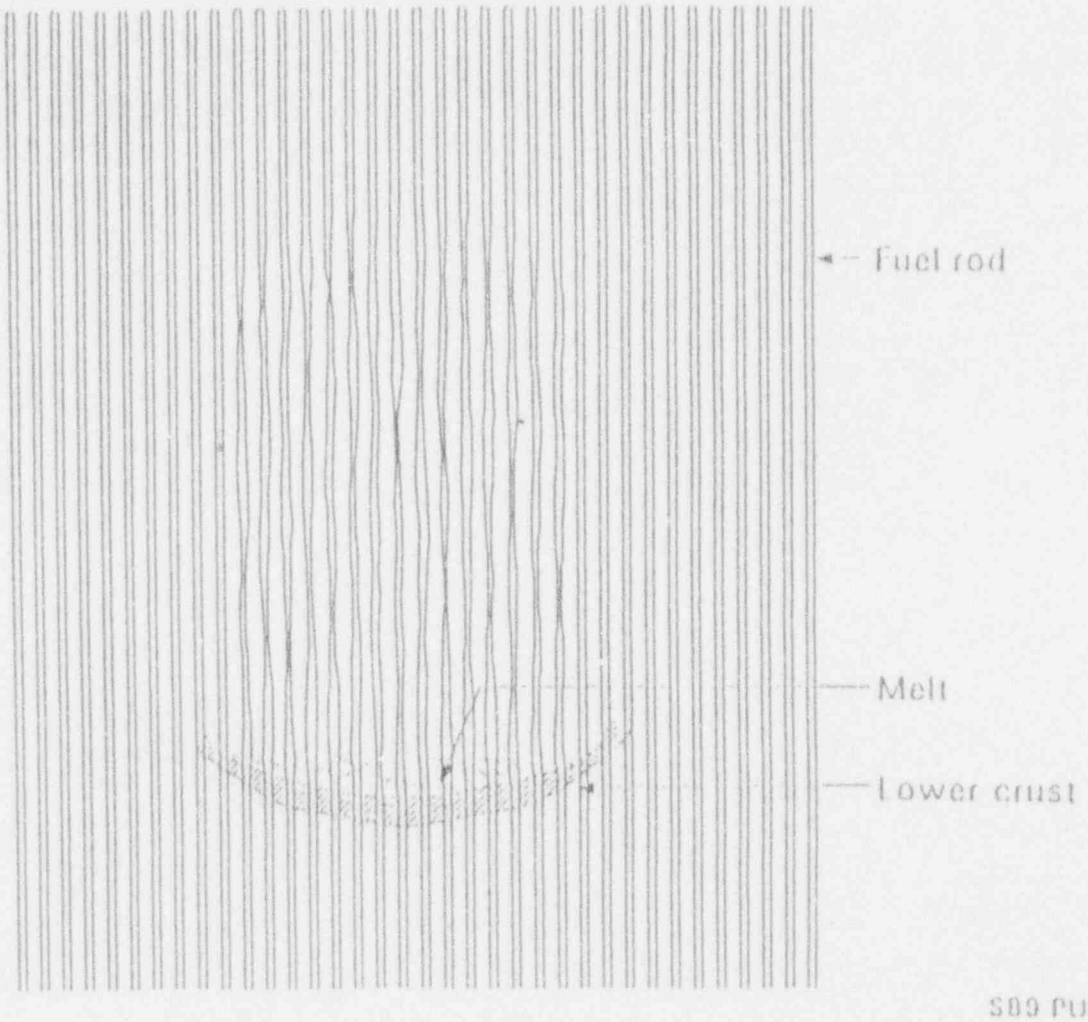


**Figure 3.** Formation of the lower crust from relocated control materials, zircaloy, and liquefied fuel shortly after rapid oxidation of the zircaloy cladding.

higher elevations toward the periphery of the core. Thus, the lower crust is expected to take the shape of a crucible. The material supported by the crust will be a pool of molten material and submerged rod stubs in the process of melting. As the submerged rod stubs melt away, mechanical support of rod stubs above the molten pool is lost, and further slumping of the rod stubs into the pool occurs. So some fuel rod remnants are expected to be submerged in the pool as long as some rod remnants stand above the pool. Figure 4 illustrates the state of the core at this stage of core damage progression.

If water is added to the core before complete slumping of fuel rod remnants into the molten pool occurs, the top surface of the molten pool may freeze to form an upper crust (Figure 5) and the fuel rod remnants above that surface may be shattered to form a particulate bed, as believed to have happened during the TMI-2 coolant pump transient [10, 12]. If the temperature of the peripheral fuel rods is still below the temperature for rapid oxidation of zircaloy by steam, they will be quenched by the incoming water [13]. Since the average temperature of the core at this stage of core heatup

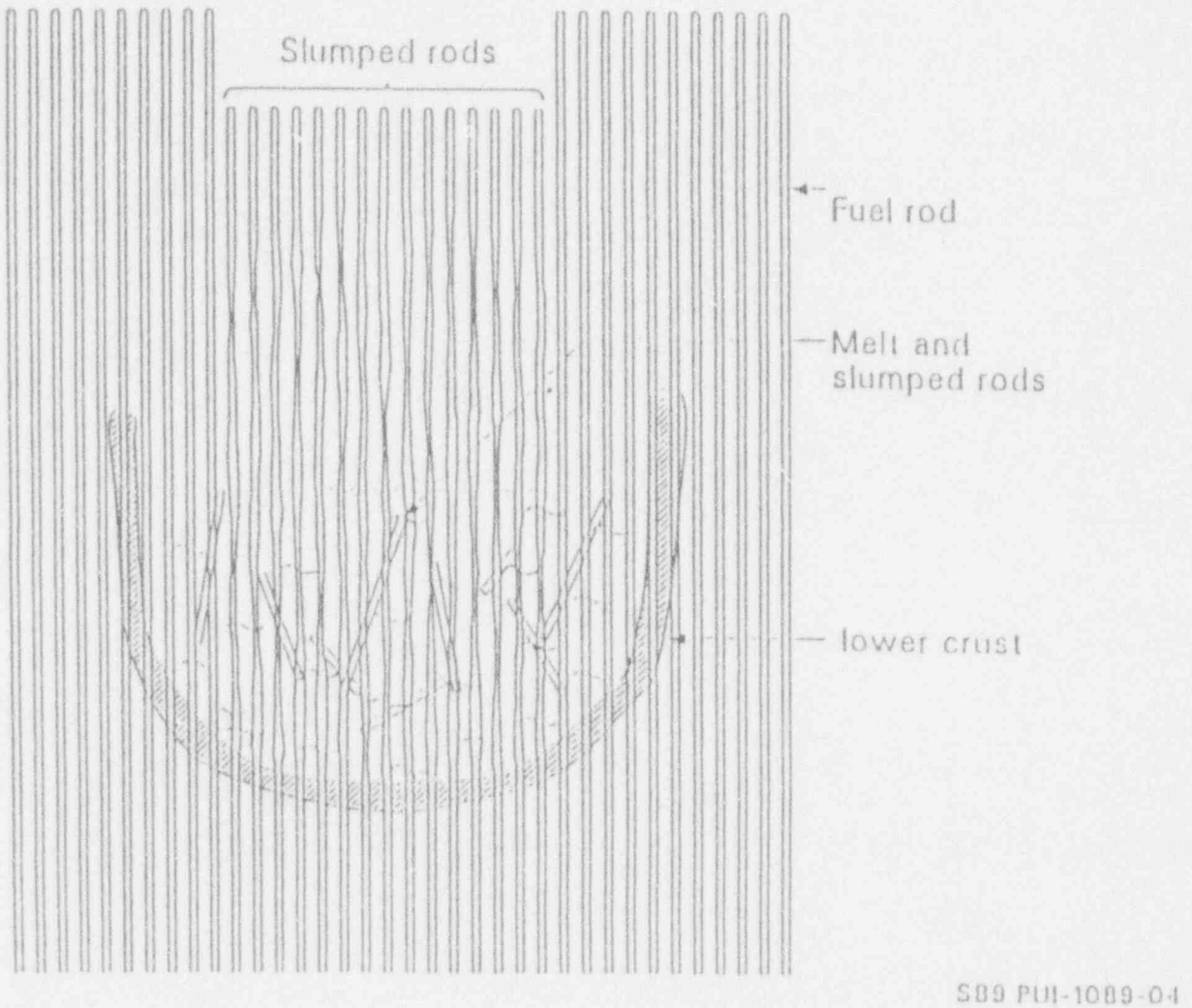


**Figure 4.** Growth of a cohesive debris bed in the central part of the core supported by a crucible-shaped lower crust containing partially molten core material.

is fairly high, copious production of steam is expected. As a result, the pressure of primary system will rise. Hydrogen generation will also increase as water is added to the core. It is estimated that, in the TMI-2 accident, one-third of the hydrogen generation during the entire accident was produced within a few minutes after water was delivered to the core at 174 min into the accident by a reactor coolant pump [14, 15]. Similarly high rates of hydrogen generation were also observed in the PBF SFD-ST [16] and the LOFT LP-FP-2 [17] tests when the test bundles were being reflooded after liquefaction of the cladding and fuel occurred.

If no water is added to the core during the growth of the cohesive debris bed, the entire upper part of the core will eventually sink into the molten pool in the center of the core. Before its complete immersion into the molten pool, the upper part of the core may retain a rod-like geometry, or alternatively, it may disintegrate into small particles even without the addition of water. The possibility of the latter scenario has been demonstrated in the PBF SFD 1-4 experiment. A particulate debris bed was formed in the upper part of the SFD 1-4 test bundle, although the bundle

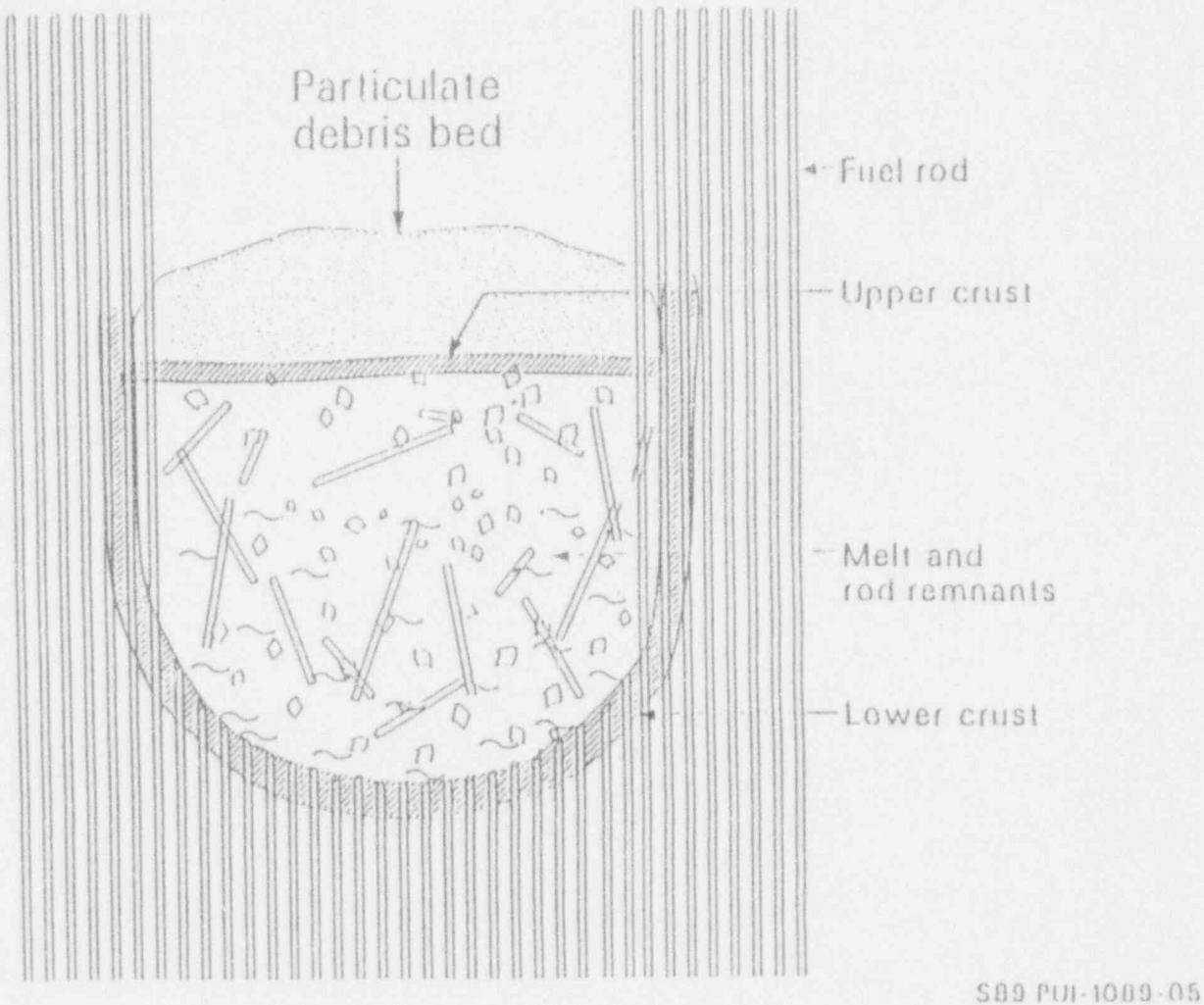


**Figure 5.** Formation of a particulate debris bed atop a cohesive debris bed as water is added to the core during cohesive bed growth.

was never reflooded by water [7]. The formation of a particulate debris bed in this experiment was due to the shattering of irradiated fuel pellets after the cladding had relocated to the lower part of the core.

If the particulate bed is shallow or composed of relatively large particles, continued water addition will quench the particulate bed. In the process, steam and hydrogen will be generated. However, because of limited water ingress into the particulate debris bed, the steam and hydrogen generation rate will be quite low and is independent of the rate of water addition to the core, as long as water covers the debris bed. Because control materials would have relocated to the lower part of the core at the time of particulate debris bed formation, recriticality may be a concern if unborated water penetrates the debris bed.

If the particulate bed of shattered fuel pellets in the upper part of the core is sufficiently deep or is composed of sufficiently small particles, water can be prevented from penetrating the bed. This

is usually referred to as dryout of the particulate bed. The dryout of particulate beds have been studied extensively both theoretically and experimentally [18 to 22]. (The conditions for dryout are given Section 4.5.2) After dryout, cooling of the particulate bed by natural convection of steam inside the bed is generally inefficient and gradual heatup of the bed will eventually lead to melting of the particles [23]. Melting of the particles will add to the growth of the cohesive debris bed.

If the cohesive bed is thin and small in radial extent, water addition may gradually cool the bed and the progression of core damage may be terminated. However, a thin and small cohesive bed could mean that a large fraction of core materials remains outside of the cohesive bed and may be in the form of a deep particulate bed that is beyond the dryout limit. Such a particulate bed resting on the cohesive bed shields water from the upper surface of the cohesive bed and prevents it from being cooled. If the cohesive bed is large, its subsequent evolution depends little on water addition [24]. Its interior will continue to heat up and melt until only a thin crust remains, regardless of water addition (Figure 6). Failure of the crust, either mechanically or by meltthrough, can lead to the relocation of the enclosed molten core material to the lower plenum of the vessel (Figure 7). The relocated amount depends on the amount of molten material in the core as well as on the location of the failure point on the crust.

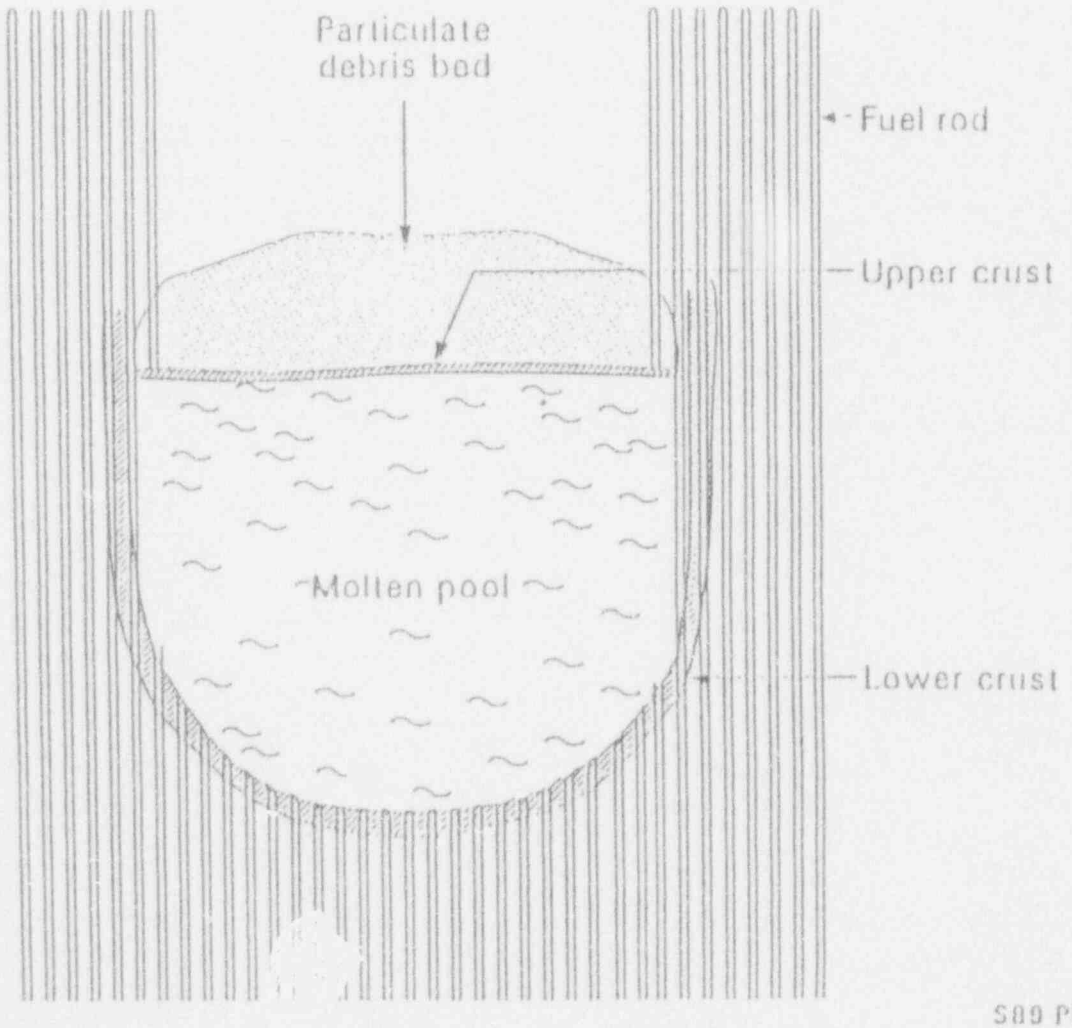


**Figure 6.** Melting of the interior of a cohesive debris bed with corresponding thinning of its crust.

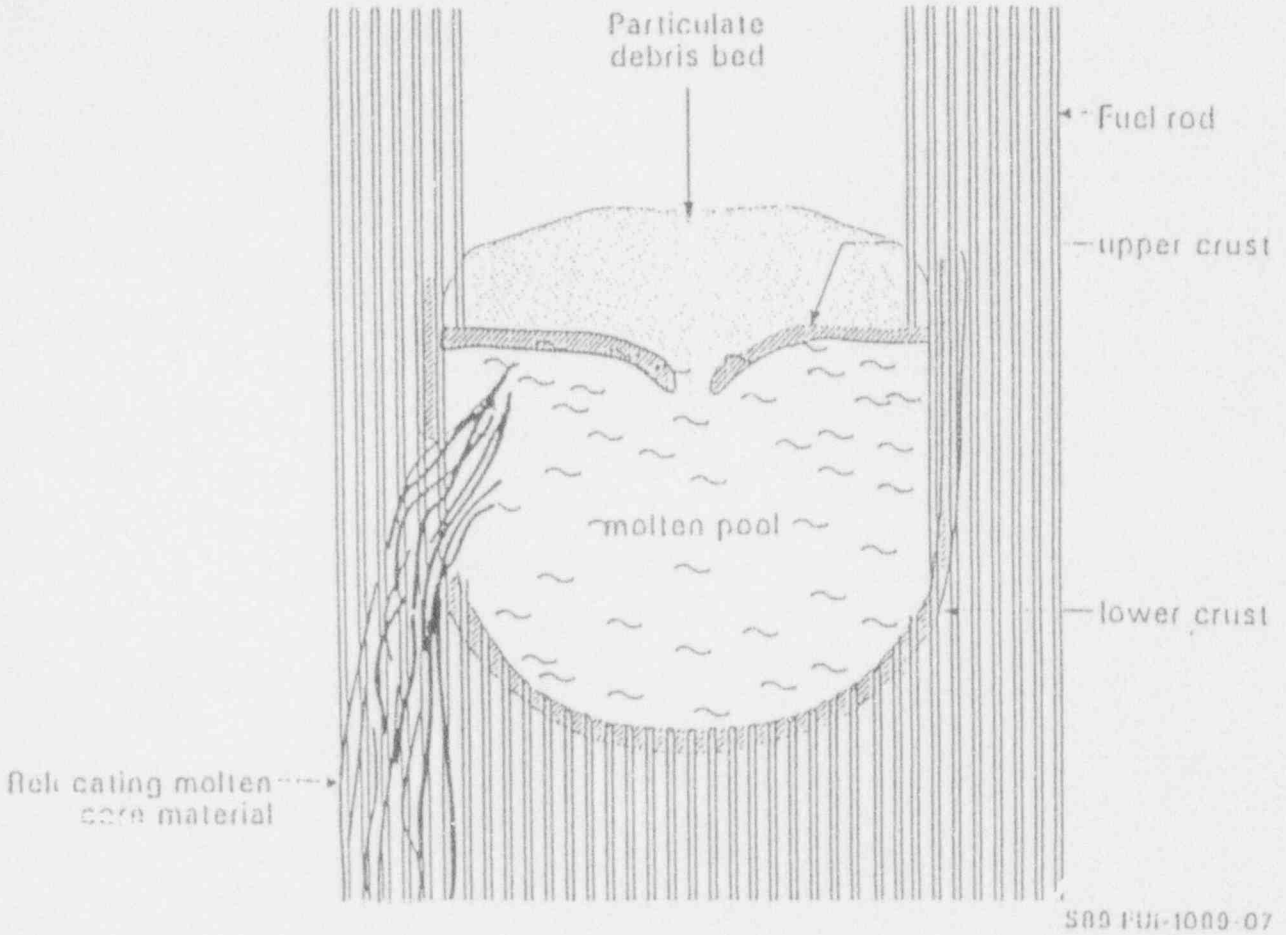


**Figure 7.** Failure of crust around cohesive bed and release of molten core materials to lower plenum of vessel.

In scenarios of small-break LOCAs where the coolant is lost through a pipe break or a relief valve, there is generally a pool of water in the lower plenum of the vessel at the time of core relocation. Release of molten core material into water invariably generates large amounts of steam. In addition, if the molten stream of core materials breaks up rapidly in water, steam explosion is also possible [25,26]. At the time of relocation, any unoxidized zirconium in the molten material can be oxidized by steam to release energy and produce hydrogen. Recriticality can also be a problem if the control materials are left behind in the core and the relocated material breaks up in unborated water in the lower plenum.

In the TMI-2 accident, progression of core damage was essentially terminated with the relocation of approximately 20 metric tons of core material into the lower plenum of the vessel. The material partially broke up to form a particulate bed and was quenched by the water in the lower plenum. The increase in pressure of the primary system at the time of relocation (224 min into the accident) indicates that both hydrogen and steam were produced for a short period of time after the

relocation. There was no evidence that the reactor ever became critical again. For postulated accident scenarios in general, however, relocation of core materials to the lower plenum is not limited to 20 metric tons. Calculations show that, for sufficiently large amounts of core material in consolidated form, the presence of water in the lower plenum cannot prevent the heatup of the material [27]. In addition, the inner surface of the vessel may be ablated by the relocating core material and the vessel is likely to fail from creep rupture of the vessel lower head [28]. The failure mode of the reactor pressure vessel and the subsequent accident progression to the exterior of the vessel is not part of the scope of the present report.

# 3. CHARACTERIZATION OF CORE DAMAGE STATES

Descriptions of the thermal characteristics of damaged cores are presented in this section. First, the basic parameters of a nominal PWR core are presented. These parameters are based on information contained in Standard Safety Analysis Reports for a Westinghouse 4-loop reactor [29] and a B&W 205 reactor [30]. Values of nominal parameters presented in this section are within approximately 10% of the specific values of large PWRs. General Electric's BWR/6 reactor design [31] is used as a model BWR whenever it is necessary to differentiate BWRs from PWRs. Second, based on these nominal parameter values, the sources of energy in the core after reactor scram are identified and evaluated. These include the decay heat and the release of energy from potential oxidation of zircaloy in the core. Third, the energy stored in core materials is calculated as a function of average core temperature. The energy released in the core is either transferred to the coolant or retained by the core materials. The amount of water whose heat of vaporization is equivalent to the stored thermal energy in the core is calculated. This is the amount of water that is required to absorb the stored energy in the core by vaporization alone. To simplify the analysis, only $UO_2$ and zircaloy are considered in the early stages of core degradation; $ZrO_2$ is added to the analysis as the zircaloy is oxidized by steam.

## 3.1 Nominal Values of PWR Parameters

The nominal values of PWR parameters used throughout this analysis are given in Table 1. Note that zircaloy comprises approximately 19% of the total core mass. The fuel mass in a BWR [31] is much higher than that in a PWR (157,000 kg for a BWR vs. 100,000 kg for a PWR) and, more significantly, because of the presence of zircaloy channel boxes around the fuel assemblies, the zircaloy in a BWR as a fraction of total core mass is also higher than that in a PWR (30% for a BWR vs. 19% for a PWR).

## 3.2 Energy Sources in a Reactor Core

Decay heat from radioactive materials is the predominant energy source in a reactor after scram. Over a short time interval, the oxidation of zircaloy by steam can also be a significant energy source. In the first hour after scram in a small-break LOCA, most of the stored heat in the fuel during reactor operation (relative to coolant saturation temperatures), residual fission heat, and decay heat would be transferred to the coolant. The core temperature would be near the saturation temperature of the coolant. Therefore, energy release during the first hour of a small-break LOCA may be ignored in calculating the stored energy of core materials. For this reason, the decay energy release is computed only for times after the first hour after scram. The results are shown in Table 2. The assumptions used in the computations are: (1) The reactor has operated continuously for one year at full power after a fresh loading of fuel, and (2) the conversion fraction of U-238 to an actinide for each fission of U-235 is 0.9. The 1979 ANSI Standard [32] is used as the decay heat model.

The decay heat table shown in Table 2 can be used to estimate the time required to dry out the core after core uncovery. To illustrate, we assume that no water is added to the core during dryout except that some of the initial water inventory in the downcomer may flow into the core to keep the water levels the same in the downcomer and the core. We also assume that the reactor

**Table 1.** Nominal PWR parameters.

| | |
|---|---|
| Rated power ($MW_t$) | 3500 |
| $UO_2$ mass (kg) | 100000 |
| Zircaloy mass (kg) | 23000 |
| Cladding thickness (mm) | 0.65 |
| Fuel rod outside diameter (mm) | 9.75 |
| Number of fuel rods | 53000 |
| Core height (m) | 3.66 |
| Volume of fuel rods ($m^3$) | 14.5 |
| Core region free volume ($m^3$) | 17.6 |
| Core bypass and inlet annulus volume ($m^3$) | 21.6 |
| Primary system volume ($m^3$) | 350 |

**Table 2.** Energy from decay heat of a nominal PWR.

| | Time after scram (h) | | | | | | | |
|---|---|---|---|---|---|---|---|---|
| | 1 | 2 | 3 | 4 | 5 | 6 | 7 | 8 |
| Cumulative energy (GJ) | 0 | 137 | 252 | 354 | 448 | 536 | 619 | 698 |
| Energy addition in preceding time interval (MJ) | — | 137 | 115 | 102 | 94 | 88 | 83 | 79 |
| Average power in preceding time interval (MW) | — | 38 | 32 | 28 | 26 | 24 | 23 | 22 |
| Average power in preceding time interval (% of full power) | — | 1.09 | 0.98 | 0.81 | 0.75 | 0.7 | 0.66 | 0.63 |

vessel is initially filled to the top of the core with saturated water at 6.9 MPa. First, we assume that during the boiloff, the core materials remain at the saturation temperature of the water. The enthalpy of vaporization of the water is 1.5 MJ/kg and the total amount of water in the core and the downcomer between the bottom and top elevations of the core is 3.08 x $10^4$ kg (41.6 $m^3$ at 740 kg/$m^3$). Therefore, the total energy, E, required to vaporize the water is 46.2 GJ. If the dryout occurs in the 4th hour after scram when the power, P, is 28.3 MW (see Table 2), the dryout time is 1600 s (4.62 x $10^{10}$ / 28.3 x $10^6$). If it is assumed more realistically that only the decay heat below the liquid level is transferred to the liquid, the liquid level will decrease exponentially with a time constant equal to E/P, or again 1600 s if core uncovery occurs in the fourth hour after scram. In Section 4, the decay heat table will be used to assess the heatup of the core.

Another energy source in the core is the oxidation of zircaloy by steam. In the process, zirconium is oxidized to $ZrO_2$ and hydrogen is produced. The energy release from the oxidation of 1 kg of zircaloy is 6.5 MJ. The energy release from the oxidation of all the zircaloy in the core (23,000 kg) is 151 GJ, which is slightly greater than the energy release from decay heat in the second hour after scram. (Oxidation of all the zircaloy in the core of a BWR yields 430 GJ.) Although the energy release from oxidation can be potentially equivalent to approximately an hour of decay heat, the power from the oxidation of zircaloy at high temperatures is considerably higher than the power from decay heat. For example, at 1800 K, oxidation of 20% of the original thickness of the cladding starting from an unoxidized state takes 150 s [33]; at 2000 K, the time required is shortened to 30 s [34]. If the cladding is oxidized uniformly in the core at such rates, the powers from oxidation are 200 MW and 1000 MW, respectively, which correspond to 5 and 25 times the decay power in the second hour after scram (see Table 2). Consequently, the heatup of fuel rods due to rapid oxidation of the cladding can be many times faster than that due to decay heat.

## 3.3 Energy Stored in a Degraded Core

The sources of energy in the core were discussed in the previous section. In this section, the energy stored in a degraded core is estimated. When the energy source and the amount of stored energy in a degraded core in a particulate stage of degradation are compared, the adiabatic heatup rate of the core, or the time to achieve such a degraded configuration, can be estimated. When a portion of the energy output is transferred to the coolant, the heatup rate would be proportionally reduced.

To simplify the analysis, we assume that the core consists of only $UO_2$ and zircaloy in the amounts given in Table 1. (The inclusion of $ZrO_2$ would give a slightly higher energy content for a given temperature than would the present estimate because of the higher specific heat of $ZrO_2$.) The specific heats used are given in Table 3. In addition, it is assumed that zircaloy changes phase at 2100 K and $UO_2$ at 2800 K. (The liquidus temperature of a mixture of Zr, $ZrO_2$, and $UO_2$ is approximately 2800 K.) During phase changes, the heats of fusion, as given in Table 3, are absorbed by the materials while their temperatures remain constant. The heats of fusion are derived from MATPRO [35, 36].

The energy stored in a core at different stages of degradation, as characterized by a temperature scale, is shown in Table 4. The stored energy is defined to be zero at 560 K, which is slightly higher than the saturation temperature (558 K) of water at 6.9 MPa. Comparing the

**Table 3.** Specific heats and heats of fusion of uranium dioxide and zircaloy.

| Material | Specific heat (J/kg-K) | Temperature range (K) | Heat of fusion (J/kg) | Melting temperature (K) |
|---|---|---|---|---|
| $UO_2$ | 300 | <1200 | $2.7 \times 10^5$ | 2800 |
| | 500 | ≥1200 | | |
| Zircaloy | 430 | <1200 | $2.3 \times 10^5$ | 2100 |
| | 360 | ≥1200 | | |

**Table 4.** Stored energy in a degraded core.

| Temperature (K) | 560 | 1200 | 1500 | 1700 | 2400 | 2800 | 3000 |
|---|---|---|---|---|---|---|---|
| Stored energy (GJ) | 0 | 26 | 43 | 55 | 101 | 151 | 163 |
| Equivalent water mass $(10^3 \text{ kg})_a$ | 0 | 17 | 28 | 36 | 67 | 100 | 108 |

a. Heat of vaporization of water mass at 6.9 MPa = Stored energy.

energy source from decay heat, as given in Table 2, and the stored energy in a degraded core, as given in Table 4, it can be estimated that adiabatic heatup of a dry core to 2800 K takes approximately an hour during the second hour after scram. Energy released from the complete oxidation of the zircaloy in the core is also approximately equivalent to the energy stored in core materials at 2800 K.

Using information given in Tables 2 and 4, the average adiabatic heatup rate of the core in the second hour after scram is calculated to be approximately 0.8 K/s in the temperature interval from 600 K to 1200 K. Above 1500 K, the rapid oxidation of zircaloy can contribute significantly to the heatup rate. Given that the power from oxidation at 1800 K is 5 times the power from decay heat and, at 2000 K, 25 times, the heatup rate from oxidation can be as high as 4 K/s and 20 K/s at these

temperatures, respectively. A more refined calculation of the adiabatic heatup of the core is given in Section 4.2.

The last row of numbers shown in Table 4 gives the equivalent mass of water whose heat of vaporization at 6.9 MPa is equal to the stored heat in the degraded core. Conceptually, if this amount of water is instantaneously injected into the hot core, its complete vaporization by the hot core will remove all the stored heat in the core. Superheating the steam is not considered in the calculation. Therefore, this is a conservative estimate of the amount of water required to remove stored heat in the core.

# 4. ENERGY REMOVAL FROM DEGRADED CORES

In this section, the heat transfer characteristics of degraded cores during water addition are considered. Simplified bounding calculations are performed to determine the minimum rate of water addition that can prevent the core from progressing to a higher stage of degradation. In addition, the time required and the total amount of water injected through the core to remove its energy are also determined. The calculations include those for a core at: (1) 1000 K (pre-damage stage), (2) 1200 K (the ballooning stage), (3) 1500 K (the early rapid oxidation stages), and (4) 2000 K (late rapid oxidation stage). When debris beds are formed in the core, because of the degradation of heat transfer resulting from drastic decreases in heat transfer areas, the rate of water addition becomes a secondary issue compared with the ability of water to remove energy from the debris bed. Critical limits of heat removal are determined for the debris beds as functions of their characteristics.

In Section 4.1, the formulation for the determination of minimum rates of water addition to degraded cores is described. The formulation applies to energy removal from a core in the pre-damage heatup stage to the late rapid oxidation stage. This section is followed by calculations of adiabatic heatup of the core, including energy addition from oxidation, to a maximum core temperature of 2100 K (Section 4.2). The results of the adiabatic heatup are used in calculations that determine the required minimum rates of water addition for the pre-damage stage, the ballooning stage, and the rapid oxidation stage. The required minimum rates of water addition are presented in Section 4.3 for the pre-damage and the ballooning stages, and in Section 4.4 for the rapid oxidation stage up to a core temperature of 2000 K. At higher temperatures, water addition to the core may shatter the cladding of the fuel and induce the formation of a particulate debris bed. Because we still cannot confidently quantify the phenomenology of shattering and enhanced hydrogen production due to the exposure of fresh zircaloy, the effects of water addition to degraded cores above 2100 K are not evaluated. However, the heat transfer characteristics of debris beds are discussed in Section 4.5.

## 4.1 Criteria for Minimum Required Rates of Water Addition to Degraded Cores

The objective of adding water to degraded cores is to arrest core damage progression and bring the core to a stable condition so that recovery from heatup of the core can be achieved. To prevent further heatup of the core, the rate of water addition must be such that the rate of heat transfer from the core to the water must be greater than the rate of heat generation in the core. Heat transfer from core materials to the incoming water includes vaporization of the water and superheating the steam to near the peak temperature of the core materials. In the subsequent formulation, it is assumed that injected water flows to the core through the downcomer and the lower plenum of the reactor vessel. It is further assumed that the incoming water is heated to saturation before it reaches the high temperature portion of the core, so there is no heat transfer to subcooled water from the high temperature portion of the core. Vaporization takes place in the lower elevations of the core and the steam is superheated in the upper elevations of the core.

Reflooding a core at high temperatures is a complicated process that involves film boiling, transition boiling, and nucleate boiling. The purpose of this study is not to model the reflooding process in detail, but rather to provide rough estimates of water addition rates that can adequately remove energy from degraded cores. These estimates can then be used as guides for detailed code

calculations if more precisely defined rates are desired. Based on this philosophy, nominal values of heat transfer coefficients or heat transfer fluxes will be used in the calculations.

In the lower high temperature core region where boiling takes place, an average heat flux of 60 $kW/m^2$ will be assumed. This is based on experimental heat fluxes between 20 $kW/m^2$ and 200 $kW/m^2$ for flow through tubes heated between 650 K and 1250 K [37]. At higher temperatures, the heat flux is dominated by radiative losses and is taken to be $\sigma T^4$, where $\sigma$ is the Stefan-Boltzmann constant and T is the temperature of the fuel rods. The elevation at which the incoming water is completely vaporized is determined by the average heat flux in the boiling region and the rate of water addition: The total heat transfer rate in the boiling region is equated to the total enthalpy gain by the water as it is completely vaporized. In a unit cell containing a fuel rod, the height of the boiling zone is calculated from the following equation:

$$GA_f \Delta H = q_{quench} (\pi D \Delta l) \quad (1)$$

where G is the mass flux of water, $A_f$ is the unit cell flow area, $\Delta H$ is the heat of vaporization of water, $q_{quench}$ is the heat flux, D is the fuel rod diameter, and $\Delta l$ is the height of the boiling zone. Equation (1) can also be written as

$$(G/4) D_H \Delta H = q_{quench} \Delta l \quad (2)$$

where $D_H$ is the hydraulic diameter of the flow.

Above the boiling zone, heat is transferred from the fuel rods to the steam by convection. The heat transfer coefficient, h, is taken as the maximum of the laminar flow heat transfer coefficient inside a circular tube whose wall is at constant temperature [38] and the heat transfer coefficient given by the Dittus-Boelter correlation for turbulent flow [39]. The steam temperature increase along the height of the core is given by

$$(G/4) D_H C_p (dT/dl) = h (T_0 - T) \quad (3)$$

where $C_p$ is the specific heat of steam and $T_0$ is the fuel rod temperature. Both $C_p$ and $T_0$ are taken as constants in the calculations. In particular, $T_0$ is taken as the average temperature of the fuel rods above the boiling zone. The heat transfer coefficient is given by

$$h = \max \{ 3.66\, k/D_H,\ 0.023\, Re^{0.8}\, Pr^{0.4}\, k/D_H \} \quad (4)$$

where k is the thermal conductivity of steam, Re is the Reynolds number of the flow, and Pr is the Prandtl number of steam.

With the boundary condition, $T = T_{sat}$ at $l = 0$ (top of the boiling zone), the solution of Equation (3) is

$$T_L = T_0 - (T_0 - T_{sat}) \exp(-4hL/GD_HC_p) \quad (5)$$

where $T_L$ is the steam temperature at $l = L$.

The quenching of the core is approximated by a series of n discreet steps. Each step consists of two distinct heat transfer zones: a boiling zone in the lower elevations of length $\Delta l$ and a forced steam convection zone of length L above the boiling zone. Heat transfer to steam above the zone of length L is ignored and the rods are assumed to heat up adiabatically. The length L is determined by conditions described below.

If the high temperature section of the core is of height $L_H$, we require

$$n \Delta l + L = L_H. \tag{6}$$

At the beginning of the last step of the quenching process, we impose the condition that the heat flux to the steam from the fuel rods be equal to the heat generation rate per unit surface area of the fuel rods. The heat generation rate includes that from decay heat and from oxidation of the zircaloy cladding. A second condition we impose is that at the beginning of the last step of the quenching process, adiabatic heatup of the core limits the peak core temperature to some specified $T_{fin}$. The peak temperature could be taken as the minimum temperature characterizing a higher stage of core degradation. If the above two conditions are satisfied, it can be assured that the core will not heat up to the higher stage of degradation.

To obtain the solution of the required mass flux of water (G) going through the core that satisfy the above-mentioned conditions, we assume that throughout the quenching process, the core is at uniform temperature represented by the average of the temperature at the beginning of the quench and the peak temperature attained by the core from adiabatic heatup during the quench. This assumption leads to a set of algebraic equations involving the mass flux, G, the number of quenching steps, n, the length of the boiling zone, $\Delta l$, and the length of convective heat transfer zone, L.

Two of the equations required to solve for G, n, $\Delta l$, and L are given by Equations (2) and (6). Another equation is obtained by equating the heat flux derived from Equation (5) and the heat generation rate per unit surface area of fuel rods, i.e.,

$$h (T_0 - T_{sat}) \exp(-4hL/GD_HC_p) = q_{heat} \tag{7}$$

where $q_{heat}$ is the heat flux equivalent of the heat generation rate.

A fourth equation is obtained by equating the time required to adiabatically heat up the core from $T_{ini}$, the core temperature before quench, to $T_{fin}$, the imposed limiting peak core temperature attained during quench, and the time required to remove the stored heat in the fuel rods in n steps of quenching. This equation is approximated by

$$nC (T_0 - T_{sat}) / (A q_{quench} + A q_{steam}) = (T_{fin} - T_{ini}) / R \tag{8}$$

where C is the heat capacity per unit length of fuel rod, A is the heat transfer area per unit length of fuel rod, R is the adiabatic heatup rate, $q_{quench}$ is the heat flux in the boiling zone, and $q_{steam}$ is a correction heat flux due to heat removal by steam convection before the rods enter the boiling zone and is given by

$$q_{steam} = (L / 2\,\Delta l) \bullet [(h\,(T_0 - T_{sat}) + q_{heat})] / 2. \quad (9)$$

Equations (2), (6), (8), and (9) are solved simultaneously for the unknown quantities G (required mass flux), n (number of quenching steps), $\Delta l$ (height of boiling zone), and L (height of steam convective cooling zone).

## 4.2 Adiabatic Heatup of the Core

In the last section, the method of estimating the minimum rate of water addition that would prevent the core from progressing to a higher stage of degradation was formulated. In that formulation, the power density and the adiabatic heatup rate of the core are treated as input parameters. In this section, a simplified calculation of adiabatic heatup is performed. This calculation gives both the power density and the rate of adiabatic heatup of the core.

The decay heat of a core undergoing a loss of coolant accident is assumed to be a constant at 30 MW. This power corresponds to the decay heat generation at approximately two hours after scram (Table 2, Section 3.2). Using information given in Section 3, the average heat flux that can be sustained by the decay heat on the surface of the cladding is

$$q_{decay} = \text{Power} / (\text{number of fuel rods x surface area of fuel rods})$$

$$= 30 \times 10^6 / (53{,}000 \times 3.66 \times 0.00975 \times \pi)$$

$$= 5049\ W/m^2. \quad (10)$$

If the diameter of the fuel rods is increased by a factor, f, due to ballooning, $q_{decay}$ will be reduced by the same factor, f.

The power from oxidation depends on temperature as well as on the availability of zircaloy and steam. It will be assumed that there is enough steam supply required by the oxidation kinetics. The results of the calculation will show that during core heatup below 2100 K, not all the zircaloy can be consumed in the oxidation.

The oxidation of the zircaloy cladding by steam is represented by the following parabolic kinetics:

$$w^2 = w_0^2 + \alpha \exp(-\beta/T)\, t \quad (11)$$

where w is mass of zircaloy oxidized per unit surface area at the end of time t, $w_0$ is the initial mass of zircaloy oxidized per unit surface area, T is the temperature of the cladding, and $\alpha$ and $\beta$ are constants. The kinetics predicts the amount of zircaloy oxidized if the temperature is kept constant during the oxidation. The constants $\alpha$ and $\beta$ are given by the Cathcart-Pawel correlation [33] for temperatures below 1850 K and by the Urbanic-Heidrick correlation [34] above 1850 K. Specifically,

$$\alpha = 294.3\ kg^2\text{-}s/m^4 \quad T < 1850\ K$$
$$= 87.9\ kg^2\text{-}s/m^4 \quad T \geq 1850\ K$$

$$\beta = 20{,}100\ K \quad T < 1850\ K$$
$$= 16{,}610\ K \quad T \geq 1850\ K. \qquad (12)$$

Equation (11) can be converted to one describing the thickness of oxidized zircaloy, $\delta$, by dividing w by the density of zircaloy (6500 $kg/m^3$).

During core heatup, because the core temperature is constantly increasing, Equation (11) cannot be used directly to predict the amount of zircaloy oxidized. For sufficiently short time intervals, $\Delta t = t_2 - t_1$, the heatup rate may be considered constant. The temperature can be approximated by $T_2 = T_1 + R\,\Delta t$, where R is the constant heatup rate during time interval $\Delta t$. With this approximation, Equation (11) can be integrated to give

$$w^2 = w_0^2 + (\alpha/R)\cdot[T_2E_2(\beta/T_2) - T_1E_2(\beta/T_1)] \qquad (13)$$

where $E_2(x)$ is the exponential integral of index 2.

Equation (13) gives the amount of zircaloy oxidized per unit surface area as a function of temperature instead of as a function of time. The power from oxidation, $q_{oxid}$, expressed as a surface heat flux is given by

$$q_{oxid} = (w_2 - w_1)\cdot H_R \cdot R / (T_2 - T_1) \qquad (14)$$

where $H_R$ is the heat released per unit mass of zircaloy oxidized (6.5 MJ/kg). The constant heatup rate, R, during the heatup from $T_1$ to $T_2$ may be approximated by the heatup rate during the previous heatup interval, which can be calculated from the fuel rod heat capacity and the total power ($q_{decay} + q_{oxid}$).

For core temperatures below 1200 K, the oxidation of zircaloy is negligible, so the heatup is almost entirely driven by decay heat. For temperatures above 1200 K, the central fuel rods are assumed to have ballooned and blocked 40 % of the flow area (4), which corresponds to a fuel rod diameter increase by a factor of 1.22. With this modification of the fuel rod diameter, an adiabatic heatup calculation is performed, starting from a core temperature of 1200 K and ending at a core temperature of 2100 K. The core temperature as a function of time is shown in Figure 8. The heatup rate is approximately 0.75 K/s at 1200 K, and increases to approximately 28 K/s at 2100 K. At 2100 K, approximately 105 $\mu$m of zircaloy (approximately 17 % of the cladding thickness) is oxidized and the power from oxidation corresponds to a heat flux of 152 $kW/m^2$.

As a by-product of the calculation, the cumulative hydrogen production is calculated to be 86 kg when the core is heated to 1800 K, and 150 kg when the core is heated to 2100 K. The hydrogen production rates at those temperatures are 1.2 kg/s and 5.5 kg/s, respectively. Note that enhanced hydrogen production due to the exposure of fresh zircaloy from cladding fracturing is not considered in the calculations.

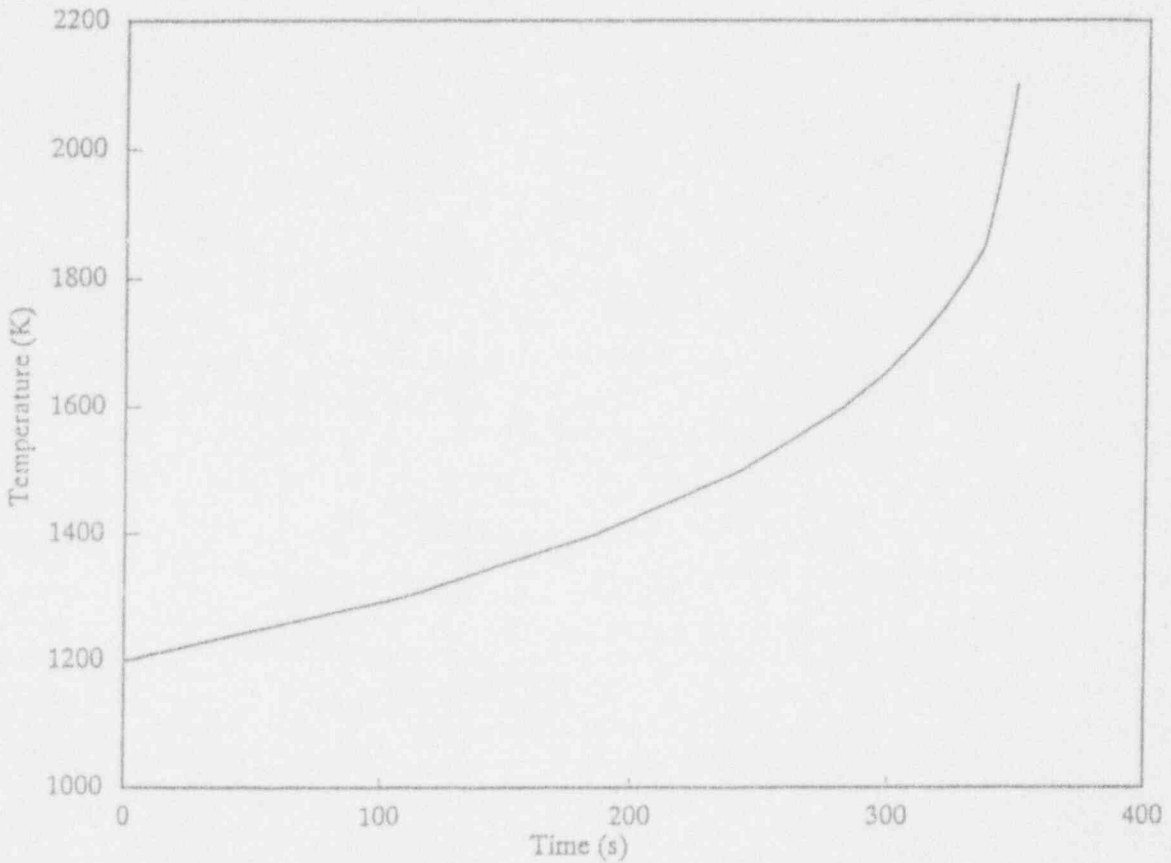


**Figure 8.** Adiabatic heatup of a reactor core.

## 4.3 Water Addition During Pre-Damage and Ballooning Stages

The temperature range during pre-damage core heatup can be considered to be from the saturation temperature of the water to 1100 K when fuel rod ballooning is expected to occur. Based on the formulation described in Section 4.1, a representative calculation is performed for a temperature at 1000 K over a 2.75 m height of core (75 % of the height of the core). The system pressure is taken as 6.9 MPa. The criterion determining the minimum rate of water addition to the core is that the core be prevented from heating up to 1100 K. Between 1000 K and 1100 K, the oxidation of zircaloy is negligible, so only the decay heat is considered in the core heatup during quench. The minimum rate of water addition is determined to be 30 kg/s, or 470 gpm (water volume measured at 300 K). This is within the injection capacity of a single high pressure injection pump (capacity between 500 gpm and 700 gpm) if most of the injected water goes through the core. The time required to completely quench the core is calculated to be 225 s, and the total amount of water added to the core during quench is 6700 kg.

A calculation is performed for the ballooning stage to determined the minimum rate of water addition to prevent the core from heating up to the rapid oxidation stage. The initial temperature of the core is taken to be 1200 K and the limiting temperature of the core is taken to be 1500 K, the minimum temperature for the core to be considered to have entered the rapid oxidation stage.

Again, the high temperature portion of the core is taken to be 2.75 m in height. Unlike the calculations for the pre-damage stage, the calculations for the ballooning stage include energy input from oxidation. At 1500 K, the power from oxidation of zircaloy is approximately 1.8 times that from decay heat.

In the calculations for the ballooning stage, it is assumed that the fuel rods in the central 80% of the core have ballooned and the flow area in the ballooned region is reduced by 40%. Consequently, the hydraulic diameter in the ballooned region is reduced by approximately 50%. The calculations yield a minimum required rate of water addition at 34.4 kg/s for the ballooned region. The flow through the unblocked peripheral region is calculated based on the assumption that the pressure drop in the core in uniform across the core. This gives a required minimum rate of flow through the peripheral region at 17.3 kg/s. The total minimum required flow through the core is 51.7 kg/s, or 820 gpm, again within the capacity of the high pressure injection system (a minimum of two operating pumps) if most of the injected water goes through the core. The time required to completely quench the core is calculated to be 192 s, and the total amount of water added to the core during quench is 9930 kg. Note that the stored energy in three-fourths of the core at 1200 K is equivalent to the heat of vaporization of 12,000 kg of water (see Table 4). The minimum required amount of water calculated is somewhat less than that. This is due to the effect of steam cooling, which more than compensates for the heating of the upper portion of the core during quenching the lower part of the core.

The above results show that a core heated to less than 1200 K can be recovered with full-capacity injection from the high pressure injection system if most of the injected water goes through the core. However, to translate water injection rates into the primary cooling system to rates of water flow through the core, detailed code calculations for specific loss-of-coolant scenarios are necessary.

## 4.4 Water Addition During Rapid Oxidation Stage

Two calculations are performed to determine the minimum required rates of water addition to a degraded core during the rapid oxidation stage, one at an initial temperature of 1500 K (early rapid oxidation stage), and another at an initial temperature of 2000 K (late rapid oxidation stage). For the early rapid oxidation stage, the determining criterion is that the core be prevented from heating up to 1800 K, a temperature slightly below the transition temperature from the slower Cathcart-Pawel oxidation kinetics to the more rapid Urbanic-Heidrick kinetics. For the late oxidation stage, the determining criterion is that the core be prevented from heating up to the melting point of zircaloy, or 2100 K. Above 2100 K, large debris beds may form in the core due to material relocation.

The height of the high temperature portion of the core is again assumed to be 2.75 m and all the fuel rods are assumed to have ballooned, contributing to a flow blockage of 40 % as indicated by code calculations [4]. The minimum required rates of water addition are calculated to be 148 kg/s, or 2350 gpm, for an initial temperature of 1500 K, and 1230 kg/s, or 19,500 gpm, for an initial temperature of 2000 K. These required rates are clearly much above the water addition capacity of the high pressure injection system, but they are within the injection capacity of the accumulators if the system pressure is lowered to 0.7 MPa below the accumulator set-point (approximately 4.2 MPa). If the cold legs of the primary cooling system are filled with water, operation of the reactor coolant pumps can also provide the necessary flow through the core.

For an initial core temperature of 1500 K, the time required to completely quench the core is calculated to be 64.6 s, and the total amount of water added to the core during quench is 9540 kg. For an initial core temperature of 2000 K, the time required to completely quench the core is calculated to be 7.6 s and the total amount of water added during the quench is 9350 kg. Note that for a core at high temperature, the time required to cool the core is much shorter than for a core at low temperature, otherwise the core would progress to a higher stage (higher temperature) of degradation. This is because of the rapid escalation of temperature due to the rapidly increasing oxidation rate as the temperature increases. Because of heat transfer to superheated steam, the total amount of water required to cool the core is not very sensitive to the initial core temperature.

If the rates of water addition to the core are higher than those calculated above, the additional hydrogen production during the brief periods of temperature escalation before the complete cooldown of the core is calculated to be limited to 55 kg during the early oxidation stage, and to 20 kg during the late oxidation stage.

## 4.5 The Effects of the Geometry of a Degraded Core on Its Energy Removal

As discussed in Section 2, several major changes in core geometry occur during core degradation. The core geometry changes when the cladding of fuel rods balloons at a temperature of approximately 1100 K. Small scale experiments [6, 7, 16, 17] have shown that blockage of the core by ballooned rods does not inhibit cooling of the rods when enough water is introduced into the core. Results of calculations presented in Section 4.3 indicate that if less than 40 % of the flow area in the central part of the core is blocked by ballooning, full capacity high pressure injection can prevent the core from heating up to the rapid oxidation stage.

A second major change in core geometry is the formation of a cohesive debris bed from the solidification of relocated molten materials. Because water is prevented from penetrating a cohesive bed, heat is conducted from the interior of the debris bed to its surface if it remains solid, or is convected to its surface if its interior re-melts. Heat loss by a cohesive debris bed then occurs only on its surface. Such a mode of heat transfer considerably limits the rate of energy removal.

A third major change in core geometry is the formation of a particulate debris bed. As described in Section 2 on the sequence of core damage, a particulate debris bed can form from the collapse of rod remnants in the upper part of the core after a substantial fraction of the zircaloy cladding has relocated to the lower part of the core. A particulate debris bed can form regardless of water addition to the core, although its formation can be greatly facilitated by rapid water addition. A particulate debris bed can also form in the lower plenum of the vessel when molten material in the core drops into a pool of water in the lower plenum. Energy removal from a particulate debris bed depends in the ability of water to penetrate the bed.

For purposes of this study, an unstable debris bed is defined as one that continues to heat up in its interior in spite of water addition. Such continual heatup of the debris bed eventually leads to a change in its geometry: A particulate debris bed may melt, and the molten materials in the interior of a cohesive debris bed may break out of its crust and relocate to lower elevations of the reactor vessel. For a particulate debris bed, the dryout of the bed provides a sufficient condition that the bed is stable. In the case of a cohesive debris bed, the criterion for stability is more difficult to define.

If water contacts or surrounds the surface of a cohesive bed, the convective and radiative heat losses from its surface generally limit the temperature of its surface to below 2000 K, which is lower than the melting point of most of the materials in the bed. Therefore, a direct meltthrough of the crust around the bed is unlikely. (For a sphere 1.5 m in radius, the radiative heat loss from its surface at 2000 K is over 20 MW, comparable to the total decay power of the entire core a few hours after scram.) However, a sufficiently thin crust around the cohesive region may fail under mechanical or thermal stress. It is assumed in the subsequent analysis that if three-fourths or more of the mass of a cohesive region becomes molten, the crust will fail and a change in debris geometry occurs. Then, by our definition, such a cohesive debris bed is termed unstable. It should be borne in mind that the choice of such a melt fraction that defines stability is somewhat arbitrary and is for the purpose of illustrating the stability behavior. As our understanding of crust failure improves, the definition of stable configurations can be refined, but the principle of analysis would remain the same.

The following sections describe the results of analyses that define the stability limits of both cohesive and particulate debris beds.

### 4.5.1 Stability Limits of Cohesive Debris Beds

Based on the above criterion of the stability of a cohesive debris bed, the stability limits are calculated for spherical cohesive debris beds as functions of their radii and thermal conductivities. Steady-state conditions are assumed in the calculations. The boundary temperatures of the crust are assumed to be 600 K (saturation temperature of water) on the outer surface and 2800 K (melting point of U-Zr-O) on the inner surface. The material enclosed by the crust is assumed to be molten and to comprise three-fourths of the mass of the cohesive debris bed. If the decay heat generated exceeds that conducted through the crust, the excess heat will melt part of the crust so that the crust will become thinner than that required to maintain geometric integrity, and, by definition, the bed is unstable. The results of calculations using two power densities for the debris bed are shown in Figure 9.

The position of a cohesive debris bed in Figure 9 is defined by two parameters: Its radius and its thermal conductivity. Two curves are shown in the figure, one labeled by a power density of 3.0 $MW/m^3$, which is a typical power density for a bed formed approximately two hours after scram, and another labeled by a power density of 1.5 $MW/m^3$, which is a typical power density for a bed formed approximately 8 hours after scram. These curves delineate the stability limits of cohesive beds having those power densities. For example, if a cohesive bed having a power density of 1.5 $MW/m^3$ is positioned by its radius and thermal conductivity in the figure to the right of the curve characterized by the power density of 1.5 $MW/m^3$, it is unstable; if it is positioned to the left, it is stable.

The use of the stability diagram is best illustrated by reference to a particular cohesive debris bed. The cohesive debris bed is taken to be spherical in shape, having a radius of 0.5 m, a power density of 3.0 $MW/m^3$, and a thermal conductivity of 10 W/m-K. The position of such a bed in the stability diagram lies on the curve labeled by a power density of 3.0 $MW/m^3$, and is therefore at the limit of stability. The bed will become stable with the passage of time when its power density decreases below 3.0 $MW/m^3$, because its position then on the stability diagram will be to the left of a curve labeled by the decreased power density. For a power density of 3.0 $MW/m^3$, beds whose radii

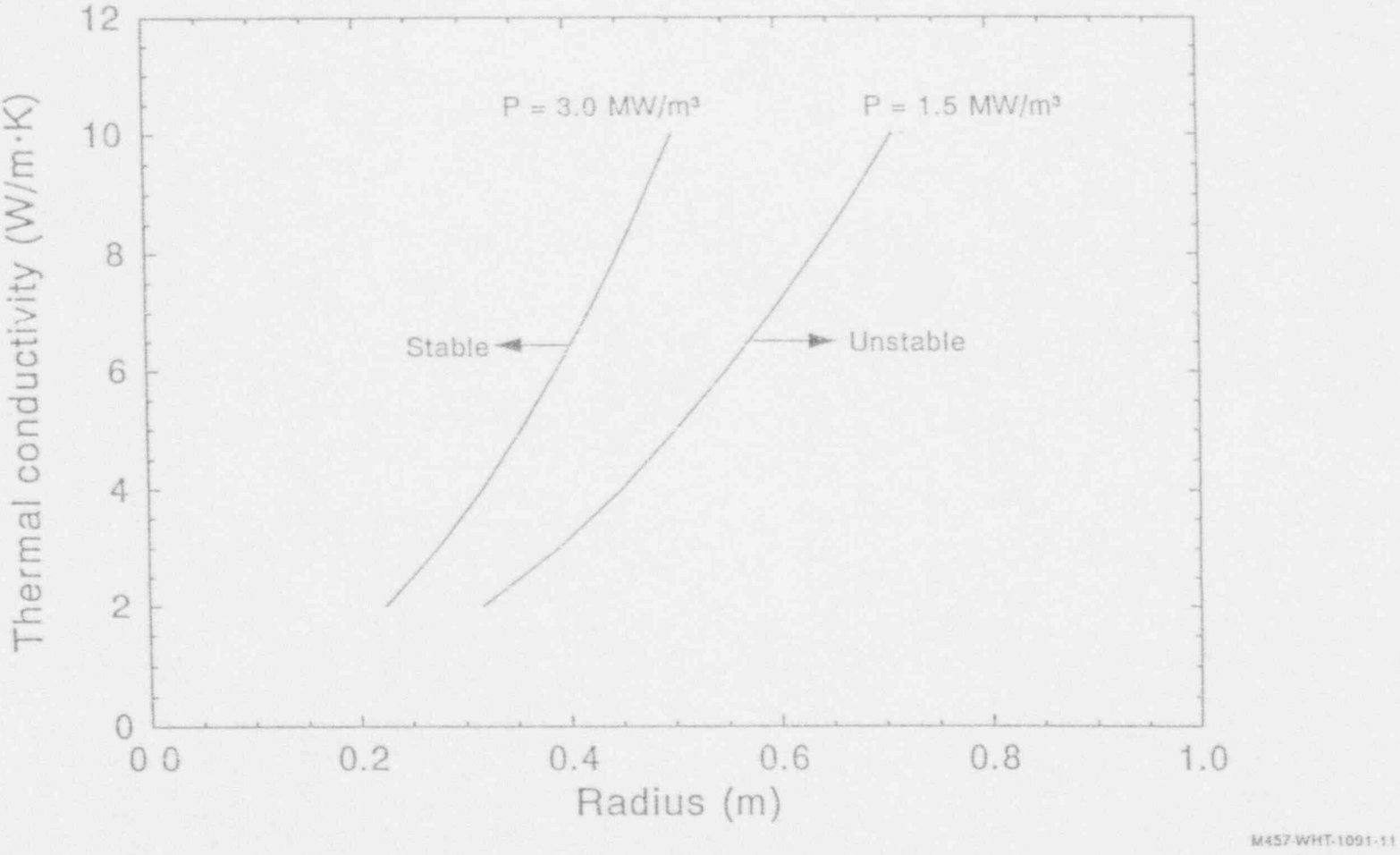


**Figure 9.** Power density (P) contours separating stable region from unstable region for spherical cohesive debris beds.

are less than 0.5 m are generally stable, because their positions are to the left of the curve labeled by the power density of 3.0 MW/m$^3$, but beds having materials with thermal conductivities less than 10 W/m-K are not stable because their positions are to the right, or below, the curve labeled by the power density of 3.0 MW/m$^3$.

A fully-developed stability diagram for cohesive debris beds is envisioned to have many similar contours of stability limits as the two shown in Figure 9, each one of which is characterized by a power density. During an accident, an operator may estimate the power density based on the time after scram, and identify the contour on the stability diagram labeled by that power density. If the operator, by probing the core with the movable SPNDs, can ascertain the size of a cohesive debris bed formed in the core, and use engineering estimates of the thermal conductivity of the materials comprising the bed, the position of the cohesive debris bed in the stability diagram is determined. By examining the position of the cohesive debris bed in the stability diagram in relation to the stability limit contour characterized by its power density, the stability of the cohesive debris bed can be determined, as discussed above.

### 4.5.2 Stability (Dryout) Limits of Particulate Debris Beds

The stability of a particulate debris bed can be defined by the ability of water to penetrate the bed. If water can penetrate the bed, energy can be efficiently removed from the bed and the particles in the bed can be prevented from melting. Otherwise, melting of the particle transforms the particulate bed to a cohesive bed. The ability of water to penetrate a homogeneous particulate debris bed on top of an impermeable plate (e.g., the top crust of a cohesive debris bed) depends on the bed's porosity, the size of the particles comprising the bed, and the power density in the bed.

Unlike the difficulties encountered in defining the stability criterion for cohesive debris beds, the ability of water to penetrate a particulate debris bed can be more precisely characterized by the dryout heat fluxes of these beds. The Lipinski model [40] is used to calculate the dryout heat flux for particulate beds in one dimension along the vertical direction. The model has been shown to agree quite well with recent data from experiments simulating the behavior of particulate debris beds formed in severe reactor accidents [22] and with models derived from flooding data [41].

Figure 10 shows the dryout limits of particulate debris beds characterized by porosity and particle size at a system pressure of 6.9 MPa. Similar to the stability diagram for cohesive debris beds, the dryout limits diagram for particulate beds is divided into regions where water cannot penetrate the bed and regions where water can penetrate the bed by curves labeled by the dryout heat flux. For simplicity, these curves are termed the coolability limits.

When a particulate debris bed is positioned by its particle size and porosity in the diagram, whether energy can be efficiently removed from the bed can be determined as follows. First, the heat flux that would emerge from its top surface if all the power produced within the bed is transferred to the surface is calculated. Second, a curve on the dryout limits diagram labeled by the dryout heat flux that is equal to the calculated heat flux in step one is identified. If the position of the debris bed in the dryout limits diagram is to the right of (larger particle size), or above (higher porosity), that curve, energy can be efficiently removed from the bed, i.e., water ingress into the bed is possible; if its position is to the left or below the curve, energy removal from the bed is inefficient, i.e., water

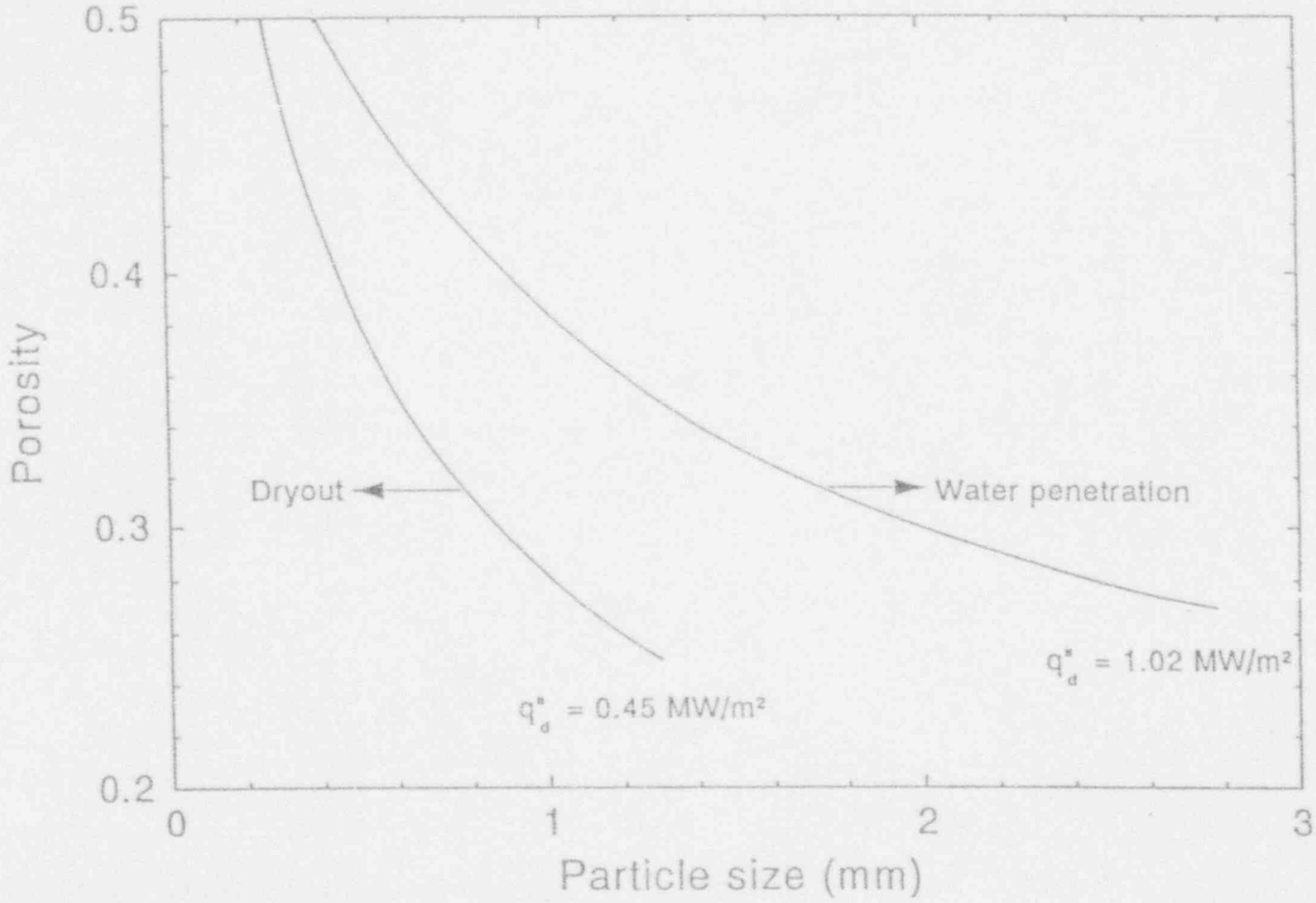


**Figure 10.** Dryout heat flux ($q''_d$) contours delineating dryout boundaries in the particle size - porosity plane for a one-dimensional particulate debris bed.

would be prevented from penetrating the bed by upward steam flow, regardless of the amount of water that is poured over the bed.

The dryout heat fluxes associated with the two curves of dryout limits shown in Figure 10 (1.02 $MW/m^2$ and 0.45 $MW/m^2$) correspond approximately to the heat fluxes of beds that are 1 m thick, 0.4 in porosity, and formed 2 hours and 8 hours after scram, respectively, if all the decay power generated within the bed is transferred to the top surface and if there is no exothermic oxidation within the bed. If a 1 m thick particulate bed is formed at two hours after scram (surface heat flux at 1.02 $MW/m^2$), has a porosity of 0.4, and is comprised of particles that are 1 mm in diameter, then it falls on the dryout limit curve labeled by 1.02 $MW/m^2$. Water can barely penetrate such a bed. As time goes on, the decay power in the bed decreases, and the bed is positioned in the diagram to the right of the dryout limit curve corresponding to a lower dryout heat flux. Water can then penetrate the bed. Water can also penetrate a one-meter thick particulate debris beds formed two hours after scram (surface heat flux at 1.02 $MW/m^2$) that have porosities higher than 0.4 or are comprised of particles that are larger than 1 mm in diameter, because these characteristics of the bed would position it in the dryout limits diagram to the right of the curve labeled by the dryout heat flux of 1.02 $MW/m^3$.

In the dryout limits diagram for particulate debris beds, the dryout heat flux associated with each contour of dryout limit corresponds to the potential heat flux that can emerge from a particulate debris bed on the verge of preventing water from entering it when water is poured over it. The heat flux could come from several sources. One source is the heat stored in the particles at elevated temperatures. Another source is the decay heat being generated in the debris bed. A third source is the heat liberated from the oxidation of zirconium in the bed when water penetrates the bed. However, only the decay heat truly defines the dryout limits. Heat fluxes to the water from stored heat in the particles only materialize when water penetrates the bed. Such heat fluxes slow the rate of ingress but do not prevent water from penetrating the bed. Similarly, oxidation takes place only when water penetrates the bed. Heat fluxes from stored heat disappear when the particles are quenched, and heat fluxes from oxidation disappear when either the particles are quenched or when the zircaloy is exhausted in the oxidation.

During an accident, the size and characteristics of a particulate debris bed formed in the reactor core cannot be ascertained with existing instruments. However, if a particulate debris bed exists in the core and water can penetrate the bed, steam will be generated when the water added to the core quenches the bed. There will also be a temporary increase in system pressure during the early stage of water addition when there is not yet enough water to condense the steam coming out of the particulate debris bed. If water cannot penetrate the bed, there will not be much steam production when water is added. In this case, system response to water addition may be deceptively quiescent.

## 5. SUMMARY AND CONCLUSION

The unmitigated core damage sequence presented in this study consists of: (1) Ballooning and rupture of fuel rod cladding, (2) rapid oxidation of zircaloy by steam, (3) failure of control rods, (4) formation of a cohesive region in lower regions of the reactor core or at the lower core support plate from relocated molten zircaloy and liquefied fuel, and (5) the relocation of core materials to the lower plenum of the reactor vessel. Concurrent with the formation of a cohesive bed near the bottom of the core, a particulate bed may also form from fuel pellets or oxidized cladding on top of the cohesive bed. The above sequence of core damage is essentially a temperature sequence, ranging from ballooning of the fuel rod cladding at approximately 1100 K to melting of the $UO_2$ fuel at 3100 K.

As water is added to the core at each stage of core degradation, steam is invariably produced because of rapid heat transfer from the overheated core materials to the incoming water. Up to the ballooning stage, core recovery can be assured if the high pressure injection system is operating at full capacity and if most of the injected water goes through the core. Core uncovery can be verified by readings of core exit thermocouples going back to the saturation temperature of water. If the core is heated to the rapid oxidation stage, the high pressure injection system is found to be below the water addition capacity that would arrest the progression of core degradation to a higher stage. If the primary system is not depressurized to allow accumulator injection, or no alternative method of quick delivery of water to the core is exercised, such as the use of reactor coolant pumps, the core will be heated to the stage of zircaloy and $UO_2$ liquefaction. The relocation of the liquified material will form a cohesive debris bed in the core.

If enough water is added to the core during the rapid oxidation stage by accumulator injection or by the exercise of reactor coolant pumps to deliver any remaining water in the cold legs, recovery of the core becomes possible if the fuel rods maintain more or less their intact geometry. Additional hydrogen will be produced during the water addition, but this is found to be significant compared with the overall hydrogen production if the core can be prevented from heating up to more than 2100 K. Because temperature measurements would have become unreliable during this stage, confirmation of recovery of the core at this stage has to rely on measurements of system pressure and responses of the SPNDs.

Movement of core materials first occur when the stainless steel cladding of the control rods melts. Besides the molten stainless steel, the relocating materials would also include the Ag-In-Cd control material in the case of PWRs and $B_4C$ control material in the case of BWRs. Some zircaloy may also be liquefied by the molten control materials at this stage. If unborated water is added to the core after the control materials have relocated, there is a possibility of re-criticality of the reactor. However, this issue is still unresolved.

If a cohesive debris bed is formed in the vessel from the relocation of core materials (stainless steel, control materials, zircaloy, fuel, and their eutectics), energy removal from the degraded core cannot be assured even if unlimited amounts of water is added to the vessel. The ability of water to remove energy from a cohesive debris bed depends on the bed's size, the power density in the bed, and the thermal conductivity of the materials comprising the bed. The power density and the thermal conductivities can be estimated from design and operating parameters of the reactor, while the size the debris bed may be obtained by probing the core with the use of the movable SPNDs, if these

instruments can still be moved in and out of the core. System responses to water addition at this stage of core damage progression depends on the amount and configuration of loose materials above the cohesive bed. If a particulate bed has already formed on top of the cohesive bed, the rates of steam and hydrogen production during water addition will be moderate because of the limited rate of water ingress into the particulate bed. If remnants of fuel rods and unoxidized zircaloy remain above the cohesive bed, flooding the core will lead to rapid generation of steam and hydrogen, and to collapse of the materials to form a particulate bed. In both cases, the interaction between the cohesive bed and the incoming water may not be noticeable because of the low rate of heat transfer from the cohesive bed to the water.

The interpretation of the response of system pressure to water addition after the formation of a cohesive debris bed could be quite counterintuitive. Because the core materials can be in the form of a cohesive bed, a particulate bed, and loose debris, the larger the cohesive and particulate beds, the smaller would be the amount of materials in the form of loose debris. If water addition to the core produces a rapid pressure rise, it is more likely that the cohesive and the particulate beds are small and energy can be easily removed from them by the incoming water. If there is little system pressure rise when water is added to the core, the debris beds are more likely to be large and energy cannot be efficiently removed from their interiors. The interiors of large debris beds are likely to melt and eventually relocate to the lower plenum of the reactor vessel.

Steam explosion at the time of relocation of molten materials to the lower plenum is still an unresolved issue. First, the probability of a steam explosion is unknown. Second, the amount of molten materials involved in a steam explosion should it occur is uncertain. However, if the movable SPNDs can be used to probe the core to determine a cohesive debris bed's size, the amount of core materials that will eventually relocate to the lower plenum can be bounded by the amount of materials comprising the cohesive debris. Conservative estimates of the impact of steam explosions, should they occur, can then be estimated.

This report has given a broad outline of core damage progression. However, additional work needs to be performed to evaluate the consequences of water addition to degraded cores for use in the development of an accident management plan. First, special characteristics of individual plants should be considered in the construction of a core damage sequence. Second, the consequences of water addition at each stage of core degradation need to be better quantified as functions of the amount of water added to the core. These include the temperature distributions at the exit of the core during the rod ballooning stage, the pressure responses during later stages, and neutronic and $\gamma$ signatures corresponding to what could be measured with the SPNDs when core geometry changes. Third, a time sequence needs to be better defined for the various stages of core degradation. As shown in Section 3 of this report, core damage could begin in less than an hour after core uncovery when emergency core cooling is unavailable. Oxidation of the zircaloy in the core can rapidly increase the core temperature to over 2000 K. After the rapid oxidation of zircaloy, there is a time interval of tens of minutes to an hour when the core geometry slowly changes from a rod-like geometry to one of cohesive mass and particulate bed. These estimates of the time intervals need to be refined by code calculations that include heat transfer between the core materials and the remaining coolant in the core. Finally, consequences of the relocation of molten materials to the lower plenum need to be carefully examined. These include the possibility of vessel failure from a steam explosion or failure of the lower head of the vessel from attack by the molten materials.

With the completion of the examination of the damaged core of the TMI-2 reactor and the analysis of numerous severe fuel damage experiments, the scenario of unmitigated core damage from ballooning of the fuel rods to the relocation of molten core materials to the lower plenum is firmly established. However, because of the dynamic nature of the interaction between water and core materials at high temperatures and the paucity of experiments simulating such an interaction, the consequences of water addition to a reactor core during advanced stages of degradation are not as well established. The situation may be remedied by detailed and realistic computer analysis, in addition to the simple, conservative, bounding calculations presented in this report.

## 6. REFERENCES


1. P. D. Bayless, "Experiment Results Report for LOFT Nuclear Experiment L3-5, L3-6, and L8-1," EGG-LOFT-5471, July 1981.

2. M. H. Schankula, D. S. Cox, and D. A. Leach, "Recent Post-Irradiation Examination Results from Battelle FLHT-2 and FLHT-4 Test Assemblies," presentation at the Severe Accident Research Program Partners Review Meeting, Idaho Falls, Idaho, April 1-14, 1989.

3. W. J. Camp, M. F. Young, J. L. Timkins, J. E. Kelly, P. J. Maudin, and R. J. Henninger, "MELPROG-PWR/MOD0: A Mechanistic Code for Analysis of Reactor Core Melt Progression and Vessel Attack under Severe Accident Conditions," NUREG/CR-4909, SAND85-0237, April 1987.

4. C. M. Allison and S. T. Polkinghorne, "SCDAP/MOD1 Analysis of the Progression of Core Damage during the TMI-2 Accident," EGG-SAR-7104, November 1985.

5. P. D. Bayless, "Analysis of Natural Circulation during a Surry Station Blackout using SCDAP/RELAP5," NUREG/CR-5214, EGG-2547, October 1988.

6. Z. R. Martinson, D. A. Petti, and B. A. Cook, "PBF Severe Fuel Damage Test 1-1 Test Results Report," NUREG/CR-4684, EGG-2643, Vol. 1-2, October 1986.

7. D. A. Petti, et al., "Power Burst Facility (PBF) Severe Fuel Damage Test 1-4 Test Results Report, "NUREG/CR-5136, EGG-2542, April 1989.

8. P. Kuan, "Stability of Zircaloy Oxidation during Severe LWR Accidents," Heat Transfer - Pittsburgh 1987, AIChE Symposium Series, No. 257, Vol. 83, pp. 297-300, August 1987.

9. R. O. Gauntt, R. D. Gasser, and L. J. Ott, "The DF-4 BWR Control Blade/Channel Box Fuel Damage Experiment," Draft, NUREG/CR-4671, SAND86-1443, March 1988.

10. J. M. Broughton, P. Kuan, D. A. Petti, and E. L. Tolman, "A Scenario of the Three Mile Island Unit 2 Accident, "Nuclear Technology, Vol. 87, pp. 34-53, August 1989.

11. P. Hofmann, S. J. L. Hagen, G. Schanz, and A. Skokan, "Reactor Core Materials Interactions at Very High Temperatures," *Nuclear Technology*, Vol. 87, pp. 146-186, August 1989.

12. P. Kuan and D. W. Golden, "Thermal Behavior of Cohesive Debris Beds in a Degraded Nuclear Reactor," AIChE Symposium Series, Vol. 85, No. 269, pp. 42-47, August 1989.

13. T. L. Van Witbeck and J. Putnam, "Three Mile Island Unit 2, Annotated Sequence of Events, March 18, 1979," GPUN Corp. TDR-044.

14. P. Kuan, J. L. Anderson, and E. L. Tolman, "Thermal Interactions during the TMI-2 2-B Coolant Pump Transient," *Transactions American Nuclear Society*, Vol. 57, pp. 410-411, October-November 1988.

15. P. Kuan, J. L. Anderson, and E. L. Tolman, "Thermal Interactions during the TMI-2 2-B Coolant Pump Transient," *Nuclear Technology*, Vol. 87, No. 1, August 1989.

16. A. D. Knipe, S. A. Ploger, and D. J. Osetek, "PBF Severe Fuel Damage Scoping Test - Test Results Report," NUREG/CR-4683, EGG-2413, August 1986.

17. J. P. Adams, et al., "Quick-Look Report on OECD LOFT Experiment LP-FP-2," OECD LOFT-T-3804, September 1985.

18. E. S. Sowa, J. C. Hesson, R. H. Gebner, and G. T. Goldfuss, "Heat Transfer Experiments through Beds of $UO_2$ in Boiling Sodium," *Transactions American Nuclear Society*, Vol. 14, p. 725, November 1981.

19. R. J. Lipinski, "A Model for Boiling and Dryout in Particle Beds," NUREG/CR-2646, SAND82-0765, June 1982.

20. D. Squarer, L. E. Hochreiter, and A. T. Pieczynski, "Modes of Heat Removal from a Heat-Generating Debris Bed," *Nuclear Technology*, Vol. 65, pp. 16-22, April 1984.

21. G. Hofmann, "Dryout in Very Deep Particulate Beds," *Nuclear Engineering Design*, Vol. 99, p. 177, 1987.

22. A. W. Reed, et al., "DCC-1/DCC-2 Degraded Core Coolability Analysis," NUREG/CR-4390, SAND85-1967, October 1985.

23. S. S. Dosanjh, "Melt Progression in Severely Damaged Reactor Cores," NUREG/CR-5029, December 1987.

24. E. L. Tolman and R. Moore, "TMI-2 Degraded Core Heatup and Cooldown Analysis," *Transactions American Nuclear Society*, Vol. 57, p. 411, October 1988.

25. D. E. Mitchell, M. L. Corradini, and W. W. Tarbell, "Intermediate Scale Steam Explosion Phenomena: Experiment and Analysis," NUREG/CR-2145, SAND81-0124, September 1981.

26. T. G. Theofanous, et al., "An assessment of Steam-Explosion-Induced Containment Failure," NUREG/CR-5050, February 1989.

27. R. Moore, "TMI-2 Reactor Vessel Lower Head Heatup Calculations," EGG-TMI-7784, September 1987.

28. G. L. Thinnes and R. L. Moore, "Comparison of Thermal and Mechanical Responses of the Three Mile Island Unit 2 Reactor Vessel," *Nuclear Technology*, Vol. 87, No. 1, August 1989.

29. Reference Safety Analysis Report, Westinghouse Nuclear Energy Systems, 1975.

30. Babcock and Wilcox Standard Safety Analysis Report, 1978.

31. BWR/6 Standard Safety Analysis Report, General Electric Corporation.

32. ANSI/ANS-5.1, 1979 Decay Heat Standard for Light Water Reactors.

33. R. E. Pawel, J. V. Cathcart, and R. A. McKee, "The Kinetics of Oxidation of Zircaloy-4 in Steam at High Temperatures," *Electrical Chemical Science and Technology*, Vol. 126, No. 7, July 1979.

34. V. F. Urbanic and T. R. Heidrick, "High-Temperature Oxidation of Zircaloy-2 and Zircaloy-4 in Steam," *Journal of Nuclear Materials*, Vol. 75, pp. 251-261, 1978.

35. D. L. Hagrman, G. A. Reymann, and R. E. Mason, "MATPRO-Version 11 (Revision 2), A Handbook of Materials Properties for Use in the Analysis of Light Water Reactor Fuel Rod Behavior," NUREG/CR-0479, TREE-1280, Rev. 2, August 1981.

36. D. L. Hagrman, "Materials Properties Models for Severe Core Damage Analysis," EGG-CDD-5801, May 1982.

37. R. C. Gottula, et al., "Forced Convective, Non-Equilibrium, Post-CHF Heat Transfer Experiment Data and Correlation Comparison Report," NUREG/CR-3193, EGG-2245, March 1985.

38. F. Kreith and M. S. Bohn, *Principles of Heat Transfer*, 4th Edition, Harper & Row Publishers, New York, 1986, p. 302.

39. F. W. Dittus and L. M. K. Boelter, "Heat Transfer in Automobile Radiators of the Tubular Type," *Publications in Engineering*, 2, University of California, Berkeley, 1930, pp. 443-461.

40. R. J. Lipinski, "A Coolability Model for Post-Accident Nuclear Reactor Debris," *Nuclear Technology*, Vol. 65, pp. 53-56, April 1984.

41. P. Kuan, "A Deep Particle Bed Dryout Model Based on Flooding," *Transactions American Nuclear Society*, Vol. 55, p. 751, November 1987.

# Appendix C

# SCDAP/RELAP5/MOD3 Surry Model Description

# Appendix C

# SCDAP/RELAP5/MOD3 Model Description

SCDAP/RELAP5/MOD3[C-1] is an integrated computer code package designed for nuclear reactor accident analysis. Modules for simulation of thermal-hydraulics, heat transfer, severe core damage, and fission product transport are included, as discussed in Appendix A. The code user is allowed to select those modules necessary to simulate the problem of interest. In this assessment of the Surry nuclear power plant (NPP) during a TMLB' sequence (the complete loss of all ac power and auxiliary feedwater without subsequent recovery or operator action), an appropriate SCDAP/RELAP5/MOD3 model required use of (a) the RELAP5 module for simulation of plant thermal-hydraulics and heat transfer affecting the plant structural mass; (b) the SCDAP module for simulation of core components during degradation, melt, and relocation to the lower reactor vessel head; and (c) the COUPLE module for simulation of the lower head to the time of creep rupture failure resulting from thermal attack by relocated core materials.

A SCDAP/RELAP5/MOD3 model was not developed from scratch for use in this assessment. Instead, modifications were made to the inputs of an existing SCDAP/RELAP5/MOD0 model. The existing model, as developed by Bayless,[C-2] has been the subject of critical internal reviews and at least one independent external review.[a] The existing model is believed to be a very good starting point for this assessment on that basis. All input modifications to the existing model are described separately in the following sections for RELAP5, SCDAP, and COUPLE modules. In addition, basic information is provided as needed to understand the input modifications and some of the general features of the model with respect to the current assessment. Other model details are adequately described by Bayless.

Before the input modifications are described, it should be noted that all calculations in this assessment were made using a code execution option known as MOD2.5 time smoothing. This option invokes a numerical method designed to improve calculational stability, as implemented as a default feature in SCDAP/RELAP5/MOD2.5. It is particularly helpful during shifts between flow regimes, heat transfer correlations, etc., where those shifts introduce functional discontinuities. The use of MOD2.5 time smoothing was justified in this assessment since (a) it produces only minor differences in scoping results out to the onset of core heatup, (b) it reduces the magnitude of integrated mass errors, and (c) it allows the code to run faster with fewer calculational problems.

## C-1. RELAP5 INPUT

The RELAP5 module was used to simulate the thermal-hydraulics of the reactor vessel, the piping in all three primary coolant loops, the pressurizer, all three steam generators, and selected parts of the secondary systems. Reactor vessel nodalization, as developed by Bayless,[C-2] is shown

---

a. G. M. Martinez et al., *Independent Review of SCDAP/RELAP5 Natural Circulation Calculations*, SAND91-2089 (to be published).

in Figure C-1. As indicated, three parallel flow channels extend from the lower plenum through the core to the upper reactor vessel head. If the appropriate conditions exist, this arrangement will allow development of in-vessel natural circulation. Heat structures, which are shown as shaded areas, represent the structural mass of the reactor vessel walls, the core barrel and baffle, the thermal shield, the upper and lower core support plates, and structures in the upper and lower plena. External surfaces of all heat structures were assumed to be adiabatic.

A junction connecting the top of the downcomer (Volume 102) to the upper plenum (Volume 172) at the hot leg elevation is shown in Figure C-1. This junction represents a small leak path associated with clearances between the hot leg nozzles (which are welded to the reactor vessel wall) and the internal hot leg piping (which is welded to the core barrel). The resulting gap in the hot leg piping, which allows flow to bypass the core, is a design requirement for removal of core internals.

Nodalizations of the primary coolant loop containing the pressurizer, as developed by Bayless, are shown in Figures C-2 and C-3. With the exception of the pressurizer and associated surge line piping, similar nodalizations were included in the model to separately represent the other two primary coolant loops in the Surry NPP.

The nodalization shown in Figure C-2 was used in conjunction with the reactor vessel nodalization from TMLB' initiation to core heatup. (In this assessment, it was assumed that the onset of core heatup coincided with a core exit vapor superheat of 2.78 K.) During this portion of the transient, full loop natural circulation of subcooled and saturated liquid can develop. As the core heats the primary coolant toward saturation, however, voids begin to form and collect at the top of the steam generator U-tubes. Once that occurs, full loop natural circulation of liquid is interrupted.

At the onset of core heatup, Figure C-2 nodalization was replaced by Figure C-3 nodalization in all calculations except those associated with Case 2. This substitution provided the flow paths needed to represent hot leg countercurrent natural circulation. (Figure C-3 nodalization was never used in Case 2, which was performed to evaluate conditions with minimum ex-vessel heat transfer.) Hot leg countercurrent natural circulation became possible after saturated liquid in the hot legs drained to the vessel and/or flashed. At that time, temperature gradients from the core to the steam generator U-tubes can drive steam flow along the top half of the hot leg (represented by components 400, 402, and 404), through a portion of the steam generator U-tubes (represented by component 408), and back to the vessel through a cooler portion of the steam generator U-tubes and the lower half of the hot leg (represented by components 409 and 430). (Note that if reactor coolant pump (RCP) loop seals clear, both Figure C-2 and C-3 nodalizations will also allow full loop natural circulation of superheated steam.) Flow areas and loss coefficients in the split hot legs, split U-tubes, and associated components were established to match experimental countercurrent flow data as explained by Bayless.

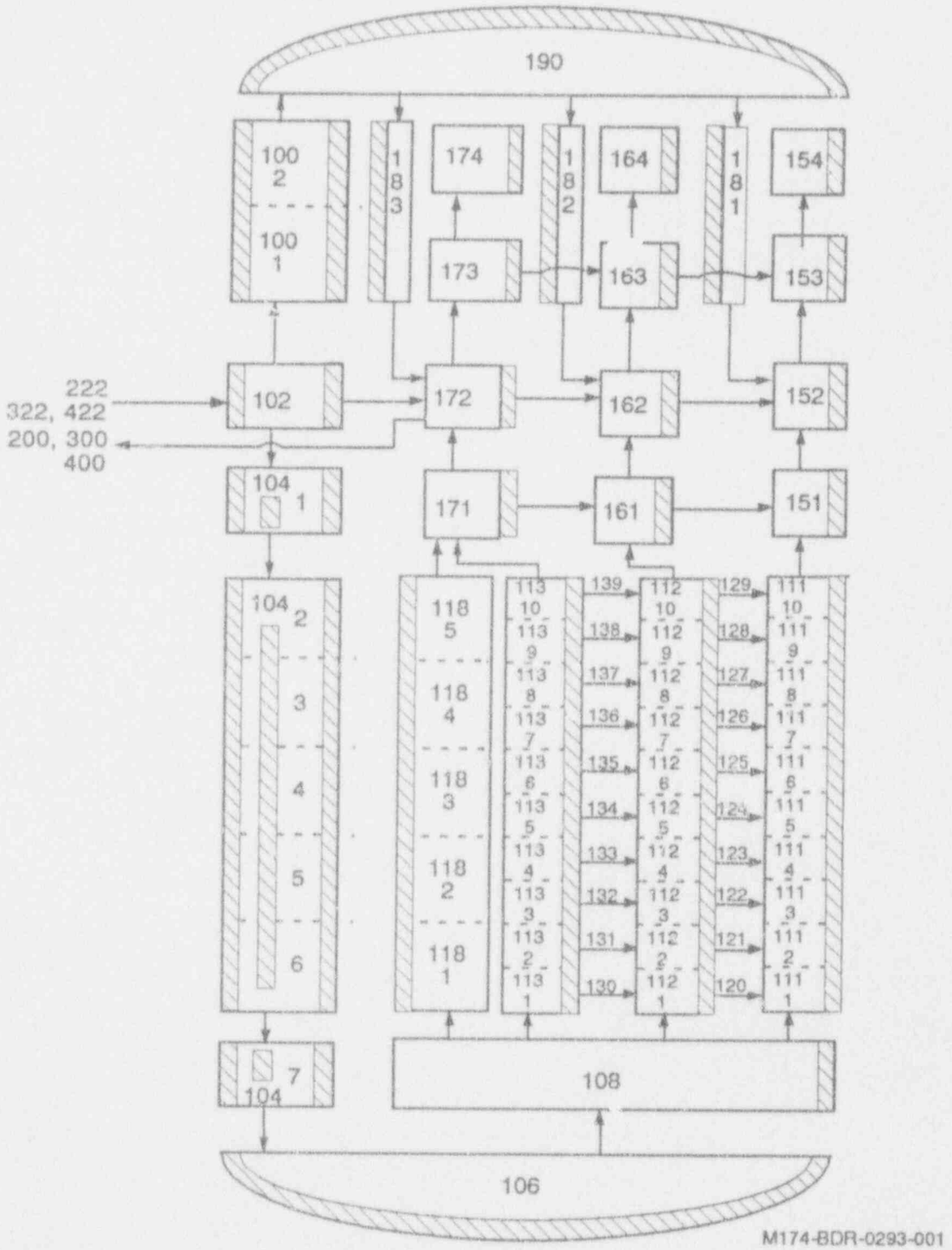


**Figure C-1.** Surry NPP reactor vessel nodalization with provisions for in-vessel natural circulation.

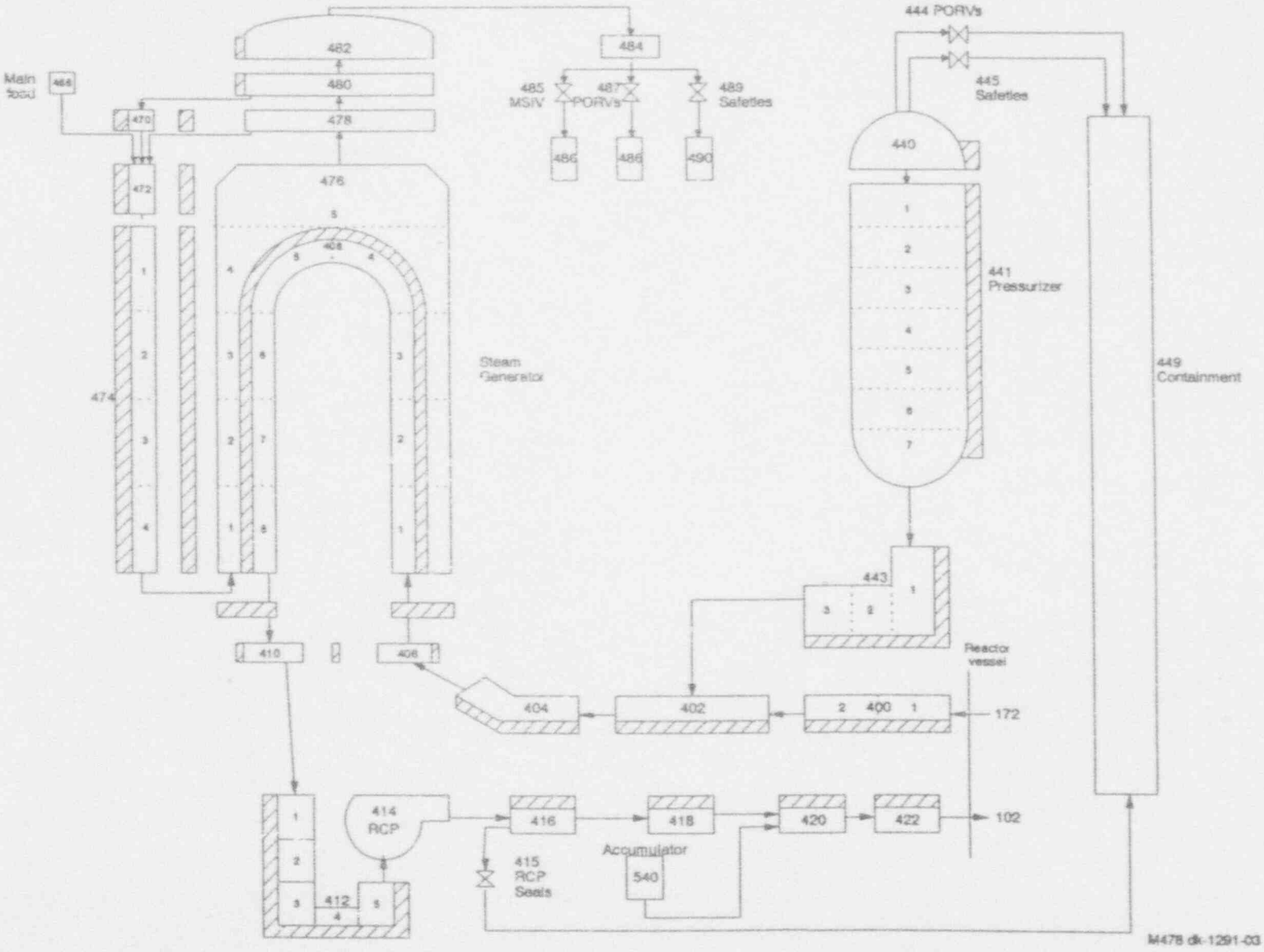


**Figure C-2.** Pressurizer coolant loop nodalization for the Surry NPP without provisions for hot leg countercurrent natural circulation.

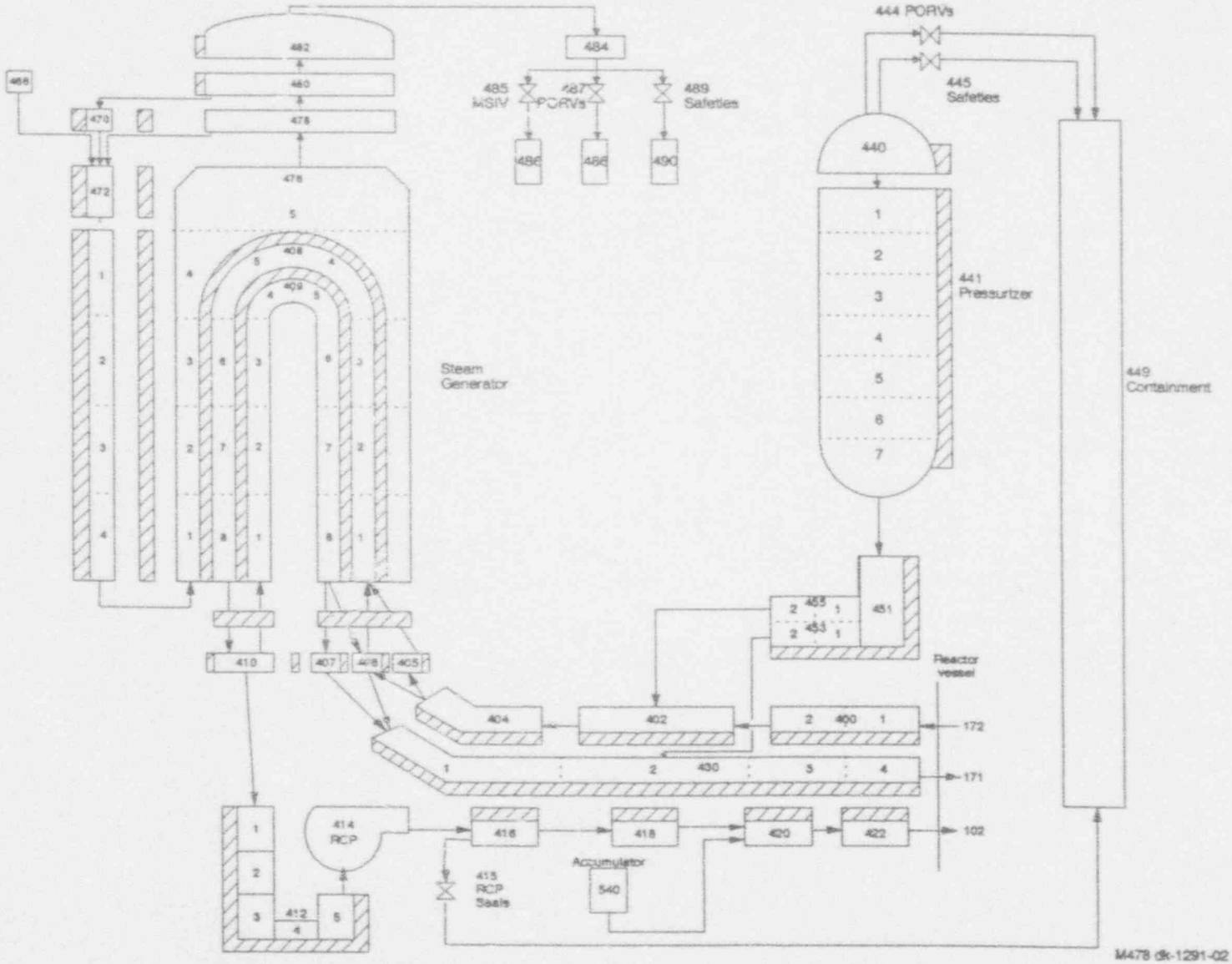


**Figure C-3.** Pressurizer coolant loop nodalization for the Surry NPP with provisions for hot leg countercurrent natural circulation.

As indicated in Figures C-2 and C-3, both fluid volumes and heat structures were included to represent the primary coolant loop piping, the pressurizer and associated surge line, and the steam generator with associated relief valves. Without ac power, the accumulator is the only emergency core cooling system that required simulation. The steam generator main feedwater system and associated piping were only needed to establish steady-state conditions prior to transient initiation. Auxiliary feedwater systems were not modeled, since they are not operational in a TMLB' sequence. The external surfaces of all heat structures were assumed to be adiabatic.

A single valve was used to represent both power-operated relief valves (PORVs) connected to the pressurizer. The valve was appropriately sized to represent the flow capacity of both PORVs in the Surry NPP. Similarly, a single valve was used to represent all three safety relief valves. It was assumed that there was sufficient plant air and battery power to allow operation of the valves throughout all transients. Other (potential) valve failure modes were not considered.

Trip valves were added to the existing model to represent potential leakage from RCP seals. As indicated in Figures C-2 and C-3, this leak was modeled at the discharge elevation of each RCP. (SCDAP/RELAP5/MOD3 allows only one connection to a pump outlet. However, the inlet of the connected pipe is hydraulically equivalent to the RCP outlet in SCDAP/RELAP5/MOD3.) The relationship between transient time and valve flow areas used to model seal leakage in this assessment is described in the body of this report.

RCP seal leaks (and discharges from the pressurizer) were directed into a single volume representing the Surry NPP containment, as indicated in Figures C-2 and C-3. However, there was no attempt to model containment in detail based on the assumption that flows from the reactor coolant system (RCS) to containment should be choked. Containment pressure response was then monitored during all calculations to check the validity of that assumption. In Cases 4, 5, and 6, it was found that RCP seal leak flows did come unchoked late in the transients. For those cases, a more accurate representation of containment pressure was obtained by restarting the affected calculations with heat structures representing the containment masses of concrete and carbon steel. The resulting heat sinks reduced containment pressure by condensing RCS flows. Further refinement of the containment model was unnecessary, since the pressure reduction was more than enough to produce choking of all flows from the RCS.

An interphase friction correlation for flow past rodded geometries was added to SCDAP/RELAP5/MOD3. Based on recommendations from the code development staff, input was added to the model to use that correlation in the core and steam generator secondary volumes. As an associated input addition, the minimum tube-to-tube spacing was used in place of the heated equivalent diameter for the secondary side of U-tube heat structures. (A corresponding rod-to-rod spacing input for the core could not be made, since SCDAP components, not RELAP5 heat structures, were used to represent the fuel.)

Several other RELAP5 inputs were added and/or altered in the transition from SCDAP/RELAP5/MOD0 to SCDAP/RELAP5/MOD3 (the addition of junction hydraulic diameter input, the alteration of the heated equivalent diameter input for heat structures, and so on). To the extent possible, all necessary input additions/alterations were implemented to retain comparability with the Bayless model.

## C-2. SCDAP INPUT

The three core flow channels shown in Figure C-1 were selected so that similarly powered fuel assemblies would be grouped together. A cross-section of the resulting three channel model is shown in Figure C-4. The number of fuel assemblies in each channel and their relative power is indicated.

A typical 15x15 fuel assembly used in the Surry NPP consists of fuel rods, control rods, and instrument tubes, as shown in Figure C-5. Therefore, separate SCDAP components representing fuel rods, control rods, and empty control rod guide tubes and instrument tubes were used by Bayless to model each channel.[C-2] As a result, a total of nine SCDAP components was required.

Scoping calculations were performed to determine if SCDAP components representing the control rods could be combined with SCDAP components representing the empty control rod guide tubes and instrument tubes (by channel). In those calculations, a one-channel model was developed using the three-component approach. In a second one-channel model, control rods, empty control rod guide tubes, and instrument tubes were combined into a single SCDAP control rod component. In that case, the total number of rods plus tubes was not altered. However, a control rod of reduced size had to be used to conserve the masses of control rod materials and the cladding. Calculations using both models were allowed to proceed through core degradation, melt, and relocation. Results from the two models were found to be virtually identical.

Based on the results of the scoping calculations, control rods were combined with empty control rod guide tubes and instrument tubes in each flow channel of the SCDAP/RELAP5/MOD3 model. Compared to the Bayless model, this simplification reduced the number of SCDAP components from nine to six.

SCDAP fuel rod components were linked to a table to provide an appropriate decay power curve for the Surry NPP following the loss of ac power (and associated reactor scram). The decay power curve was based on an ORIGEN2 calculation from scram to 20,000 s (333.3 min) as used in the sensitivity calculations described by Bayless. As indicated in Table C-1, however, the decay power curve was extended to 36,000 seconds (600.0 minutes) to accommodate the anticipated duration of calculations in this assessment. The accuracy of the extension, which was made with a least-squares fit of the last seven data points in the original table, should not adversely impact results. In addition, the Bayless data was scaled by a factor of 0.998 to obtain a match between MOD0 and MOD3 steady-state power levels.

SCDAP input is required to define certain parameters that control severe core damage progression. In general, best-estimate parameters were selected where there were data or some basic understanding of the associated process. For parameters with higher degrees of uncertainty, values were selected to minimize the time to lower head failure. This approach provides the basis for a conservative evaluation of the potential for high pressure melt ejection and the associated problem of direct containment heating, since the time available for generation of an ex-vessel failure by natural convection heating is minimized and since the system pressure at the time of failure should be maximized (at least for RCP seal leak cases). The resulting parameter set, including a full discussion of the logic used to establish each value, is described in the body of this report.

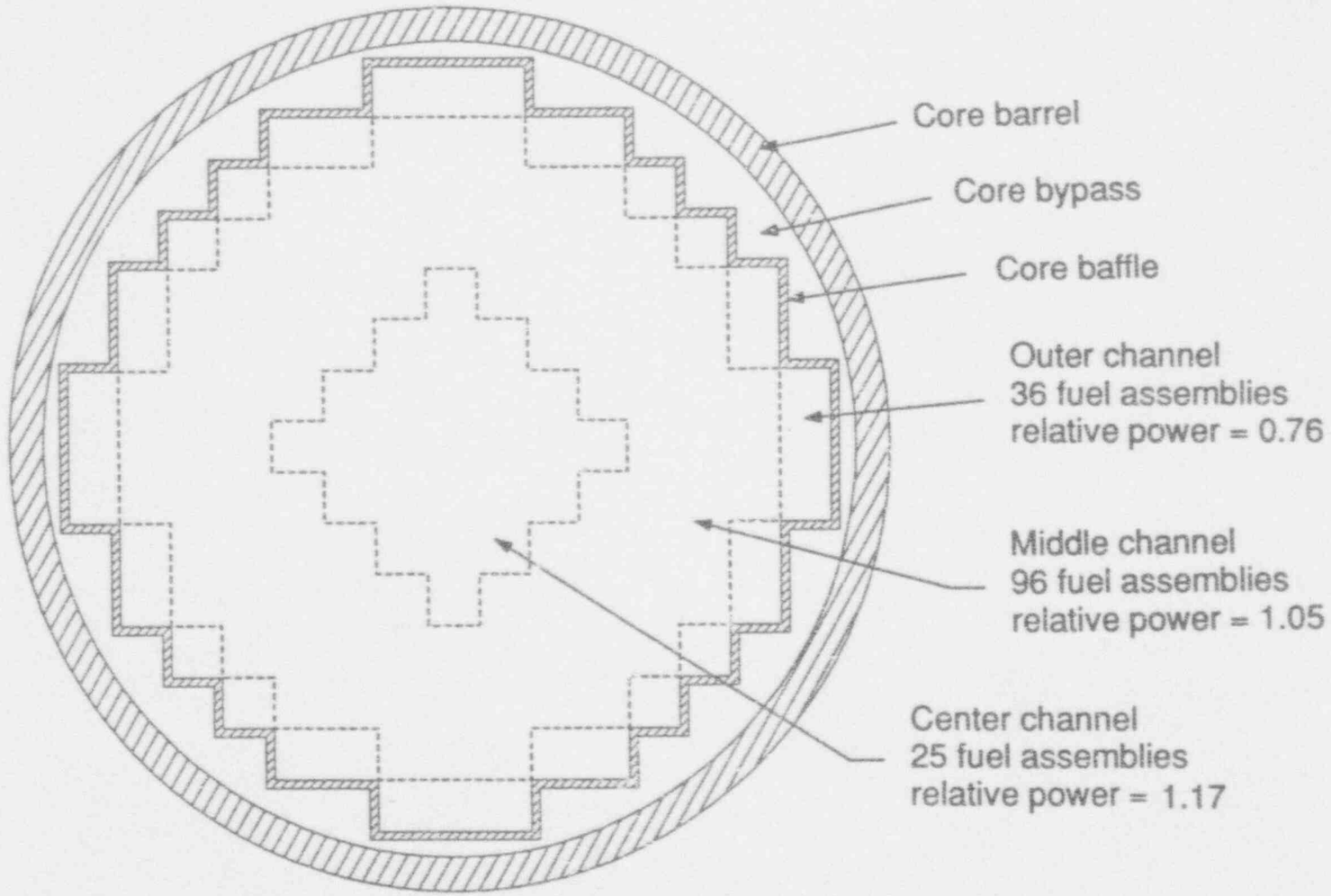


**Figure C-4.** A cross section of the three-channel core region.

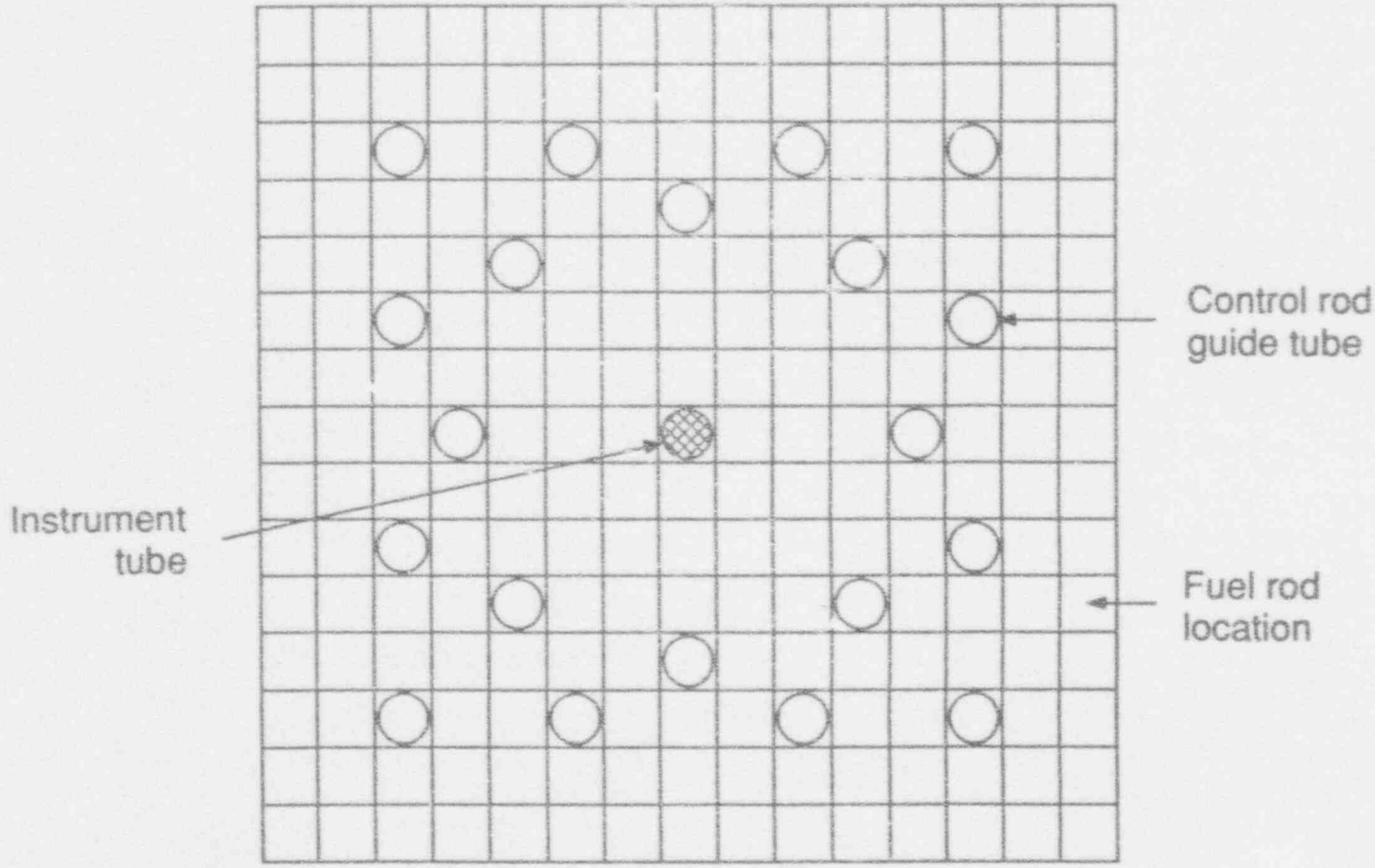


**Figure C-5.** A typical 15x15 Surry NPP fuel assembly.

**Table C-1.** Decay power curve.

| Time (s) | Center Channel (MW) | | | Middle Channel (MW) | | | Outer Channel (MW) | | |
|---|---|---|---|---|---|---|---|---|---|
| | Prompt | Fission Product | Actinide | Prompt | Fission Product | Actinide | Prompt | Fission Product | Actinide |
| 0.0 | 426.75 | 25.804 | 1.4094 | 1470.1 | 89.974 | 4.3161 | 398.42 | 25.198 | 1.0112 |
| 0.7 | 426.75 | 25.804 | 1.4094 | 1470.1 | 89.974 | 4.3161 | 398.42 | 25.198 | 1.0112 |
| 1.0 | 382.11 | 25.804 | 1.4094 | 1316.3 | 89.974 | 4.3161 | 356.74 | 25.198 | 1.0112 |
| 1.5 | 323.73 | 24.634 | 1.4092 | 1115.3 | 85.803 | 4.3152 | 302.23 | 23.991 | 1.0112 |
| 2.0 | 275.83 | 23.872 | 1.4092 | 950.24 | 83.131 | 4.3152 | 257.52 | 23.217 | 1.0112 |
| 3.0 | 61.178 | 22.820 | 1.4087 | 210.75 | 79.444 | 4.3132 | 57.117 | 22.164 | 1.0109 |
| 6.0 | 8.8713 | 20.987 | 1.4077 | 30.561 | 73.022 | 4.3104 | 8.2822 | 20.332 | 1.0102 |
| 11.0 | 5.5405 | 19.328 | 1.4060 | 19.087 | 67.213 | 4.3056 | 5.1726 | 18.679 | 1.0087 |
| 16.0 | 4.1075 | 18.267 | 1.4043 | 14.150 | 63.521 | 4.2998 | 3.8347 | 17.641 | 1.0077 |
| 21.0 | 3.2849 | 17.491 | 1.4025 | 11.316 | 60.810 | 4.2941 | 3.0669 | 16.883 | 1.0062 |
| 31.0 | 2.3029 | 16.378 | 1.3987 | 7.9338 | 56.949 | 4.2826 | 2.1501 | 15.797 | 1.0037 |
| 51.0 | 1.2969 | 14.956 | 1.3919 | 4.4680 | 52.016 | 4.2615 | 1.2108 | 14.428 | 0.9987 |
| 101.0 | 0.3965 | 13.031 | 1.3750 | 1.3660 | 45.365 | 4.2088 | 0.3702 | 12.585 | 0.9861 |
| 201.0 | 0.0679 | 11.270 | 1.3421 | 0.2338 | 39.252 | 4.1072 | 0.0634 | 10.888 | 0.9620 |
| 501.0 | 0.0013 | 9.3085 | 1.2525 | 0.0046 | 32.400 | 3.8312 | 0.0012 | 8.9838 | 0.8962 |
| 1001.0 | 0.0 | 7.9034 | 1.1297 | 0.0 | 27.531 | 3.4518 | 0.0 | 7.6400 | 0.8057 |
| 2501.0 | 0.0 | 6.0192 | 0.8979 | 0.0 | 20.986 | 2.7359 | 0.0 | 5.8287 | 0.6357 |
| 5001.0 | 0.0 | 4.7465 | 0.7429 | 0.0 | 16.52: | 2.2586 | 0.0 | 4.5747 | 0.5225 |
| 10001.0 | 0.0 | 3.7534 | 0.6738 | 0.0 | 12.966 | 2.0479 | 0.0 | 3.5601 | 0.4729 |
| 20001.0 | 0.0 | 3.2092 | 0.6448 | 0.0 | 11.087 | 1.9616 | 0.0 | 3.0214 | 0.4535 |
| 36000.0 | 0.0 | 2.7197 | 0.5548 | 0.0 | 9.4023 | 1.6836 | 0.0 | 2.5731 | 0.3877 |

Several other SCDAP inputs were added and/or altered in the transition from SCDAP/RELAP5/MOD0 to SCDAP/RELAP5/MOD3 (the addition of fuel rod gap conductance, the alteration in the number of radial nodes required to define a control rod component, and so on). To the extent possible, all necessary input additions/alterations were implemented to retain comparability with the Bayless model.

## C-3. COUPLE INPUT

SCDAP/RELAP5/MOD0 calculations by Bayless were terminated when fuel relocation began.[C-2] For that reason, detailed modeling of the lower reactor vessel head was not performed. In this assessment, however, determining the time of lower head failure was a primary objective that required COUPLE input.

The COUPLE mesh used to represent the lower reactor vessel head is shown in Figure C-6. The axisymetric mesh includes a total of 320 nodes with 285 elements. Two elements were used to represent the thickness of the carbon steel portion of the lower head, with an adjoining single element representing the stainless steel liner. (Because the liner is relatively thin, the elements representing it appear to be a heavy line in the figure.)

A layer of zero-width gap elements coincided with the inner surface of the liner. The gap elements provided a way to model contact resistance between the debris and liner. In this assessment, a large conductance was used to simulate perfect debris/liner contact. (This approach is consistent with the effort to minimize the time to lower head failure.) The remaining elements are initially filled with primary coolant. During molten relocation, the coolant can boil off and/or be displaced by debris.

Convection and radiation heat transfer were modeled at all interfaces between the coolant and debris. In addition, convection and radiation heat transfer were modeled along the vessel wall at all nodes that are not submerged by debris (those nodes exposed to primary coolant/steam). The external surface of the lower head was assumed to be adiabatic.

## C-4. REFERENCES

C-1. C. M. Allison et al., *SCDAP/RELAP5/MOD3 Code Manual*, NUREG/CR-5273, EGG-2555 (Draft), Revision 2, Volumes 1-4, September 1991 (available from EG&G Idaho, Inc.).

C-2. P. D. Bayless, *Analyses of Natural Circulation During a Surry Station Blackout Using SCDAP/RELAP5*, NUREG/CR-5214, EGG-2547, October 1988.

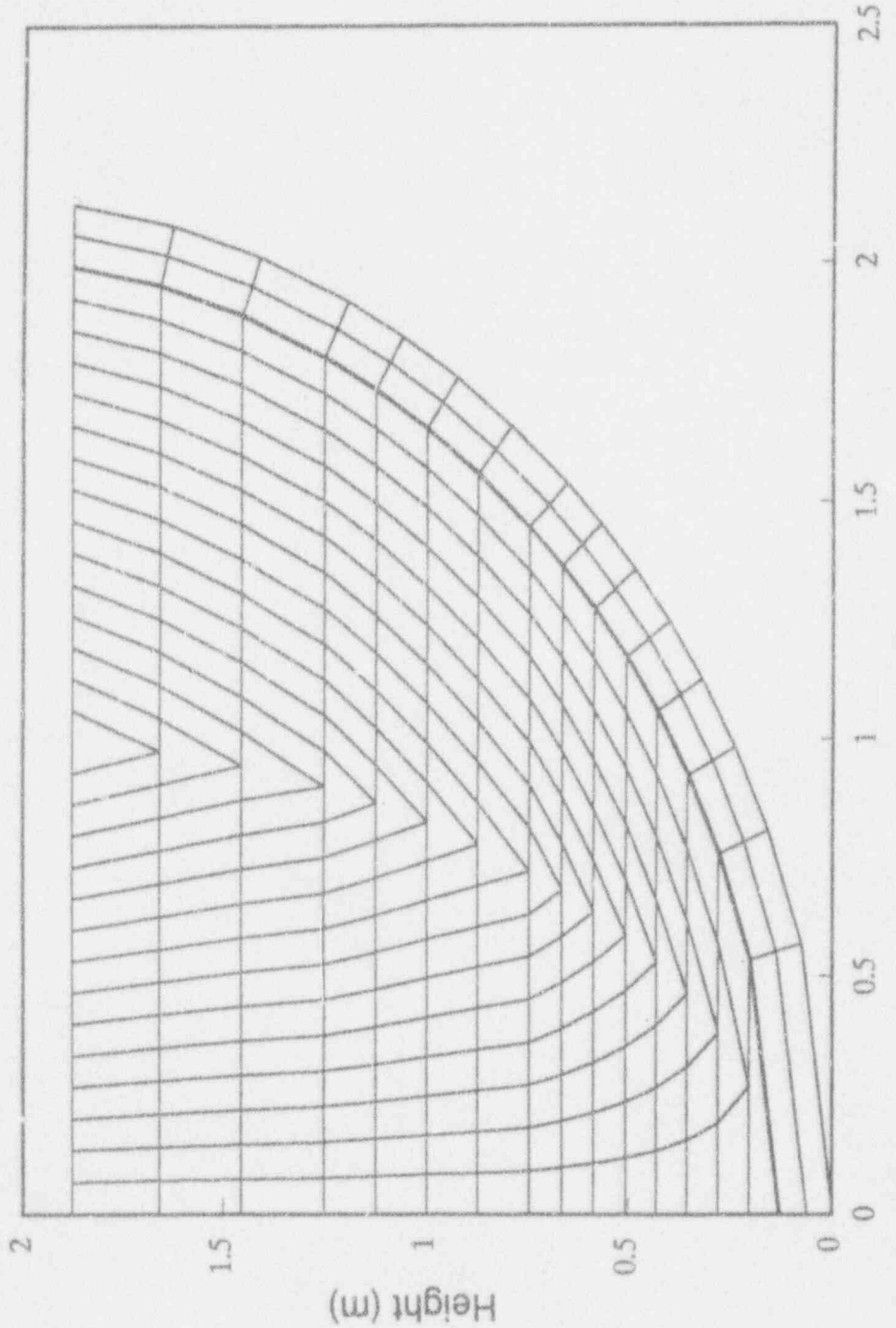


**Figure C-6.** COUPLE mesh representing the lower reactor vessel head.

NRC FORM 335 (2-89) NRCM 1102, 3201, 3202

U.S. NUCLEAR REGULATORY COMMISSION

# BIBLIOGRAPHIC DATA SHEET

(See instructions on the reverse)

1. REPORT NUMBER (Assigned by NRC, Add Vol., Supp., Rev., and Addendum Numbers, if any.)

NUREG/CR-6158
EGG-2644

2. TITLE AND SUBTITLE

Implications for Accident Management of Adding Water to a Degrading Reactor Core

3. DATE REPORT PUBLISHED

MONTH: February YEAR: 1994

4. FIN OR GRANT NUMBER

B5995

5. AUTHOR(S)

P. Kuan, D.J. Hanson, D.J. Pafford, K.S. Quick

6. TYPE OF REPORT

Technical

7. PERIOD COVERED (Inclusive Dates)

8. PERFORMING ORGANIZATION – NAME AND ADDRESS (If NRC, provide Division, Office or Region, U.S. Nuclear Regulatory Commission, and mailing address; if contractor, provide name and mailing address.)

Idaho National Engineering Laboratory
EG&G Idaho, Inc.
Idaho Falls, Idaho 83415

9. SPONSORING ORGANIZATION – NAME AND ADDRESS (If NRC, type "Same as above"; if contractor, provide NRC Division, Office or Region, U.S. Nuclear Regulatory Commission, and mailing address.)

Division of Systems Research
Office of Nuclear Regulatory Research
U.S. Nuclear Regulatory Commission
Washington, D.C. 20555

10. SUPPLEMENTARY NOTES

11. ABSTRACT (200 words or less)

This report evaluates both the positive and negative consequences of adding water to a degraded reactor core during a severe accident. The evaluation discusses the earliest possible stage at which an accident can be terminated and how plant personnel can best respond to undesired results. Specifically discussed are (a) the potential for plant personnel to add water for a range of severe accidents, (b) the time available for plant personnel to act, (c) possible plant responses to water added during the various stages of core degradation, (d) plant instrumentation available to understand the core condition and (e) the expected response of the instrumentation during the various stages of severe accidents.

12. KEY WORDS/DESCRIPTORS (List words or phrases that will assist researchers in locating the report.)

Accident Management
Severe Accident
Degraded Core
Water Addition
ECC Injection
Core Damage

13. AVAILABILITY STATEMENT

Unlimited

14. SECURITY CLASSIFICATION

(This Page) Unclassified

(This Report) Unclassified

15. NUMBER OF PAGES

16. PRICE

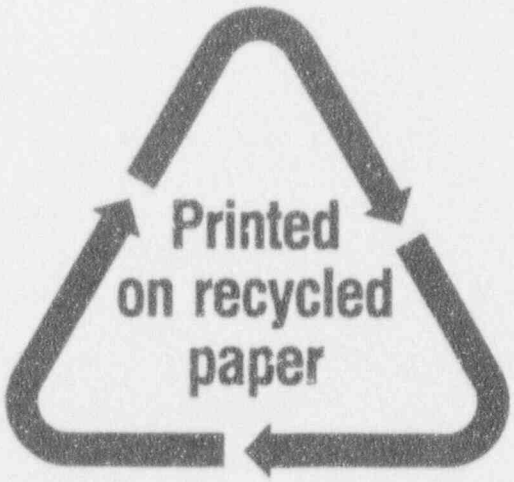


Federal Recycling Program

UNITED STATES
NUCLEAR REGULATORY COMMISSION
WASHINGTON, D.C. 20555-0001





120555139531 1 1AN1PR
US NRC-OADM
DIV FOIA & PUBLICATIONS SVCS
TPS-PDR-NUREG
P-211
WASHINGTON DC 20555